이학박사 학위논문

Excited-State Transition Metal-Catalyzed C–N and C–S Bond Formations

들뜬 상태 전이금속 촉매를 사용한 탄소–질소 및 탄소–황 결합형성

2019 년 2 월

서울대학교 대학원

화학부 유기화학 전공

김 태 훈

Excited-State Transition Metal-Catalyzed C–N and C–S Bond Formations

지도교수 이 철 범

이 논문을 이학박사 학위논문으로 제출함
2019 년 2 월

서울대학교 대학원
화학부 유기화학 전공
김 태 훈

김태훈의 이학박사 학위논문을 인준함
2019 년 2 월

위 원 장 David Yu-Kai Chen (인)

부위원장 이 철 범 (인)

위 원 김 병 철 (인)

위 원 조 은 진 (인)

위 원 이 홍 근 (인)

Abstract

Iridium and ruthenium polypyridyl complexes have become a powerful tool for harvesting visible-light photonic energy in organic reactions (**Chapter 1**). The ^{3}MLCT complex formed after photo-excitation can activate molecules to their different electronic structures which can not be attained through thermal activation strategies. Moreover, an excited-state metal complex that can act as both strong reductant and oxidant in a redox catalytic cycle enables the cyclometalated complexes to mediate facile one-electron reduction and oxidation in a single reaction system. Additionally, triplet-excited states accessed via the Dexter energy transfer of the photocatalyst allow for organic chemists to bypass the poor absorbance and spin-orbit coupling during the unfavored intersystem crossing of most organic compounds.

Using the single electron transfer mechanism of the photocatalyst, we developed a mild aromatic C–H functionalization protocol for the efficient synthesis of aniline derivatives (**Chapter 2**). The activation of an N–Cl bond via photoredox catalysis generated an electron-deficient nitrogen radical intermediate which subsequently furnished aryl amines from unactivated aromatic compounds. More specifically, in the presence of a catalytic amount of an iridium photocatalyst, irradiation with visible light-induced reduction of an N–Cl bond and oxidation of cyclohexadienyl radical intermediate, thus forming C–N bond by substituting aryl C_{sp^2}–H bond.

Transition metal-catalyzed cross-coupling of amines with aromatic halides have been widely utilized for the synthesis of aromatic amines which are mainstay fragments of widespread utility in various areas (**Chapter 3**). Decades of investigations have led to the structural sophistication of transition metal complexes to promote more efficient catalytic amination reactions. Recently, visible-light-activated photocatalysts have added a new dimension to this transition metal-catalyzed amination by involving a different electronic state of the cross-coupling catalyst. In this strategy, the insufficient reactivity of first-row transition metals is circumvented by changing the electronic structure of the organometallic intermediates. We have invented a nickel-catalyzed method for the sulfonamidation of aryl halides making use of a photocatalyst that helps bypass disfavored reductive elimination of Ni^{II} (**Chapter 4**). Using this dual-catalytic strategy, two complementary reaction conditions have been developed for the sulfonamidation of aromatic halides, one using ligand-free nickel and the other employing a small amount of dtbbpy ligand. Applying these two protocols, we have demonstrated that efficient sulfonamidation take place with a broad array of aromatic halides. Preliminary mechanistic studies have revealed that the triplet-excitation of the nickel center facilitates the C–N bond-making reductive elimination of the

otherwise unreactive Ni^{II} amido complex. In addition, we have detected the bipyridyl ligand decomposition of an iridium photocatalyst. This observation further inspired us to propose the ligand to play an additional role in the recovery of a decomposed photocatalyst.

Recently, there has been increased interest in the development of SO_2 surrogates for the efficient synthesis of sulfinate salts en route to sulfones and sulfonamides. However, the arylation of sulfinates has relied on the harsh palladium-catalyzed sulfonylation process, which was developed more than ten years ago. Considering the importance of aryl sulfones in various pharmaceutical, agrochemical, and materials areas, we embarked on a research program aimed at the development of an alternative, more efficient palladium-catalyzed method for sulfonylation. We postulated that the inconvenient reaction conditions utilized in the traditional sulfone synthesis might be due to the impediment of a sulfinate ligand in the oxidative addition of the palladium center. Thus, we proposed a change of the oxidative addition pathway to involve the formation of an aryl radical intermediate by using visible light activation, which might provide rapid access to the palladium sulfinato complex. Based on this mechanistic proposition, our investigations led to the discovery of a visible-light-activated palladium-catalyzed sulfonylation reaction (**Chapter 5**). Preliminary mechanistic studies hinted at the involvement of a radical intermediate in the cross-coupling process. An alternative mechanism is also proposed which involves a one-electron oxidative addition to be responsible for electron transfer mediated radical formation.

Keyword: photocatalyst, C–H functionalization, aniline, cross-coupling, nickel, palladium, sulfone
Student Number: 2013-20261

Table of Contents

List of Figures

List of Schemes

List of Tables

List of Abbreviations

Ac	acetyl
Ar	generic aryl substituent
BINAP	2,2'-bis(diphenylphosphaneyl)-1,1'-binaphthalene
BIPHEP	2,2'-bis(diphenylphosphaneyl)-1,1'-biphenyl
Boc	*tert*-butoxycarbonyl
bpy	2,2'-bipyridine
Bs	benzenesulfonyl
Bz	benzoyl
CFL	compact fluorescent lamp
cod	cyclooctadiene
DABSO	1,4-Diazabicyclo[2.2.2]octane bis(sulfur dioxide) adduct
DBU	1,8-diazabicyclo(5.4.0)undec-7-ene
DCM	dichloromethane
dF(CF3)ppy	2-(2,4-difluorophenyl)-5-(trifluoromethyl)pyridine
dF(Me)ppy	2-(2,4-difluorophenyl)-5-(methyl)pyridine
dFppy	2-(2,4-difluorophenyl)pyridine
DIPEA	diisopropylethylamine
DMA	dimethylacetamide
DMAP	4-dimethylaminopyridine
DMF	dimethylformamide
DMSO	dimethylsulfoxide

dtbbpy	4,4’-di-tert-butyl-2,2'-bipyridine
EAS	electrophilic aromatic substitution
EI	electron impact
ESI	electrospray ionization
Et	ethyl
FAB	fast atom bombardment
FRET	Förster resonance energy transfer
HEH	Hantzsch ester
HLF	Hofmann-Löffler-Freytag
HOMO	highest occupied molecular orbital
HRMS	high-resolution mass spectrometry
***i*-Pr**	isopropyl
IR	infrared
ISC	intersystem crossing
L	generic ligand
LED	light emitting diode
LUMO	lowest unoccupied molecular orbital
M	generic metal
MC	metal centered
MC	metal centered
Me	methyl
MeCN	acetonitrile

MLCT	metal to ligand charge transfer
Ms	methanesulfonyl
MTBD	7-methyl-1,5,7-triazabicyclo[4.4.0]dec-5-ene
NMR	nuclear magnetic resonance
Ph	phenyl
phen	1,10-phenanthroline
ppy	2-phenylpyridine
rt	room temperature
SCE	saturated calomel electrode
SET	single electron transfer
TBAI	tetrabutylammonium iodide
***t*-Bu**	*tert*-Bu
TEA	triethylamine
TEMPO	(2,2,6,6-Tetramethylpiperidin-1-yl)oxyl
TFA	trifluoroacetic acid
THF	tetrahydrofuran
TIPS	triisopropylsilyl
TLC	thin-layer chromatography
TMEDA	tetramethylethylenediamine
TMG	1,1,3,3-tetramethylguanidine
Ts	*p*-toluenesulfonyl
TTET	triplet-triplet energy transfer

UV	ultraviolet
X	generic anionic ligand
Xantphos	4,5-Bis(diphenylphosphino)-9,9-dimethylxanthene

Chapter 1. Visible-Light-Activated Ruthenium and Iridium Photocatalysts

1.1. Brief Introduction to Photochemical Organic Reactions

A fundamental principle in the development of a useful organic transformation is selective activation of a molecule to elicit the desired reactivity that can address issues unresolvable by previous approaches. Enlisting new types of reactive organic or organometallic intermediates has been widely studied on this purpose and showed remarkable success in chemical synthesis.

Approaches to access reactive intermediates may be classified into two major categories – thermal and photochemical activations. Thermal activation relies on the inherent reactivity of compounds in their ground states and adjusting the HOMO-LUMO (highest occupied molecular orbital-lowest occupied molecular orbital) energy level often facilitates bond-forming or bond-breaking events. Endeavors to enhance the reactivity in this way has led to successful development of a variety of catalyst systems, such as Brøsted/Lewis acid catalysts, organocatalysts, and organometallic catalysts, broadening the synthetic scope of otherwise unreactive substrates. The photochemical activation has also received much attention as it renders alternative activation modes by taking advantage of transient excited states (**Figure 1.1**).[1] The torquoselectivity of electrocyclization reactions governed by the Woodward-Hoffmann selection rule is an illustrative example of the paradigmatic reactivity difference between thermal and photochemical reactions (**Figure 1.1a**).[2] The excited state molecules take part in electron transfer, hydrogen atom abstraction, and photodissociation, which may be of significant utility in organic synthesis (**Figure 1.1b, 1.1c, and 1.1d**).[3] The inefficient light absorption of most organic and organometallic molecules, unfortunately, prevents the general use of this unique activation strategy, while necessitating inconvenient, and often expensive, high-energy light sources that might hamper all too important selective activation of specific functional groups.

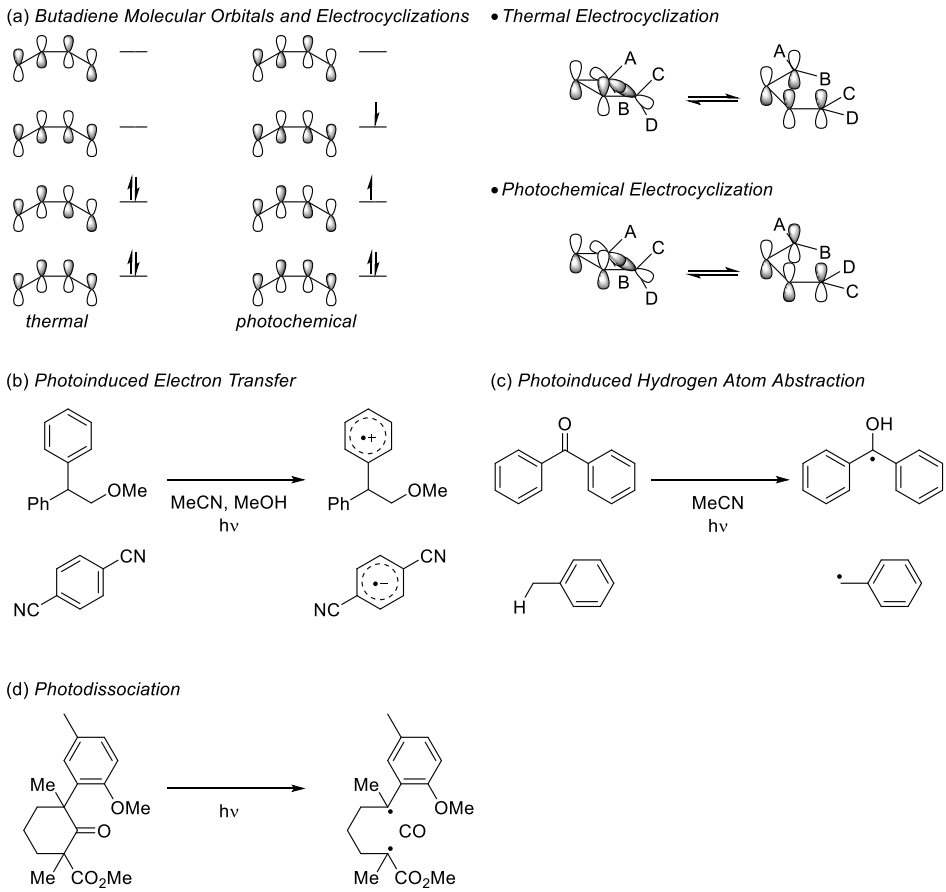

Figure 1.1. Photochemical Reaction Pathways

Photon absorbing catalysts may serve as photosensitized intermediates, efficiently converting photonic energy into a chemical form in a controlled manner. After the light-harvesting process, the excited photocatalyst effects an electronic modification of a broad array of organic substrates, a feature that can be utilized for new reaction development. In particular, visible light as a tool for initiating photochemical reactions should be the most sustainable way for photochemical engineering of reactivity owing to its abundance, mild, and green nature.

1.2. Ruthenium and Iridium Photocatalysts in Organic Synthesis

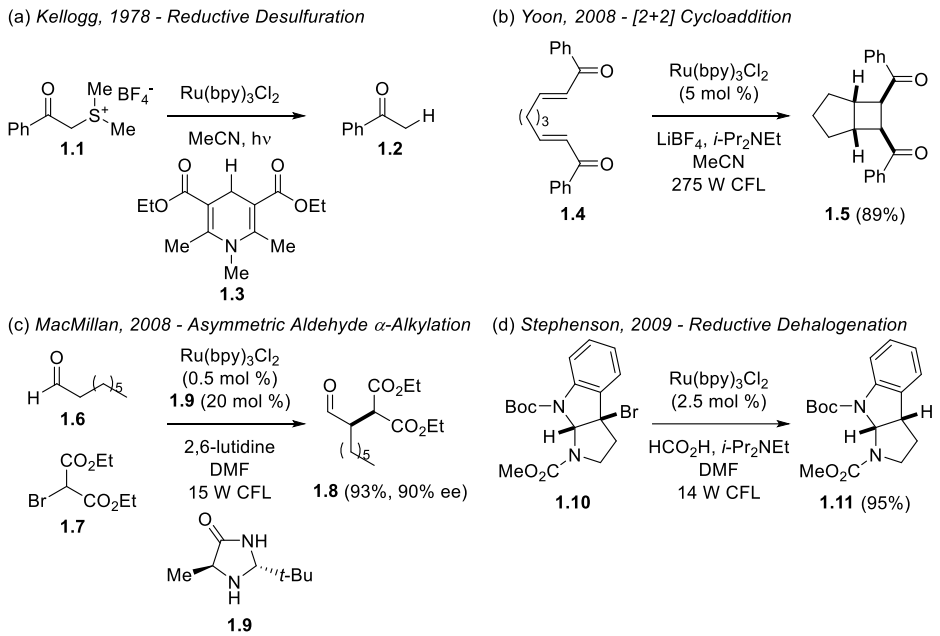

Scheme 1.1. Seminal Reports of Cyclometalated Photocatalysts in Organic Synthesis

Among various photocatalysts, polypyridyl ruthenium and iridium complexes have been widely utilized in visible-light-mediated organic reactions, leading to the remarkable growth of visible-light-driven organic synthesis for the past decade.[4] These catalysts, after absorbing light energy, activate molecules by either single electron transfer (SET) or triplet-triplet energy transfer (TTET) to generate reactive organic or organometallic intermediates useful for various organic reactions. In 1978, Kellogg reported the first example making use of these cyclometalated complexes in the reduction of sulfonium salt **1.1** to ketone **1.2** by employing Hantzsch ester **1.3** as a hydrogen and electron donor (**Scheme 1.1a**).[5] This pioneering work, however, did not immediately lead to the development of visible-light photoredox systems for use in organic synthesis, while most of the applications were focused on the organic light emitting diodes (OLEDs), photovoltaic cells, carbon dioxide reduction, and hydrogen production from water.[6] In 2008 and 2009, Yoon, MacMillan, and Stephenson illustrated new applications of $Ru(bpy)_3^{2+}$, revisiting this old catalyst for use in organic synthesis (**Scheme 1.1b, 1.1c, and 1.1d**).[7] The

Yoon group reported [2+2] cycloaddition of enones **1.4** to afford cyclobutane **1.5**.[7a] Concurrently, the MacMillan group disclosed α-alkylation of aldehyde **1.6** via combination of a photoredox and organocatalyst **1.9**, which afforded enantioenriched aldehyde **1.8**.[7b] Stephenson also demonstrated a mild radical reduction of tertiary alkyl halide **1.10** to indoline **1.11**.[7c] These examples were exciting discoveries, as mild catalysis under visible light irradiation enabled challenging bond activation. The breakthrough made by these seminal studies prompted the synthetic community to consider visible-light-activated ruthenium and iridium polypyriyl complexes as sustainable and powerful tools in organic synthesis.

1.3. Photochemical Properties of Ruthenium and Iridium Polypyridyl Complexes

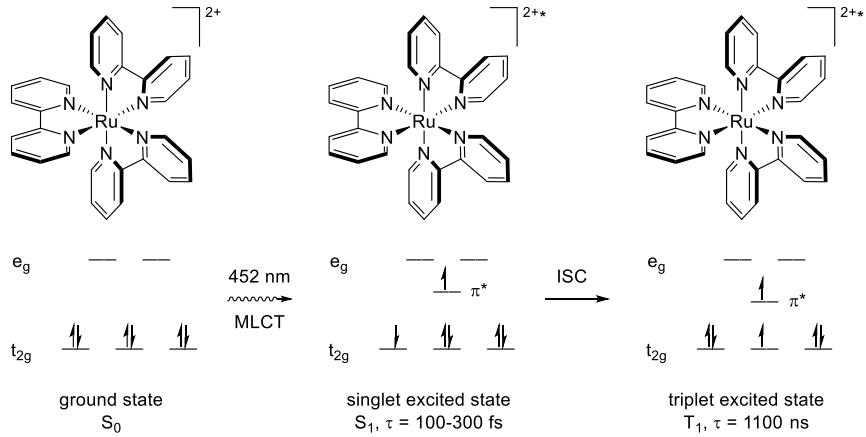

Figure 1.2. Excitation of $Ru(bpy)_3^{2+}$ using Visible Light

The usefulness of ruthenium and iridium photocatalysts in visible-light mediated organic transformations comes from their photochemical behavior after light irradiation (**Figure 1.2**). In the case of $Ru(bpy)_3^{2+}$, for instance, light energy is converted into chemical energy through metal to ligand charge transfer (MLCT) that gives an electron from the metal to the ligand π^* orbital forming a relatively short-lived (100-300 fs) singlet-excited MLCT complex. After the intersystem crossing (ISC), the complex turns into a relatively long-lived (1100 ns) triplet-excited MLCT complex inverting the spin state of an electron by spin-orbit coupling.[8] In its triplet-excited state, the photocatalyst possesses a lifespan of 1100 ns that is long enough to interact with molecules in an intermolecular fashion. The catalyst in a long-lived state can generate radical ions or triplet-excited intermediates from organic substrates either by SET or TTET.

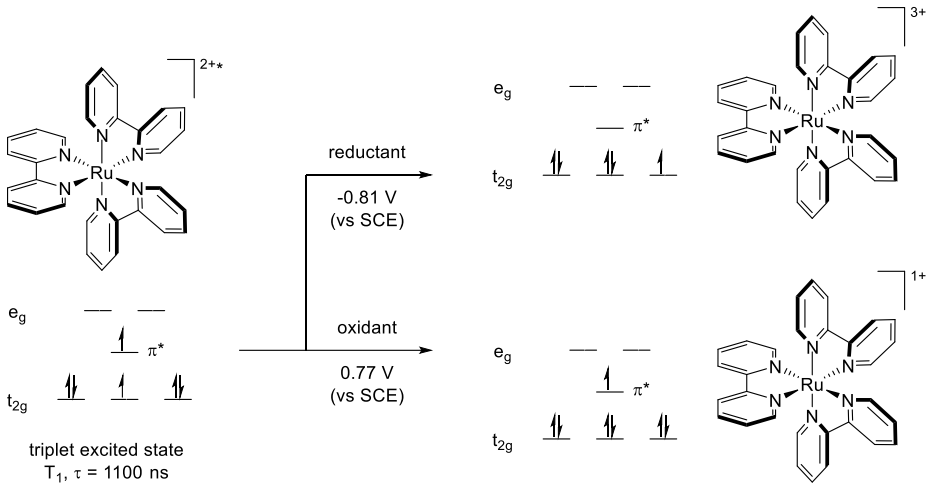

Figure 1.3. Single Electron Transfer of ^{3}MLCT Ru(bpy)$_3^{2+}$ Complex

Organic synthesis using photoredox catalysis has flourished presumably thanks to the unique SET process enabled by photocatalysts. As a result of the dominant MLCT process by light activation of Ru(bpy)$_3^{2+}$, the bpy portion has the high electron density and the metal center becomes electron deficient, causing the highest singly occupied molecular orbital (HSOMO, π*) to be positioned on the bpy moiety with the lowest singly unoccupied molecular orbital (LSUMO, t_{2g}) at the metal center. Owing to the spatial distribution of HSOMO and LSUMO, the bpy ligand can be readily oxidized, and the Ru center may be reduced by other molecules. As a consequence, the ^{3}MLCT complex can act as both strong single electron reductant ($E_{1/2}$ = -0.81 V vs. SCE) and strong oxidant ($E_{1/2}$ = +0.77 V vs. SCE). This feature enables facile conversion of diverse organic molecules into ionic radical species, rendering a reaction system capable of oxidizing and reducing at the same time, which is infeasible with thermal redox-active catalysts (**Figure 1.3**).[8a]

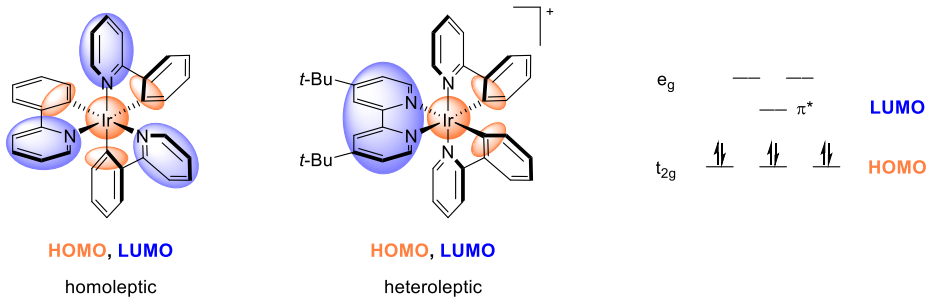

Figure 1.4. Simplified HOMO and LUMO of Ground-State Iridium Complexes

Electrochemical properties of a photocatalyst lend themselves to the essential parameters in designing new reactions, particularly those driven by the SET mechanism, as fine-tuning of ligands on iridium and ruthenium complexes broadens reduction potentials that can be accessed by photocatalysts. The range of the reduction potential available with the ruthenium metal center, however, is rather narrow on account of thermally accessible triplet excited states (^{3}MC) by d→d transition which decomposes the metal complex.[9] Iridium catalysts, on the other hand, are more widely utilized in reactions involving more challenging redox processes. They can adopt ppy (2-phenylpyridine) type ligands which are not compatible with ruthenium photocatalysts.[10] The incorporation of ppy ligands in the cyclometalated structure allows for iridium photocatalysts to adopt two distinct structures – homoleptic and heteroleptic (**Figure 1.4**). In homoleptic complexes, the highly electron-donating ppy ligand makes the catalyst more reducing, and the non-symmetric structure allows modification of electron density in HOMO and LUMO separately, thus enabling adjustment of the reduction potential of one ligand without too much affecting the other.[11a] In heteroleptic complexes, even more dramatic spatial detachment of HOMO from LUMO in the ppy ligand vis-à-vis the bpy ligand allows for the modification of redox potentials to produce more oxidizing cationic iridium photocatalysts.[11b]

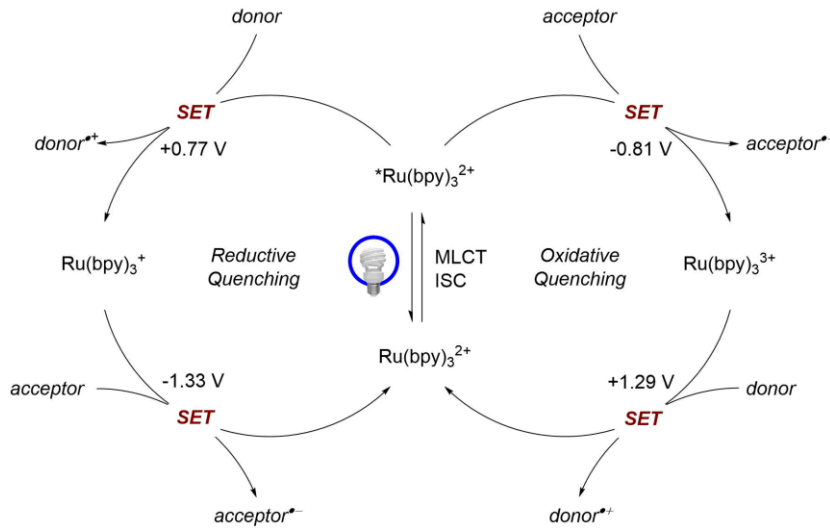

Figure 1.5. Oxidative and Reductive Quenching Cycles of $Ru(bpy)_3^{2+}$

Engaging organic molecules in reactions using an SET process of the visible-light photoredox catalysis entails rational design of a catalytic cycle. An excited photoredox catalyst undergoes either reductive quenching or oxidative quenching by a donor or an acceptor molecule, and an electron transfer event must be accompanied by an additional compensating electron transfer to complete a catalytic cycle (**Figure 1.5**). As an illustration, the excited $Ru(bpy)_3^{2+}$ in a reductive quenching cycle accepts an electron from a donor molecule to form a $Ru(bpy)_3^{1+}$ species ($E_{1/2}$ [$*Ru^{2+}/Ru^{1+}$] = +0.77 V vs. SCE) and this reduced ruthenium complex gives off an electron ($E_{1/2}$ [Ru^{2+}/Ru^{1+}] = -1.33 V vs. SCE) to an acceptor, closing a catalytic cycle.[8a] Alternatively, in an oxidative quenching cycle, an electron is provided to an acceptor at the beginning ($E_{1/2}$ [$Ru^{3+}/*Ru^{2+}$] = -0.81 V vs. SCE), and the oxidized ruthenium complex gets an electron from a donor to go back to the ground state $Ru(bpy)_3^{2+}$ ($E_{1/2}$ [Ru^{3+}/Ru^{2+}] = +1.29 V vs. SCE).[8a] In the SET processes, the reduction potential values of catalysts, donors, and acceptors govern the thermodynamics and kinetics of electron transfer reactions. Thermodynamic feasibility and rate of electron transfer can be approximated by the Rehm-Weller equation and Marcus theory.[12]

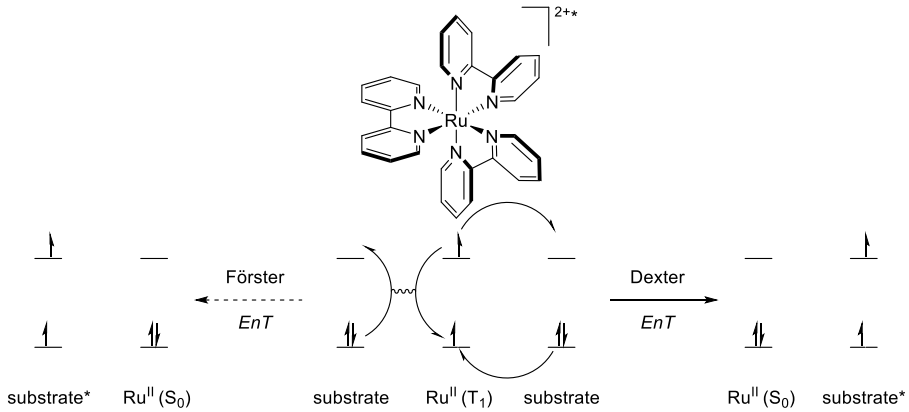

Figure 1.6. Förster Resonance and Dexter Energy Transfer

Another fundamental reactivity that can be accessed by a ^{3}MLCT complex is the excitation of other molecules through energy transfer, a process in which change in energy occurs between two chromophores. More specifically, an excited donor molecule goes to a lower-lying state by giving its energy to an acceptor molecule through a non-radiative pathway, for which there have been two proposed mechanisms – Förster energy transfer and Dexter energy transfer (**Figure 1.6**).[13] Förster energy transfer (Förster resonance energy transfer, FRET) relies on the coulombic interaction between two molecular orbitals. Electronic oscillation of a donor molecule interacts "through space" with a ground-state acceptor molecule by the charge repulsion resulting in electronic oscillation in the acceptor molecule, and this allows the acceptor molecule to go to its excited singlet state. However, FRET is a forbidden process for ^{3}MLCT complexes as it requires spatially-separated two spin inversions which are a violation of Wigner's spin conservation rules.[14] Dexter energy transfer mechanism, on the other hand, happens through two sequential electron transfer events by a "physical contact" between two chromophores. The overlap of molecular orbitals between excited and ground-state molecules allows the simultaneous exchange of two electrons, transferring the triplet energy. Two factors affect the rate of energy transfer events – diffusion rate and overlap integral J of the normalized donor emission spectrum and the normalized absorption spectrum of the acceptor. The diffusion rate takes control

over the process if the energy transfer in a collision complex is sufficiently fast. However, in the opposite case, the kinetics of energy transfer in a collision complex becomes the rate-determining step, and the overlap integral *J* determines the rate of a reaction.

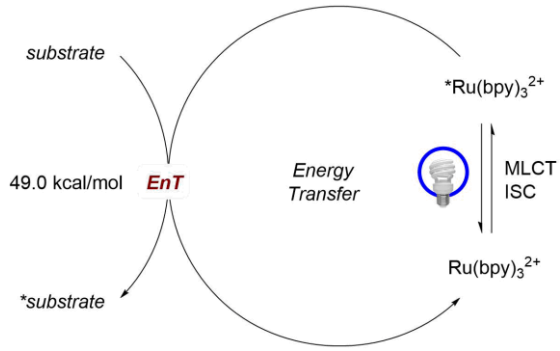

Figure 1.7. Energy Transfer Catalytic Cycle of $Ru(bpy)_3^{2+}$

Photocatalysts can induce the formation of triplet-excited organic or inorganic intermediates in a reaction system through TTET, thus offering opportunities for new reaction development. Acting as a light-harvesting antenna, for instance, $Ru(bpy)_3^{2+}$ delivers its triplet energy (49.0 kcal/mol) to an energy accepting molecule generating another photosensitized organic or inorganic architectures in a reaction system and goes back to its ground state to close a catalytic cycle (**Figure 1.7**).[8a, 15] By charging the light harvesting role to a catalyst that can be turned into a triplet photosensitizer, this approach can bypass the barriers for intersystem crossing processes of most compounds.

1.4. Conclusion

Photocatalysts permit the use of photochemical activation for the development of new methodologies that can offer an alternative means for the thermal activation strategy. The novel intermediates in photochemical reactions enter on reaction pathways distinct from those of ground-state intermediates, thus providing opportunities to formulate new synthetic methodologies with additional chemical dimensions. Ruthenium and iridium polypyridyl complexes, in particular, have made their ways to elegant use in organic synthesis through elaborate ligand tuning that provides a broad range of redox potentials and triplet energies. With a single reaction system oxidizing and reducing at the same time under mild visible light irradiation, the unique potential of the ruthenium and iridium photoredox system lies in the ability to modulate oxidative and reductive quenching cycles.

1.5. References

1) For a review, see Hoffmann, N. *Chem. Rev.* **2008,** *108*, 1052.

2) Hoffmann, R.; Woodward, R. B. *J. Am. Chem. Soc.* **1965,** *87*, 2046.

3) (a) Arnold, D. R.; Maroulis, A. J. *J. Am. Chem. Soc.* **1976,** *98*, 5931. (b) Wagner, P. J.; Truman, R. J.; Puchalski, A. E.; Wake, R. *J. Am. Chem. Soc.* **1986,** *108*, 7727. (c) Ng, D.; Yang, Z.; Garcia-Garibay, M. A. *Org. Lett.* **2004,** *6*, 645.

4) (a) Shaw, M. H.; Twilton, J.; MacMillan, D. W. C. *J. Org. Chem* **2016,** *81*, 6898. (b) Strieth-Kalthoff, F.; James, M. J.; Teders, M.; Pitzer, L.; Glorius, F. *Chem. Soc. Rev.* **2018**.

5) Hedstrand, D. M.; Kruizinga, W. H.; Kellogg, R. M. *Tetrahedron Lett.* **1978,** *19*, 1255.

6) (a) Meyer, T. J. *Acc. Chem. Res.* **1989,** *22*, 163. (b) Kalyanasundaram, K.; Grätzel, M. *Coord. Chem. Rev.* **1998,** *177*, 347. (c) Takeda, H.; Ishitani, O. *Coord. Chem. Rev.* **2010,** *254*, 346.

7) (a) Ischay, M. A.; Anzovino, M. E.; Du, J.; Yoon, T. P. *J. Am. Chem. Soc.* **2008,** *130*, 12886. (b) Nicewicz, D. A.; MacMillan, D. W. C. *Science* **2008,** *322*, 77. (c) Narayanam, J. M. R.; Tucker, J. W.; Stephenson, C. R. J. *J. Am. Chem. Soc.* **2009,** *131*, 8756.

8) (a) Wrighton, M.; Markham, J. *J. Phys. Chem.* **1973,** *77*, 3042. (b) Demas, J. N.; Harris, E. W.; McBride, R. P. *J. Am. Chem. Soc.* **1977,** *99*, 3547. (c) Ding, Z.; Wellington, R. G.; Brevet, P. F.; Girault, H. H. *J. Phys. Chem.* **1996,** *100*, 10658. For book chapters see: (d) Campagna, S.; Puntoriero, F.; Nastasi, F.; Bergamini, G.; Balzani, V. Photochemistry and Photophysics of Coordination Compounds: Ruthenium. In *Photochemistry and Photophysics of Coordination Compounds I*, Balzani, V.; Campagna, S., Eds. Springer Berlin Heidelberg: Berlin, Heidelberg, 2007. (e) Flamigni, L.; Barbieri, A.; Sabatini, C.; Ventura, B.; Barigelletti, F. Photochemistry and Photophysics of Coordination Compounds: Iridium. In *Photochemistry and Photophysics of Coordination Compounds II*, Balzani, V.; Campagna, S., Eds. Springer Berlin Heidelberg: Berlin, Heidelberg, 2007. For a review, see (f) Tucker, J. W.; Stephenson, C. R. J. *J. Org. Chem* **2012,** *77*, 1617.

9) Durham, B.; Caspar, J. V.; Nagle, J. K.; Meyer, T. J. *J. Am. Chem. Soc.* **1982,** *104*, 4803.

10) (a) Li, E. Y.; Cheng, Y.-M.; Hsu, C.-C.; Chou, P.-T.; Lee, G.-H.; Lin, I. H.; Chi, Y.; Liu, C.-S. *Inorg. Chem.* **2006,** *45*, 8041. (b) Bomben, P. G.; Robson, K. C. D.; Sedach, P. A.; Berlinguette, C. P. *Inorg. Chem.* **2009,** *48*, 9631.

11) (a) Tamayo, A. B.; Alleyne, B. D.; Djurovich, P. I.; Lamansky, S.; Tsyba, I.; Ho, N. N.; Bau, R.; Thompson, M. E. *J. Am. Chem. Soc.* **2003,** *125*, 7377. (b) Lowry, M. S.; Goldsmith, J. I.; Slinker, J. D.; Rohl, R.; Pascal, R. A.; Malliaras, G. G.; Bernhard, S. *Chem. Mater.* **2005,** *17*, 5712. For summarized electrochemical properties and synthesis, see (c) Singh, A.; Teegardin, K.; Kelly, M.; Prasad, K. S.; Krishnan, S.; Weaver, J. D. *J. Organomet. Chem.* **2015,** *776*, 51.

12) (a) Marcus, R. A. *J. Chem. Phys.* **1956,** *24*, 966. (b) Rehm, D.; Weller, A. *Isr. J. Chem.* **1970,** *8*, 259. (c) M D Newton, a.; Sutin, N. *Annu. Rev. Phys. Chem.* **1984,** *35*, 437. (d) Hoffman, M. Z. *J. Phys. Chem.* **1988,** *92*, 3458. (e) Closs, G. L.; Miller, J. R. *Science* **1988,** *240*, 440.

13) (a) Turro, N. J. *Modern molecular photochemistry*. University Science Books: Mill Valley, Cal., **1991**. (b) Balzani, V.; Ceroni, P.; Juris, *A. Photochemistry and photophysics: concepts, research, applications*. Wiley-VCH: Weinheim, **2014**.

14) E. Wigner. *Group theory and applications to quantum mechanics*. Academic Press: San Diego, **1959**.

15) Strieth-Kalthoff, F.; James, M. J.; Teders, M.; Pitzer, L.; Glorius, F. *Chem. Soc. Rev.* **2018,** *47*, 7190.

Chapter 2. Radical C–H Amination of Aromatic Compounds

2.1. Introduction to Nitrogen-Centered Radicals

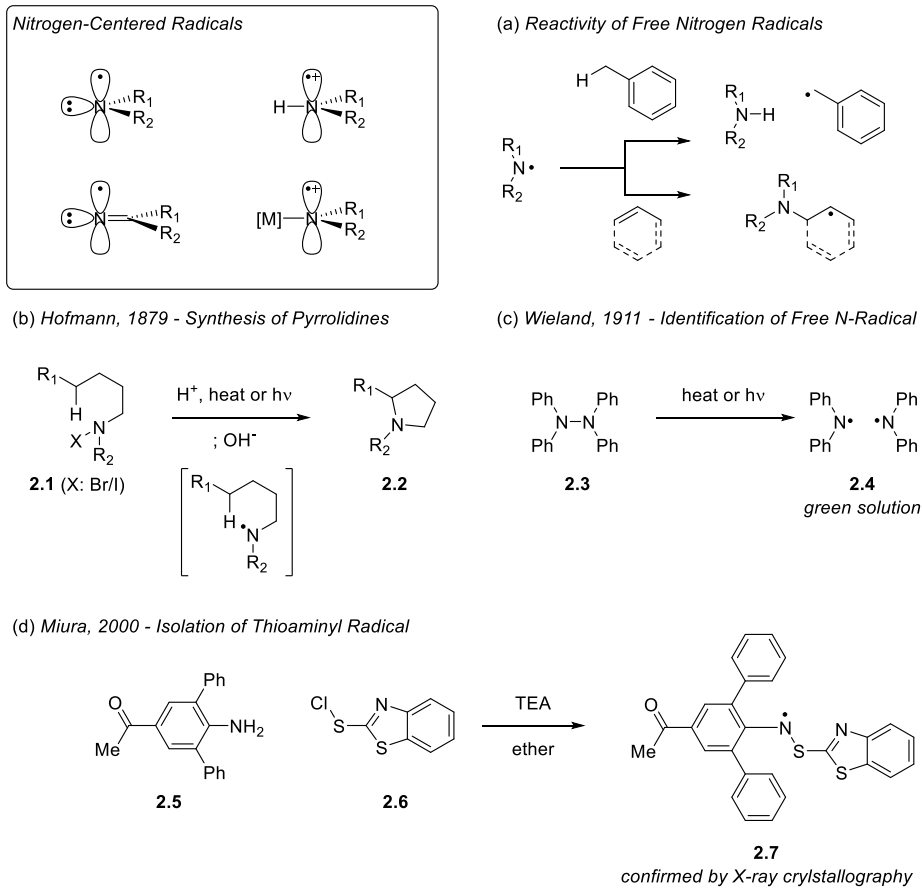

Figure 2.1. Nitrogen-Centered Radicals

Nitrogen radicals are versatile intermediates exhibiting a broad range of reactivity that can be modulated by substituents or coordination states. For example, they participate in hydrogen atom abstraction, addition to electron-rich unsaturated compounds or other bond-forming processes mediated by organometallic complexes (**Figure 2.1**).[1] The nitrogen radical first appeared in the literature more than a century ago as a mediator for the C–H bond activation, as exemplified by the Hofmann-Löffler-Freytag (HLF) reaction (**Figure 2.1b**).[1,2] In 1879, Hofmann disclosed a straightforward synthesis of pyrrolidine **2.2** by photolysis or thermal decomposition of *N*-haloamine **2.1**. After this work, the Wieland group reported in 1911 the first example of a free aminyl radical generated via irradiation or thermolysis of tetraphenyl hydrazines **2.3** forming a green solution of the diphenyl aminyl radical **2.4** (**Figure 2.1c**).[3a] In 2000, Miura and coworkers achieved the first isolation of *N*-centered radical **2.7** during a reaction between sterically hindered aniline **2.5** and sulfenyl chloride **2.6** (**Figure 2.1d**) which was confirmed by X-ray crystallographic analysis and magnetic studies.[3b]

Even with its early emergence in the history of organic chemistry, the nitrogen radical had received relatively little attention as compared with carbon-centered radicals. However, as understanding of the factors governing chemical properties of radicals, such as polarity, bond dissociation energies, and kinetics, became sophisticated, explorations of the N-radicals for use in organic synthesis were initiated.[4] Many catalytic reactions utilizing nitrogen-centered radicals as key intermediates have become available, including an array of reactions under photoredox catalysis.[5] By overcoming two demanding electron transfers using an excited-state redox-active intermediate, the visible-light activated redox catalysts provided new concepts in nitrogen radical-mediated transformations.

2.2. Visible-Light-Mediated Formation of Nitrogen Radicals

The most notable aspect in the generation of nitrogen-centered radicals under visible-light photoredox catalysis is the mild catalytic platform on which various precursors can be selectively activated.[5] Compared to traditional protocols relying on high-temperature thermolysis, UV photolysis, and stoichiometric redox agents, the electron transfer-mediated radical initiation approach offers a sustainable means for performing nitrogen radical-mediated reactions.

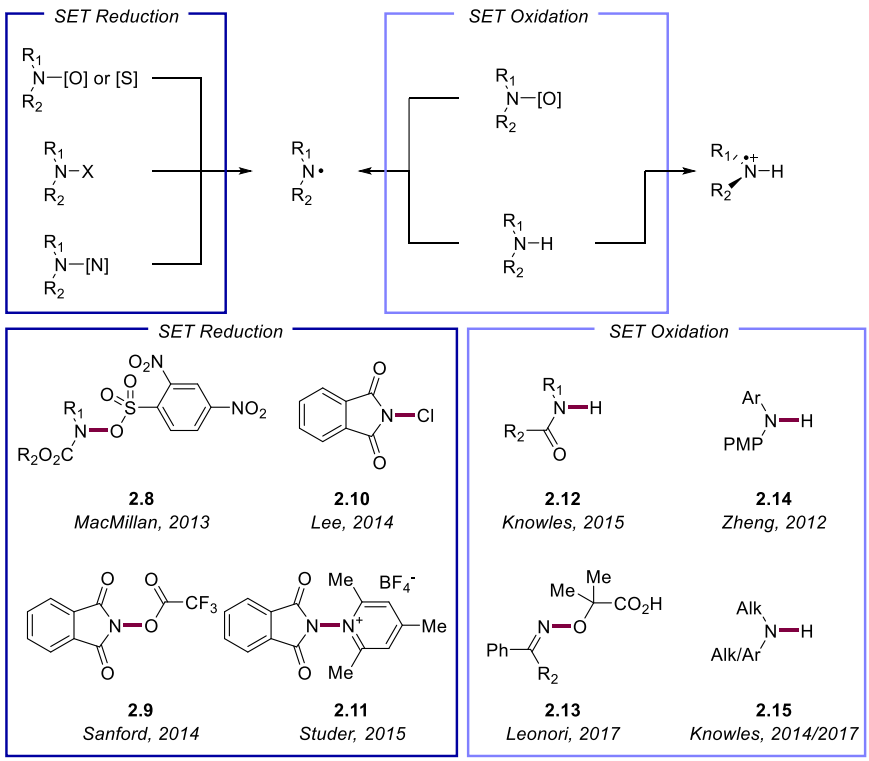

Figure 2.2. Nitrogen Radical Synthesis and Precursors Using Electron Transfer

There are two ways for generation of nitrogen-centered radicals using SET process; 1) reduction of N–heteroatom bonds to induce mesolytic cleavage of the radical anion, and 2) oxidation of amine-containing molecules (**Figure 2.2**). In 2013, MacMillan and coworkers reported a sulfonamidyl radical-mediated organic transformation using one-electron reduction of the N–O bond-containing compound **2.8**.[6] Merging asymmetric

enamine catalysis with photocatalytic sulfonamidyl radical generation, an efficient method was developed for asymmetric α-amination of aldehydes. In this work, incorporation of an electron-deficient sulfonate as a leaving group in the parent nitrogen-containing molecules successfully modulated the reduction potential so that the efficient photocatalytic SET process followed by mesolytic cleavage of the N–O bond could occur. In 2014, the Sanford group published a Minisci type amination of aromatics and heteroaromatics using a similar strategy,[7] which employed *N*-acyloxyphthalimide ester **2.9** in a visible-light-driven catalytic cycle for aryl C–H amination. In the same year, the first photocatalytic generation and utilization of an N-centered radical using reductive cleavage of N–halogen bond were reported by the Lee group.[8] Through screening of various potential amine radical precursors, *N*-chlorophthalimide **2.10**, a well-known reagent for chlorination, was determined to be a most efficient imidyl radical precursor which could effect homolytic C–H functionalization of arenes and heteroarenes. Studer pioneered the use of *N*-aminopyridnium salt **2.11**, prepared from commercially available pyrylium salts, as an efficient electron acceptor engendering nitrogen radical.[9]

Oxidative generation of neutral amine radicals, compared to reductive strategies, was slow to evolve in visible-light-mediated photocatalysis. Possible explanations for the late appearance of oxidative approaches are the nitrogen radical center shift to an adjacent $C_{sp}{}^3$ carbon atom, the formation of an iminium, and the high electronic barrier associated with oxidation of secondary amines, especially those proximal to electron withdrawing groups.[10,11] In 2015, Knowles reported a strategy that addressed the thermodynamic and kinetic barriers associated with the SET oxidation using a proton-coupled electron transfer (PCET) approach.[11] The PCET process is a simultaneous transfer of a proton and an electron from the amine substrate to separate acceptor and oxidant molecules, which at times has a lower activation barrier that those of individual proton and electron transfers.[12] Use of the PCET mechanism allowed direct homolytic activation of the N–H bond of amide **2.12** in a carboamination under mild reaction conditions. Leonori and coworkers also

synthesized iminyl radicals through an oxidative strategy involving decarboxylation of pendent carboxylic acid **2.13** and β-fragmentation.[13]

Formation of aminium radical cations from aniline derivatives (**2.14** and **2.15**) was accomplished by Zheng and Knowles, which enabled the generation of protonated nitrogen-centered radicals without employing strong acidic conditions. The protonated amine radicals reacted with olefins to form indoles and azacycles, and the Knowles group also accomplished *anti*-Markovnikov hydroamination of unactivated olefins using aliphatic secondary amines.[14]

The development of neutral nitrogen radical formation from a variety of precursors has led to widespread applications in visible-light-mediated organic transformations. The HLF (Hofmann-Löffler-Freytag) C–H activation strategy led to a mild catalytic platform for the carbon-centered radical generation. Several groups have reported the use of this carbon-centered radical intermediate for C–C and C–heteroatom bond formations.[13,15] A notable breakthrough has been made in the nitrogen-centered radical-mediated aniline synthesis, leading to the development of several new methods for catalytic aromatic amine synthesis using well-designed electron transfer events. The addition of nitrogen radicals to alkenes enabled efficient preparation of C–N containing sp^3-carbon frameworks via a radical polar crossover or a radical-mediated mechanism.[14b,16]

2.3. Nitrogen-Centered Radical-Mediated C–H Imidation of Arenes

The ubiquity of nitrogen-containing organic compounds in a diverse range of areas has provided the synthetic community with undeniable motivation to explore reactive nitrogen intermediates for the efficient synthesis of amine building blocks, in particular, by substituting the most common functional group in organic molecules, the C–H bond.[17] Various approaches based on the use of transition metal complexes, nitrenes, and nitrogen radicals as reactive intermediates have been studied to forge C–N bonds directly from aromatic compounds. However, intermolecular aryl C-H amination for aniline synthesis presents fundamental challenges of functionalizing unactivated aromatic substrates. For example, to achieve a high level of efficiency, the use of an excess amount of arene substrates or a directing group was necessary for the C–H metalation approach which significantly reduced the generality and scope of the reaction.[17] The Minisci type amination utilizing electron-deficient "N•" species has also been a way to install nitrogen groups in unactivated aromatic compounds, but the necessity of inconvenient radical initiation protocols limited the practical application of this chemistry.[1,2,3,18] In light of the drawbacks associated with previous approaches, we decided to develop a new strategy for the aromatic C–H amination by modulating the reactivity of the nitrogen-centered radical using photoredox catalysis.

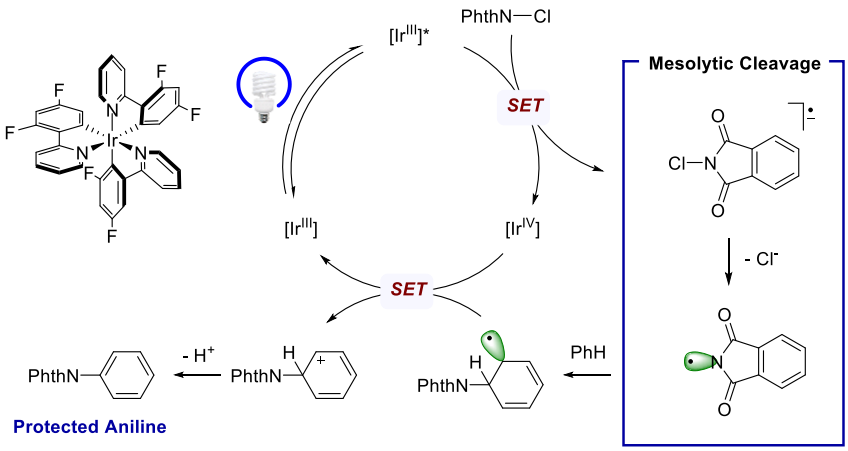

Figure 2.3. Proposed Mechanism for Radical C–H Imidation

Depicted above is the detailed mechanistic picture of our proposal (**Figure 2.3**). We postulated that the one-electron reduction of an N–halogenated molecule using visible-light excited iridium complex would destabilize it to form a radical anion intermediate, subsequently giving rise to a nitrogen-centered radical through mesolytic cleavage. The electron-deficient nitrogen radical might then react with a relatively electron-rich aromatic compound to give a cyclohexadienyl radical intermediate, which would act as an electron donor for the oxidized iridium catalyst to close the catalytic cycle while becoming a carbocation. Deprotonation of the Wheland intermediate would afford the desired product.

2.3.1. Discovery and Optimization of Reaction Conditions

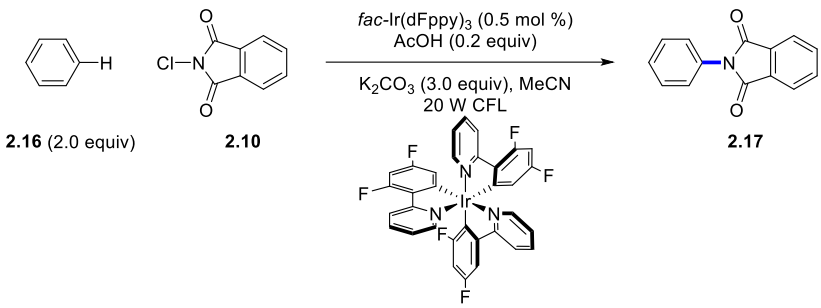

entry	*derivatization from standard reaction conditions*	2.17 (%)
1	none	65
2	*fac*-Ir(ppy)$_3$ instead of *fac*-Ir(dFppy)$_3$	54
3	without AcOH	55
4	TFA instead of AcOH	36
5	Without photocatalyst, visible-light or base	<2
6	*t*-BuOCl (1.0 equiv), *t*-BuOH (1.0 equiv) phthalimide (1.0 equiv) instead of **2.10**	58
7	NaOCl (1.0 equiv), *t*-BuOH (1.0 equiv) AcOH (1.0 equiv), phthalimide (1.0 equiv) instead of **2.10**	52

[a]Yields are determined by the NMR analysis with an internal standard using the general procedure.

Table 2.5. Derivatization of Photocatalytic C–H Imidation Conditions[a]

With the proposed mechanistic picture, we initially investigated this reaction using benzene (**2.16**) and *N*-chlorosuccinimide. Through a series of optimization studies performed by Dr. Hyejin Kim, it became evident that the phthalimide structure and chloride leaving group were essential for the high performance of the reaction. In addition, more oxidizing *fac*-Ir(dFppy)$_3$ ($E_{1/2}$ [Ir^{4+}/Ir^{3+}] = +0.98 V vs. SCE) compared to *fac*-Ir(ppy)$_3$ ($E_{1/2}$ [Ir^{4+}/Ir^{3+}] = +0.78 V vs. SCE) showed better efficiency in this reaction (**Table 2.1**, *entries* 1, and 2).[19] Still, more experiments would seems necessary, as the radical addition step appeared to be reversible with the possibility of existing a catalytic dead end owing to the transient nature of the electron deficient *N*-radical.[1] Addition of a small amount of acetic acid showed a 10% yield increase of the product, but trifluoroacetic acid had a deleterious effect (*entry* 3, and 4). The increase in yield with an acetic acid additive was reproduced with other substrates as well. While 5-10% yield enhancement took place, however, no plausible hypothesis could be advanced for these observations. Photocatalyst, visible light,

and a base were crucial ingredients for this imidation chemistry (*entry* 5). Also, the in situ generation of *N*-chlorophthalimide using *t*-BuOCl or NaOCl was feasible for this protocol without significant loss of reaction efficiency (*entries* 6, and 7).[20] With the optimal conditions in hand, we sought to examine the scope of this reaction.

2.3.2. Reaction Scope

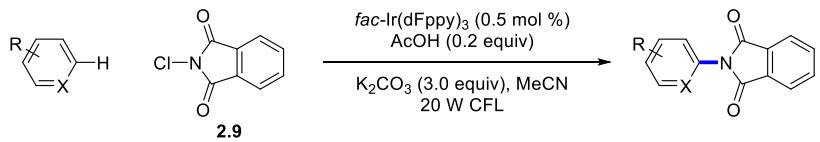

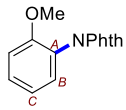

2.18 41% (15:1:13)

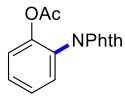

2.19 46% (3.2:2:1)

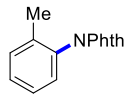

2.20 47% (2.5:1:1.3)

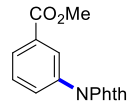

2.21 60% (7.2:11:4)

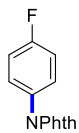

2.22 47% (7.4:4:9.3)

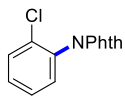

2.23 60% (2.3:1:2)

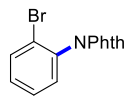

2.24 43% (3.3:2:2.7)

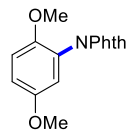

2.25 44%[b]

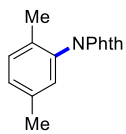

2.26 50%[b]

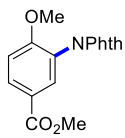

2.27 48%

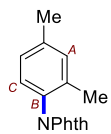

2.28 72%[b] (4:9:1)

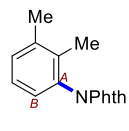

2.29 34%[b] (1:1)

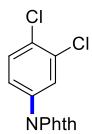

2.30 37% (4:4.9)

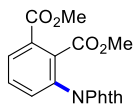

2.31 27% (1:1)

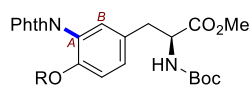

2.32 46%[b] (7.1:1, R = Me)
2.33 36% (1.1:1, R = Ac)

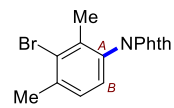

2.34 47% (4:1)

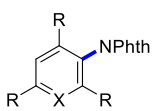

2.35 52% (R = Me, X = C)
2.36 10% (R = *t*-Bu, X = C)
2.37 45%[b] (R = Me, X = N)

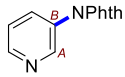

2.38 38% (1:2.1)

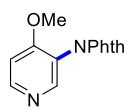

2.39 40%[b]

2.40 50%[b] (R = Me)
2.41 29%[b] (R = *t*-Bu)

[a]Yields are determined by the isolated products using the general procedure unless otherwise noticed. [b]Arene (0.5 mmol), and *N*-chlorophthalimide (1.0 mmol).

Table 6.2. Scope of C–H Imidation with 6-Membered Aromatics[a]

The iridium photoredox-catalyzed C–H imidation successfully employed a broad range of 6-membered aromatics and heteroaromatics (**Table 2.2**). Due to the electrophilic character of the nitrogen radical, regioselectivity of this reaction followed the trends noted in electrophilic aromatic substitution (EAS) reactions. Mono-substituted electron-rich and electron-poor aromatic substrates both provided good yields. Arenes with an ortho/para-director predominantly formed ortho-products (**2.18**-**2.20**, and **2.23**-**2.24**). In the presence of an electron-withdrawing group, the reaction afforded a meta-substituted product (**2.21**) as the major product. The fluoride substituent showed a slight preference for para-substitution (**2.22**), which could be explained by the inductive effect of this highly electronegative element. Disubstituted aromatics were also good coupling partners (**2.25**-**2.31**), albeit the efficiency dropped to a certain degree with two deactivating groups (**2.30**, and **2.31**). As an illustration of complex aniline synthesis, we conducted imidation of tyrosine derivatives possessing diverse functional groups which gave moderate yields of the products (**2.32**, and **2.33**). Pyridines showed a preference for 3-substitution in this amination (**2.37**-**2.41**). Interestingly, high steric congestion, such as tri-substitution and *t*-Bu group in substrates, was tolerated to a certain level (**2.35**-**2.37**, and **2.41**).

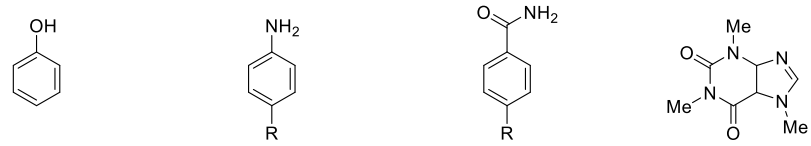

2.42

2.43 R: Cl
2.44 R: OMe

2.45 R: Cl
2.46 R: OMe

2.47

2.48 R = NAc
2.49 R = O

2.50 R = NH
2.51 R = O
2.52 R = S

2.53

2.54 R = H
2.55 R = Br

Table 2.7. Unsuccessful Coupling Partners of C–H Imidation[a]

The established reaction conditions were incompatible with the arenes described in **Table 2.3**. Substrates with a protic group (**2.42**-**2.46**) and fused heteroaromatics (**2.47**-**2.55**) were not tolerated due to the decomposition of substrates and imidation reagents caused by a competitive thermal chlorination process. The chlorinated compounds could be isolated as the major products in a few cases (**2.47**, and **2.54**).

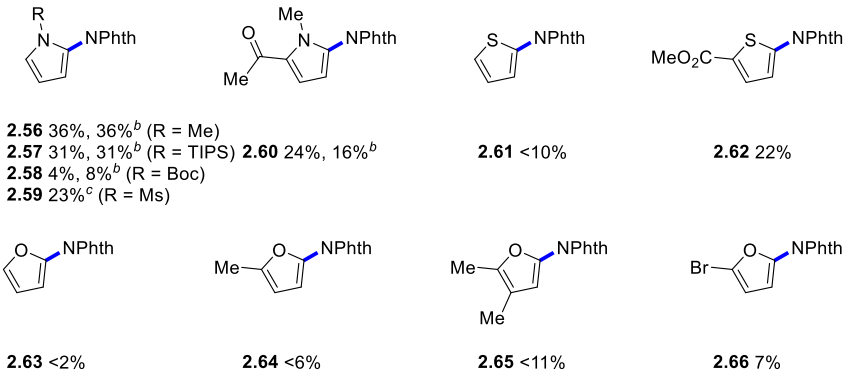

2.56 36%, 36%[b] (R = Me)
2.57 31%, 31%[b] (R = TIPS) **2.60** 24%, 16%[b]
2.58 4%, 8%[b] (R = Boc)
2.59 23%[c] (R = Ms)

2.61 <10%

2.62 22%

2.63 <2%

2.64 <6%

2.65 <11%

2.66 7%

[a]Yields are determined by the isolated products using the general procedure. [b]Without *fac*-Ir(dFppy)$_3$. [c]using 5 mol % *fac*-Ir(dFppy)$_3$

Table 2.8. Scope of C–H Imidation with 5-Membered Heterocycles[a]

For electron rich 5-membered heterocycles, poor yields were generally observed (**Table 2.4**). It was noteworthy that imidated compounds were formed even in the absence of photocatalyst with similar efficiency (**2.56-2.58**). Although more detailed studies are necessary, one plausible explanation for this observation might be the favorable formation of a visible-light-active charge-transfer complex with electron-rich pyrroles. Like previous observations, decomposition of reactants by thermal chlorination could also be responsible for the poor efficiency in these reactions.

2.3.3. Photoredox-Catalyzed C–H Amination of Arenes

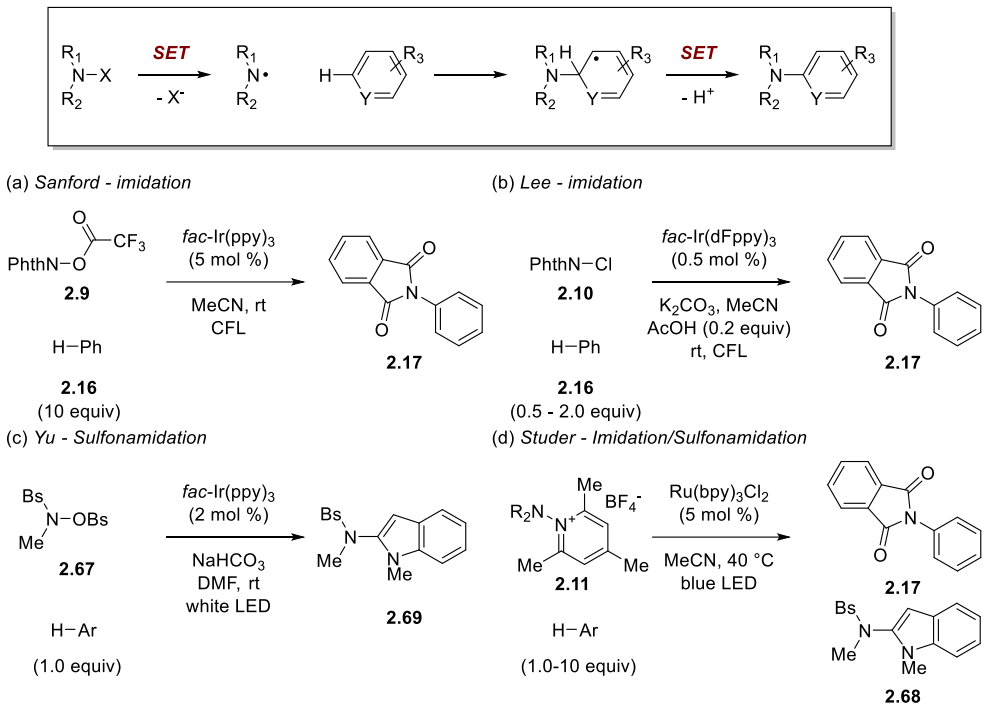

Scheme 2.1. Photoredox-Catalyzed C–H Amination of Arenes

The approach based on reductive cleavage of N–X bonds was also found to be useful in the functionalization of unactivated aromatic compounds by other groups as well (**Scheme 2.1**).[5] The efficiency of this strategy stemmed from the redox-neutral nature of radical C–H amination strategy as the cyclohexadienyl radical after the formation of C–N bonds can serve as a reductant for oxidized photocatalysts. Since Sanford's seminal report, many groups made attempts to improve this strategy.[7] Our protocol dramatically decreased the amount of arene, even using the arene as a limiting reagent in some cases.[8] Shortly after disclosure of our imidation method, Yu and Studer broadened the scope of amines.[9,21] Also, Studer's work employed a less reducing photocatalyst, with pyridinium salts **2.11** as radical precursors, although the catalyst loading was high. The homolytic C-H functionalization under mild visible-light irradiation conditions constitutes a sustainable platform for C–H amination chemistry, offering an alternative to the traditional nitration requiring harsh

reaction conditions.

2.4. Conclusion

Visible-light photoredox catalysis has emerged as a powerful tool for generating nitrogen-centered radicals, a breakthrough in improving traditional approaches for amine radical formation requiring harsh conditions. Thanks to the unique nature of electron transfer catalysis, remarkable progress has been made in nitrogen radical-mediated chemistry. We have developed a protocol based on N-radical generation via homolytic activation of an N–Cl bond for mild catalytic aniline synthesis from various aromatic compounds, a valuable transformation considering the widespread utility of anilines in organic synthesis. The use of catalytic iridium activated under visible-light irradiation proved highly efficient for generating a phthalimidyl *N*-radical from easily accessed *N*-chlorophthalimide and inducing aryl C-H imidation. Also developed is the one-pot protocol for the formation of the radical precursor and photocatalytic imidation. Under the optimized reaction conditions, a phthalimidyl substituent, a versatile nitrogen functional group, could be incorporated into various commercial aromatic compounds to furnish protected anilines.

2.5. References

1) Stella, L. Nitrogen-Centered Radicals. In *Radicals in Organic Synthesis*; Renaud, P. and Sibi, M. P. Ed.; Wiley-VCH: Weinheim: New York, 2001; Vol. 2; p 407.

2) (a) Hofmann, A. W. *Ber. Dtsch Chem. Ges.* **1879,** *12*, 984. (b) Wolff, M. E. *Chem. Rev.* **1963,** *63*, 55.

3) (a) Wieland, H. *Justus Liebigs Ann. Chem.* **1911,** *381*, 200. (b) Miura, Y.; Tomimura, T.; Teki, Y. *J. Org. Chem* **2000,** *65*, 7889.

4) Studer, A.; Curran, D. P. *Angew. Chem. Int. Ed.* **2016,** *55*, 58.

5) For reviews, see (a) Chen, J.-R.; Hu, X.-Q.; Lu, L.-Q.; Xiao, W.-J. *Chem. Soc. Rev.* **2016,** *45*, 2044. (b) Kärkäs, M. D. *ACS Cat.* **2017,** *7*, 4999. (c) Xiong, T.; Zhang, Q. *Chem. Soc. Rev.* **2016,** *45*, 3069.

6) Cecere, G.; König, C. M.; Alleva, J. L.; MacMillan, D. W. C. *J. Am. Chem. Soc.* **2013,** *135*, 11521.

7) Allen, L. J.; Cabrera, P. J.; Lee, M.; Sanford, M. S. *J. Am. Chem. Soc.* **2014,** *136*, 5607.

8) Kim, H.; Kim, T.; Lee, D. G.; Roh, S. W.; Lee, C. *Chem. Commun.* **2014,** *50*, 9273.

9) Greulich, T. W.; Daniliuc, C. G.; Studer, A. *Org. Lett.* **2015,** *17*, 254.

10) Selective examples for aminium radical cation in photoredox catalysis see (a) Condie, A. G.; González-Gómez, J. C.; Stephenson, C. R. J. *J. Am. Chem. Soc.* **2010,** *132*, 1464. (b) Rueping, M.; Leonori, D.; Poisson, T. *Chem. Commun.* **2011,** *47*, 9615. (c) McNally, A.; Prier, C. K.; MacMillan, D. W. C. *Science* **2011,** *334*, 1114. (d) DiRocco, D. A.; Rovis, T. *J. Am. Chem. Soc.* **2012,** *134*, 8094.

11) Choi, G. J.; Knowles, R. R. *J. Am. Chem. Soc.* **2015,** *137*, 9226.

12) Weinberg, D. R.; Gagliardi, C. J.; Hull, J. F.; Murphy, C. F.; Kent, C. A.; Westlake, B. C.; Paul, A.; Ess, D. H.; McCafferty, D. G.; Meyer, T. J. *Chem. Rev.* **2012,** *112*, 4016.

13) Davies, J.; Sheikh, N. S.; Leonori, D. *Angew. Chem. Int. Ed.* **2017,** *56*, 13361.

14) (a) Maity, S.; Zheng, N. *Angew. Chem. Int. Ed.* **2012,** *51*, 9562. (b) Musacchio, A. J.; Nguyen, L. Q.; Beard, G. H.; Knowles, R. R. *J. Am. Chem. Soc.* **2014,** *136*, 12217. (c)

Musacchio, A. J.; Lainhart, B. C.; Zhang, X.; Naguib, S. G.; Sherwood, T. C.; Knowles, R. R. *Science* **2017,** *355*, 727.

15) (a) Qin, Q.; Yu, S. *Org. Lett.* **2015,** *17*, 1894. (b) Choi, G. J.; Zhu, Q.; Miller, D. C.; Gu, C. J.; Knowles, R. R. *Nature* **2016,** *539*, 268. (c) O'Broin, C. Q.; Fernández, P.; Martínez, C.; Muñiz, K. *Org. Lett.* **2016,** *18*, 436. (d) Becker, P.; Duhamel, T.; Stein, C. J.; Reiher, M.; Muñiz, K. *Angew. Chem. Int. Ed.* **2017,** *56*, 8004. (e) Shu, W.; Nevado, C. *Angew. Chem. Int. Ed.* **2017,** *56*, 1881. (f) Jiang, H.; Studer, A. *Angew. Chem. Int. Ed.* **2018,** *57*, 1692. (h) Morcillo, S. P.; Dauncey, E. M.; Kim, J. H.; Douglas, J. J.; Sheikh, N. S.; Leonori, D. *Angew. Chem.* **2018,** *130*, 12945.

16) (a) Qin, Q.; Ren, D.; Yu, S. *Org. Biomol. Chem.* **2015,** *13*, 10295. (b) Miyazawa, K.; Koike, T.; Akita, M. *Chem. A Eur. J.* **2015,** *21*, 11677.

17) Park, Y.; Kim, Y.; Chang, S. *Chem. Rev.* **2017,** *117*, 9247.

18) Lüring, U.; Kirsch, A. *Chem. Ber.* **1993,** *126*, 1171.

19) Singh, A.; Teegardin, K.; Kelly, M.; Prasad, K. S.; Krishnan, S.; Weaver, J. D. *J. Organomet. Chem.* **2015,** *776*, 51.

20) Zhong, Y.-L.; Zhou, H.; Gauthier, D. R.; Lee, J.; Askin, D.; Dolling, U. H.; Volante, R. P. *Tetrahedron Lett.* **2005,** *46*, 1099.

21) Qin, Q.; Yu, S. *Org. Lett.* **2014,** *16*, 3504.

2.6. Experimental Section

2.6.1. General Information

Anisole, phenyl acetate, fluorobenzene, chlorobenzene, bromobenzene, methyl benzoate, 1,4dimethoxybenzene, methyl *p*-anisate, *o*-xylene, *m*-xylene, *p*-xylene, 1,2-dichlorobenzene, dimethylphthalate, 2-bromo-1,3-dimethylbenzene, mesitylene, 1,3,5-tri-tert-butylbenzene, 4methoxypyridine, 2,6-lutidine, 2,6-di-*tert*-butylpyridine, 2,4,6-collidine, phthalimide, *N*-chlorophthalimide, *N*-bromophthalimide, glacial acetic acid, *tert*-butanol, potassium carbonate, sodium hypochlorite, hydrazine monohydrate and tris[2-(4,6-difluorophenyl)pyridinatoC2,N]iridium(III) ($Ir(dFppy)_3$) were purchased from commercial sources and used as received without further purification. *tert*-butyl hypochlorite was prepared by using a literature procedure. Benzene, toluene, pyridine and solvents were obtained by passing through activated alumina columns of solvent purification systems from Glass Contour. The progress of reaction was checked on thin layer chromatography (TLC) plates (Merck 5554 Kiesel gel 60 F254), and the spots were visualized under 254 nm UV light and/or charring after dipping the TLC plate into a vanillin solution (15.0 g of vanillin and 2.5 mL of concentrated sulfuric acid in 250 mL of ethanol), a $KMnO_4$ solution (3.0 g of $KMnO_4$, 20.0 g of K_2CO_3, and 5.0 mL of 5% NaOH solution in 300 mL of water), or a ninhydrin solution (1.5 g of ninhydrin, 5 mL of acetic acid, 500 mL of 95% ethanol). Column chromatography was performed on silica gel (Merck 9385 Kiesel gel 60) using hexanes-EtOAc (v/v). NMR spectra were obtained on a Bruker DPX-300 (300 MHz), an Agilent 400-MR DD2 Magnetic Resonance System (400 MHz) and a Varian/Oxford As-500 (500 MHz) spectrophotometer. Chemical shift values were recorded as parts per million relatives to tetramethylsilane as an internal standard unless otherwise indicated, and coupling constants in Hertz. The following abbreviations (or combinations thereof) were used to explain the multiplicities: s = singlet, d = doublet, t = triplet, q = quartet, m = multiplet, b = broad. IR spectra were measured on a Thermo Scientific Nicolet 6700 spectrometer. High resolution mass spectra were recorded on a JEOL JMS-600W, JMS-700, Agilent 6890 Series or a JEOL JMS-AX505WA, HP 5890 Series II spectrometer using electron impact (EI) or fast atom bombardment (FAB) method. Gas chromatography data were obtained on a Hewlett Packard HP 6890 Series GC systems.

2.6.2. General Imidation Procedure

Method A for imidation using N-chlorophthalimide

To a reaction vessel with a magnetic stirring bar were added *N*-chlorophthalimide (90.8 mg/0.50 mmol or 181.6 mg/1.00 mmol), potassium carbonate (207.3 mg, 1.50 mmol), and *fac*-Ir(dFppy)$_3$ (1.9 mg, 0.0025 mmol, 0.5 mol % for the limiting agent). After addition of acetonitrile (5.0 ml), arene/heteroarene substrate (1.00 mmol or 0.50 mmol) and acetic acid (5.7 µl) were added. The mixture was placed in the irradiation apparatus equipped with a 20 W household compact fluorescent lamp (CFL). After 24 h, the reaction was quenched by addition of saturated $Na_2S_2O_3$ aqueous solution and the aqueous phase was then extracted with dichloromethane. The resulting organic phase was washed with 2 N NaOH aqueous solution to remove the remaining phthalimide, dried over anhydrous sodium sulfate, filtered and concentrated under reduced pressure. The resulting crude mixture was purified by flash column chromatography on silica gel, which furnished the title compounds as described.

Method B for imidation using phthalimide and tert-butyl hypochlorite

To a reaction vessel with a magnetic stirring bar were added phthalimide (147.1 mg, 1.00 mmol), potassium carbonate (207.3 mg, 1.50 mmol), *tert*-butanol (95.6 µl, 1.00 mmol) and *fac*-Ir(dFppy)$_3$ (1.9 mg, 0.0025 mmol). After addition of acetonitrile (5.0 ml), *tert*-butyl hypochlorite (113 µl, 1.00 mmol) was added in one portion and the reaction mixture was vigorously stirred at room temperature without light. After 2 h, arene/heteroarene substrate (0.50 mmol) was added and the mixture was placed in the irradiation apparatus equipped with a 20 W CFL. After 24 h, the reaction was quenched by addition of saturated $Na_2S_2O_3$ aqueous solution and the aqueous phase was then extracted with dichloromethane. The resulting organic phase was washed with 2 N NaOH aqueous solution to remove the remaining phthalimide, dried over anhydrous sodium sulfate, filtered and concentrated under reduced pressure. The resulting crude mixture was purified by flash column chromatography on silica gel, which furnished the title compounds as described.

Method C for imidation using phthalimide and sodium hypochlorite

To a reaction vessel with a magnetic stirring bar were added phthalimide (227.0 mg, 1.25 mmol), *tert*-butanol (95.6 µl, 1.00 mmol) and acetonitrile (5.0 ml). Aqueous solution of sodium hypochlorite containing 11–14% chlorine (0.44 ml, 1.00 mmol) and acetic acid (57.2 µl, 1.00 mmol) were slowly added at the same time and the resulting solution was stirred vigorously at room temperature without light. After 2 h, *fac*-Ir(dFppy)$_3$ (1.9 mg, 0.0025 mmol) and arene/heteroarene substrate (0.50 mmol) were added and the mixture was placed in the irradiation apparatus equipped with a 20 W CFL. After 24 h, the reaction was quenched by addition of saturated $Na_2S_2O_3$ aqueous solution and the aqueous phase was then extracted with dichloromethane. The resulting organic phase was washed with 2 N NaOH aqueous solution to remove the remaining phthalimide, dried over anhydrous sodium sulfate, filtered and concentrated under reduced pressure. The resulting crude mixture was purified by flash column chromatography on silica gel, which furnished the title compounds as described.

2.6.3. Experimental Data for Imidation Products

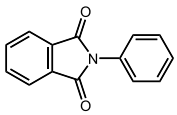

***N*-phenylphthalimide (2.17)**[i]

^{1}H NMR (500 MHz, $CDCl_3$): δ 8.00–7.92 (m, 2H), 7.83–7.77 (m, 2H), 7.54–7.48 (m, 2H), 7.47–7.38 (m, 3H). 13C NMR (125 MHz, $CDCl_3$): δ 167.5, 134.6, 131.9, 131.8, 129.3, 128.3, 126.8, 123.9.

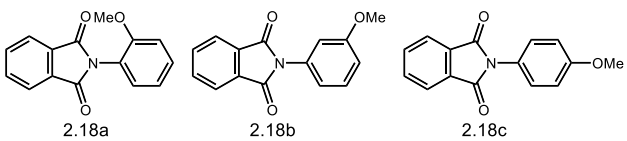

2.18a 2.18b 2.18c

***N*-(methoxyphenyl)phthalimide (2.18)**[ii,iii]

Following the general procedure for photocatalytic imidation (method A), starting from anisole (109 μl, 1.00 mmol) and *N*-chlorophthalimide (90.8 mg, 0.50 mmol), the isomeric mixture of 2.18a, 2.18b and 2.18c was afforded as a light yellow solid after column chromatography (52.3 mg, 0.207 mmol, 41%). The structures and the relative ratios of isomers were determined by synthesis of authentic samples and their ^{1}H NMR spectra.

Isomeric ratio (15:1.0:13).

***N*-(2-methoxyphenyl)phthalimide (2.18a)** ^{1}H NMR (400 MHz, $CDCl_3$): δ 7.96–7.86 (m, 2H), 7.80–7.70 (m, 2H), 7.48–7.37 (m, 1H), 7.26 (dd, J = 7.7, 1.7 Hz, 1H), 7.13–7.00 (m, 2H), 3.80 (s, 3H). ^{13}C NMR (100 MHz, $CDCl_3$): δ 167.6, 155.6, 134.3, 132.5, 130.9, 130.2, 123.9, 121.1, 120.4, 112.3, 56.0.

***N*-(3-methoxyphenyl)phthalimide (2.18b)** ^{1}H NMR (400 MHz, CDCl3): δ 7.99–7.90 (m, 2H), 7.84–7.76 (m, 2H), 7.41 (t, J = 8.1 Hz, 1H), 7.06–6.86 (m, 3H), 3.84 (s, 3H). ^{13}C NMR (100 MHz, $CDCl_3$): δ 167.4, 160.2, 134.6, 132.9, 132.0, 130.0, 124.0, 119.1, 114.3, 112.6, 55.7.

***N*-(4-methoxyphenyl)phthalimide (2.18c)** ^{1}H NMR (400 MHz, $CDCl_3$): δ 7.98–7.91 (m, 2H), 7.81–7.74 (m, 2H), 7.34 (d, J = 8.3 Hz, 2H), 7.03 (d, J = 8.5 Hz, 2H), 3.85 (s, 3H). ^{13}C NMR (100 MHz, $CDCl_3$): δ 167.8, 159.4, 134.5, 132.0, 128.1, 124.4, 123.9, 114.7, 55.7.

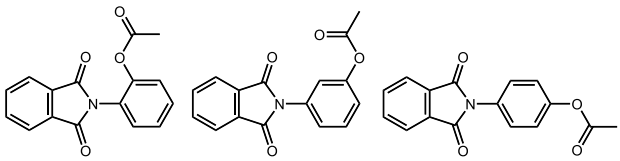

***N*-(acetoxyphenyl)phthalimide (2.19)**[i]

Following the general procedure for photocatalytic imidation (method A), starting from phenyl acetate (127 μl, 1.00 mmol) and *N*-chlorophthalimide (90.8 mg, 0.50 mmol), the isomeric mixture of 2.19a, 2.19b and 2.19c was afforded as a white solid after column chromatography (64.1 mg, 0.228 mmol, 46%). The structures and the relative ratios of isomers were determined by ^{1}H NMR spectraoscopy described in the reference literature.

Isomeric ratio (3.2:2.0:1.0).

^{1}H NMR (400 MHz, $CDCl_3$): δ 8.00–7.94 (m, 2H), 7.85–7.78 (m, 2H), 7.55–7.46 (m, 1.2H), 7.43– 7.35 (m, 2H), 7.32 (t, J = 2.0 Hz, 0.2H), 7.29–7.23 (m, 0.4H), 7.17 (dd, J = 8.2, 1.3 Hz, 0.4H), 2.34 (s, 0.5H), 2.32 (s, 1H), 2.15 (s, 1.6H). ^{13}C NMR (100 MHz, $CDCl_3$): δ 169.3, 169.1, 168.2, 167.3, 167.0, 166.7, 151.0, 150.1, 146.5, 134.7, 134.6, 132.8, 132.0, 131.8, 131.7, 130.0, 129.8, 129.6, 129.3, 127.6, 126.4, 124.1, 124.03, 123.99, 123.95, 123.8, 123.6, 122.4, 121.2, 119.8, 21.3, 21.1.

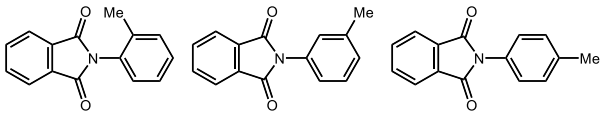

2.20a 2.20b 2.20c

***N*-(methylphenyl)phthalimide (2.20)**[i]

Following the general procedure for photocatalytic imidation (method A), starting from toluene (106 μl, 1.00 mmol) and *N*-chlorophthalimide (90.8 mg, 0.50 mmol), the isomeric mixture of 2.20a, 2.20b and 2.20c was afforded as a white solid after column chromatography (55.9 mg, 0.236 mmol, 47%). In the case following the method B starting from toluene (53.1 μl, 0.50 mmol), the isomeric mixture was provided in 46% yield (54.5 mg, 0.230 mmol). The structures and the relative ratios of isomers were determined by synthesis of authentic samples and their ^{1}H NMR spectra.

Isomeric ratio (2.5:1.0:1.3).

***N*-(2-methylphenyl)phthalimide (2.20a)** ^{1}H NMR (400 MHz, $CDCl_3$): δ 8.00–7.93 (m, 2H), 7.83–7.77 (m, 2H), 7.39–7.38 (m, 1H), 7.37 (d, J = 1.1 Hz, 1H), 7.36–7.31 (m, 1H), 7.21 (d, J = 7.5 Hz, 1H), 2.22 (s, 3H). ^{13}C NMR (100 MHz, $CDCl_3$): δ 167.6, 136.7, 134.5, 132.2, 131.4, 130.8, 129.7, 128.9, 127.1, 124.0, 18.3.

***N*-(3-methylphenyl)phthalimide (2.20b)** ^{1}H NMR (400 MHz, $CDCl_3$): δ 7.95 (dd, J = 5.5, 3.0 Hz, 2H), 7.79 (dd, J = 5.4, 3.1 Hz, 2H), 7.42– 7.35 (m, 1H), 7.24–7.19 (m, 3H), 2.42 (s, 3H). ^{13}C NMR (100 MHz, $CDCl_3$): δ 167.6, 139.3, 134.5, 132.0, 131.7, 129.3, 129.1, 127.5, 124.0, 123.9, 21.6.

***N*-(4-methylphenyl)phthalimide (2.20c)** ^{1}H NMR (400 MHz, $CDCl_3$): δ 7.95 (dd, J = 5.4, 3.1 Hz, 2H), 7.79 (dd, J = 5.5, 3.0 Hz, 2H), 7.31 (s, 4H), 2.41 (s, 3H). ^{13}C NMR (100 MHz, $CDCl_3$): δ 167.6, 138.4, 134.5, 132.0, 130.0, 129.2, 126.7, 123.9, 21.4.

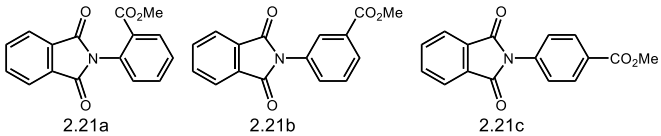

***N*-(methoxycarbonylphenyl)phthalimide (2.21)**[v,vi]

Following the general procedure for photocatalytic imidation (method A), starting from methyl benzoate (136.2 mg, 1.00 mmol) and *N*-chlorophthalimide (90.8 mg, 0.50 mmol), the isomeric mixture of 2.21a, 2.21b and 2.21c was afforded as a white solid after column chromatography (48.3 mg, 0.172 mmol, 34%). The structures and the relative ratios of isomers were determined by synthesis of authentic samples and their ^{1}H NMR spectra.

Isomeric ratio (7.2:11:4.0).

***N*-(2-methoxycarbonylphenyl)phthalimide (2.21a)** ^{1}H NMR (400 MHz, $CDCl_3$): δ 8.21–8.11 (m, 1H), 8.00–7.91 (m, 2H), 7.84–7.75 (m, 2H), 7.69 (ddd, J = 7.7, 1.5, 0.8 Hz, 1H), 7.60–7.50 (m, 1H), 7.40 (dd, J = 7.9, 1.0 Hz, 1H), 3.74 (s, 3H). ^{13}C NMR (100 MHz, $CDCl_3$): δ 167.7, 165.4, 134.5, 133.5, 132.3, 132.0, 131.8, 130.5, 129.3, 128.2, 123.9, 52.5.

***N*-(3-methoxycarbonylphenyl)phthalimide (2.21b)** ^{1}H NMR (400 MHz, $CDCl_3$): δ 8.15 (dd, J = 2.7, 1.0 Hz, 1H), 8.09 (ddd, J = 7.7, 1.9, 1.0 Hz, 1H), 8.01–7.94 (m, 2H), 7.85–7.79 (m, 2H), 7.69–7.64 (m, 1H), 7.60 (t, J = 7.9 Hz, 1H), 3.94 (s, 3H). ^{13}C NMR (100 MHz, $CDCl_3$): δ 167.2, 166.3, 134.8, 132.1, 131.8, 131.5, 131.1, 129.4, 129.3, 127.9, 124.1, 52.6.

***N*-(4-methoxycarbonylphenyl)phthalimide (2.21c)** ^{1}H NMR (400 MHz, $CDCl_3$): δ 8.16 (dd, J = 8.7, 2.1 Hz, 2H), 8.00–7.95 (m, 2H), 7.83–7.76 (m, 2H), 7.58 (dd, J = 8.5, 1.5 Hz, 2H), 3.93 (s, 3H). ^{13}C NMR (100 MHz, $CDCl_3$): δ 166.9, 166.5, 136.0, 134.8, 131.7, 130.6, 129.4, 126.1, 124.1, 52.5.

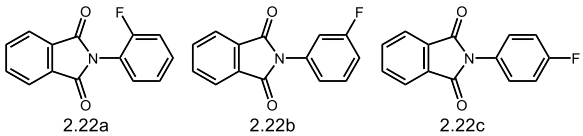

***N*-(fluorophenyl)phthalimide (2.22)**[ii,iv]

Following the general procedure for photocatalytic imidation (method A), starting from fluorobenzene (94.2 μl, 1.00 mmol) and *N*-chlorophthalimide (90.8 mg, 0.50 mmol), the isomeric mixture of 2.22a, 2.22b and 2.22c was afforded as a white solid after column chromatography (56.7 mg, 0.235 mmol, 47%). In the case following the method B starting from fluorobenzene (47.1 μl, 0.50 mmol), the isomeric mixture was provided in 40% yield (48.6 mg, 0.201 mmol). The structures and the relative ratios of isomers were determined by synthesis of authentic samples and their ^{1}H NMR spectra.

Isomeric ratio (7.4:4.0:9.3).

***N*-(2-fluorophenyl)phthalimide (2.22a)** ^{1}H NMR (400 MHz, $CDCl_3$): δ 8.00–7.93 (m, 2H), 7.84–7.76 (m, 2H), 7.49–7.41 (m, 1H), 7.37 (td, J = 7.7, 2.0 Hz, 1H), 7.32–7.23 (m, 2H). ^{13}C NMR (100 MHz, $CDCl_3$): δ 166.7, 159.3, 156.8, 134.7, 132.1, 131.0, 130.9, 130.1, 124.9, 124.8, 124.1, 119.6, 119.5, 117.1, 116.9. ^{19}F NMR (376 MHz, $CDCl_3$): δ -118.71, -118.73, -118.73, -118.74, -118.75, -118.75, -118.76, -118.77.

N-(3-fluorophenyl)phthalimide (2.22b) ^{1}H NMR (400 MHz, $CDCl_3$): δ 8.01–7.93 (m, 2H), 7.85–7.77 (m, 2H), 7.48 (td, J = 8.2, 6.3 Hz, 1H), 7.29 (ddd, J = 8.0, 1.9, 0.9 Hz, 1H), 7.27–7.22 (m, 1H), 7.12 (tdd, J = 8.4, 2.5, 0.9 Hz, 1H). ^{13}C NMR (100 MHz, $CDCl_3$): δ 167.1, 164.1, 161.6, 134.8, 133.3, 133.2, 131.7, 130.5, 130.4, 124.1, 122.23, 122.19, 115.3, 115.1, 114.3, 114.0. ^{19}F NMR (376 MHz, $CDCl_3$): δ -111.18, -111.20, -111.21, -111.23, -111.23, -111.25.

N-(4-fluorophenyl)phthalimide (2.22c) ^{1}H NMR (400 MHz, $CDCl_3$): δ 8.01–7.91 (m, 2H), 7.85–7.76 (m, 2H), 7.47–7.39 (m, 2H), 7.24–7.15 (m, 2H). ^{13}C NMR (100 MHz, $CDCl_3$): δ 167.4, 163.4, 160.9, 134.7, 131.8, 128.6, 128.5, 127.78, 127.75, 124.0, 116.5, 116.2. ^{19}F NMR (376 MHz, $CDCl_3$): δ -113.06, -113.07, -113.08, -113.08, 113.09, -113.10, -113.10, -113.11, -113.13.

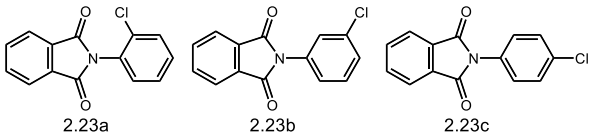

***N*-(chlorophenyl)phthalimide (2.23)**[i]

Following the general procedure for photocatalytic imidation (method A), starting from chlorobenzene (101 μl, 1.00 mmol) and *N*-chlorophthalimide (90.8 mg, 0.50 mmol), the isomeric mixture of 2.23a, 2.23b and 2.23c was afforded as a white solid after column chromatography (77.0 mg, 0.299 mmol, 60%). The structures and the relative ratios of isomers were determined by synthesis of authentic samples and their ^{1}H NMR spectra.

Isomeric ratio (2.3:1.0:2.0).

***N*-(2-chlorophenyl)phthalimide (2.23a)** ^{1}H NMR (400 MHz, $CDCl_3$): δ 8.03–7.93 (m, 2H), 7.86–7.77 (m, 2H), 7.62–7.54 (m, 1H), 7.48–7.40 (m, 2H), 7.39–7.32 (m, 1H). ^{13}C NMR (100 MHz, $CDCl_3$): δ 166.9, 134.7, 133.4, 132.1, 130.9, 130.7, 129.8, 127.9, 124.2.

***N*-(3-chlorophenyl)phthalimide (2.23b)** ^{1}H NMR (400 MHz, $CDCl_3$): δ 8.03–7.93 (m, 2H), 7.86–7.77 (m, 2H), 7.53–7.49 (m, 1H), 7.48–7.42 (m, 1H), 7.41–7.36 (m, 2H). ^{13}C NMR (100 MHz, $CDCl_3$): δ 167.0, 134.8, 133.0, 131.8, 130.3, 128.4, 126.9, 124.8, 124.1.

***N*-(4-chlorophenyl)phthalimide (2.23c)** ^{1}H NMR (400 MHz, $CDCl_3$): δ 8.01–7.92 (m, 2H), 7.84–7.78 (m, 2H), 7.51–7.45 (m, 2H), 7.45–7.39 (m, 2H). ^{13}C NMR (100 MHz, $CDCl_3$): δ 167.2, 134.8, 134.0, 131.8, 130.4, 129.5, 127.9, 124.1.

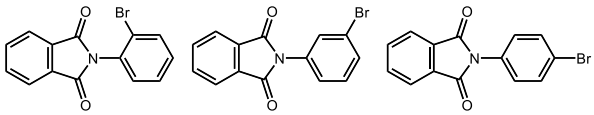

***N*-(bromophenyl)phthalimide (2.24)**[i,vii]

Following the general procedure for photocatalytic imidation (method A), starting from bromobenzene (105 µl, 1.00 mmol) and *N*-chlorophthalimide (90.8 mg, 0.50 mmol), the isomeric mixture of 2.24a, 2.24b and 2.24c was afforded as a white solid after column chromatography (65.7 mg, 0.217 mmol, 43%). The structures and the relative ratios of isomers were determined by synthesis of authentic samples and their ^{1}H NMR spectra.

Isomeric ratio (3.3:2.0:2.7).

***N*-(2-bromophenyl)phthalimide (2.24a)** ^{1}H NMR (400 MHz, $CDCl_3$): δ 8.01–7.96 (m, 2H), 7.85–7.79 (m, 2H), 7.78–7.73 (m, 1H), 7.50–7.44 (m, 1H), 7.40–7.33 (m, 2H). ^{13}C NMR (100 MHz, $CDCl_3$): δ 166.8, 134.7, 133.8, 132.1, 131.6, 131.2, 131.0, 128.7, 124.2, 123.5.

***N*-(3-bromophenyl)phthalimide (2.24b)** ^{1}H NMR (400 MHz, $CDCl_3$): δ 8.01–7.92 (m, 2H), 7.86–7.77 (m, 2H), 7.65 (t, J = 1.7 Hz, 1H), 7.57–7.51 (m, 1H), 7.46–7.33 (m, 2H). ^{13}C NMR (100 MHz, $CDCl_3$): δ 167.0, 134.8, 133.1, 131.7, 131.3, 130.5, 129.7, 125.3, 124.1, 122.6.

***N*-(4-bromophenyl)phthalimide (2.24c)** ^{1}H NMR (400 MHz, $CDCl_3$): δ 7.99–7.93 (m, 2H), 7.84–7.77 (m, 2H), 7.67–7.61 (m, 2H), 7.39–7.33 (m, 2H). ^{13}C NMR (100 MHz, $CDCl_3$): δ 167.1, 134.8, 132.5, 131.8, 130.9, 128.2, 124.1, 122.0.

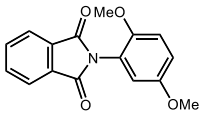

_N_-(2,5-dimethoxyphenyl)phthalimide (2.25)

Following the general procedure for photocatalytic imidation (method A), starting from 1,4-dimethoxybenzene (138.2 mg, 1.00 mmol) and *N*-chlorophthalimide (90.8 mg, 0.50 mmol), the titled compound 2.25 was afforded as a light yellow solid after column chromatography (62.1 mg, 0.219 mmol, 44%) with *N*-(4-methoxyphenyl)phthalimide (12.3 mg, 0.049 mmol, 10%).

^{1}H NMR (400 MHz, $CDCl_3$): δ 7.97–7.91 (m, 2H), 7.81–7.72 (m, 2H), 7.00–6.95 (m, 2H), 6.85–6.80 (m, 1H), 3.78 (s, 3H), 3.75 (s, 3H). ^{13}C NMR (100 MHz, $CDCl_3$): δ 167.5, 153.8, 149.9, 134.3, 132.4, 123.9, 120.9, 116.1, 115.8, 113.4, 56.6, 56.0. IR (neat): νmax 3093, 3009, 2956, 2836, 1786, 1769, 1724, 1510, 1461, 1384, 1278, 1227, 1204, 1114, 1045, 1023, 928, 893, 861, 734 cm^{-1}. HRMS (EI) calcd. for $C_{16}H_{13}NO_4^+$ (M^+): 283.0844, found 283.0845.

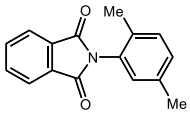

_N_-(2,5-dimethylphenyl)phthalimide (2.26)[i]

Following the general procedure for photocatalytic imidation (method A), starting from *p*-xylene (123 μl, 1.00 mmol) and *N*-chlorophthalimide (90.8 mg, 0.50 mmol), the titled compound 2.26 was afforded as a white solid after column chromatography (50.1 mg, 0.199 mmol, 40%). In the case following the method A starting from *p*-xylene (61.7 μl, 0.50 mmol) and *N*-chlorophthalimide (181.6 mg, 1.00 mmol), the product was provided in 50% yield (63.0 mg, 0.251 mmol).

^{1}H NMR (400 MHz, CDCl3): δ 7.99–7.92 (m, 2H), 7.83–7.75 (m, 2H), 7.29–7.22 (m, 1H), 7.21–7.14 (m, 1H), 7.02 (s, 1H), 2.36 (s, 3H), 2.16 (s, 3H). ^{13}C NMR (100 MHz, $CDCl_3$): δ 167.7, 136.9, 134.5, 133.5, 132.2, 131.1, 130.54, 130.48, 129.3, 123.9, 21.0, 17.8.

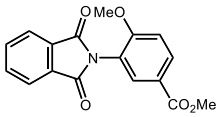

***N*-(2-methoxy-5-methoxycarbonylphenyl)phthalimide (2.27)**

Following the general procedure for photocatalytic imidation (method A), starting from methyl *p*-anisate (166.0 mg, 1.00 mmol) and *N*-chlorophthalimide (90.8 mg, 0.50 mmol), the titled compound 2.27 was afforded as a colorless crystal after column chromatography (75.0 mg, 0.241 mmol, 48%). In the case following the method A starting from methyl *p*-anisate (83.1 mg, 0.50 mmol) and *N*-chlorophthalimide (181.6 mg, 1.00 mmol), the product was provided in 39% yield (60.3 mg, 0.194 mmol) which was not changed in open-air conditions. When the reaction was carried out in the conditions following the method B starting from methyl *p*-anisate (83.1 mg, 0.50 mmol), the product yield was 41% (63.7 mg, 0.205 mmol).

^{1}H NMR (400 MHz, $CDCl_3$): δ 8.13 (dd, J = 8.8, 2.1 Hz, 1H), 7.96 (d, J = 2.1 Hz, 1H), 7.92 (dd, J = 5.4, 3.1 Hz, 2H), 7.77 (dd, J = 5.4, 3.1 Hz, 2H), 7.06 (d, J = 8.8 Hz, 1H), 3.87 (s, 3H), 3.83 (s, 3H). ^{13}C NMR (75 MHz, $CDCl_3$): δ 167.2, 166.2, 159.4, 134.5, 132.9, 132.4, 132.1, 124.0, 123.3, 120.5, 111.8, 56.4, 52.3. IR (neat): νmax 2952, 2844, 1782, 1724, 1611, 1512, 1447, 1377, 1317, 1294, 1273, 1214, 1185, 1148, 1119, 1086, 1022, 985, 915, 881, 830, 795, 767, 720 cm^{-1}. HRMS (EI) calcd. for $C_{17}H_{13}NO_5^+$ (M^+): 311.0793, found 311.0789.

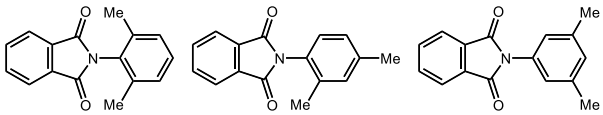

***N*-(dimethylphenyl)phthalimide (2.28)**[viii]

Following the general procedure for photocatalytic imidation (method A), starting from *m*-xylene (123 μl, 1.00 mmol) and *N*-chlorophthalimide (90.8 mg, 0.50 mmol), the isomeric mixture of 2.28a, 2.28b and 2.28c was afforded as a white solid after column chromatography (72.2 mg, 0.287 mmol, 57%). In the case following the method A starting from m-xylene (61.7 μl, 0.50 mmol) and Nchlorophthalimide (181.6 mg, 1.00 mmol), the isomeric mixture was provided in 72% yield (90.8 mg, 0.361 mmol). The structures and the relative ratios of isomers were determined by synthesis of authentic samples and their ^{1}H NMR spectra.

Isomeric ratio (4.0:9.0:1.0).

***N*-(2,6-dimethylphenyl)phthalimide (2.28a)** ^{1}H NMR (400 MHz, $CDCl_3$): δ 8.01–7.94 (m, 2H), 7.84–7.77 (m, 2H), 7.31–7.25 (m, 1H), 7.19 (d, J = 7.5 Hz, 2H), 2.17 (s, 6H). ^{13}C NMR (100 MHz, $CDCl_3$): δ 167.4, 137.1, 134.5, 132.2, 130.0, 129.7, 128.7, 124.0, 18.3.

***N*-(2,4-dimethylphenyl)phthalimide (2.28b)** ^{1}H NMR (400 MHz, $CDCl_3$): δ 7.99–7.91 (m, 2H), 7.83–7.75 (m, 2H), 7.18 (s, 1H), 7.14 (dd, J = 8.5, 0.5 Hz, 1H), 7.08 (d, J = 7.9 Hz, 1H), 2.38 (s, 3H), 2.17 (s, 3H). ^{13}C NMR (100 MHz, $CDCl_3$): δ 167.7, 139.7, 136.3, 134.5, 132.2, 132.1, 128.6, 128.0, 127.8, 123.9, 21.4, 18.1.

N-(3,5-dimethylphenyl)phthalimide (2.28c) ^{1}H NMR (400 MHz, $CDCl_3$): δ 7.98–7.92 (m, 2H), 7.82–7.76 (m, 2H), 7.05 (s, 1H), 7.02 (s, 2H), 2.38 (s, 6H). ^{13}C NMR (100 MHz, $CDCl_3$): δ 167.7, 139.1, 134.5, 132.0, 131.5, 130.4, 124.7, 123.9, 21.5.

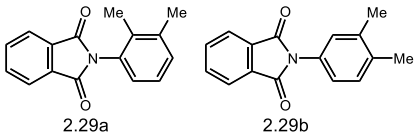

***N*-(dimethylphenyl)phthalimide (2.29)**[i]

Following the general procedure for photocatalytic imidation (method A), starting from *o*-xylene (121 μl, 1.00 mmol) and *N*-chlorophthalimide (90.8 mg, 0.50 mmol), the isomeric mixture of 2.29a and 2.29b was afforded as a white solid after column chromatography (41.5 mg, 0.164 mmol, 33%). In the case following the method A starting from *o*-xylene (60.3 μl, 0.50 mmol) and *N*-chlorophthalimide (181.6 mg, 1.00 mmol), the isomeric mixture was provided in 34% yield (43.1 mg, 0.171 mmol). When the reaction was carried out in the conditions following the method B starting from *o*-xylene (121 μl, 1.00 mmol) and phthalimide (73.6 mg, 0.50 mmol), the product yield was 35% (43.9 mg, 0.174 mmol). The structures and the relative ratios of isomers were determined by synthesis of authentic samples and their ^{1}H NMR spectra.

Isomeric ratio (1.0:1.0).

***N*-(2,3-dimethylphenyl)phthalimide (2.29a)** ^{1}H NMR (400 MHz, $CDCl_3$): δ 8.00–7.91 (m, 2H), 7.84–7.75 (m, 2H), 7.30–7.19 (m, 2H), 7.09– 7.01 (m, 1H), 2.36 (s, 3H), 2.08 (s, 3H). ^{13}C NMR (100 MHz, $CDCl_3$): δ 167.8, 138.6, 135.3, 134.5, 132.3, 131.2, 130.7, 126.48, 126.46, 124.0, 20.7, 14.9.

***N*-(3,4-dimethylphenyl)phthalimide (2.29b)** ^{1}H NMR (400 MHz, $CDCl_3$): δ 7.98–7.91 (m, 2H), 7.82–7.75 (m, 2H), 7.29–7.25 (m, 1H), 7.19–7.16 (m, 1H), 7.14 (dd, J = 8.0, 2.2 Hz, 1H), 2.31 (d, J = 2.9 Hz, 6H). ^{13}C NMR (100 MHz, $CDCl_3$): δ 167.7, 137.8, 137.2, 134.5, 132.0, 130.5, 129.3, 127.9, 124.3, 123.8, 20.1, 19.7.

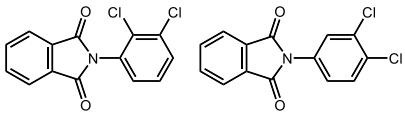

2.30a 2.30b

***N*-(dichlorolphenyl)phthalimide (2.30)**[i]

Following the general procedure for photocatalytic imidation (method A), starting from 1,2-dichlorobenzene (113 μl, 1.00 mmol) and *N*-chlorophthalimide (90.8 mg, 0.50 mmol), the isomeric mixture of 2.30a and 2.30b was afforded as a white solid after column chromatography (53.7 mg, 0.184 mmol, 37%). The structures and the relative ratios of isomers were determined by synthesis of authentic samples and their ^{1}H NMR spectra.

Isomeric ratio (4.0:4.9).

***N*-(2,3-dichlorophenyl)phthalimide (2.30a)** ^{1}H NMR (400 MHz, CDCl3): δ 7.96 (dd, J = 5.4, 3.1 Hz, 2H), 7.81 (dd, J = 5.4, 3.1 Hz, 2H), 7.59 (dd, J = 8.1, 1.5 Hz, 1H), 7.36 (t, J = 8.1 Hz, 1H), 7.31–7.23 (m, 1H). ^{13}C NMR (100 MHz, CDCl3): δ 166.5, 134.8, 134.5, 132.5, 131.9, 131.6, 131.5, 129.2, 127.9, 124.2.

***N*-(3,4-dichlorophenyl)phthalimide (2.30b)** ^{1}H NMR (400 MHz, CDCl3): δ 8.00–7.94 (m, 2H), 7.85–7.78 (m, 2H), 7.64 (d, J = 2.4 Hz, 1H), 7.58 (d, J = 8.6 Hz, 1H), 7.37 (dd, J = 8.6, 2.4 Hz, 1H). ^{13}C NMR (100 MHz, CDCl3): δ 166.8, 135.0, 133.2, 132.3, 131.7, 131.3, 130.9, 128.4, 125.7, 124.2.

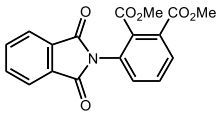

2.31a

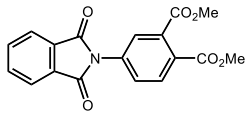

2.31b

***N*-(dimethoxycarbonylphenyl)phthalimide (2.31)**

Following the general procedure for photocatalytic imidation (method A), starting from dimethylphthalate (163 µl, 1.00 mmol) and *N*-chlorophthalimide (90.8 mg, 0.50 mmol), the isomeric mixture of 2.31a and 2.31b was afforded as a white solid after column chromatography (46.6 mg, 0.137 mmol, 27%). The structures and the relative ratios of isomers were determined by synthesis of authentic samples and their ^{1}H NMR spectra.

Isomeric ratio (1.0:1.0).

***N*-(2,3-dimethoxycarbonylphenyl)phthalimide (2.31a)** 1H NMR (400 MHz, CDCl 3): δ 7.99 (dd, J = 7.9, 1.2 Hz, 1H), 7.97– 7.93 (m, 2H), 7.82–7.79 (m, 2H), 7.66 (t, J = 7.9 Hz, 1H), 7.52 (dd, J = 7.9, 1.2 Hz, 1H), 3.91 (s, 3H), 3.75 (s, 3H). 13C NMR (75 MHz, CDCl3): δ 167.1, 166.6, 166.4, 134.8, 133.3, 133.2, 132.99, 131.96, 131.0, 130.7, 130.6, 124.2, 53.2, 53.1. IR (neat): νmax 2953, 2360, 1786, 1726, 1596, 1468, 1433, 1381, 1284, 1235, 1205, 1153, 1133, 1111, 1085, 1066, 914, 885, 763, 717 cm^{-1}. HRMS (EI) calcd. for $C_{18}H_{13}NO_6^+$ (M^+): 339.0743, found 339.0746.

***N*-(3,4-dimethoxycarbonylphenyl)phthalimide (2.31b)** 1H NMR (500 MHz, CDCl3): δ 7.99–7.96 (m, 2H), 7.93 (d, J = 2.1 Hz, 1H), 7.86 (d, J = 8.3 Hz, 1H), 7.84–7.81 (m, 2H), 7.72 (dd, J = 8.3, 2.1 Hz, 1H), 3.93 (s, 3H), 3.93 (s, 3H). 13C NMR (100 MHz, CDCl3): δ 167.6, 167.3, 166.7, 135.0, 134.6, 133.1, 131.6, 131.2, 130.0, 128.5, 126.6, 124.3, 53.1, 53.0. IR (neat): νmax 2954, 1782, 1724, 1607, 1468, 1436, 1416, 1376, 1283, 1219, 1192, 1129, 1070, 961, 881, 846, 823, 789, 771, 718 cm^{-1}. HRMS (EI) calcd. for $C_{18}H_{13}NO_6^+$ (M^+): 339.0743, found 339.0749.

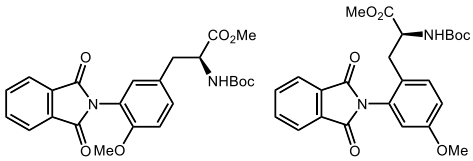

2.32a 2.32b

(*S*)-Methyl2-(*tert*-butoxycarbonylamino)-3-(3-(phthalimidyl)-4-methoxyphenyl)propanoate (2.32a)

and

(*S*)-methyl2-(*tert*-butoxycarbonylamino)-3-(2-(phthalimidyl)-4-methoxyphenyl)propanoate (2.32b)

Following the general procedure for photocatalytic imidation (method A), starting from (*S*)-methyl 2-(*tert*-butoxycarbonylamino)-3-(4-methoxyphenyl)propanoate (S1, 309.4 mg, 1.00 mmol) and *N*-chlorophthalimide (90.8 mg, 0.50 mmol), the isomeric mixture of 2.32 was afforded as a light yellow oil after column chromatography (93.1 mg, 0.205 mmol, 40%). In the case following the method A starting from S1 (154.7 mg, 0.50 mmol) and *N*-chlorophthalimide (181.6 mg, 1.00 mmol), the product was provided in 46% yield (103 mg, 0.228 mmol). The products were characterized as a mixture because they could not be separated into the each of isomers by silica gel chromatography or preparative TLC.

Isomeric ratio (7.1:1.0).

^{1}H NMR (500 MHz, $CDCl_3$) δ 7.99–7.96 (m, 0.28H), 7.95–7.92 (m, 2H), 7.82–7.80 (m, 0.28H), 7.79–7.77 (m, 2H), 7.31–7.28 (m, 0.28H), 7.24–7.20 (m, 1H), 7.02–6.96 (m, 2H), δ 6.72 (d, J = 2.5 Hz, 0.14H), 5.15–5.13 (m, 0.14H), 5.09–5.02 (m, 1H), 4.62–4.55 (m, 1H), 4.49–4.46 (m, 0.14H), 3.80 (s, 0.42H), 3.78 (s, 3H), 3.73 (s, 3H), 3.60 (s, 0.42H), 3.13–3.05 (m, 2H), 2.98–2.93 (m, 0.14H), 2.88–2.84 (m, 0.14H), 1.44 (s, 9H), 1.34 (s, 1.26H). ^{13}C NMR (100 MHz, $CDCl_3$) δ 172.7, 172.4, 167.9, 167.8, 167.4, 167.3, 159.3, 155.3, 154.6, 134.6, 134.3, 132.4, 132.2, 131.5, 131.4, 131.0, 128.7, 124.1, 124.0, 123.8, 120.4, 116.1, 114.5, 112.4, 80.2, 79.9, 56.1, 55.6, 54.6, 54.0, 52.6, 52.5, 37.5, 33.4, 28.5, 28.4. IR (neat): νmax 3372, 2977, 1782, 1722, 1614, 1513, 1447, 1380, 1287, 1258, 1166, 1112, 1086, 1025, 879, 719 cm^{-1}. HRMS (FAB) calcd. for $C_{24}H_{27}N_2O_7^+$ ($M+1^+$): 455.1818, found 455.1817.

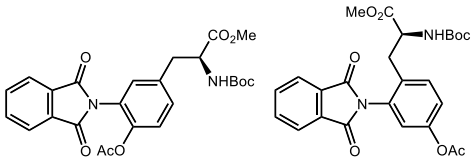

2.33a 2.33b

(*S*)-Methyl 3-(4-acetoxy-3-(phthalimidyl)phenyl)-2-(*tert*-butoxycarbonylamino)propanoate (2.33a)

and

(*S*)-methyl 3-(4-acetoxy-2-(phthalimidyl)phenyl)-2-(*tert*-butoxycarbonylamino)propanoate (2.33b)

Following the general procedure for photocatalytic imidation (method A), starting from (*S*)-methyl 3-(4-acetoxyphenyl)-2-(*tert*-butoxycarbonylamino)propanoate (S2, 337.4 mg, 1.00 mmol) and *N*-chlorophthalimide (90.8 mg, 0.50 mmol), the isomeric mixture of 18b was afforded as a light yellow oil after column chromatography (88.0 mg, 0.182 mmol, 36%). In the case following the method A starting from S2 (168.7 mg, 0.50 mmol) and *N*-chlorophthalimide (181.6 mg, 1.00 mmol), the product was provided in 33% yield (78.6 mg, 0.163 mmol). The products were characterized as a mixture because they could not be separated into the each of isomers by silica gel chromatography or preparative TLC.

Isomeric ratio (1.1: 1.0).

^{1}H NMR (500 MHz, $CDCl_3$): δ 8.01–7.91 (m, 4H), 7.85–7.77 (m, 4H), 7.41 (d, J = 8.6 Hz, 1H), 7.31 (d, J = 8.4 Hz, 1H), 7.26 (dd, J = 8.3, 1.7 Hz, 1H), 7.22 (dd, J = 8.5, 2.4 Hz, 1H), 7.15 (s, 1H), 7.03 (d, J = 2.4 Hz, 1H), 5.13 (dd, J = 41.8, 8.2 Hz, 2H), 4.56 (dd, J = 51.8, 7.2 Hz, 2H), 3.73 (s, 3H), 3.60 (s, 3H), 3.15 (d, J = 4.4 Hz, 2H), 3.01 (dd, J = 14.7, 5.9 Hz, 1H), 2.91 (dd, J = 14.7, 7.8 Hz, 1H), 2.27 (s, 3H), 2.12 (s, 3H), 1.43 (s, 9H), 1.33 (s, 9H). ^{13}C NMR (100 MHz, $CDCl_3$): δ 172.5, 172.2, 168.9, 168.2, 167.6, 167.4, 166.5, 155.4, 155.3, 150.0, 145.4, 134.7, 134.6, 132.9, 132.04, 131.98, 131.7, 131.2, 130.8, 130.3, 124.2, 124.1, 124.0, 123.7, 122.9, 122.5, 80.3, 80.1, 54.4, 53.8, 52.7, 52.5, 37.7, 33.6, 28.5, 28.4, 21.3, 21.1. IR (neat): νmax 3376, 2978, 1768, 1727, 1608, 1505, 1436, 1375, 1241, 1180, 1110, 1015, 887, 721 cm^{-1}. HRMS (FAB) calcd. for $C_{25}H_{27}N_2O_8^+$ ($M+1^+$): 483.1767, found 483.1767.

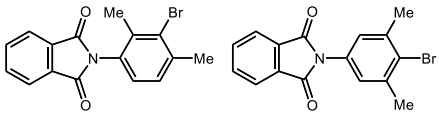

***N*-(bromodimethylphenyl)phthalimide (2.34)**

Following the general procedure for photocatalytic imidation (method A), starting from 2-bromo-1,3-dimethylbenzene (133 μl, 1.00 mmol) and *N*-chlorophthalimide (90.8 mg, 0.50 mmol), the isomeric mixture of 2.34a and 2.34b was afforded as a white solid after column chromatography (77.5 mg, 0.235 mmol, 47%). The structures and relative ratios of isomers were determined by isolation of the isomers and assigning their ^{1}H NMR spectra.

Isomeric ratio (4.0: 1.0).

***N*-(3-bromo-2,4-dimethylphenyl) phthalimide (2.34a)** ^{1}H NMR (400 MHz, $CDCl_3$): δ 8.01–7.92 (m, 2H), 7.85–7.76 (m, 2H), 7.24 (d, J = 8.0 Hz, 1H), 7.08 (d, J = 8.0 Hz, 1H), 2.48 (s, 3H), 2.28 (s, 3H). ^{13}C NMR (100 MHz, $CDCl_3$): δ 167.5, 140.3, 137.3, 134.7, 132.1, 129.1, 129.0, 128.6, 127.5, 124.1, 24.5, 19.7. IR (neat): νmax 1733, 1713, 1481, 1381, 1235, 1110, 887, 721, 695 cm^{-1}. HRMS (EI) calcd. for $C_{16}H_{12}BrNO_2$ (M^+): 329.0051, found 329.0050.

***N*-(4-bromo-3,5-dimethylphenyl)phthalimide (2.34b)** ^{1}H NMR (400 MHz, $CDCl_3$): δ 8.00–7.91 (m, 2H), 7.84–7.76 (m, 2H), 7.26 (s, 2H), 2.47 (s, 6H). ^{13}C NMR (100 MHz $CDCl_3$): δ 167.4, 139.6, 134.7, 131.9, 130.1, 127.7, 126.4, 124.0, 24.3. IR (neat): νmax 1717, 1590, 1468, 1414, 1378, 1110, 1086, 1031, 857, 711 cm^{-1}. HRMS (EI) calcd. for $C_{16}H_{12}BrNO_2$ (M^+): 329.0051, found 329.0051.

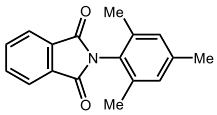

***N*-mesitylphthalimide (2.35)**[i]

Following the general procedure for photocatalytic imidation (method A), starting from mesitylene (139 μl, 1.00 mmol) and *N*-chlorophthalimide (90.8 mg, 0.50 mmol), the titled compound 2.35 was afforded as a white solid after column chromatography (46.4 mg, 0.175 mmol, 35%). In the case following the method C starting from mesitylene (66.0 μl, 0.50 mmol), the product was provided in 52% yield (68.7 mg, 0.259 mmol).

^{1}H NMR (400 MHz, $CDCl_3$): δ 7.99–7.93 (m, 2H), 7.83–7.77 (m, 2H), 7.01 (s, 2H), 2.33 (s, 3H), 2.12 (s, 6H). ^{13}C NMR (100 MHz, $CDCl_3$): δ 167.6, 139.6, 136.7, 134.5, 132.2, 129.5, 127.2, 124.0, 21.4, 18.2.

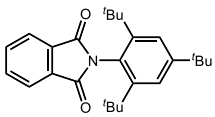

***N*-(2,4,6-tri-tert-butylphenyl)phthalimide (2.36)**

Following the general procedure for photocatalytic imidation (method A), starting from 1,3,5-tri-tertbutylbenzene (246.4 mg, 1.00 mmol) and *N*-chlorophthalimide (90.8 mg, 0.50 mmol), the titled compound 2.36 was afforded as a white solid after column chromatography (19.7 mg, 0.0503 mmol, 10%).

1H NMR (400 MHz, CDCl3): δ 7.99–7.95 (m, 2H), 7.81–7.77 (m, 2H), 7.55 (s, 2H), 1.35 (s, 9H), 1.28 (s, 18H). 13C NMR (100 MHz, CDCl3): δ 170.5, 151.0, 148.6, 134.5, 132.9, 125.1, 124.2, 124.1, 37.3, 35.2, 33.1, 31.6. IR (neat): νmax 2949, 2904, 1728, 1710, 1597, 1461, 1439, 1377, 1364, 1275, 1198, 1107, 1078, 882, 764, 750, 723, 701 cm^{-1}. HRMS (EI) calcd. for $C_{26}H_{33}NO_2^+$ (M^+): 391.2511, found 391.2513.

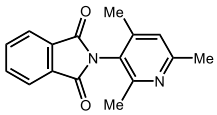

_N_-(2,4,6-trimethylpyridin-3-yl)phthalimide (2.37)

Following the general procedure for photocatalytic imidation (method A), starting from 2,4,6-collidine (132 μl, 1.00 mmol) and *N*-chlorophthalimide (90.8 mg, 0.50 mmol), the titled compound 2.37 was afforded as a light yellow solid after column chromatography (48.4 mg, 0.185 mmol, 37%). In the case following the method A starting from 2,4,6-collidine (66.0 μl, 0.50 mmol) and *N*-chlorophthalimide (181.6 mg, 1.00 mmol), the product 2.37 was provided in 45% yield (59.4 mg, 0.226 mmol).

^{1}H NMR (500 MHz, $CDCl_3$): δ 8.00–7.96 (m, 2H), 7.85–7.81 (m, 2H), 7.02 (s, 1H), 2.55 (s, 3H), 2.36 (s, 3H), 2.14 (s, 3H). ^{13}C NMR (75 MHz, $CDCl_3$): δ 167.1, 158.9, 156.4, 146.6, 134.8, 132.1, 124.2, 123.8, 123.4, 24.4, 21.1, 17.9. IR (neat): νmax 2925, 1783, 1728, 1602, 1469, 1373, 1317, 1224, 1111, 1087, 1029, 8884, 722 cm^{-1}. HRMS (EI) calcd. for $C_{16}H_{14}N_2O_2^+$ (M^+): 266.1055, found 266.1056.

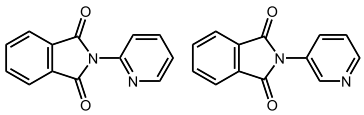

2.38a 2.38b

***N*-(pyridinyl)phthalimide (2.38)**[iii]

Following the general procedure for photocatalytic imidation (method A), starting from pyridine (80.6 μl, 1.00 mmol) and *N*-chlorophthalimide (90.8 mg, 0.50 mmol), 2.38a (13.8 mg, 0.062 mmol, 12%) and 2.38b (29.3 mg, 0.131 mmol, 26%) were afforded as white solid after column chromatography. The structures and relative ratios of isomers were determined by isolation and comparing with synthesized authentic samples by assigning their 1H NMR spectra.

Isomeric ratio (1.0:2.1).

***N*-(2-pyridinyl)phthalimide (2.38a)** ^{1}H NMR (400 MHz, $CDCl_3$): δ 8.73–8.68 (m, 1H), 8.01–7.96 (m, 2H), 7.93–7.87 (m, 1H), 7.84–7.79 (m, 2H), 7.48–7.42 (m, 1H), 7.40–7.35 (m, 1H). ^{13}C NMR (100 MHz, $CDCl_3$): δ 166.9, 149.9, 146.4, 138.5, 134.8, 132.0, 124.2, 123.7, 122.3.

***N*-(3-pyridinyl)phthalimide (2.38b)** ^{1}H NMR (400 MHz, $CDCl_3$): δ 8.81–8.78 (m, 1H), 8.65 (dd, J = 4.8, 1.5 Hz, 1H), 8.01–7.96 (m, 2H), 7.87–7.81 (m, 3H), 7.47 (ddd, J = 8.2, 4.8, 0.7 Hz, 1H). ^{13}C NMR (100 MHz, $CDCl_3$): δ 167.0, 149.0, 147.6, 135.0, 133.78, 131.77, 129.0, 124.2, 123.9.

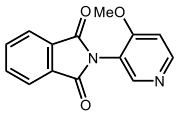

***N*-(4-methoxypyridin-3-yl)phthalimide (2.39)**

Following the general procedure for photocatalytic imidation (method A), starting from 4-methoxypyridine (102 μl, 1.00 mmol) and *N*-chlorophthalimide (90.8 mg, 0.50 mmol), the titled compound 2.39 was afforded as a light yellow solid after column chromatography (44.4 mg, 0.175 mmol, 35%). In the case following the method A starting from 4-methoxypyridine (50.7 μl, 0.50 mmol) and *N*-chlorophthalimide (181.6 mg, 1.00 mmol), the product 2.39 was provided in 40% yield (51.2 mg, 0.251 mmol).

^{1}H NMR (400 MHz, $CDCl_3$): δ 8.59 (d, J = 5.7 Hz, 1H), 8.41 (s, 1H), 7.99–7.94 (m, 2H), 7.83–7.79 (m, 2H), 6.99 (d, J = 5.7 Hz, 1H), 3.87 (s, 3H). ^{13}C NMR (100 MHz, $CDCl_3$): δ 167.0, 161.8, 152.4, 150.8, 134.6, 132.2, 124.1, 117.9, 107.6, 56.1. IR (neat): νmax 2360, 2342, 1717, 1593, 1511, 1433, 1381, 1288, 1192, 1102, 1016, 881, 828, 716 cm^{-1}. HRMS (EI) calcd. for $C_{14}H_{10}N_2O_3^+$ (M^+): 254.0691, found 254.0692.

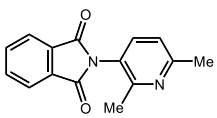

***N*-(2,6-dimethylpyridin-3-yl)phthalimide (2.40)**

Following the general procedure for photocatalytic imidation (method A), starting from 2,6-lutidine (116 μl, 1.00 mmol) and *N*-chlorophthalimide (90.8 mg, 0.50 mmol), the titled compound 2.40 was afforded as a light yellow solid after column chromatography (52.3 mg, 0.207 mmol, 41%). In the case following the method A starting from 2,6-lutidine (57.9 μl, 0.50 mmol) and *N*-chlorophthalimide (181.6 mg, 1.00 mmol), the product 2.40 was provided in 50% yield (63.1 mg, 0.250 mmol).

^{1}H NMR (500 MHz, $CDCl_3$): δ 7.99–7.94 (m, 2H), 7.84–7.80 (m, 2H), 7.42 (d, J = 8.0 Hz, 1H), 7.15 (d, J = 8.0 Hz, 1H), 2.60 (s, 3H), 2.42 (s, 3H). ^{13}C NMR (75 MHz, $CDCl_3$): δ 167.2, 159.2, 156.2, 136.9, 134.8, 132.1, 124.5, 124.1, 121.7, 24.6, 21.4. IR (neat): νmax 2925, 1783, 1764, 1728, 1582, 1474, 1381, 1266, 1229, 1107, 1084, 885, 828, 719 cm^{-1}. HRMS (EI) calcd. for $C_{15}H_{12}N_2O_2^+$ (M^+): 252.0899, found 252.0899.

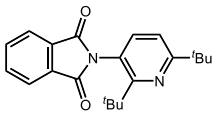

***N*-(2,6-di-*tert*-butylpyridin-3-yl)phthalimide (2.41)**

Following the general procedure for photocatalytic imidation (method A), starting from 2,6-di-*tert*-butylpyridine (224 μl, 1.00 mmol) and *N*-chlorophthalimide (90.8 mg, 0.50 mmol), the titled compound 2.41 was afforded as a white solid after column chromatography (59.2 mg, 0.176 mmol, 35%). In the case following the method A starting from 2,6-di-*tert*-butylpyridine (112 μl, 0.50 mmol) and *N*-chlorophthalimide (181.6 mg, 1.00 mmol), the product 2.41 was provided in 29% yield (48.0 mg, 0.143 mmol).

^{1}H NMR (400 MHz, $CDCl_3$): δ 7.98–7.92 (m, 2H), 7.82–7.76 (m, 2H), 7.26 (d, *J* = 8.2 Hz, 1H), 7.23 (d, *J* = 8.1 Hz, 1H)., 1.38 (s, 9H), 1.34 (s, 9H). ^{13}C NMR (100 MHz, $CDCl_3$): δ 168.9, 168.5, 164.7, 139.1, 134.6, 132.4, 124.1, 122.7, 117.4, 39.4, 38.1, 30.6, 30.3. IR (neat): νmax 2960, 2868, 1786, 1766, 1732, 1715, 1587, 1483, 1456, 1383, 1356, 1266, 1226, 1132, 1108, 1084, 904, 887, 831, 761, 721, 706, 690, 530 cm^{-1}. HRMS (EI) calcd. for $C_{21}H_{24}N_2O_2^+$ (M^+): 336.1838, found 336.1837.

2.6.4. References Cited

[i] Kim, H. J.; Kim, J.; Cho, S. H.; Chang, S. *J. Am. Chem. Soc.*, **2011**, *133*, 16382.

[ii] Shrestha, R.; Mukherjee, P.; Tan, Y.; Litman Z. C.; Hartwig J. F. *J. Am. Chem. Soc.* **2013**, *135*, 8480.

[iii] Khedkar, M. V.; Khan, S. R.; Sawant, D. N.; Bagal D. B.; Bhanage, B. M. *Adv. Synth. Catal.* **2011**, *353*, 3415.

[iv] Chen, D. C.; Ye H. Q.; Wu, H.; *Catal. Commun.* 2007, 8, 1527.

[v] Vamecq, J.' Bac, P.; Herrenknecht, C.; Maurois, P.; Delcourt P.; Stables, J. P. *J. Med. Chem.* **2000**, *43*, 1311.

[vi] Zhou, Y.; Rodriguez, A. L.; Williams, R.; Weaver, C. D.; Conn, P. J.; Lindsley, C. W.; *Bioorg. Med. Chem. Lett.* **2009**, *19*, 6502.

[vii] Khedkar, M. V.; Khan, S. R.; Dhake K. P.; Bhanage, B. M.; *Synthesis* **2012**, *44*, 2623.

[viii] Kantak, A. A.; Potavathri, S.; Barham, R. A.; Romano K. M.; DeBoef, B. *J. Am. Chem. Soc.* **2011**, *133*, 19960.

Chapter 3. Transition Metal-Catalyzed C–N Bond Formation

3.1. Cross-Coupling of Aromatic Bromides and Amines

Aryl bromides, prior to the emergence of cross-coupling reactions mediated by "transition metal" catalysis, participated in substitution processes as electrophiles only in limited settings. Due to the development of various protocols using transition metal catalysts, the traditionally unreactive electrophiles have been rendered as valuable building blocks in a variety of substitution reactions. In particular, the palladium-catalyzed protocols became one of the most widely utilized organic transformations, and the C–C bond-forming methods was recognized by the Nobel prize in 2010.[1] Extensive efforts to expand the usefulness of this chemistry to the formation of other types of chemical bonds, especially C–heteroatom bonds, have been made for the past decades, leading to the development of an array of mild and efficient protocols. Aromatic amine synthesis using cross-coupling reactions especially has received much attention due to the widespread application of aniline derivatives in pharmaceutical, agrochemical and materials. Thus, development of transition metal catalyst systems for efficient amination has represented one of the most important goals of the research in the field.

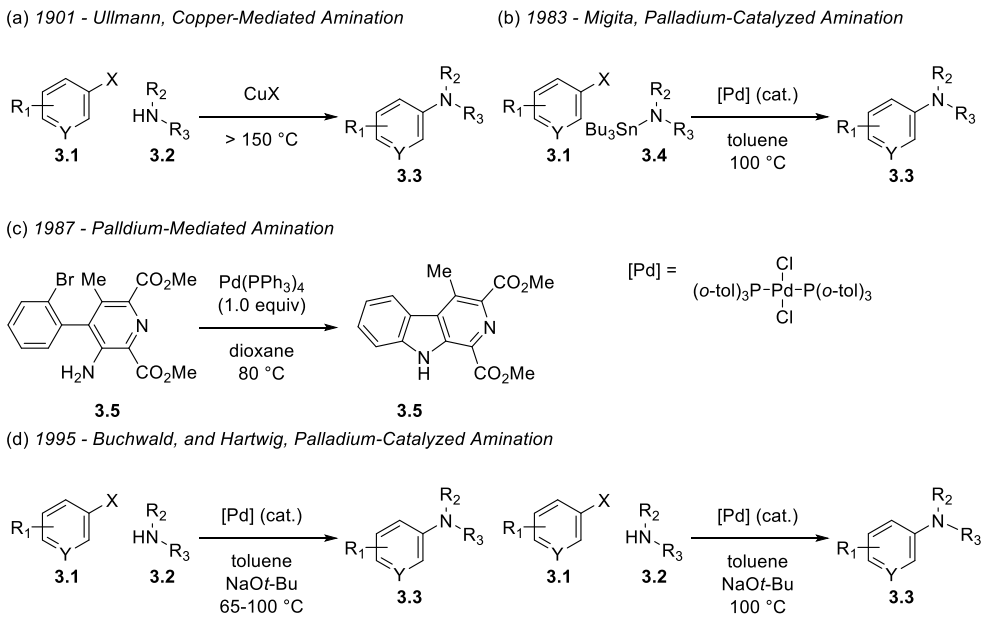

Scheme 3.1. Seminal Reports of Aryl Halides Amination

The synthetic plan based on disconnection of $C_{sp}{}^2$–N bonds allowed direct access to various aniline structures utilized in areas of primary and applied research.[2] The use of aryl amines as nucleophiles in a cross-coupling, in this regard, has been almost a century-old interest for organic chemists. In 1901, Ullmann reported the first C–N bond formation via amination of aromatic halides using copper as a mediator (**Scheme 3.1a**).[3] At this time, the mechanism of this transition metal-mediated amination was obscure, and no catalytic approach was available until 1983. Using a tin amide as a nucleophile used in the analogous Migita-Stille coupling, Migita first discovered the feasibility of performing catalytic amination using palladium (**Scheme 3.1b**). In 1987, the Boger group developed the tin free amination mediated by palladium (**Scheme 3.1c**).[4,5] Despite these pioneering observations, it was not until the Buchwald and Hartwig's striking discoveries that the transition metal-catalyzed *N*-arylation of amine nucleophiles became a cornerstone of modern organic synthesis of aromatic amines.[6] The recognition of the importance of a base assisted ligand exchange process provided a crucial basis for transition metal-catalyzed amination

chemistry (**Scheme 3.1d**).

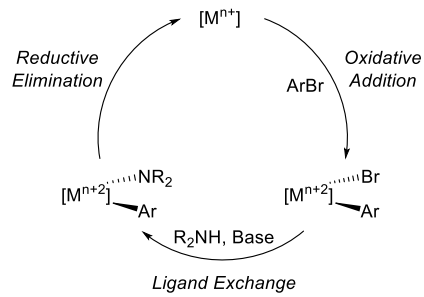

Figure 3.1. Elementary Steps in Transition Metal-Catalyzed Amination

Transition metal-catalyzed amination of aryl halides consists of three elementary steps – oxidative addition, amine substitution and reductive elimination (**Figure 3.1**). In the catalytic cycle, a low-valent transition metal activates an aryl halide by oxidative addition forming an organometallic intermediate which subsequently undergoes ligand exchange to bring an amine fragment to the metal center. The amido complex then affords the desired aromatic amine via reductive elimination and closes the catalytic cycle. Based on this general catalytic mechanism, many groups have explored new catalytic systems to improve the efficiency of the reaction and come up with distinct strategies for amination chemistry.

3.1.1. Palladium- and Nickel-Catalyzed Amination

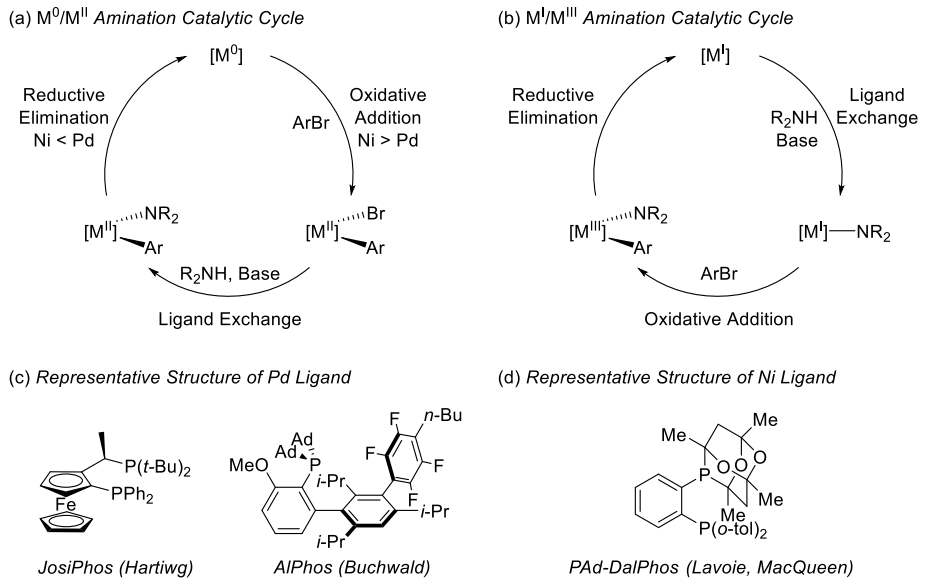

Figure 3.2. Palladium- and Nickel-Catalyzed Amination

With better mechanistic understanding, elaborated ligands and more efficient precatalysts, remarkable advances have been made in the palladium-catalyzed amination reactions for the past decades.[6c] However, nickel, the same Group 10 element as palladium, have remained largely unexplored since its seminal report.[7] The fundamental reactivity difference between nickel and palladium and the lack of studies on nickel catalysts might be the reason for the scarcity of new development in nickel-catalyzed amination reactions. Nickel possesses a higher oxidative addition rate because it is more electropositive compared to palladium, while palladium is more reactive toward the reductive elimination process (**Figure 3.2a**). This primary reactivity difference is evident as the initial research with palladium catalysts focused on the use of aryl bromides and aryl iodides, while nickel catalysts were utilized for unreactive electrophiles such as aryl fluorides, aryl nitriles, and aryl ethers.[8] Studies on the nickel complexes capable of forming C–N bonds have revealed that the Ni^{II} reductive elimination suffers from high energy barrier and that the facile C–N bond formation is possible with Ni^{III} intermediates as proposed by Hillhouse.[9] Since the

nickel can access multiple oxidation states, an alternative Ni^{I}/Ni^{III} mechanism is also viable (**Figure 3.2b**). The palladium catalyst system overcomes the slow oxidative addition by increasing the electron density and the steric hindrance of ancillary ligands. A notable example of this class of ligands is the biaryl phosphine invented by the Buchwald group (**Figure 3.2c**).[6c,10] The tailored ligand enhances not only the oxidative addition but also the reductive elimination. Facilitating two electronically opposing processes is possible as the ligand can adopt the mono-ligated form of palladium during all the elementary steps in cross-coupling. The destabilized palladium due to the coordination deficiency helps out the approach of Pd^{0} towards C_{sp^2}–X bonds. At the same time, the Pd^{II} species goes through rapid reductive elimination assisted by the mono-ligated complex's high energy state. Hartwig, on the other hand, focused on the stability of the cross-coupling catalyst which was enhanced by the high steric hindrance, structural rigidity, and electron-donating character of JosiPhos ligand.[11] Research on nickel catalysis also has been studied along the same line. Some breakthroughs in addressing the slow reductive elimination of nickel seem working with the modulation of ligand structure, but the mechanistic ambiguity of nickel-catalyzed aminations hampers the rationalization of these observations as the ligand might change the oxidation state preference of nickel intermediates (**Figure 3.2d**).[12]

3.1.2. Copper-Catalyzed Amination

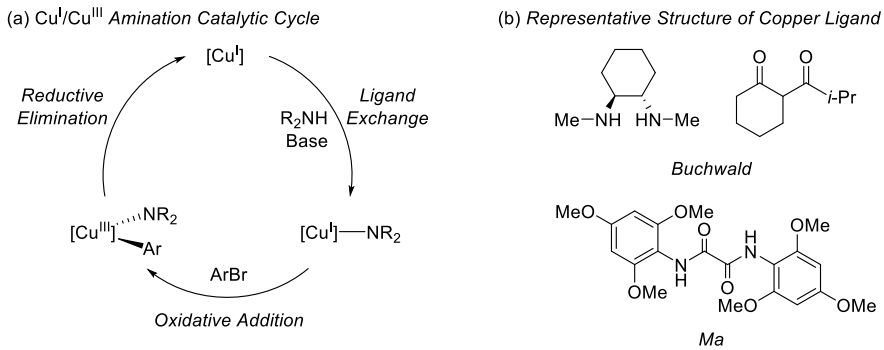

Figure 3.3. Copper-Catalyzed Amination

Among Group 11 transition metals, the most representative metal studied for amination is copper. A most widely believed working mechanism for the copper-catalyzed amination is the Cu^{I}/Cu^{III} redox cycle which is isoelectronic with palladium catalysis (**Figure 3.3a**).[13] Interestingly, copper as a catalyst for amination has not received much attention in early research even though the first seminal example of *N*-arylation of amines utilized organometallic copper as an intermediate. The energy barrier during the oxidative addition of a low-valent copper in comparison to palladium and nickel might have posed a challenge for the elaboration of reaction conditions.[14] Unlike palladium and nickel, the ligands developed for copper adopts second-row elements as the coordination centers (**Figure 3.3b**). Initial attempts by the Buchwald group demonstrated the reactivity enhancement in the amination of aryl iodides with diamine or diketone compounds.[15] Recently, the Ma group further elaborated the structure of the ligand expanding the scope of aryl halides to aryl chlorides.[16] However, the thermal cross-coupling approaches using a copper still suffers from the slow oxidative addition despite considerable endeavors in designing ligands to promote the catalytic activity of copper.

3.1.3. Recent Palladium-, Nickel, and Copper-Catalyzed Amination

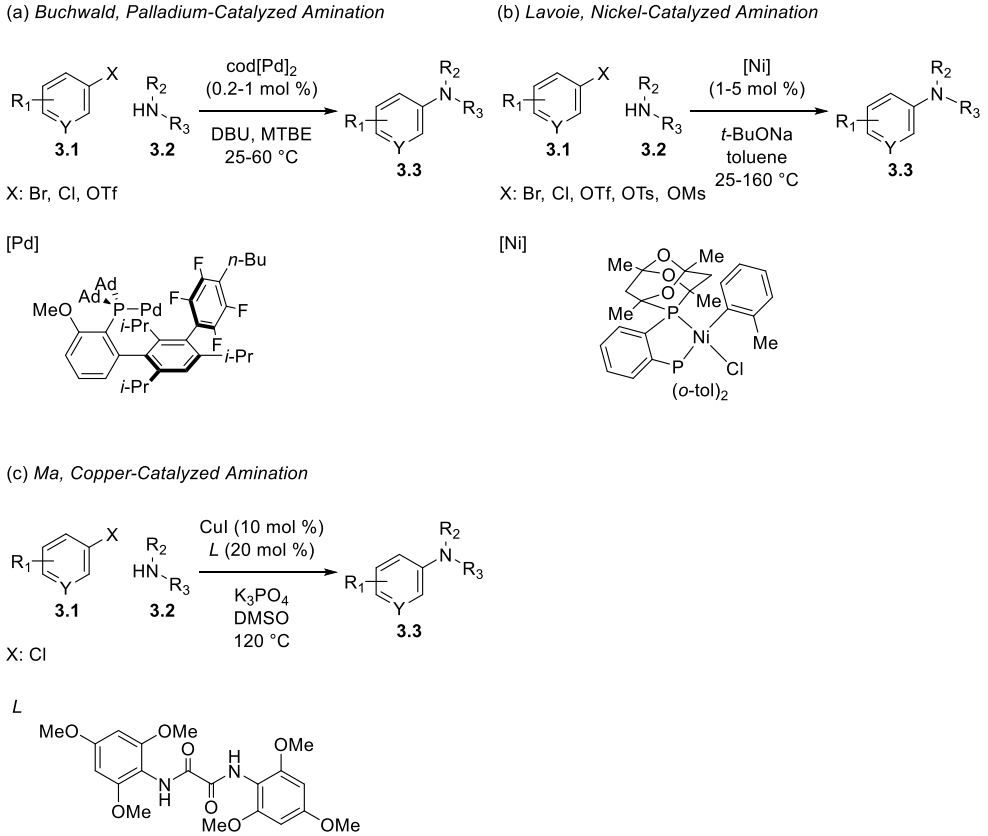

Scheme 3.2. State of The Art of Transition Metal-Catalyzed Amination

The current state of the art of palladium-, nickel-, and copper-catalyzed aminations features much milder and efficient conditions thanks to the designed ligands for overcoming the intrinsic reactivity limitations of these transition metals. As illustrated, the Buchwald's pioneering works on palladium catalysis enabled the most effective coupling even with aryl chloride substrates owing to the exquisite design of Pd^0 precatalysts and ligands (**Scheme 3.2a**).[10b] Similar efforts to design ligands and precatalysts for nickel catalysis also led to a breakthrough (**Scheme 3.2b**).[12] The Ma's new ligand imparted good catalytic efficiency to copper in amination (**Scheme 3.2c**).[16] Notably, all the reactions can be carried out with reduced catalyst loadings and reaction temperatures as compared with those of their initial discoveries.

3.2. Photoinduced Cross-Coupling Chemistry

An alternative approach of changing the electronic structure of transition metals using photochemical activation, rather than elaborating the ligand structure, became a popular platform to address reactivity dilemma.[17] The use of a cross-coupling catalyst in conjunction with photocatalysts or the direct excitation of the metal catalysts proved to be effective strategies circumventing the insufficient reactivity of ground-state transition metals.

3.2.1. Photoredox/Nickel-Catalyzed Amination

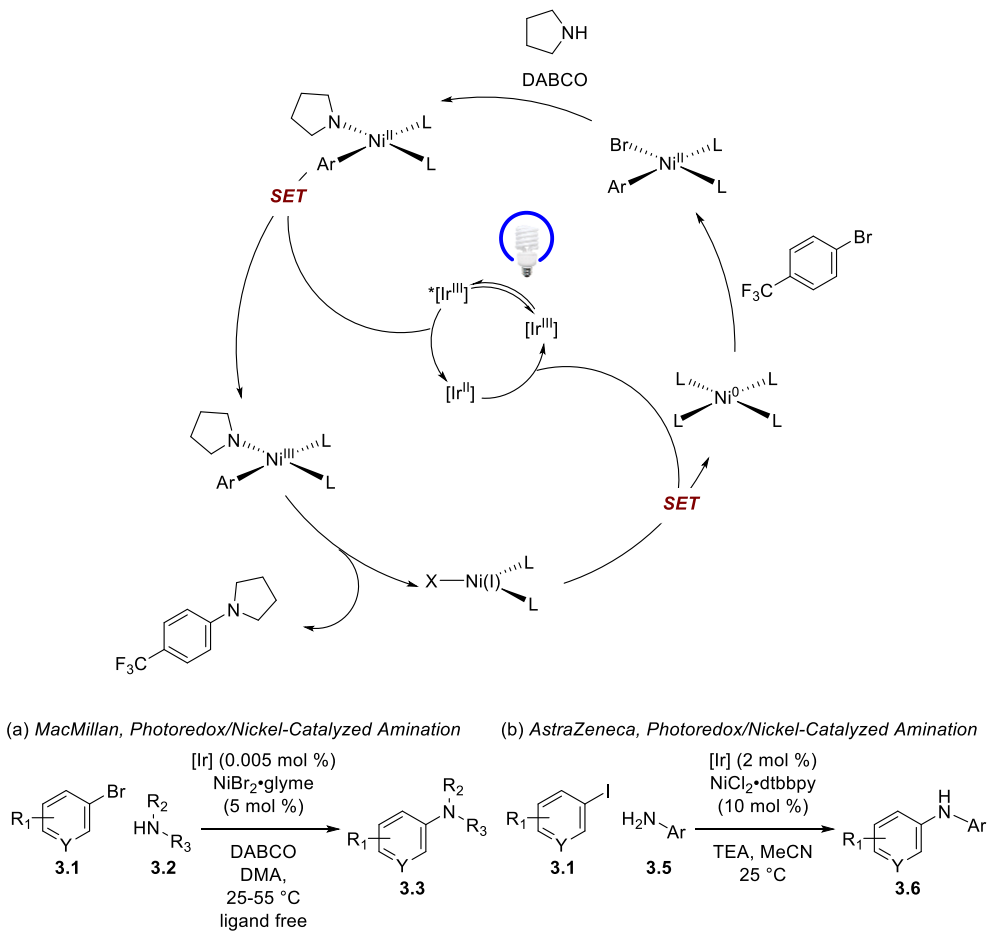

Figure 3.4. Photoredox/Nickel-Catalyzed Amination

The photoredox/nickel dual-catalyzed reaction presented a new approach to address the slow reductive elimination problem of the nickel-catalyzed *N*-arylation. With the photoredox catalysts capable of mediating both the one-electron oxidation and reduction, two independent Ni^{0}/Ni^{II} oxidative addition and Ni^{III}/Ni^{I} reductive elimination could be operative in a single reaction system, thus enabling efficient oxidative addition and rapid reductive elimination at the same time (**Figure 3.4**).[17b] The critical step in this metallaphotoredox-catalyzed amination is proposed to be the single-electron oxidation of the organometallic Ni^{II}, concurrently synthesized from an aryl bromide, to the Ni^{III} intermediate, which upon reductive elimination affords the aromatic amine and Ni^{I} species. The Ni^{I} complex is further reduced to close the catalytic cycle. In 2016, MacMillan and coworkers published a protocol using this metallaphotoredox catalysis, and notably, this approach proceeded without employing an ancillary ligand for the cross-coupling catalyst (**Figure 3.4a**).[18] The photocatalyst taking over the role of ligands in cross-coupling proved successful strategy achieving *N*-arylation of a broad range of aromatic amines. The research group of AstraZeneca also published a similar approach, although a ligated nickel complex was used as the catalyst (**Figure 3.4b**).[19]

3.2.2. Photoinduced Copper-Catalyzed Amination

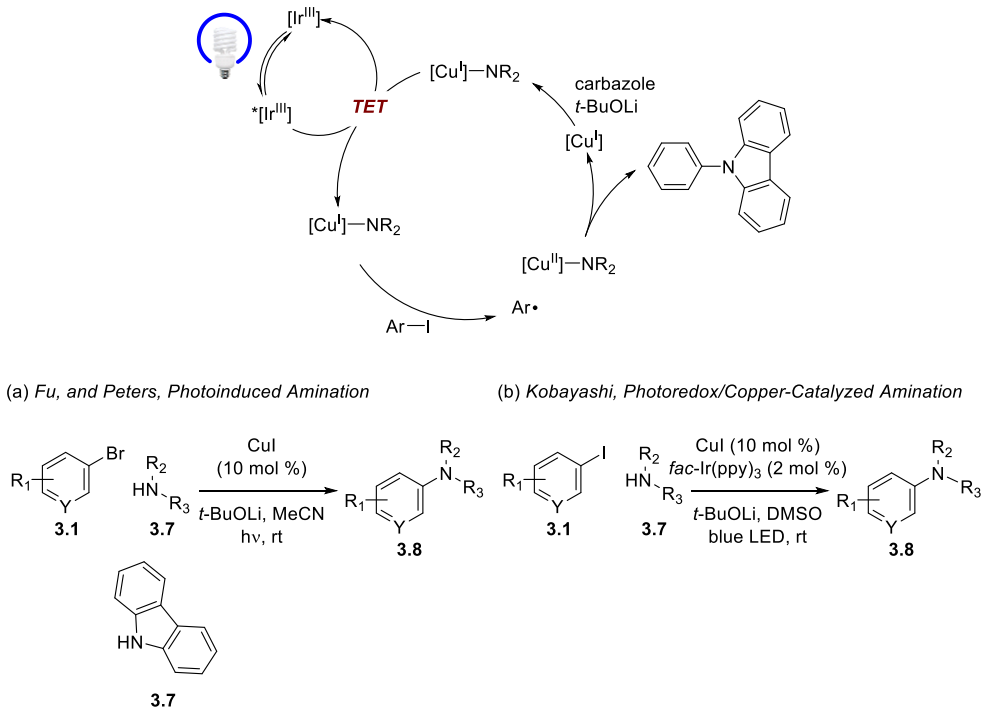

Figure 3.5. Photoinduced Copper-Catalyzed Amination

Studies toward the development of copper-catalyzed amination reactions suggested a possibility of the involvement of single electron transfer in oxidative addition processes.[14a,c] A series of experiments performed by the Hartwig group showed that the reaction between Cu^{II}-amido complex and carbon-centered radical could rapidly form a C–N bond.[20] Taking into account these observations, the work by Fu and Peters presented an alternative way of activation for copper-catalyzed C-N cross-coupling that made use of light to initiate the arylation of carbazole **3.7 (Figure 3.5)**.[17a] The excited-state copper acts as a one-electron reductant for organohalides while serving as a cross-coupling catalyst at the same time. Initial reports utilized the UV region photonic energy to activate the catalysts for *N*-arylation of carbazole with aromatic halides. Engineering of the ligand further allowed the use of visible light as the energy source for the $C_{sp}{}^3$–N bond formation with alkyl halides and amines, albeit without arylation reactivity.[21] In 2015, the Kobayashi

group realized the visible-light-driven arylation of carbazoles using an external iridium photocatalyst as a photosensitizer.[22] However, notwithstanding the success of these approaches, it is important to note that the photoinduced copper-catalyzed arylation reactions are efficient only with limited nucleophiles. The narrow choice of potential amine coupling partners in this photoinduced copper-catalyzed amination is due to the photochemical and electrochemical property of copper dependent critically on coupling nucleophiles.

3.3. Conclusion

There have been many endeavors toward the development of efficient transition metal-catalyzed C–N bond-forming reactions. Notably, the utilization of specially designed ligands for promoting the elementary steps of cross-coupling processes have been the primary approaches. With the deep understanding of the mechanism of the catalytic *N*-arylation, the palladium-catalyzed amination has risen to prominence while progress have also been made in nickel and copper catalysis through the ligand manipulation. Visible-light-driven catalysis, on the other hand, provides a new paradigm for driving the catalytic cycle of amination. The separation of metal oxidation states for oxidative addition, and reductive elimination enabled by the electron transfer mediated via photoredox catalysis allows for energetically favored two processes to be used in a single reaction. Copper catalysis with light irradiation also offers an alternative mode of activating organic halides by forming carbon-centered radical intermediates via light-driven SET, thus bypassing the slow oxidative addition of copper.

3.4. References

1) Johansson Seechurn, C. C. C.; Kitching, M. O.; Colacot, T. J.; Snieckus, V. *Angew. Chem. Int. Ed*. **2012,** *51*, 5062.

2) (a) Schlummer, B.; Scholz, U. *Adv. Synth. Catal.* **2004,** *346*, 1599. (b) Torborg, C.; Beller, M. *Adv. Synth. Catal.* **2009,** *351*, 3027.

3) Ulmann, F. *Chem. Ber.* **1903**, *36*, 2382. Goldberg, I *Chem. Ber.* **1906**, *39*, 1691.

4) Masanori, K.; Masayuki, K.; Toshihiko, M. *Chem. Lett.* **1983,** *12*, 927.

5) Dale Boger, L.; Panek, J. S. *Tetrahedron Lett.* **1984,** *25*, 3175.

6) (a) Guram, A. S.; Rennels, R. A.; Buchwald, S. L. *Angew. Chem. Int. Ed.* **1995,** *34*, 1348. (b) Louie, J.; Hartwig, J. F. *Tetrahedron Lett.* **1995,** *36*, 3609. For a review, see (c) Ruiz-astillo, P.; Buchwald, S. L. *Chem. Rev.* **2016,** *116*, 12564.

7) Wolfe, J. P.; Buchwald, S. L. *J. Am. Chem. Soc.* **1997,** *119*, 6054.

8) Selected examples for the nickel-catalyzed aryl fluoride activation, see (a) Mesganaw, T.; Garg, N. K. *Org. Process Res. Dev.* **2013**, *17*, 29. (b) Li, B.-J.; Yu, D.-G.; Sun, C.-L.; Shi, Z.-J. *Chem. Eur. J.* **2011**, *17*, 1728. (c) Penney, J. M.; Miller, J. A. *Tetrahedron Lett.* **2004**, *45*, 4989. For the aryl nitriles, see (d) García, J. J.; Brunkan, N. M.; Jones, W. D. *J. Am. Chem. Soc.* **2002**, *124*, 9547. For the aryl ethers, see (e) Tobisu, M.; Xu, T.; Shimasaki, T.; Chatani, N. *J. Am. Chem. Soc.* **2011**, *133*, 19505. (f) Liu, X.-W.; Echavarren, J.; Zarate, C.; Martin, R. *J. Am. Chem. Soc.* **2015**, *137*, 12470.

9) Koo, K.; Hillhouse, G. L. *Organometallics* **1995,** *14*, 4421. Lin, B. L.; Clough, C. R.; Hillhouse, G. L. *J. Am. Chem. Soc.* **2002,** *124*, 2890. Macgregor, S. A.; Neave, G. W.; Smith, C. *Faraday Discuss.* **2003,** *124*, 111.

10) (a) Martin, R.; Buchwald, S. L. *Acc. Chem. Res.* **2008,** *41*, 1461. (b) Dennis, J. M.; White, N. A.; Liu, R. Y.; Buchwald, S. L. *J. Am. Chem. Soc.* **2018,** *140*, 4721.

11) (a) Shen, Q.; Shekhar, S.; Stambuli, J. P.; Hartwig, J. F. *Angew. Chem. Int. Ed.* **2005,** *44*, 1371. (b) Shen, Q.; Ogata, T.; Hartwig, J. F. *J. Am. Chem. Soc.* **2008,** *130*, 6586. (c) Ogata, T.; Hartwig, J. F. *J. Am. Chem. Soc.* **2008,** *130*, 13848. (d) Shen, Q.; Hartwig, J. F. *Org. Lett.*

2008, *10*, 4109.

12) Lavoie, C. M.; MacQueen, P. M.; Rotta-Loria, N. L.; Sawatzky, R. S.; Borzenko, A.; Chisholm, A. J.; Hargreaves, B. K. V.; McDonald, R.; Ferguson, M. J.; Stradiotto, M. *Nat. Commun.* **2016,** *7*, 11073.

13) Beletskaya, I. P.; Cheprakov, A. V. *Organometallics* **2012,** *31*, 7753.

14) (a) Jones, G. O.; Liu, P.; Houk, K. N.; Buchwald, S. L. *J. Am. Chem. Soc.* **2010,** *132*, 6205. (b) Yu, H.-Z.; Jiang, Y.-Y.; Fu, Y.; Liu, L. *J. Am. Chem. Soc.* **2010,** *132*, 18078. (c) Giri, R.; Brusoe, A.; Troshin, K.; Wang, J. Y.; Font, M.; Hartwig, J. F. *J. Am. Chem. Soc.* **2018,** *140*, 793.

15) (a) Klapars, A.; Antilla, J. C.; Huang, X.; Buchwald, S. L. *J. Am. Chem. Soc.* **2001,** *123*, 7727. (b) Shafir, A.; Buchwald, S. L. *J. Am. Chem. Soc.* **2006,** *128*, 8742.

16) Zhou, W.; Fan, M.; Yin, J.; Jiang, Y.; Ma, D. *J. Am. Chem. Soc.* **2015,** *137*, 11942.

17) (a) Creutz, S. E.; Lotito, K. J.; Fu, G. C.; Peters, J. C. *Science* **2012,** *338*, 647. (b) Twilton, J.; Le, C.; Zhang, P.; Shaw, M. H.; Evans, R. W.; MacMillan, D. W. C. *Nat. Rev. Chem.* **2017,** *1*, 0052.

18) Corcoran, E. B.; Pirnot, M. T.; Lin, S.; Dreher, S. D.; DiRocco, D. A.; Davies, I. W.; Buchwald, S. L.; MacMillan, D. W. C. *Science* **2016,** *353*, 279.

19) Oderinde, M. S.; Jones, N. H.; Juneau, A.; Frenette, M.; Aquila, B.; Tentarelli, S.; Robbins, D. W.; Johannes, J. W. *Angew. Chem. Int. Ed.* **2016,** *55*, 13219.

20) Tran, B. L.; Li, B.; Driess, M.; Hartwig, J. F. *J. Am. Chem. Soc.* **2014,** *136*, 2555.

21) (a) Kainz, Q. M.; Matier, C. D.; Bartoszewicz, A.; Zultanski, S. L.; Peters, J. C.; Fu, G. C. *Science* **2016,** *351*, 681. (b) Matier, C. D.; Schwaben, J.; Peters, J. C.; Fu, G. C. *J. Am. Chem. Soc.* **2017,** *139*, 17707.

22) Yoo, W.-J.; Tsukamoto, T.; Kobayashi, S. *Org. Lett.* **2015,** *17*, 3640.

Chapter 4. Photosensitized Nickel-Catalyzed C–N Bond Formation

4.1. Photosensitized Nickel Catalysis

Photoredox/nickel dual catalysis has become a popular research field since its original reports by MacMillan, Doyle, and Molander.[1] The change of the nickel-catalyzed cross-coupling mechanism by incorporating an SET process led to the development of new bond-forming protocols. The success of these approaches lies in the promotion of the energetically unfavorable reductive elimination of a Ni^{II} complex by formation of a reactive Ni^{III} intermediate via radicals or one-electron oxidation.[1c,2] Photosensitization of nickel has emerged as a powerful approach to address the problems associated with nickel-catalyzed cross-coupling chemistry, providing an alternative to the high-valent nickel approach. The triplet-excited Ni^{II} complex can participate in multiple chemical events, such as reductive elimination, single electron transfer, and halogen radical formation (**Figure 4.1**).[3] In these approaches, the photocatalyst not only acts as a photosensitizer playing the role of light-harvesting but activates the nickel toward its triplet-excited state via the Dexter energy transfer that circumvents the intersystem crossing process.

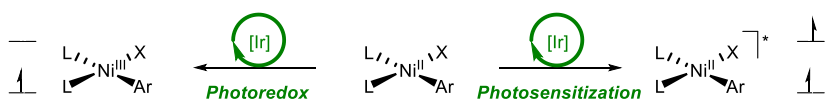

- *accessed by radical capture or direct oxidation*
- *rapid bond-making reductive elimination*

- *accessed by energy transfer or direct excitation*
- *rapid bond-making reductive elimination*
- *single electron transfer*
- *halogen atom synthesis*

Figure 4.1. Photocatalytic Activation Strategies of Nickel Complex

4.1.1. Halogen Radical Formation by Excited Nickel Catalysis

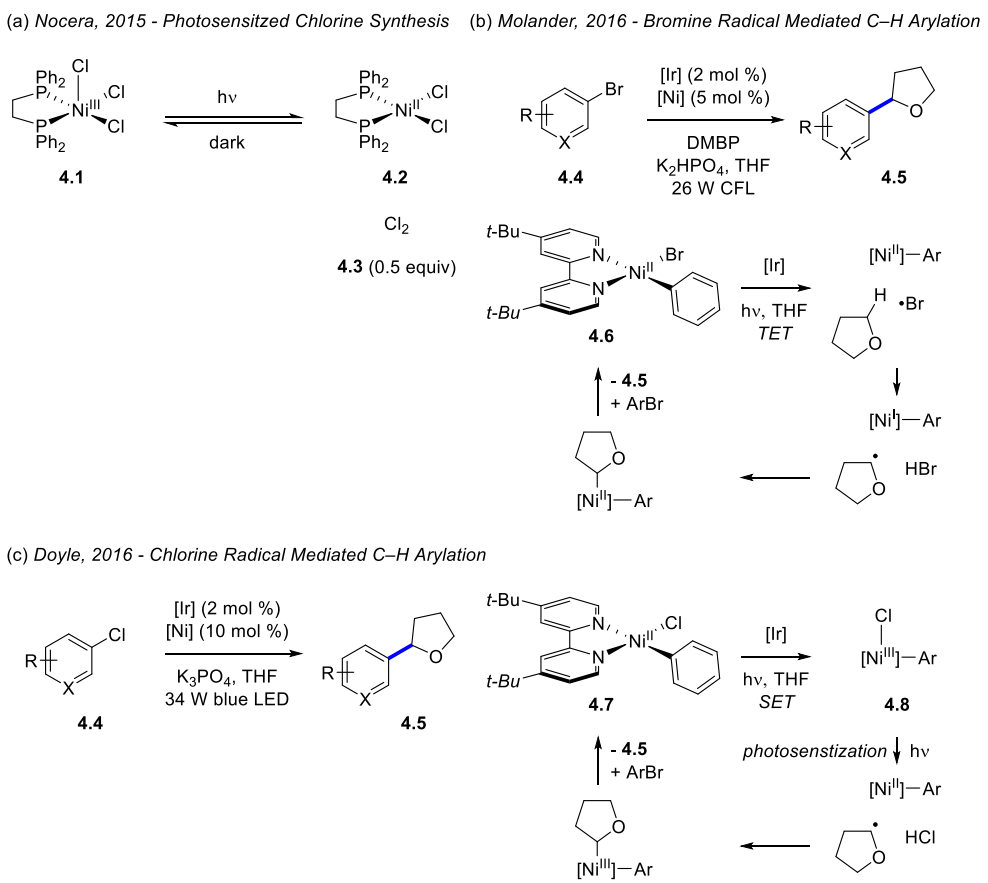

Scheme 4.1. Photosensitized Nickel-Catalyzed Halogen Radical Formation

Uncovering new reactivities of transition metals offer potential opportunities to develop new catalytic transformations that can lead to unprecedented applications in organic synthesis. As a milestone reactivity for the design of a nickel-based solar fuel cell, the production of halogen radicals using a photoexcited nickel was reported in 2015 by Nocera and colleagues, which rendered an alternative means for Cl–Cl bond formation (**Scheme 4.1a**).[3a] The excitation of Ni^{III} **4.1** showed light-dependent chlorine generation that had not been considered a plausible transformation with first-row transition metals. After this seminal report, Molander and Doyle in 2016 made similar observations, which were tapped into a photosensitization strategy for the activated C_{sp}^3–H bond arylation with the assistance of an iridium photocatalyst (**Scheme 4.1b, and 4.1c**).[3b,3c] By using the

photosensitized nickels as halogen radical precursors, various alkyl ethers could serve as nucleophiles in the nickel-catalyzed cross-coupling reaction with aryl halids giving arylated ethers **4.5**. Interestingly, Molander proposed that the photosensitization of Ni^{II} **4.6** resulted in the decomposition of the organometallic nickel liberating a bromine radical, which subsequently became another Ni^{II} containing fragments giving the product. Doyle, on the other hand, performed a systematic study with Ni^{II} intermediate **4.7** and revealed the oxidized Ni^{III} **4.8** to be the photosensitized catalyst for chlorine radical formation.

4.1.2. Ether Bond Synthesis by Excited Nickel Catalysis

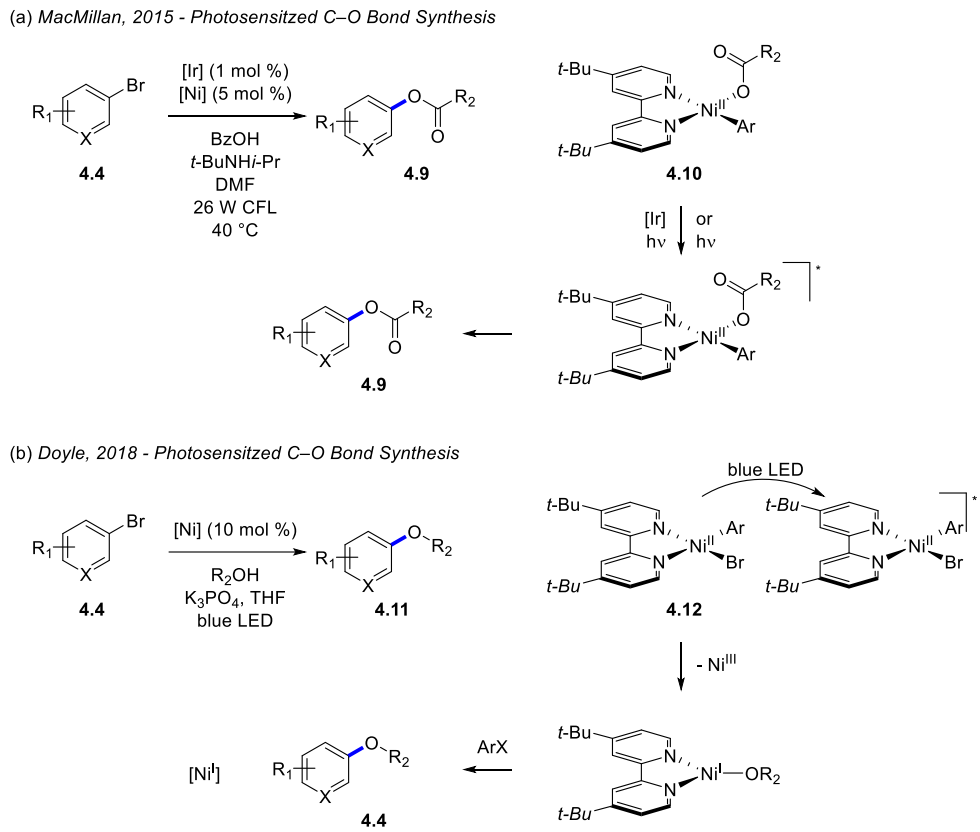

Scheme 4.2. Cross-Coupling using Excited Nickel

It is essential to activate metal intermediates that facilitate either or both oxidative addition and reductive elimination steps in the design of a catalytic cross-coupling reaction. Two approaches were proposed using excited nickel complexes for catalytic C–O bond formations. One published by MacMillan and McCusker utilizes photosensitization of the organometallic nickel intermediate to speed up the challenging reductive elimination of a Ni^{II} (**Scheme 4.2a**), and the other is to generate a reactive Ni^{I} intermediate by single electron transfer with the excited Ni^{II} complex as reported by Doyle and coworkers (**Scheme 4.2b**).[3d,3e] The work from MacMillan and McCusker achieved an unprecedented cross-coupling between aryl halides **4.4** and carboxylic acids affording ester **4.9** by photosensitization of the organometallic nickel intermediate. In this study, the light-

harvesting role by the photosensitizer catalyst circumvented the inefficient intersystem crossing of nickel **4.10** accessing a triplet-excited state that participated in the challenging C–O bond-forming reductive elimination step. Importantly, physical contacts between the two metal catalysts were characterized with UV-visible spectra, lending support to the Dexter triplet energy transfer mechanism.[4] The Doyle group demonstrated that visible light could activate Ni^{II} **4.12** to get an electron from another Ni complex **4.12** for the formation of Ni^{I} species. The Ni^{I} then participated in the Ni^{I}/Ni^{III} catalytic cycle for the etherification of aryl halides. Notably, a hot intersystem crossing process was proposed on account of the similar energy levels of ^{1}MLCT and ^{3}MLCT Ni^{II} complexes. It was also suggested that the fine-tuning of ligands on the nickel center might give rise to an alternative metal complex for the d^6 transition metal-based photocatalysts.

4.2. Photosensitized Nickel-Catalyzed Sulfonamidation of Aryl Halides

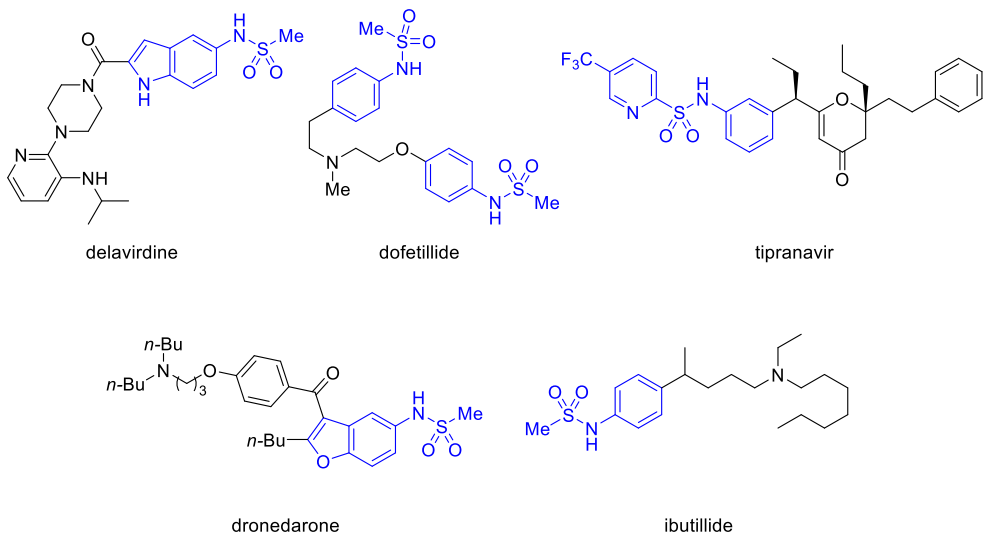

Figure 4.2. *N*-Aryl Sulfonamides in Pharmaceuticals

The sulfonamide is a mainstay structural motif of numerous bioactive compounds and one of the first systematically utilized functional groups in drug design (**Figure 4.2**).[5] In particular, secondary sulfonamides are used as bioisosteres of carboxylic acids as they have similar hydrogen bonding interaction properties and pendant aryl or heteroaryl groups can conveniently modulate the pK_a of N–H bonds.[6] Most commonly utilized methods for *N*-aryl sulfonamide synthesis have been based on substitution of sulfonyl chlorides with anilines, which is not an ideal strategy owing to the use and the formation of genotoxic reagents and byproducts.[7] In contrast, cross-coupling of sulfonamides and aryl bromides can access a broad range of sulfonamidated products without employing toxic reagents.

The palladium-catalyzed cross-coupling has emerged as a powerful means for construction of C–N bonds and decades of investigation have led to the development of an array of mild protocols.[8] Notwithstanding these developments, however, the Buchwald-Hartwig reactions using sulfonamides as nucleophiles are inefficient due to the attenuation of their nucleophilicity by the presence of strong electron-withdrawing sulfonyl groups, which impedes the amine ligand exchange step.[9] Also, the use of an earth-abundant metal such as nickel, in place of palladium, for the amination may be of enormous economic advantage but has remained unexplored.

Recently, the "switched on" reactivity of organometallics with photonic energy showed its usefulness in many chemical bond formations. The change of oxidation states or electronic structure of organometallic compounds using photonic energy provided unique activation modes for transition metal-catalyzed processes.[10] Notably, without employing elaborated ligands, these approaches modulated the reactivity of the key intermediates in organic transformations. We postulated that adopting this approach for the nickel-catalyzed C–N bond formation would address the limitations of previous sulfonamidation approaches. More specifically, we questioned whether using a triplet-excited nickel could facilitate the elementary step of the catalytic cycle leading to efficient sulfonamidation in a general sense.

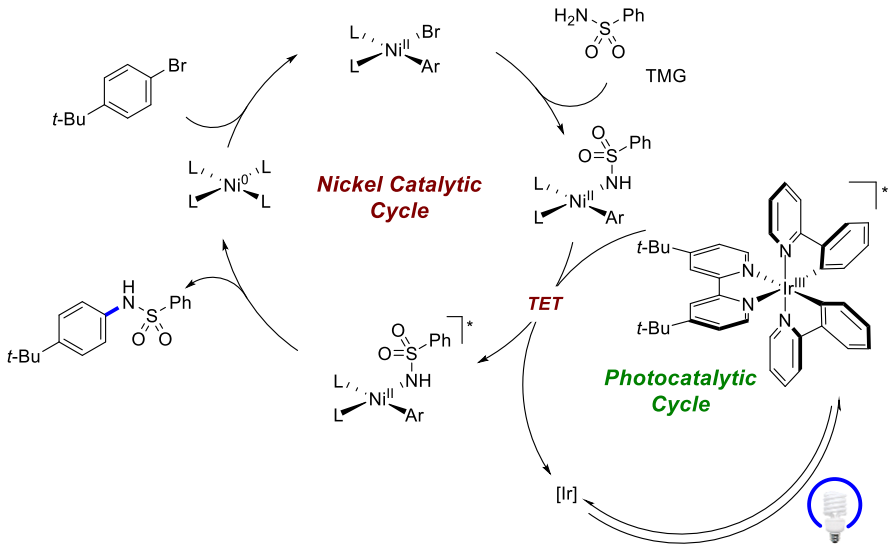

Figure 4.3. Photosensitized Sulfonamidation

Depicted is a more detailed picture of this proposal (**Figure 4.3**). In the catalytic cycle, a low-valent nickel activates the aryl halide substrate by oxidative addition forming an organometallic Ni^{II} intermediate, and a base triggers the ligand exchange furnishing a Ni^{II} sulfonamido complex. The iridium complex undergoes a ^{3}MLCT process on absorbing visible-light, and this excited iridium transfers its triplet energy to the ground state Ni^{II}.[11] The triplet-excited nickel thus formed undergoes reductive elimination, an otherwise thermodynamically unfavorable process, providing the desired product and completing the catalytic cycle. This dual-catalytic approach would bypass the inefficient light absorption problem of organometallic nickel species by involving the iridium photocatalyst, assigning the light-harvesting and the bond-making roles to separate catalysts in a reaction.

4.2.1. Discovery and Optimization of Sulfonamidation

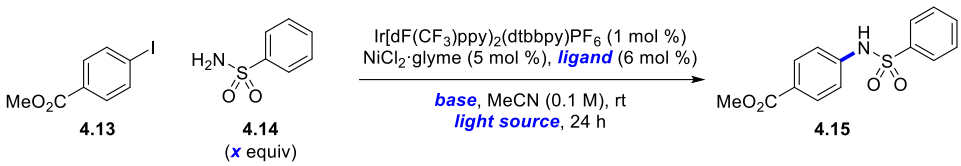

entry	*ligand*	*base*	*sulfonamide (equiv)*	*light source*	4.15 (%)
1	dtbbpy	TEA (1.0 equiv)	1	20 W CFL	33
2	phen	TEA (1.0 equiv)	1	20 W CFL	44
3	bpy	TEA (1.0 equiv)	1	20 W CFL	39
4		TEA (1.0 equiv)	1.5	20 W CFL	41
5	phen	TEA (1.0 equiv)	1.5	20 W CFL	51
6	phen	TEA (1.5 equiv)	1.5	20 W CFL	52
7	phen	TEA (1.0 equiv)	1.5	30 W blue LED	62
8	phen	TEA (1.0 equiv)	2	30 W blue LED	57
9	phen	K_2CO_3 (1.0 equiv)	1.5	30 W blue LED	29
10	phen	DIPEA (1.0 equiv)	1.5	30 W blue LED	42
11	phen	DBU (1.0 equiv)	1.5	30 W blue LED	85
12	phen	DABCO (1.0 equiv)	1.5	30 W blue LED	15
13	phen	DBU (1.5 equiv)	1.5	30 W blue LED	95
14	dtbbpy	DBU (1.5 equiv)	1.5	30 W blue LED	95
15		DBU (1.5 equiv)	1.5	30 W blue LED	95

[a]Yields are determined by NMR analysis with an internal standard using ArI **4.13** (0.2 mmol).

Table 4.1. Initial Discovery and Optimization of Sulfonamidation[a]

The reaction was initially tested and optimized with methyl 4-iodobenzoate (**4.13**) and benzenesulfonamide (**4.14**) as the substrates (**Table 4.1**). The screening experiments revealed little to no ligand effect on the reactivity, albeit the use of phen was slightly beneficial over other ligands, such as bpy and dtbbpy for the formation of arylated sulfonamide **4.15** (*entries* 1-3). It was noteworthy that in the absence of an added ligand, the reaction still showed a significant amount of product formation (*entry* 4). Changing the amount of amide **4.14** to 1.5 equivalent and the use of blue LED resulted in better yields of the product (*entries* 5-8). To further enhance the efficiency of this dual-catalytic strategy, we tested several bases and found DBU (1,8-diazabicyclo(5.4.0)undec-7-ene) to be optimal for this reaction system (*entries* 9-13). Interestingly, the involvement of DBU diminished

the ligand dependency of the reaction significantly, possibly suggesting that the nickel complex ligated with the strongly electron-donating DBU can act as an alternative catalyst for the bipyridine ligand coordinated nickel (*entries* 14 and 15).

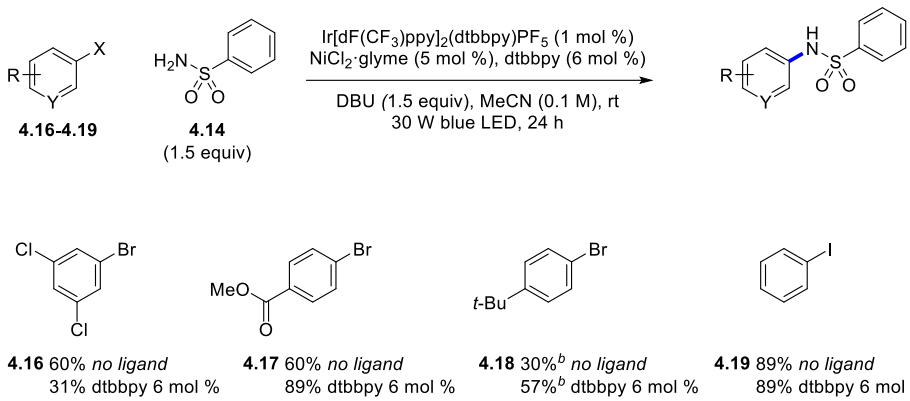

[a]Yields are determined by isolated products using ArX (0.5 mmol). [b]Using $Ir(ppy)_2(dtbbpy)PF_6$ (1 mol %), DBU (0.5 equiv), and K_2CO_3 (1.5 equiv) at 55 °C.

Table 4.2. Ligand Dependence of Substrates with The Initial Reaction Conditions[a]

The effect of ligand depended on the electronic nature of aryl halide substrates (**Table 4.2**). For some substrates, the addition of dtbbpy ligand proved more effective (**4.17**, and **4.18**) while better reactivity was detected with ligand-free conditions (**4.16**). The trend did not seem to be conducive to rationale with a single reactivity parameter. At this point, we initiated collaboration with Professor David MacMillan, along with his coworkers Stefan McCarver and Emily Corcoran, to examine whether the ligand was an essential ingredient for efficient sulfonamidation.

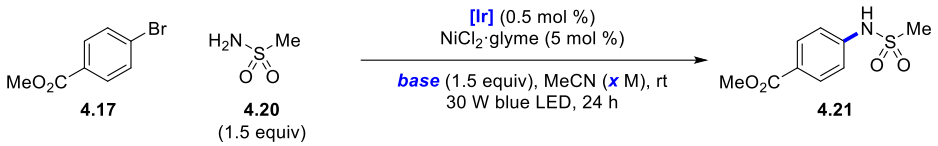

entry	[Ir]	*base*	*concentration*	4.17 (%)	4.21 (%)
1[b]	Ir[dF(CF$_3$)ppy$_2$](dtbbpy)PF$_6$	DBU	0.1	40	60
2[b,c]	Ir[dF(CF$_3$)ppy$_2$](dtbbpy)PF$_6$	DBU	0.1	46	37
3[b]	Ir[dF(CF$_3$)ppy$_2$](dtbbpy)PF$_6$	DBU	0.25	14	73
4	Ir[dF(CF$_3$)ppy$_2$](dtbbpy)PF$_6$	DBU	0.25	38	60
5[b]	Ir[dF(CF$_3$)ppy$_2$](dtbbpy)PF$_6$	TMG	0.25	21	77
6[b]	Ir(ppy$_2$)(dtbbpy)PF$_6$	TMG	0.25	15	75
7[b]	Ir(dFppy$_2$)(dtbbpy)PF$_6$	TMG	0.25	20	68
8[b]	Ir(dF(Me)ppy$_2$)(dtbbpy)PF$_6$	TMG	0.25	23	67
9[b]	Ir(ppy$_2$)(dtbbpy)PF$_6$	DBU	0.25	14	82
10	Ir(ppy$_2$)(dtbbpy)PF$_6$	DBU	0.25	8	86
11	Ir(ppy$_2$)(dtbbpy)PF$_6$	TMG	0.25	11	85

[a] Yields are determined by NMR analysis with an internal standard using ArBr **4.17** (0.2 mmol). [b]TBAI (0.1 equiv). [c][Ir] (1 mol %).

Table 4.3. Initial Ligand-Free Sulfonamidation Optimization[a]

As alkylsulfonamides showed diminished reaction efficiency under the previous conditions, the optimization studies for ligand-free conditions were carried out using methanesulfonamide (**4.20**) (**Table 4.3**). Based on the observation that tetrabutylammonium iodide (TBAI) slightly enhanced yields for the sulfonamidation of aryl bromides, the initial experiments adopted TBAI as an additive. Decreasing amount of the photocatalyst from 1mol % to 0.5mol %, and increasing the concentration from 0.1 M to 0.25 M elevated yield of the product **4.21**, while the use of TBAI was still necessary to get better results with DBU (*entries* 1-4). TMG (1,1,3,3-tetramethylguanidine), which was found to be beneficial by Emily Corcoran before leaving the project, proved to be a better choice than DBU (*entry* 5), possibly because the more electron-rich base acted as a better ligand in the oxidative addition step. Interestingly, a weaker triplet photosensitizer, Ir(ppy)$_2$(dtbbpy)PF$_6$ (50.0 kcal/mol), had efficiency comparable to that of a stronger triplet photosensitizer Ir[dF(CF$_3$)ppy]$_2$(dtbbpy)PF$_6$ (59.5 kcal/mol) despite the big difference in triplet energy between the two iridium complexes. Stronger photosensitizers, Ir(dFppy)$_2$(dtbbpy)PF$_6$ (55.4

kcal/mol) and Ir(dF(Me)ppy)$_2$(dtbbpy) (55.6 kcal/mol), showed decreased performance in this reaction (*entries* 6-8).[12] This result implies that the more oxidizing photocatalysts may have a lower concentration of the ^{3}MLCT iridium due to the presence of redox-active compounds, such as TMG, in the reaction mixture. However, the much stronger photosensitizer Ir[dF(CF$_3$)ppy]$_2$(dtbbpy)PF$_6$ did not seem to be significantly affected by the concentration. The use of Ir(ppy)$_2$(dtbbpy)PF$_6$ allowed the omission of the TBAI additive and unexpectedly resulted in excellent yields of the product (*entries* 9-11).

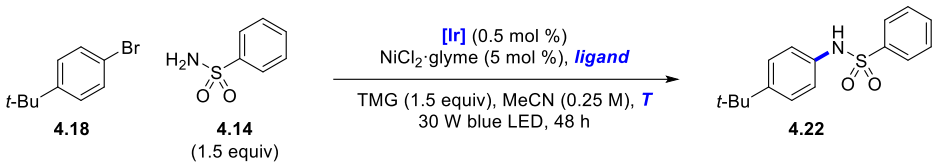

entry	[Ir]	*ligand*	*temperature*	4.18 (%)	4.22 (%)
1[b]	$Ir(ppy_2)(dtbbpy)PF_6$		rt	84	16
2[b]	$Ir(dFppy_2)(dtbbpy)PF_6$		rt	76	7
3[b]	$Ir[dF(CF_3)ppy_2](dtbbpy)PF_6$		rt	75	6
4	$Ir(ppy_2)(dtbbpy)PF_6$		rt	61	29
5[b]	$Ir(ppy_2)(dtbbpy)PF_6$		55 °C	68	32
6[b]	$Ir(ppy_2)(dtbbpy)PF_6$	dtbbpy (6 mol %)	rt	55	29
7[b]	$Ir(ppy_2)(dtbbpy)PF_6$	dtbbpy (1 mol %)	rt	53	36
8	$Ir(ppy_2)(dtbbpy)PF_6$	dtbbpy (1 mol %)	rt	0	97
9[b]	$Ir(ppy_2)(dtbbpy)PF_6$	dtbbpy (1 mol %)	55 °C	0	98
10[b,c]	$Ir(ppy_2)(dtbbpy)PF_6$		rt	99	0
11[b,c]	$Ir(ppy_2)(dtbbpy)PF_6$	dtbbpy (1 mol %)	rt	48	51
12[b,c]	$Ir(ppy_2)(dtbbpy)PF_6$	dtbbpy (5 mol %)	rt	53	46
13[c]	$Ir(ppy_2)(dtbbpy)PF_6$	dtbbpy (1 mol %)	rt	0	98
14[b,c]	$Ir(ppy_2)(dtbbpy)PF_6$	dtbbpy (1 mol %)	55 °C	0	99

[a]Yields are determined by NMR analysis with an internal standard using ArBr **4.18** (0.5 mmol). [b]24 h. [c]DMSO instead of MeCN.

Table 4.4. Electron-Neutral Aryl Bromide Optimization[a]

Electron-neutral aryl bromides were found to be less efficient coupling partners under ligand-free reaction conditions. During the optimization studies using bromide **4.18** and sulfonamide **4.14** (**Table 4.4**), all the catalysts tested for the ligand-free conditions gave poor results (*entries* 1-4). Neither the extended reaction time (*entry* 4) nor the increased reaction temperature (entry 5) seemed to solve the problem. We suspected that the slow oxidative addition rate of Ni^0 to the aryl halide was the problem for the slow conversion and decided to see the effect of bidentate ligands in this transformation with the assumption that the ligand might facilitate the oxidative addition. The reaction with 1 mol% dtbbpy outperformed the one with 6 mol % ligand (*entries* 6 and 7). The yield could be almost quantitative when the reaction was run for 48 hours (*entry* 8). The reaction went to completion in 24 hours at an elevated temperature (approximately reaching 55 ℃) giving

an excellent yield of the product (*entry* 9). The rate of the reaction slightly improved using DMSO solvent, despite the dependence of the amount of ligand wherein 1 mol % of dtbbpy was optimal (*entries* 10-14). Owing to the interesting observation from these experiments with dtbbpy ligand, we elected to separate the investigation into ligand-added and ligand-free reaction conditions.

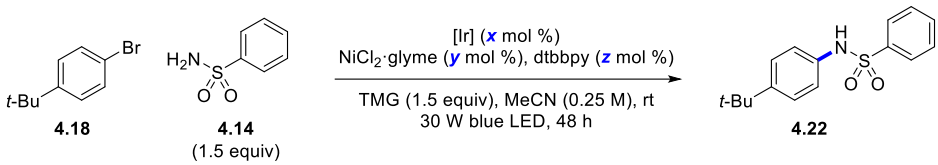

entry	[Ir]	mol %	$NiCl_2$•glyme *(mol %)*	dtbbpy (mol %)	4.18 (%)	4.22 (%)
1	$Ir(ppy_2)(dtbbpy)PF_6$	0.5	5	1	0	99
2	$Ir(ppy_2)(dtbbpy)PF_6$	0.05	5	1	94	0
3	$Ir(ppy_2)(dtbbpy)PF_6$	0.01	5	1	98	0
4[b]	$Ir(ppy_2)(dtbbpy)PF_6$	0.5	5	1	30	69
5[b]	$Ir(ppy_2)(dtbbpy)PF_6$	0.05	5	1	99	<1
6[b]	$Ir(ppy_2)(dtbbpy)PF_6$	0.01	5	1	100	0
7[b]	$Ir[dF(CF_3)ppy_2](dtbbpy)PF_6$	0.5	5	1	74	25
8[b]	$Ir[dF(CF_3)ppy_2](dtbbpy)PF_6$	0.05	5	1	82	17
9[b]	$Ir[dF(CF_3)ppy_2](dtbbpy)PF_6$	0.01	5	1	71	13
10[b]	$Ir[dF(CF_3)ppy_2](dtbbpy)PF_6$	0.01	5	0	63	8
11	$Ir(ppy_2)(dtbbpy)PF_6$	0.5	3	1	56	40
12	$Ir(ppy_2)(dtbbpy)PF_6$	0.5	1	1	77	21
13	$Ir(ppy_2)(dtbbpy)PF_6$	0.5	5	0	61	29
14	$Ir(ppy_2)(dtbbpy)PF_6$	0.5	5	0.1	40	40
15	$Ir(ppy_2)(dtbbpy)PF_6$	0.5	5	0.5	0	84

[a]Yields are determined by NMR analysis with an internal standard using ArBr **4.18** (0.5 mmol). [b]TMG (2.0 equiv), sulfonamide (2.5 equiv)

Table 4.5. Effects of Catalyst Loadings[a]

We examined the effect of the reagent amounts on the ligand-added reaction using the conditions described above (**Table 4.5**). Decreasing the photocatalyst loading to 0.05mol% or below resulted in no reaction (*entries* 1-3), and the increase of equivalents of base and sulfonamide was detrimental to the reaction (*entry* 4-6). Using a higher energy triplet sensitizer, $Ir[dF(CF_3)ppy]_2(dtbbpy)PF_6$ did not give better results although a significant amount of sulfonamide **4.22** was formed even at 0.01 mol% catalyst loadings (*entries* 7-9). The reaction also worked even in the absence of ligand (*entry* 10). At low concentrations, the photocatalyst may decompose significantly before performing the TTET. As $Ir[dF(CF)_3ppy]_2(dtbbpy)PF_6$ possesses a more favorable energy transfer profile, the formation of a small amount of the product can be reasonable. Decreasing catalyst loadings of $NiCl_2$•glyme while fixing the amount of the photocatalyst to 0.5 mol% exhibited steady

decline of the product formations (*entries* 11 and 12), illustrating 5 mol% of nickel to be essential for this sulfonamidation. Possibly, some Ni^{II} is sacrificed by scavenging the arylated sulfonamide. In the later studies, we noted the possibility of impeding the requisite Ni^{0} formation the arylated product. The equivalent of the ligand could not be reduced without diminishing the efficiency of the sulfonamidation (*entries* 13-15). Even though more experiments are necessary, it may be that both the dtbbpy chelated nickel and DBU/sulfonamide coordinated nickel work as active catalysts. It is also possible that the dtbbpy is not participating in the nickel catalytic cycle. Another possibility responsible for the ligand effect is that the added ligand may restore the decomposed iridium complex, arising from loss of dtbbpy due to light irradiation, in which the electron transfer from the metal d orbital to the dtbbpy π^* orbital is infeasible (see **Section 4.2.3** for more details).[13]

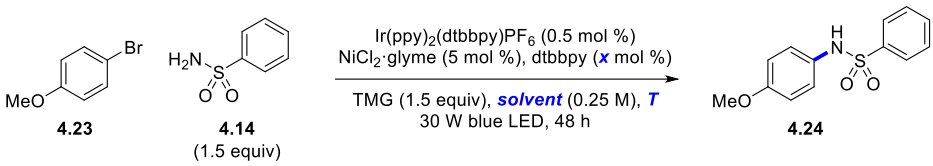

entry	*solvent*	*ligand (mol %)*	*temperature*	4.23 (%)	4.24 (%)
1	MeCN	1	rt	84	16
2	MeCN	1	55 °C	100	0
3	DMSO	1	rt	63	29
4	DMSO	1	55 °C	25	63
5[b]	DMSO	1	55 °C	25	64
6[c]	DMSO	1	55 °C	25	63
7	DMSO	5	rt	62	38
8	DMSO	5	55 °C	46	51

[a]Yields are determined by NMR analysis with an internal standard using ArBr **4.23** (0.5 mmol).
[b]10 mol % $NiCl_2$•glyme, [c]72 h

Table 4.6. Electron-Rich Aryl Bromide Optimization[a]

As depicted above, the investigation was carried out using 4-bromoanisole (**4.23**) as a standard substrate for electron-rich aryl bromides (**Table 4.6**). Use of MeCN solvent gave poor conversion, and at an elevated reaction temperature, the reaction did not proceed (*entries* 1 and 2), which might be due to decomposition of both nickel and iridium catalysts. As the Ni^0 is readily oxidized to its higher oxidation states, the slow oxidative addition with the electron-rich aryl bromide might have led to the unproductive nickel oxidation without forming an aryl nickel. The undesired consumption of nickel would have further prevented the photocatalyst from giving off its energy, causing ligand dissociation. Incorporation of a more polar solvent, DMSO is confirmed to be a better choice for the higher conversion of the aryl bromide (*entry* 3), probably owing to the increase in the rate of oxidative addition. Elevated temperatures led to the formation of the product in good yield (*entry* 4) while higher catalyst loadings and extended reaction times were not necessary (*entries* 5 and 6). It was also found that a lower equivalent of dtbbpy might be more effective (*entries* 7 and 8).

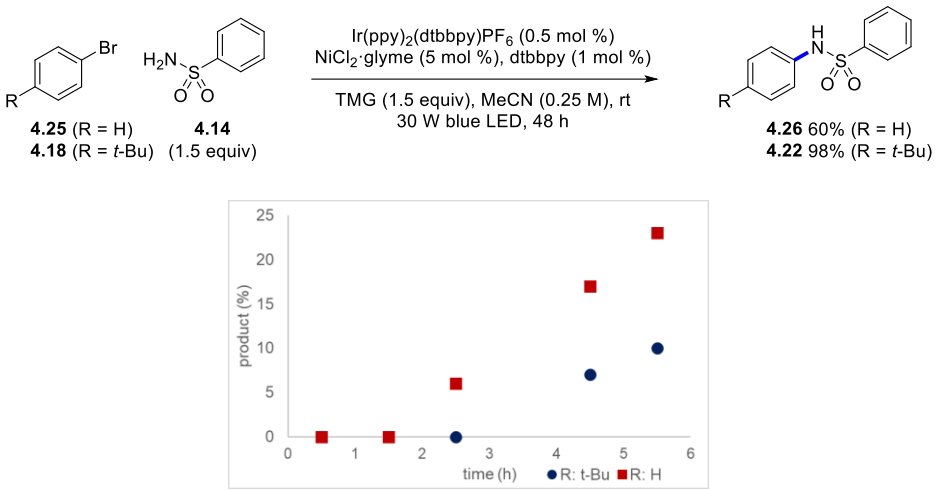

Figure 4.4. Initial Rate of Sulfonamidation

Additionally detected was the inhibition of Ni^{II} to Ni^{0} reduction by the sulfonamide product. For example, the product yield was lower with the less electron-rich bromobenzene (**4.25**) than that with bromide **4.18**, even though the initial rate was faster with **4.25** (**Figure 4.4**). It turned out that *N*-aryl sulfonamides formed as products in the reaction could prevent the Ni^{0} formation from the Ni^{II} precatalyst even in the presence of only 0.1 equivalent relatives to bromoarene **4.18** at the beginning of the reaction (**Table 4.7**). Addition of the products to the reactions with $NiCl_2$•glyme as a precatalyst completely suppressed the sulfonamidation (*entries* 1-3). In contrast, when $Ni(cod)_2$ was utilized as a catalyst, the addition of a sulfonamide had little impact on the reaction resulting in only small decrease in yields (*entries* 4-6). Stefan McCarver in the Princeton team confirmed this hypothesis of product quenching the nickel catalysis initiation by cyclic voltammetry experiments which revealed that the reduction potential of Ni^{II} became more negative when coordinated by the *N*-arylated sulfonamide. The addition of an *N*-aryl sulfonamide to a mixture of $NiBr_2$•glyme, benzenesulfonamide, and TMG shifted the Ni^{II} reduction potential from -1.0 V to -1.4 V vs. SCE. The lower pK_a value of an *N*-aryl sulfonamide might make the compound easily deprotonated in the reaction mixture which would allow the amide ion to coordinate the nickel complex even with its higher steric hindrance.

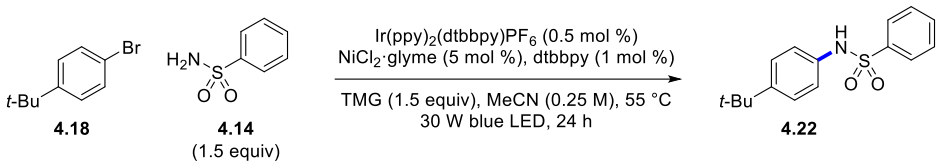

entry	[Ni]	additive	4.18 (%)	4.22 (%)
1	$NiCl_2$•glyme		0	98
2	$NiCl_2$•glyme	**4.26** (0.1 equiv)	97	0
3	$NiCl_2$•glyme	**4.22** (0.1 equiv)	96	0
4	$Ni(cod)_2$		17	82
5	$Ni(cod)_2$	**4.26** (0.1 equiv)	29	70
6	$Ni(cod)_2$	**4.22** (0.1 equiv)	23	73

[a]Yields are determined by NMR analysis with an internal standard using ArBr **4.18** (0.5 mmol).

Table 4.7. Product Quenching Experiments[a]

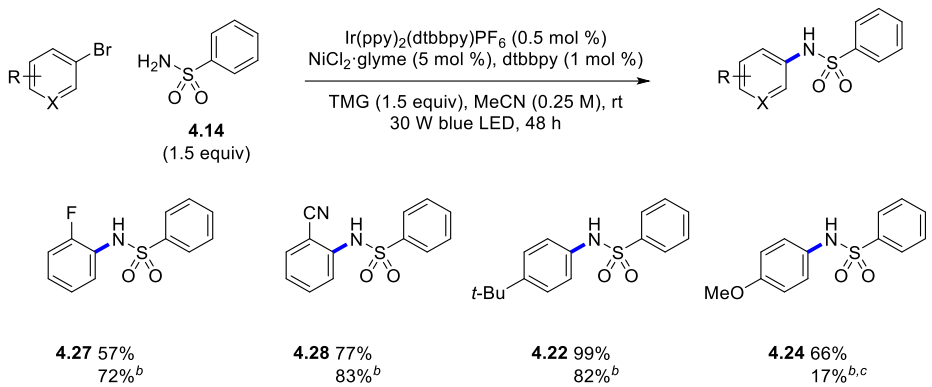

[a]Yields are determined by NMR analysis with an internal standard using ArBr (0.5 mmol). [b]$Ni(cod)_2$ instead of $NiCl_2$•glyme. [c]DMSO instead of MeCN at 55 °C.

Table 4.8. Activity Difference in Ni^0 and Ni^{II} Precatalysts[a]

Comparison of catalytic efficiency of $NiCl_2$•glyme and $Ni(cod)_2$ using different aryl bromides also supported our hypothesis of the acidic nitrogen inhibiting the formation of Ni^0 required for initiation of catalysis (**Table 4.8**). $Ni(cod)_2$ gave higher yields for the reaction of aryl halides (**4.27** and **4.28**) forming products with more acidic N-H bonds. When a Ni^0 complex, e.g., $Ni(cod)_2$, is added at the beginning of the reaction, the inhibition of Ni^{II} reduction by the arylated product does not affect the reaction. However, the catalytic efficiency of $Ni(cod)_2$ diminished when applied to electron-rich aryl halides (**4.22** and **4.24**), possibly because consumption of the Ni^0 through multiple side pathways might become more competitive due to slow oxidative addition.

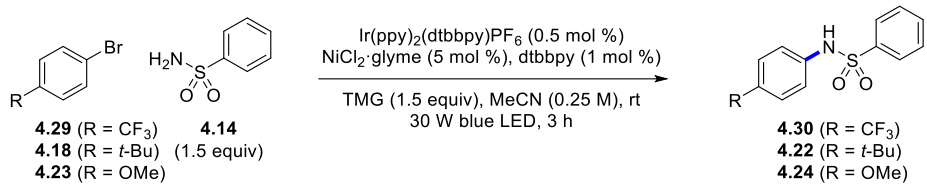

entry	ArBr	TMEDA	*product* (%)
1	**4.29**		0
2	**4.29**	0.05 equiv	26
3	**4.18**		0
4	**4.18**	0.05 equiv	7
5[b]	**4.23**		0
6[b]	**4.23**	0.05 equiv	11

[a]Yields are determined by NMR analysis with an internal standard using ArBr (0.5 mmol). [b]DMSO instead of MeCN at 55 °C.

Table 4.9. Effects of TMEDA in The Initiation of Sulfonamidation[a]

To address the slow catalyst initiation problem in the early stage of the reaction, we added catalytic tetramethylethylenediamine (TMEDA) as an organic reductant and monitored for 3 hours. The initial rate of product formation became faster with all aryl bromides (**4.18**, **4.23** and **4.29**) (**Table 4.9**). However, the reaction slowed down and overall kinetics of the reaction was almost similar at some point, and product formation at the final stage were generally lower than additive-free conditions (**Figure 4.5**).

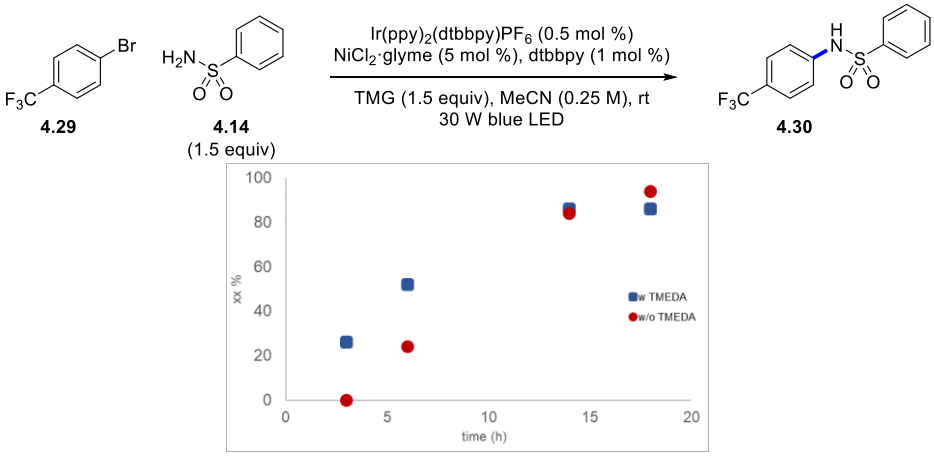

Figure 4.5. Rate of Sulfonamidation with TMEDA

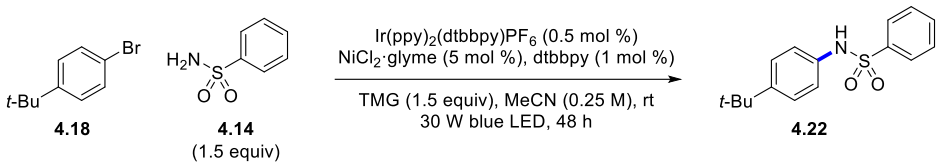

entry	*derivatization from standard reaction conditions*	4.21 (%)
1	none	98
2	without [Ni], without $Ir(ppy)_2(dtbbpy)PF_6$ or under dark	0
3	TMG (1.0 equiv)	69
4	$BsNH_2$ (1.0 equiv)	71
5	$NiBr_2$•glyme instead of $NiCl_2$•glyme	98
6	$Ni(cod)_2$ instead of $NiCl_2$•glyme, 55 °C, 24 h	82
7	bpy instead of dtbbpy	60
8	phen instead of dtbbpy	40

[a]Yields are determined by NMR analysis with an internal standard using ArBr **4.18** (0.5 mmol).

Table 4.10. Control Experiments of Sulfonamidation[a]

Finally, we conducted a series of control experiments (**Table 4.10**). The visible-light irradiation was necessary for this reaction (*entry* 2), and decreasing the amount of the base or sulfonamide showed diminished efficiency (*entries* 3 and 4) as these components might serve as ligands for the nickel. Other nickel precatalysts, such as $NiBr_2$•glyme, were compatible with the optimized reaction conditions (*entries* 5 and 6). The Ni^0 catalyst dropped the reaction efficiency a little, although Ni^0 was especially useful for electron-deficient aryl halides. The dtbbpy ligand proved to be optimal for the ligand-added reaction conditions (*entries* 7 and 8).

4.2.2. Reaction Scope

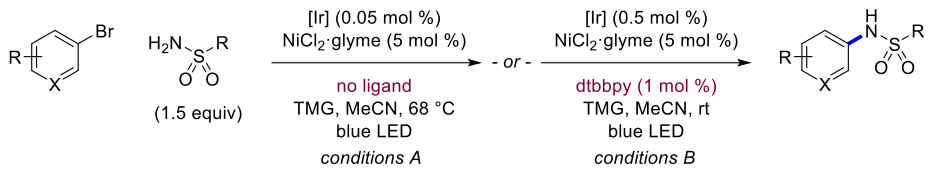

Scheme 4.3. Ligand-Free and Ligand-Added Photosensitized Sulfonamidation

After screening experiments, we came up with two complementary reaction conditions for photosensitized nickel-catalyzed sulfonamidation of aryl halides (**Scheme 4.3**). During the optimization studies, the ligand-free conditions, utilizing 0.05 mol% $Ir(ppy)_2(bpy)PF_6$, TMG and acetonitrile in combination with $NiCl_2$•glyme, proved to be more effective with electron-deficient heteroaryl halides, although higher temperatures were generally necessary (35 or 68 ℃). The ligand-added conditions utilizing 0.5 mol% $Ir(ppy)_2(dtbbpy)PF_6$ with an additional 1 mol% dtbbpy worked well particularly with electron-rich aryl halides typically at lower temperatures (rt or 55 ℃).

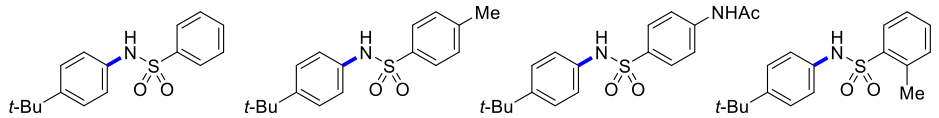

4.22 *A*: 86%
B: 98%

4.31 *A*: 86%
B: 98%

4.32 *A*: 91%
B: 99%[b]

4.33 *A*: 82%
B: 97%[b]

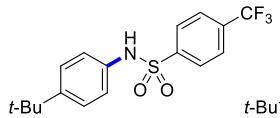

4.34 *A*: 66%[c]
B: 99%[b]

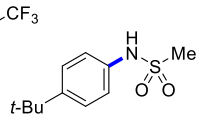

4.35 *A*: 90%
B: 97%[b]

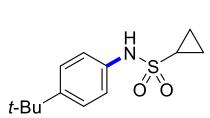

4.36 *A*: 76%
B: 98%[b]

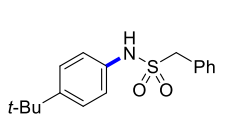

4.37 *A*: 73%
B: 99%[b]

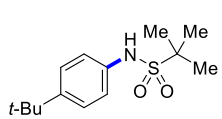

4.38 *A*: 41%[c]
B: 98%[b]

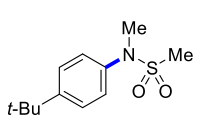

4.39 *A*:
B: 67%[b,d]

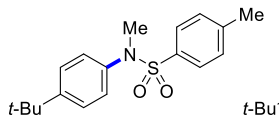

4.40 *A*: 19%[c]
B: 63%[b,d]

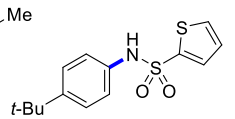

4.41 *A*: 74%
B: 96%[b]

[a]Yields are determined by the isolated products using the general procedure unless otherwise noticed. [b]55 °C. [c]TMG and sulfonamide (2.0 equiv). [d]TMG (2.0 equiv) and sulfonamide (2.5 equiv).

Table 4.11. Scope of Sulfonamides[a]

A broad array of sulfonamides was compatible with the reaction conditions (**Table 4.11**). Both primary aryl and alkyl sulfonamides gave the desired products in good to excellent yields. The ligand-free conditions conducted efficient couplings at 68 ℃, albeit requiring more amounts of the sulfonamides (e.g., 2.0 equiv) with weaker nucleophilicity (**4.34**, and **4.38**). The ligand-added conditions provided the products in almost quantitative yields, although higher reaction temperatures (e.g., 55 ℃) were necessary for most alkyl and aryl sulfonamides (**4.33**-**4.38** and **4.41**). The sulfonamidation protocol tolerated steric hindrances, such as *o*-tolyl and *t*-butyl groups, providing moderate to excellent yields under both reaction conditions (**4.33**, and **4.38**). Interestingly, only the ligand-added conditions were effective for coupling of secondary *N*-methylsulfonamides, in which case increasing the amount of nucleophile and base was beneficial (**4.39**, and **4.40**). A thiophene structure was compatible with the reaction (**4.41**). Sterically hindered secondary sulfonamides did not participate in this reaction (**Table 4.12**). Only a cyclic sultam gave the desired product **4.44** in low yield while benzofused sultam decomposed (cf. **4.45**). Sulfonamides that can

potentially act as bidentate ligands prohibited the reaction as well (cf. **4.46**, and **4.47**), preventing TMG from coordinating to the nickel center. It was detected that 0.5 equivalent of 5-methyl-2-pyridinesulfonamide completely suppressed the coupling reaction using benzenesulfonamide as a substrate.

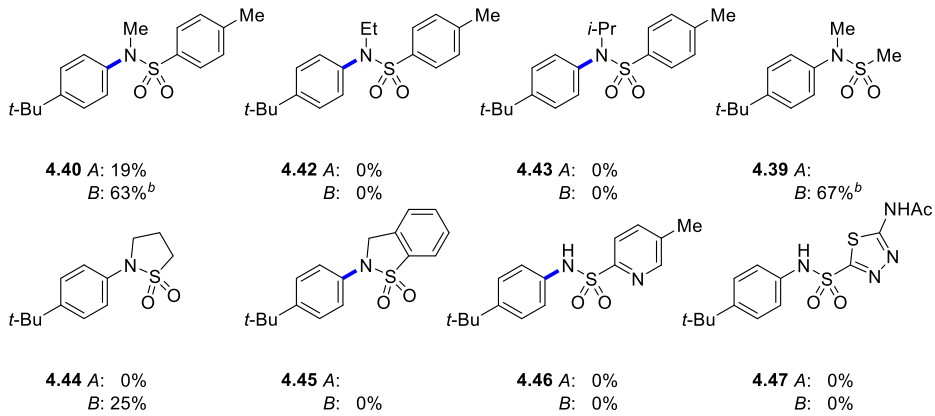

4.40 *A*: 19%
B: 63%[b]

4.42 *A*: 0%
B: 0%

4.43 *A*: 0%
B: 0%

4.39 *A*:
B: 67%[b]

4.44 *A*: 0%
B: 25%

4.45 *A*:
B: 0%

4.46 *A*: 0%
B: 0%

4.47 *A*: 0%
B: 0%

[a]Yields are determined by the NMR analysis with an internal standard using the general procedure using TMG and sulfonamide (2.0 equiv) at 68 °C for A, and TMG (2.0 equiv) and sulfonamide (2.5 equiv) at 55 °C for B unless otherwise noticed. [b]Isolated yield.

Table 4.12. Secondary Sulfonamides Reactivity Comparison[a]

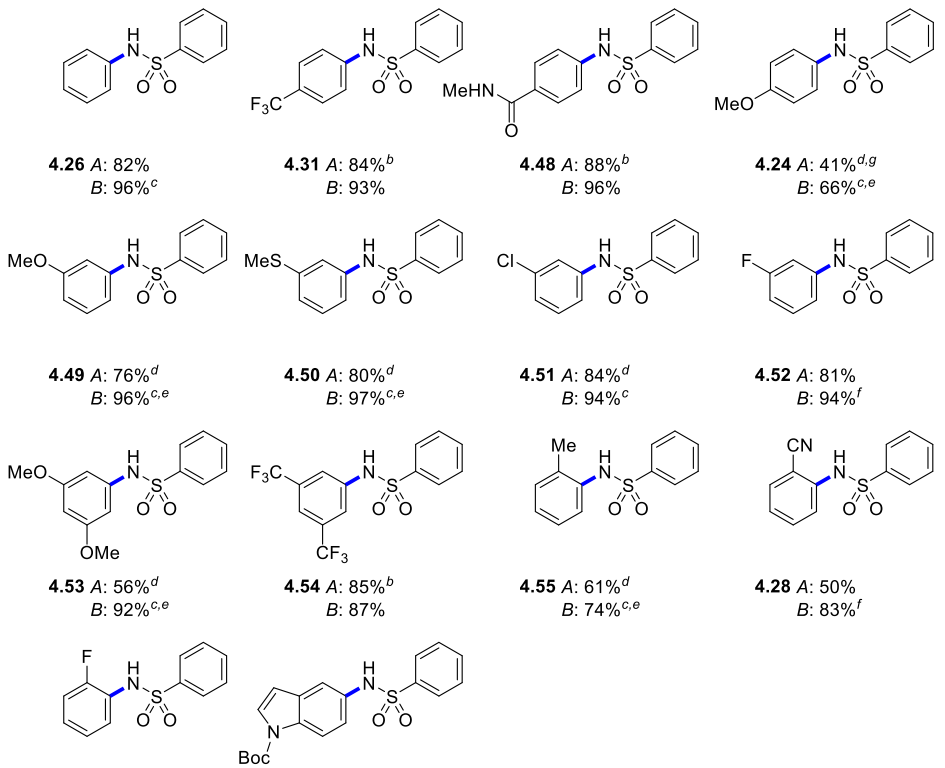

[a]Yields are determined by the isolated products using the general procedure unless otherwise noticed. [b]35 °C. [c]55 °C. [d]Ir[dF(CF$_3$)ppy]$_2$(dtbbpy)PF$_6$ instead of Ir(ppy)$_2$(bpy)PF$_6$. [e]DMSO instead of MeCN. [f]Ni(cod)$_2$ instead of NiCl$_2$•(glyme). [g]MTBD instead of TMG.

Table 4.13. Scope of Aryl Bromides[a]

The nickel-catalyzed sulfonamidation showed high efficiency with various aryl halides (**Table 4.13**). For both reaction conditions, heating the reaction mixture (68 ℃ for ligand-free conditions and 55 ℃ for ligand-added conditions) further enhanced the yield of the product from electron-rich electrophiles while the coupling with electron-deficient aryl halide partners could be coupled under ambient temperature. Interestingly, MTBD sometimes outperformed TMG for electron-rich bromoarenes in ligandless conditions (**4.24**, and **4.56**). Aryl bromides with ortho-substituents required a higher reaction temperature to overcome the steric hindrance regardless of the electronic nature (**4.27**, **4.28** and **4.55**). Also, the reaction tolerated multiple functional groups, such as fluoride and chloride (**4.27**, **4.51** and **4.52**), unprotected secondary amide (**4.48**), nitrile (**4.28**) and Boc-protected indole

(**4.56**). Substituents with the ability to coordinate to nickel, too much steric encumbrance, and high electron density were not compatible at this stage (**Table 4.14, 4.57-4.59**). The nucleophilic indole nitrogen seemed to quench the catalytic cycle forming **4.61**, and a small amount impurity contained in 5-bromo-*N*-Boc-indole appeared to cause irreproducibility of the sulfonamidation.

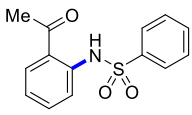

4.57 *A*: 0%
B: 0%

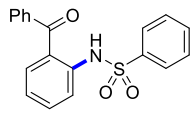

4.58 *A*: 0%
B: 0%

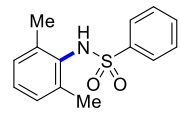

4.59 *A*:
B: 0%

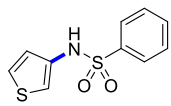

4.60 *A*:
B: 25%

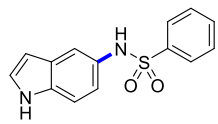

4.61 *A*:
B: 24%

[a]Yields are determined by the NMR analysis with an internal standard at 68 °C for A and using DMSO instead of MeCN at 55 °C for B.

Table 4.14. Unsuccessful Aryl Bromides[a]

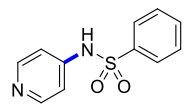

4.62 *A*: 90%[b]
B: 0%

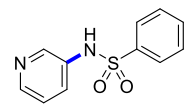

4.63 *A*: 89%[b]
B: 73%

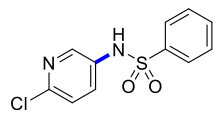

4.64 *A*: 80%[f]
B: 71%

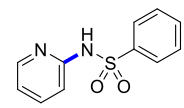

4.65 *A*: 56%[b,e]
B: 20%

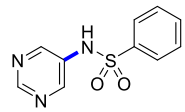

4.66 *A*: 83%[b]
B: 15%

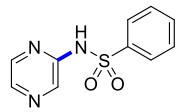

4.67 *A*: 55%[b,c,e]
B: <5%

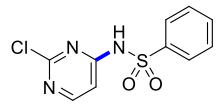

4.68 *A*: 49%[b,f,g]
B: 10%

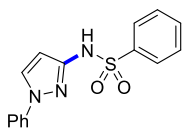

4.69 *A*: 62%[e]
B: <5%

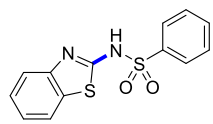

4.70 *A*: 55%[e]
B: 15%

[a]Yields are determined by the isolated products using the general procedure unless otherwise noticed. [b]35 °C. [c]Ir[dF(CF$_3$)ppy]$_2$(dtbbpy)PF$_6$ instead of Ir(ppy)$_2$(bpy)PF$_6$. [d]using 4-bromopyridinium bromide and TMG (2.5 equiv). [e]TMG (2.0 equiv). [f]DBU (2.0 equiv) instead of TMG. [g]ArCl instead of ArBr.

Table 4.15. Scope of Heteroaryl Bromides[a]

Heteroaromatics also proved excellent coupling partners especially under ligand-free conditions (**Table 4.15**). Interestingly, ligand-added conditions provided good yields only with 3-bromopyridine derivatives (**4.63**, and **4.64**) whereas ligand-free conditions successfully provided coupling products with most bromopyridines (**4.62**-**4.65**). Even more electron-poor heteroaromatics, such as pyrimidines, gave moderate to excellent yields (**4.66**-**4.68**). Also found is the coupling of 5-membered heteroaryl halides (**4.69** and **4.70**) which have been challenging for most transition metal-catalyzed cross-coupling strategies.

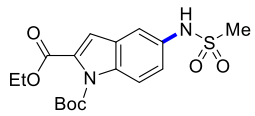

4.71 *A*:
B: 80%[b,c]

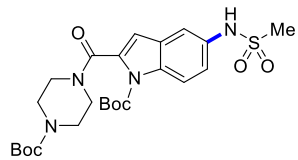

4.72 *A*:
B: 35%[b,c]

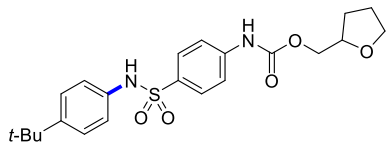

4.73 *A*:
B: 70%

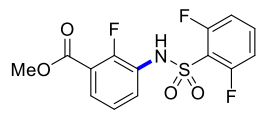

4.74 *A*: 25%
B: 49%[b,c], 83%[b,c,d,e]

[a]Yields are determined by NMR analysis using an internal standard unless otherwise noticed. [b]55 °C. [c]DMSO instead of MeCN. [d]$Ni(cod)_2$ instead of $NiCl_2$•(glyme). [e]Isolated yield.

Table 4.16. Scope of Drug-Like Structures[a]

A range of structurally diverse aryl bromides was moderately tolerable without necessitating modification of the optimized reaction conditions (**Table 4.16**). With this sulfonamidation protocol, we could access precursors for delavirdine, a non-nucleoside reverse transcriptase inhibitor, albeit the reaction efficiency decreased as the nitrogen and oxygen contents in the molecule increased (**4.71** and **4.72**).[13] Coupling of a sulfanilamide derivative with multiple heteroatoms successfully afforded the desired product as well (**4.73**). A formal synthesis of dabrafenib, a B-Raf kinase inhibitor, could also be performed, and incorporating Ni^0 raised the yield of the product (**4.74**).[14] As the results showcased the potential utility of this method in actual drug synthesis, we elected to synthesize dabrafenib using the ligand-added conditions (**Scheme 4.4**). The cross-coupling was conducted using aryl bromide **4.75** that could be synthesized in 4 steps from readily available sulfonamide **4.76**. Stefan McCarver, using the high throughput screening experiments, identified mild synthetic conditions for the formation of dabrafenib **4.77** in good yield. It was noteworthy that even a potential nucleophile for the amination, the aniline group, was tolerable.

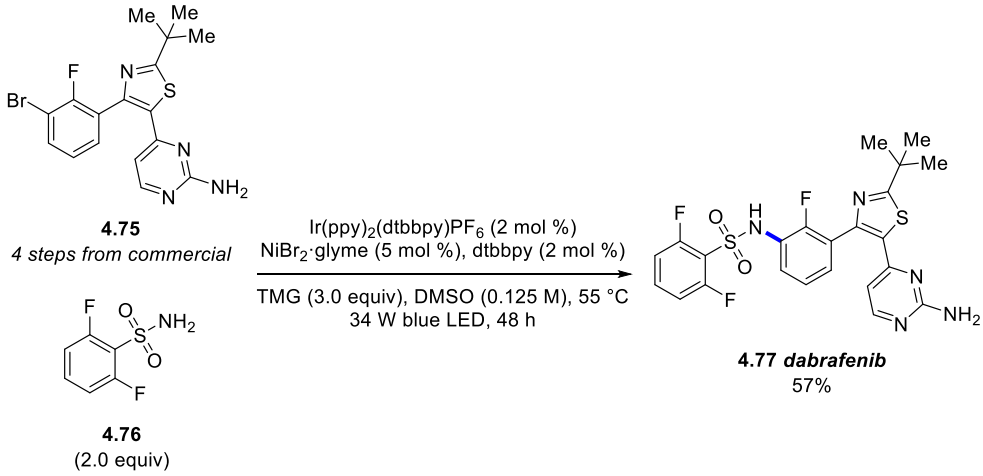

Scheme 4.4. Synthesis of Dabrafenib

4.2.3. Mechanistic Studies

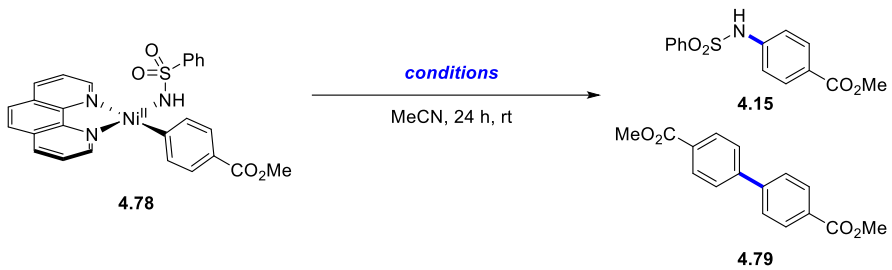

entry	*reaction conditions*	4.15 (%)	4.79 (%)
1	none	8	35
2	[Ir] (1.2 equiv.), 30 W blue LED	23	37
3	[Ir] (1.2 equiv.), no light	9	37
4	30 W blue LED	7	37
5	open to the air	6	41
6	$PhI(OAc)_2$ (1.2 equiv)	8	35

Table 4.17. Stoichiometric Ligated Nickel Reductive Elimination

To gain insight into the mechanistic of this reaction, we synthesized the ligated nickel sulfonamido complex **4.78** and investigated the reactivity of the complex under multiple conditions (**Table 4.17**). The nickel complex gave the C–N coupled product **4.15** via a thermal reaction pathway, along with a significant amount of the biaryl byproduct **4.79** (*entry* 1). Enhancement in the yield occurred with an iridium photocatalyst and light (*entries* 2-4). Interestingly, the Ni^{II} complex did not seem to be oxidized by air or a hypervalent iodine reagent, in contrast to the other observations, suggesting that reductive elimination might not proceed through the Ni^{III} intermediacy (*entry* 5-6).[11b,16] The result of the stoichiometric study suggested that the reaction under the ligand-added conditions might be operative through a triplet-excited sulfonamido nickel complex with some level of the thermal reductive elimination process.

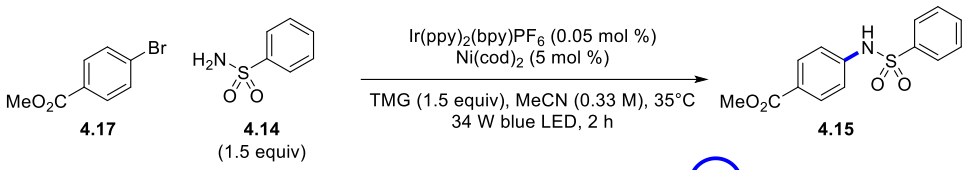

entry	*derivatization*	4.15 (%)
1	none	99
2	no light	0
3	no nickel	0
4	no photocatalyst	11
5	*entry* 4, Benzophenone (0.5 mol %)	18

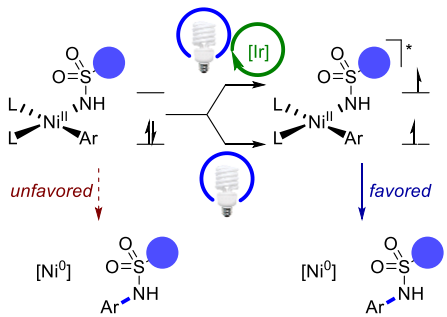

Table 4.18. Control Experiments

As no synthetic method for our actual organometallic nickel species was available, we conducted a mechanistic study on the reaction using $Ni(cod)_2$ as a catalyst (**Table 4.18**). The use of a Ni^0 precatalyst for this study was critical in order to form the organometallic nickel in the very beginning of the reaction. The Ni^{II} intermediate formed in the reaction mixture did not produce any C–N coupled product **4.15** without light or nickel (*entries* 2 and 3). Interestingly, a significant degree of product formation was observed in the absence of a photocatalyst. In this case, the yield increased with the addition of a catalytic amount of the triplet sensitizer benzophenone (*entries* 4 and 5). These observations indicated that the light source was directly exciting the nickel to go to its active triplet state. The absorbance $Ni(cod)_2$, TMG, and the aryl halide measured in MeCN showed dependence on the reagent around 500-600 nm, lending support to the mechanism involving a triplet-excited nickel in the C–N bond-forming step in our reaction system.

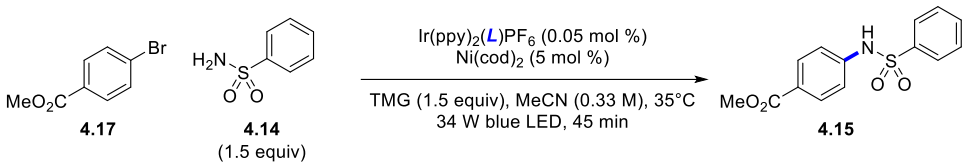

entry	*R*	E_T *(kcal/mol)*	$E_{1/2}$*(II/III*) (V)*	4.15 (%)
1	*MeO*	47.7	0.58	92
2	Me	47.6	0.59	81
3	H	46.3	0.61	83
4	Cl	42.6	0.72	10
5	CO_2Me	39.7	0.70	5
6	CF_3	39.2	0.74	5
7	no [Ir]			11

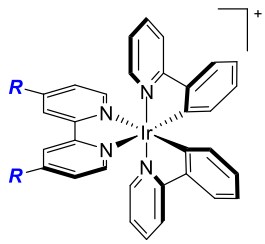

Table 4.19. Correlation between Sulfonamidaton and Photocatalyst Triplet Energy

Modification of the bipyridyl ligand on the iridium center allowed access to a series of photocatalysts that have a negative correlation between $E_{1/2}$(II/III*) reduction potentials and energies of ^{3}MLCT iridium complexes. With these iridium complexes in combination with Ni(cod)$_2$, we examined which property affected the reductive elimination under photochemical conditions (**Table 4.19**).[3d] Although the optimized reaction conditions utilized Ni^{II} sources as precatalysts, the use of Ni(cod)$_2$ in these experiments was crucial as it could exclude the electrochemical reduction of Ni^{II} catalysts. The catalysts with triplet energy higher than 46 kcal/mol showed faster C–N bond formation (*entries* 1-3) while the oxidizing power of excited photocatalysts showed no correlations with sulfonamidated product formation, resulting in yields similar to those of the reactions that did not employ iridium complexes (*entries* 4-6). From these observations, we concluded that photocatalysts were performing the light-harvesting role for the photosensitization of nickel catalysts. Considering the recent work by Doyle and Scholes proposing a triplet-excited nickel complex to be involved in the initial d→π* MLCT, the nickel complex in our reaction system also appeared to adopt structural resemblance to their ^{3}MLCT nickel system.[3e] In their studies, also proposed was the initiation of a nickel-catalyzed etherification of aryl halides by the action of ^{3}MLCT Ni^{II}–Aryl complexes, a catalytic cycle working through a

Ni^{I}/Ni^{III} oxidative addition pathway. However, there was no observation to support the Ni^{I}/Ni^{III} oxidative addition process. Possibilities exist for the reductive elimination of triplet-excited Ni^{II} complexes; the structure of a ^{3}MLCT nickel that becomes electron-deficient at the nickel center will make a resemblance between ^{3}MLCT Ni^{II} and Ni^{III} changing the unfavorable C–N reductive elimination operative by making the metal complex more electronegative.

4.2.4. Photocatalyst Decomposition Studies

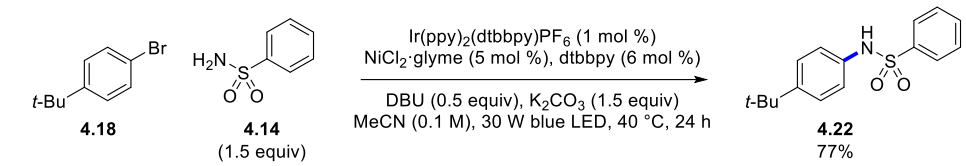

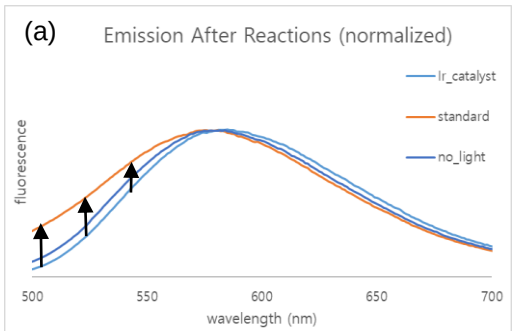

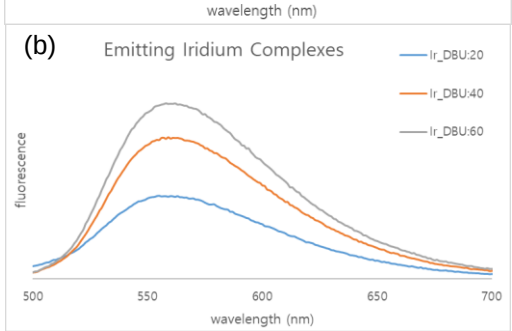

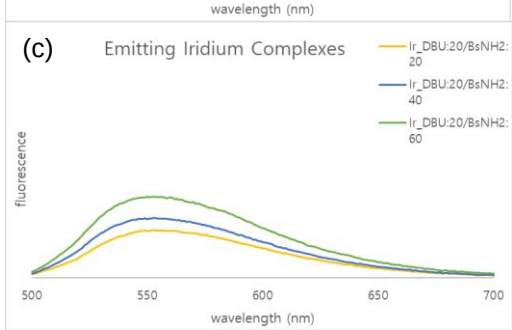

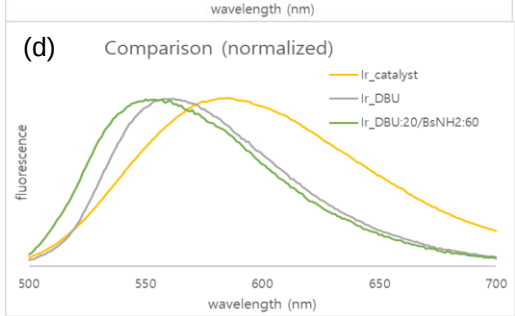

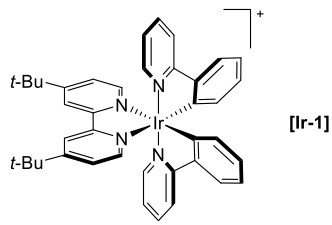

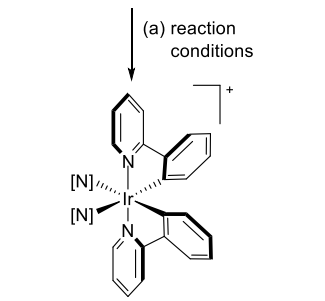

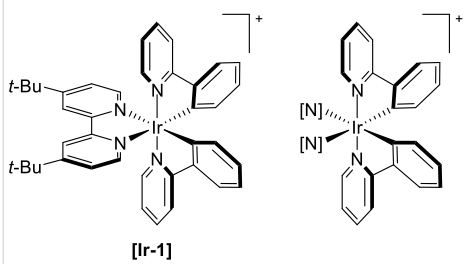

Figure 4.6. Emission Spectra of Iridium Complexes

Several pathways are possible for the decomposition of the iridium complexes in visible-light photocatalytic transformations, among which the most frequently proposed is the Minisci-type modification of the ligands.[17] The bipyridine dissociation, which was initially detected by Bernhard who developed heteroleptic iridium photocatalysts, have not been taken into consideration.[15] We also suspected during our studies that the catalyst was decomposing and the role of the added ligand for nickel was unclear. To gain more insight, we decided to chase the decomposition pathway of $Ir(ppy)_2(dtbbpy)PF_6$ **[Ir-1]** by measuring the emission spectra (**Figure 4.6**). After the depicted reaction conditions, we detected shoulders developing around 500 nm in the emission spectrum of the iridium complex which depended on light irradiation (**Figure 4.6a**). It was interesting that decomposed portions of the photocatalysts also showed luminescence characters. As several potential ligands existed in the reaction mixture, for instance, DBU and sulfonamides, we synthesized $Ir(ppy)_2(MeCN)_2PF_6$ **[Ir-2]**, a postulated decomposed iridium catalyst after the solvent coordination, and measured the emission spectra of a solution containing potential ligands (DBU and sulfonamide) and the iridium complex (**Figure 4.6b,** and **4.6c**). As expected, the non-luminescence iridium complex changed into a complex that emits light around 500 and 550 nm which could explain the additional emission observed. To further

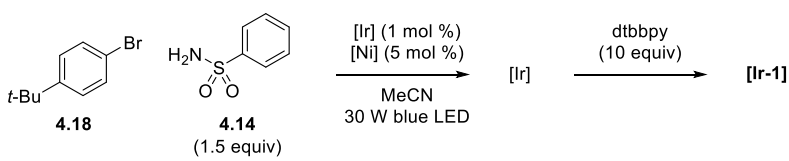

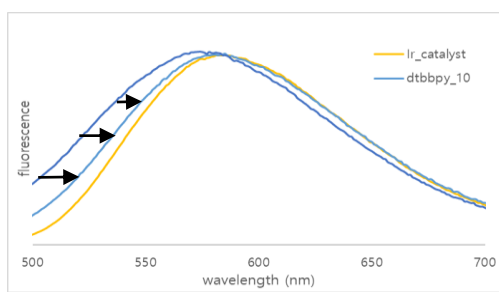

Figure 4.7. Emission Spectra Recovery

prove our postulation, we added 10.0 equivalents of dtbbpy (relatives to the iridium photocatalyst) to a solution of the decomposed iridium complex and examined if the emission spectrum of initially added **[Ir-1]** could be restored (**Figure 4.7**). The result verified the existence of ligand dissociation in the iridium complexes. Also conceivable is the possibility of decomposition of the triplet-excited nickel through a similar pathway. Thus, the chelation effect of bidentate ligands may be ignorable, and fast transferring of ligands between two metals is perhaps operating in this reaction system.

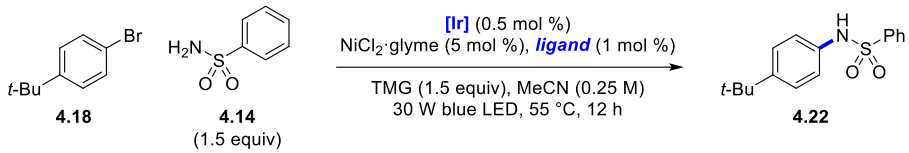

entry	[Ir]	*ligand*	4.18 (%)	4.22 (%)
1	$Ir(ppy_2)(dtbbpy)PF_6$	dtbbpy	48	51
2	$Ir(ppy_2)(dtbbpy)PF_6$	bpy	49	39
3	$Ir(ppy_2)(dtbbpy)PF_6$	phen	47	43
4	$Ir(ppy_2)(bpy)PF_6$	dtbbpy	79	6
5	$Ir(ppy_2)(bpy)PF_6$	bpy	62	29
6	$Ir(ppy_2)(bpy)PF_6$	phen	81	8

Table 4.20. Correlation between Structure of Photocatalysts and Ligands

The reactivity comparison between ligand-free and ligand-added conditions suggested that the rate-determining step for the sulfonamidation of electron-rich and neutral aryl bromides might be the oxidative addition step since dtbbpy-added conditions always outperformed the dtbbpy-free conditions. However, yields of the cross-coupling process showed dependence on both the structure of catalysts and added bipyridine ligands (**Table 4.20**). For the reactions with ($Ir(ppy)_2(dtbbpy)PF_6$) catalyst used in ligand-added conditions, the rates increased with electron-rich ligands (*entries* 1-3) whereas the optimal catalyst for ligand-free conditions ($Ir(ppy)_2(bpy)$) showed the best result with bpy, an ancillary ligand of the iridium photocatalyst (*entries* 4-6). It was striking that dtbbpy and phen ligands showed similar conversions considering the substantial rate difference between dtbbpy and phen ligands in oxidative addition (**Figure 4.8**). One plausible explanation might be that the iridium concentration is decreasing at the beginning of a catalytic cycle by losing dtbbpy or bpy to a certain equilibrium point. The addition of the corresponding ligands would have driven the equilibrium backward restoring the photocatalysts. Still, more experiments are necessary for this proposal to be advanced.

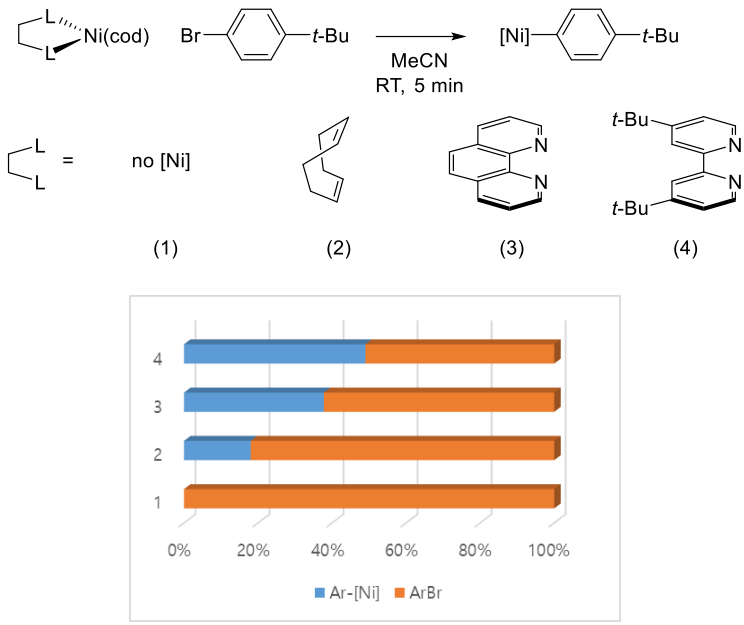

Figure 4.8. Relative Oxidative Addition Rate of Nickel

4.3. Conclusion

The photosensitization of nickel complexes using iridium photocatalysts provides an efficient method for the *N*-arylation of sulfonamides under mild conditions. We have developed two reaction conditions, one employing a small amount of dtbbpy and the other without bidentate ligands. These two protocols are complementary in reactivity, enabling sulfonamidation with a broad range of aryl halides as coupling partners. The synthesis of a drug molecule, dabrafenib, showing exclusive selectivity for the sulfonamide group over an aniline group, further prove the usefulness of this approach in complex molecule synthesis. Additionally, the results of mechanistic studies support our postulation excluding the involvement of reductive elimination of a high-valent Ni^{III} species in the catalytic cycle. Also, a proposal has been put forward for the role of dtbbpy in the reaction mixture based on the measurement of the fluorescence of decomposed iridium photocatalysts. A paper detailing this sulfonamidation protocol was published in 2018.[18]

4.4. References

1) (a) Zuo, Z.; Ahneman, D. T.; Chu, L.; Terrett, J. A.; Doyle, A. G.; MacMillan, D. W. C. *Science* **2014,** *345*, 437. (b) Tellis, J. C.; Primer, D. N.; Molander, G. A. *Science* **2014,** *345*, 433. (c)Twilton, J.; Le, C.; Zhang, P.; Shaw, M. H.; Evans, R. W.; MacMillan, D. W. C. *Nat. Rev. Chem.* **2017,** *1*, 0052.

2) (a) Weix, D. J. *Acc. Chem. Res.* **2015,** *48*, 1767. (b) Fu, G. C. *ACS Central Science* **2017,** *3*, 692.

3) (a) Hwang, S. J.; Powers, D. C.; Maher, A. G.; Anderson, B. L.; Hadt, R. G.; Zheng, S.-L.; Chen, Y.-S.; Nocera, D. G. *J. Am. Chem. Soc.* **2015,** *137*, 6472. (b) Shields, B. J.; Doyle, A. G. *J. Am. Chem. Soc.* **2016,** *138*, 12719. (c) Heitz, D. R.; Tellis, J. C.; Molander, G. A. *J. Am. Chem. Soc.* **2016,** *138*, 12715. (d) Welin, E. R.; Le, C.; Arias-Rotondo, D. M.; McCusker, J. K.; MacMillan, D. W. C. *Science* **2017,** *355*, 380. (e) Shields, B. J.; Kudisch, B.; Scholes, G. D.; Doyle, A. G. *J. Am. Chem. Soc.* **2018,** *140*, 3035.

4) (a) Turro, N. J. *Modern molecular photochemistry*. University Science Books: Mill Valley, Cal., **1991**. (b) Balzani, V.; Ceroni, P.; Juris, *A. Photochemistry and photophysics: concepts, research, applications*. Wiley-VCH: Weinheim, **2014**.

5) (a)Minghao, F.; Bingqing, T.; Steven, H. L.; Xuefeng, J. *Curr. Top. Med. Chem.* **2016,** *16*, 1200. (b)Supuran, C. T.; Angela, C.; Andrea, S. *Med. Res. Revi.* **2003,** *23*, 535. (C) Drews, J. *Science* **2000,** *287*, 1960. Kalgutkar, A. S.; Jones, R.; Sawant, A. Sulfonamide as an Essential Functional Group in Drug Design. In *Metabolism, Pharmacokinetics and Toxicity of Functional Groups*; Smith, D. A., Ed.; Royal Society of Chemistry: Cambridge, **2010**; pp 210–274.

6) (a) Ballatore, C.; Huryn, D. M.; Smith III, A. B. *ChemMedChem* **2013**, *8*, 385. (b) Şanli, N.; Şanli, S.; Ö zkan, G.; Denizli, A. *J. Braz. Chem. Soc.* **2010**, *21*, 1952.

7) (a) Pierson, D. A.; Olsen, B. A.; Robbins, D. K.; DeVries, K. M.; Varie, D. L. *Org. Process Res. Dev.* **2009,** *13*, 285. (b) Snodin, D. J. *Org. Process Res. Dev.* **2010,** *14*, 960.

8) (a) Guram, A. S.; Rennels, R. A.; Buchwald, S. L. *Angew. Chem. Int. Ed.* **1995,** *34*, 1348.

(b) Louie, J.; Hartwig, J. F. *Tetrahedron Lett.* **1995,** *36*, 3609. For a review, see (c) Ruiz-astillo, P.; Buchwald, S. L. *Chem. Rev.* **2016,** *116*, 12564.

9) For recent examples of Cu and Pd-Catalyzed sulfonamidation of aryl halides, see (a) Hicks, J. D.; Hyde, A. M.; Cuezva, A. M.; Buchwald, S. L. *J. Am. Chem. Soc.* **2009,** *131*, 16720. (b) Baffoe, J.; Hoe, M. Y.; Touré, B. B. *Org. Lett.* **2010,** *12*, 1532. (c) Rosen, B. R.; Ruble, J. C.; Beauchamp, T. J.; Navarro, A. *Org. Lett.* **2011,** *13*, 2564. (d) Wang, X.; Guram, A.; Ronk, M.; Milne, J. E.; Tedrow, J. S.; Faul, M. M. *Tetrahedron Lett.* **2012,** *53*, 7. (e) Tan, B. Y.-H.; Teo, Y.-C.; Seow, A.-H. *Eur. J. Org. Chem.* **2014,** *2014*, 1541.

10) Twilton, J.; Le, C.; Zhang, P.; Shaw, M. H.; Evans, R. W.; MacMillan, D. W. C. *Nat. Rev. Chem.* **2017,** *1*, 0052.

11) Koo, K.; Hillhouse, G. L. *Organometallics* **1995,** *14*, 4421. Lin, B. L.; Clough, C. R.; Hillhouse, G. L. *J. Am. Chem. Soc.* **2002,** *124*, 2890. Macgregor, S. A.; Neave, G. W.; Smith, C. *Faraday Discuss.* **2003,** *124*, 111.

12) Singh, A.; Teegardin, K.; Kelly, M.; Prasad, K. S.; Krishnan, S.; Weaver, J. D. *J. Organomet. Chem.* **2015,** *776*, 51.

13) Romero, D. L.; Morge, R. A.; Genin, M. J.; Biles, C.; Busso, M.; Resnick, L.; Althaus, I. W.; Reusser, F.; Thomas, R. C.; Tarpley, W. G. *J. Med. Chem.* **1993,** *36*, 1505.

14) Rheault, T. R.; Stellwagen, J. C.; Adjabeng, G. M; Hornberger, K. R.; Petrov, K. G.; Waterson, A. G.; Dickerson, S. H.; Mook, R. A. Jr.; Laquerre, S. G.; King, A. J.; Rossanese, O. W.; Arnone, M. R.; Smitheman, K. N.; Kane-Carson, L. S.; Han, C.; Moorthy, G. S.; Moss, K. G.; Uehling, D. E. *ACS Med. Chem. Lett.* **2013**, *4*, 358.

15) (a) Lowry, M. S.; Goldsmith, J. I.; Slinker, J. D.; Rohl, R.; Pascal, R. A.; Malliaras, G. G.; Bernhard, S. *Chem. Mater.* **2005,** *17*, 5712. (b) Tinker, L. L.; McDaniel, N. D.; Curtin, P. N.; Smith, C. K.; Ireland, M. J.; Bernhard, S. *Chem. A Eur. J.* **2007,** *13*, 8726.

16) Tasker, S. Z.; Jamison, T. F. *J. Am. Chem. Soc.* **2015,** *137*, 9531.

17) Devery Iii, J. J.; Douglas, J. J.; Nguyen, J. D.; Cole, K. P.; Flowers Ii, R. A.; Stephenson, C. R. J. *Chem. Sci.* **2015,** *6*, 537.

18) Kim, T.; McCarver, S. J.; Lee, C.; MacMillan, D. W. C. *Angew. Chem. Int. Ed.* **2018,** *57*, 3488.

4.5. Experimental Section

4.5.1 General Information

Aryl halides and sulfonamides were purchased from commercial sources and used as received. $Ir[dF(CF_3)ppy]_2(dtbbpy)PF_6$, $Ir(ppy)_2(bpy)PF_6$, and $Ir(ppy)_2(dtbbpy)PF_6$ were prepared according to the literature procedures.[i] All solvents were purified according to the method of Grubbs.[ii] Non-aqueous reagents were transferred under nitrogen or argon via syringe or cannula. Organic solutions were concentrated under reduced pressure on a Büchi rotary evaporator using a water bath. Chromatographic purification of products was accomplished using forced-flow chromatography on silica gel (Merck 9385 Kiesel gel 60). Thin-layer chromatography (TLC) was performed on Silicycle 0.25 mm silica gel F-254 plates. Visualization of the developed chromatogram was performed by fluorescence quenching or $KMnO_4$ stain. ^1H NMR spectra were recorded on an Agilent 400-MR DD2 400 MHz, Varian/Oxford As-500 500 MHz, or Bruker UltraShield Plus 500 MHz and are internally referenced to residual protio $(CD_3)_2CO$ (2.05 ppm), $(CD_3)_2SO$ (2.50 ppm), or $CDCl_3$ signals (7.27 ppm). Data for ^1H NMR are reported as follows: chemical shift (δ ppm), integration, multiplicity (s = singlet, d = doublet, t = triplet, q = quartet, m = multiplet, dd = doublet of doublets, dt = doublet of triplets, br = broad), coupling constant (Hz), and assignment. ^{13}C NMR spectra were recorded on an Agilent 400-MR DD2 400 MHz, Varian/Oxford As-500 500 MHz, or Bruker UltraShield Plus 500 MHz and data are reported in terms of chemical shift relative to $(CD_3)_2CO$ (29.9 ppm), $(CD_3)_2SO$ (39.5 ppm), or $CDCl_3$ (77.0 ppm). IR spectra were recorded on a Thermo Scientific Nicolet 6700, Shimadzu IRTracer-100, or Perkin Elmer Spectrum 100 FTIR spectrometer and are reported in wavenumbers (cm^{-1}). High Resolution Mass Spectra were recorded on an Agilent 5973N using electrospray (ESI) technique. Emission spectra of photocatalysts were collected on a PTI QuantaMaster™ 400 with Felix32 software.

4.5.2. Preparation of Substrates

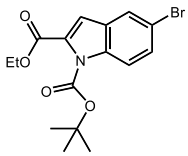

1-(*tert*-butyl) 2-ethyl 5-bromo-1*H*-indole-1,2-dicarboxylate

A flask was charged with ethyl 5-bromoindole-2-carboxylate (1.34 g, 5.0 mmol, 1.0 equiv.), and DMAP (61.0 mg, 5 mmol, 0.1 equiv.) then the reactants were dissolved in MeCN (15 ml). To this reaction mixture was added Boc_2O (1.4 ml, 6 mmol, 1.2 equiv.) and the resulting solution was stirred overnight. The crude reaction mixture was evaporated. Purification by flash column chromatography provided the title compound (1.86 g, 5 mmol, 99%) as a greenish yellow oil.

^{1}H NMR (400 MHz, $CDCl_3$) δ 7.96 (d, *J* = 8.9 Hz, 1H), 7.73 (d, *J* = 1.6 Hz, 1H), 7.54 – 7.43 (m, 1H), 7.00 (s, 1H), 1.62 (s, 9H).

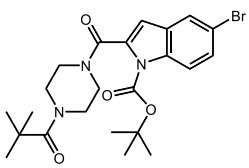

***tert*-butyl 5-bromo-2-(4-pivaloylpiperazine-1-carbonyl)-1*H*-indole-1-carboxylate (4.75)**

To a solution 1-boc-piperazine (298 mg, 1.6 mmol, 1.0 equiv.), and 5-bromoindole-2-carboxylic acid (457 mg, 1.9 mmol, 1.2 equiv.) in THF (11 ml) was added CDI (288 mg, 1.8 mmol 1.1 equiv.) and stirred for 48 h. The reaction mixture was concentrated *in vacuo* and the resulting residue was diluted with EtOAc. The organic layer was washed 3x using aq. $NaHCO_3$, dried (Na_2SO_4) and concentrated *in vacuo*. To the resulting crude mixture was added DMAP (20 mg, 0.16 mmol, 0.1 equiv.), and MeCN (16 ml). To this solution was added Boc_2O (1.1 ml, 4.8 mmol, 3.0 equiv.), and the resulting solution was stirred for 24 h. The solvent was concentrated *in vacuo*, and purification of the crude product by flash column chromatography provided the title compound (810 mg, 1.6 mmol, 99%) as a yellow oil.

^{1}H NMR (400 MHz, $CDCl_3$) δ 7.99 (d, *J* = 8.9 Hz, 1H), 7.68 (s, 1H), 7.44 (d, *J* = 8.9 Hz, 1H), 6.54 (s, 1H), 3.74 (s, 2H), 3.54 (s, 2H), 3.41 (s, 2H), 3.34 (s, 2H), 1.61 (s, 9H), 1.46 (s, 9H); ^{13}C NMR (101 MHz, $CDCl_3$) δ 162.9, 154.5, 148.6, 134.4, 133.5, 130.2, 128.3, 123.8, 116.9, 116.6, 107.3, 85.4, 80.4, 46.8, 41.7, 28.3, 28.0.

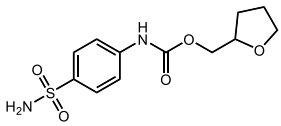

(tetrahydrofuran-2-yl)methyl (4-sulfamoylphenyl)carbamate

To a solution of sulfanilamide (517 mg, 3.0 mmol, 1.0 equiv.), and triphosgene (297 mg, 1.0 mmol, 0.33 equiv.) in THF (0.04 mmol) was added TEA (1.25 ml, 9.0 mmol, 3.0 equiv.), and tetrahydrofurfuryl alcohol (0.44 ml, 4.5 mmol, 1.5 equiv.) at 0 ℃. The resulting reaction mixture was stirred overnight and concentrated *in vacuo*. The resulting solid residue was recrystallized using EtOAc and hexane to provide the title compound (420 mg, 1.4 mmol, 47%) as a white solid.

^{1}H NMR (400 MHz, $(CD_3)_2SO$) δ 10.12 (s, 1H), 7.73 (d, *J* = 8.8 Hz, 2H), 7.61 (d, *J* = 8.8 Hz, 2H), 7.21 (s, 2H), 4.17 – 3.97 (m, 3H), 3.77 (dd, *J* = 14.6, 6.9 Hz, 1H), 3.66 (dd, *J* = 14.1, 7.6 Hz, 1H), 1.95 (ddd, *J* = 21.5, 12.4, 7.7 Hz, 1H), 1.89 – 1.74 (m, 2H), 1.64 – 1.51 (m, 1H).

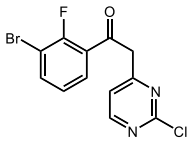

1-(3-Bromo-2-fluorophenyl)-2-(2-chloropyrimidin-4-yl)ethan-1-one

A 500 mL flask was charged with methyl 3-bromo-2-fluorobenzoate (4.66 g, 20.0 mmol, 1.0 equiv.) and THF (140 mL) then cooled to 0 ℃ in an ice water bath. A freshly prepared LiHMDS solution (6.69 g, 40.0 mmol, 2.0 equiv., 65 mL THF) was added followed by slow addition of 2-chloro-4-methylpyrimidine (3.21 g, 25.0 mmol, 1.25 equiv.) as a solution in THF (40 mL). The reaction was allowed to warm to room temperature over 1 hour. The volume of the solution was reduced by half under reduced pressure and then 6 M HCl was added, at which point a solid precipitate formed. The solution was filtered and washed with H_2O and Et_2O to provide the product (4.63 g, 14.1 mmol, 70%). The ^{1}H NMR data show a mixture of keto and enol tautomers.

^{1}H NMR (400 MHz, $CDCl_3$) δ 13.39 (s, 1H), 8.76 (d, *J* = 5.0 Hz, 1H), 8.66 (d, *J* = 5.4 Hz, 1H), 8.01 (ddd, *J* = 8.2, 6.4, 1.7 Hz, 1H), 7.94 – 7.83 (m, 2H), 7.83 – 7.75 (m, 1H), 7.59 (d, *J* = 5.0 Hz, 1H), 7.54 (d, *J* = 5.4 Hz, 1H), 7.32 (dt, *J* = 11.7, 7.9 Hz, 2H), 6.33 (s, 1H), 4.63 (d, *J* = 2.3 Hz, 2H); ^{13}C NMR (100 MHz, $CDCl_3$) δ 193.2, 193.1, 168.1, 166.7, 161.3, 161.2, 160.7, 160.4, 160.2, 158.6, 157.6, 157.0, 156.6, 155.0, 138.8, 136.1, 130.4, 129.3, 126.8, 126.7, 126.7, 126.7, 126.6, 124.7, 124.6, 122.2, 117.9, 110.4, 110.2, 110.1, 109.9, 100.2, 100.1, 50.6, 50.6; HRMS (ESI) calcd. for $C_{12}H_8BrClFN_2O$ [$(M+H)^+$]: 328.94469, found 328.94583.

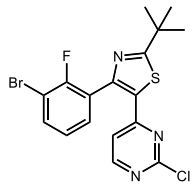

4-(3-Bromo-2-fluorophenyl)-2-(*tert*-butyl)-5-(2-chloropyrimidin-4-yl)thiazole

To a solution of 1-(3-Bromo-2-fluorophenyl)-2-(2-chloropyrimidin-4-yl)ethan-1-one (3.95 g, 12.0 mmol, 1.0 equiv.) in DMA (100 mL) was added NBS (2.14 g, 12.0 mmol, 1.0 equiv) and the reaction stirred for 15 minutes at room temperature. To the mixture was added 2,2-dimethylpropanethioamide (1.41 g, 12.0 mmol, 1.0 equiv.) and then the solution was heated to 120 ℃ for 2 hours. The reaction was cooled to room temperature and partitioned between H_2O and EtOAc. The aqueous layer was extracted 2x with EtOAc and the combined organic layers washed with H_2O and brine then dried with Na_2SO_4, filtered, and concentrated. The residue was purified by column chromatography (10% EtOAc/hexanes) to provide the product (3.65 g, 8.6 mmol, 71%).

^{1}H NMR (400 MHz, $CDCl_3$) δ 7.96 – 7.80 (m, 1H), 7.72 – 7.53 (m, 1H), 7.29 (q, J = 10.3, 9.1 Hz, 1H), 7.15 (d, J = 5.6 Hz, 1H), 1.43 (d, J = 9.1 Hz, 9H); ^{13}C NMR (100 MHz, $CDCl_3$) δ 184.1, 161.6, 160.4, 156.7, 154.8, 147.9, 135.2, 131., 131.6, 126.9, 124.5 (d, J = 15.5 Hz), 116.6, 109.6 (d, J = 21.2 Hz), 38.4, 30.7; HRMS (ESI) calcd. for $C_{17}H_{17}BrClFN_3S$ [$(M+H)^+$]: 425.98371, found 425.98249.

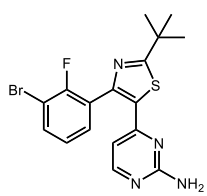

4-(4-(3-Bromo-2-fluorophenyl)-2-(*tert*-butyl)thiazol-5-yl)pyrimidin-2-amine (44)

A suspension of 4-(3-bromo-2-fluorophenyl)-2-(*tert*-butyl)-5-(2-chloropyrimidin-4-yl)thiazole (0.85 g, 2.0 mmol, 1.0 equiv.), NH_4OH (28 wt%, 13.8 mL, 200 mmol), and dioxane (20 mL) was heated in a sealed tube to 90 ℃ for 24 hours. H_2O was added and the mixture was filtered to provide the product as a white solid (0.49 g, 1.2 mmol, 60%)

IR (neat) ν_{max} x cm^{-1}; ^{1}H NMR (400 MHz, $CDCl_3$) δ 8.10 (d, *J* = 5.2 Hz, 1H), 7.85 (ddd, *J* = 8.2, 6.6, 1.7 Hz, 1H), 7.56 (ddd, *J* = 7.9, 6.6, 1.7 Hz, 1H), 7.30 (t, *J* = 7.9 Hz, 1H), 6.78 (s, 2H), 6.08 (d, *J* = 5.2 Hz, 1H), 1.43 (s, 9H); ^{13}C NMR (100 MHz, $CDCl_3$) δ 182.0, 163.9, 159.5, 157.9, 156.8, 154.8, 145.3, 135.0, 134.8, 131.7, 126.8, 125.2, 109.5, 105.9, 30.8; HRMS (ESI) calcd. for $C_{17}H_{17}BrClFN_3S$ [$(M+H)^+$]: 407.03358, found 407.03162.

4.5.3. General Sulfonamidation Procedure

General procedure A:

To an oven dried 8 mL vial equipped with a stir bar was added $NiCl_2$•glyme (5.5 mg, 0.025 mmol, 0.05 equiv), sulfonamide (0.75 mmol, 1.5 equiv), TMG (89 mg, 0.75 mmol, 1.5 equiv), aryl halide (0.5 mmol, 1.0 equiv), and MeCN (0.333 M). The solution was sonicated for 10 minutes and then photocatalyst (0.25 μmol, 0.0005 equiv) was added as a 0.0125 M stock solution in MeCN. The reaction was placed in an ice bath and sparged with N_2 for 15 minutes, after which the cap was sealed with electric tape. The reaction was stirred and irradiated with a 34 W blue LED lamp in an enclosed system with the reaction temperature reaching 68 ℃ (without fan cooling) or 35 ℃ (with fan cooling) for the indicated time. The reaction was quenched with saturated NH_4Cl (2 mL). The reaction was then extracted 4x from saturated NH_4Cl with either EtOAc (for carbocyclic aryl halides) or 4:1 CH_2Cl_2:isopropanol (for heterocyclic aryl halides). Organic extracts were combined, dried ($MgSO_4$), and concentrated *in vacuo*. Purification by flash column chromatography yielded the sulfonamidation product.

General procedure B:

To an oven dried vial equipped with a stir bar was added the bromoarene (if solid, 0.50 mmol, 1.0 equiv.), the sulfonamide (if solid, 0.75 mmol, 1.50 equiv.), $Ir(ppy)_2(dtbbpy)PF_6$ (2.3 mg, 2.5 μmol, 0.005 equiv.), $NiCl_2$·glyme (5.5 mg, 25 μmol, 0.05 equiv.) or $Ni(cod)_2$ (6.9 mg, 25 μmol, 0.05 equiv. weighed in a glove box after adding all solid materials) and dtbbpy (1.3 mg, 5 μmol, 0.01 equiv.). Degassed MeCN or DMSO (Degassed by sparging with Ar for 15 minutes, 0.25 M) was added to the vial followed by the bromoarene (if liquid), the sulfonamide (if liquid) and TMG (86 mg, 0.75 mmol, 1.50 equiv.). The vial was replenished with Ar and placed approximately 6 cm away from one 30 W blue LED and stirred for indicated reaction time. 25 ℃ reactions were performed with fan cooling and 55 ℃ reactions were performed without fan cooling. After completion of the reaction aq. NH_4Cl was added. For the reactions performed with MeCN the aqueous phase was extracted with CH_2Cl_2 (3x) and dried ($MgSO_4$). For the reactions performed with DMSO the aqueous phase was extracted with EtOAc (3x). The organic extracts were combined and washed with water (2x), brine (1x), dried ($MgSO_4$) and concentrated *in vacuo*. Purification by flash column chromatography yielded the sulfonamidation product.

Reaction Apparatus for Procedure A

Reaction Apparatus for Procedure B

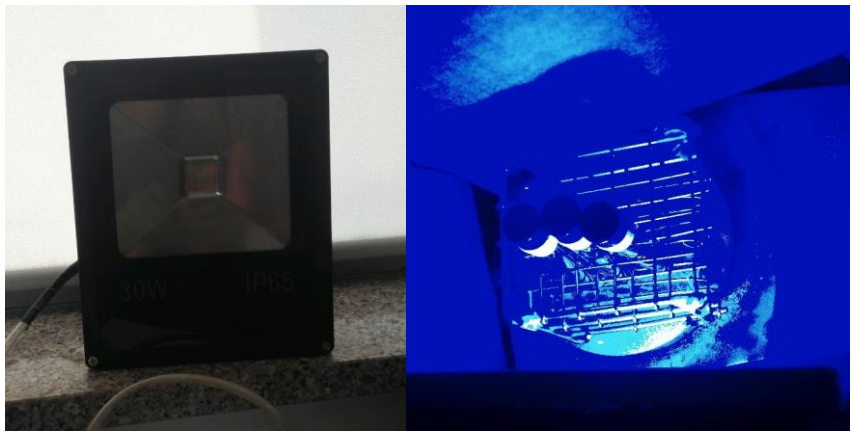

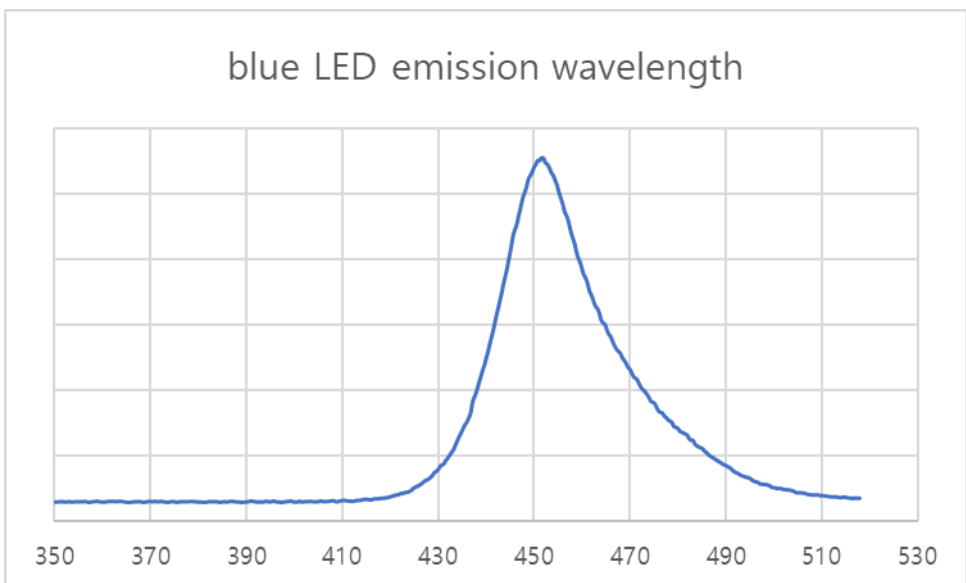

The light source and the reactions are performed with a 30 W blue LED. The emission maximum of the light source is approximately 450 nm.

Wavelength output of blue LED used was collected on Spectral Products SM240.

4.5.4. Experimental Data for Sulfonamidation Products

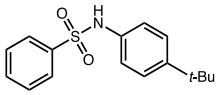

***N*-(4-(*tert*-butyl)phenyl)-4-methylbenzenesulfonamide (4.22)**

Procedure A: Prepared following the general procedure outlined above using 1-bromo-4-*tert*-butylbenzene (107 mg, 0.50 mmol, 1.0 equiv.), benzenesulfonamide (118 mg, 0.75 mmol, 1.50 equiv.), $Ir[dF(CF_3)ppy]_2(dtbbpy)PF_6$ (0.28 mg, 0.25 μmol, 0.0005 equiv.), $NiCl_2$·glyme (5.5 mg, 25 μmol, 0.05 equiv.), TMG (86 mg, 0.75 mmol, 1.5 equiv.), and MeCN (1.3 mL). After 24 hours of blue LED irradiation at 68 ℃, the reaction mixture was subjected to the workup procedure outlined in the general procedure. Purification by flash column chromatography (ethyl acetate/hexane) provided the title compound (124 mg, 0.43 mmol, 86%) as a white solid.

Procedure B: Prepared following the general procedure outlined above using 1-bromo-4-*tert*-butylbenzene (107 mg, 0.50 mmol, 1.0 equiv.), benzenesulfonamide (118 mg, 0.75 mmol, 1.50 equiv.), $Ir(ppy)_2(dtbbpy)PF_6$ (2.3 mg, 2.5 μmol, 0.005 equiv.), $NiCl_2$·glyme (5.5 mg, 25 μmol, 0.05 equiv.), dtbbpy (1.3 mg, 5 μmol, 0.01 equiv.), TMG (86 mg, 0.75 mmol, 1.50 equiv.), and MeCN (2.0 mL). After 48 hours of blue LED irradiation at 25 ℃, the reaction mixture was subjected to the workup procedure outlined in the general procedure. Purification by flash column chromatography (10% to 30% ethyl acetate/hexane) provided the title compound (142 mg, 0.49 mmol, 98%) as a white solid.

The compound matched previously reported characterization data.[v]

^{1}H NMR (400 MHz, $CDCl_3$) δ 7.80 (d, *J* = 7.7 Hz, 2H), 7.53 (t, *J* = 7.4 Hz, 1H), 7.43 (t, *J* = 7.6 Hz, 2H), 7.24 (d, *J* = 8.6 Hz, 2H), 7.00 (d, *J* = 8.5 Hz, 3H), 1.25 (s, 9H); ^{13}C NMR (101 MHz, $CDCl_3$) δ 148.7, 139.4, 133.7, 133.0, 129.1, 127.4, 126.3, 121.8, 34.5, 31.4.

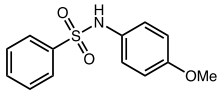

***N*-(4-methoxyphenyl)benzenesulfonamide (4.24)**

Procedure A: Prepared following the general procedure outlined above using 4-bromoanisole (94 mg, 0.50 mmol, 1.0 equiv.), benzenesulfonamide (118 mg, 0.75 mmol, 1.50 equiv.), $Ir[dF(CF_3)ppy]_2(dtbbpy)PF_6$ (0.28 mg, 0.25 μmol, 0.0005 equiv.), $NiCl_2$·glyme (5.5 mg, 25 μmol, 0.05 equiv.), MTBD (115 mg, 0.75 mmol, 1.5 equiv.), and MeCN (1.3 mL). After 24 hours of blue LED irradiation at 68 ℃, the reaction mixture was subjected to the workup procedure outlined in the general procedure. Purification by flash column chromatography (ethyl acetate/hexane) provided the title compound (54 mg, 0.21 mmol, 41%) as a white solid.

Procedure B: Prepared following the general procedure outlined above using 4-bromoanisole (94 mg, 0.50 mmol, 1.0 equiv.), benzenesulfonamide (118 mg, 0.75 mmol, 1.50 equiv.), $Ir(ppy)_2(dtbbpy)PF_6$ (2.3 mg, 2.5 μmol, 0.005 equiv.), $NiCl_2$·glyme (5.5 mg, 25 μmol, 0.05 equiv.), dtbbpy (1.3 mg, 5 μmol, 0.01 equiv.), TMG (86 mg, 0.75 mmol, 1.5 equiv.), and DMSO (2.0 mL). After 48 hours of blue LED irradiation at 55 ℃, the reaction mixture was subjected to the workup procedure outlined in the general procedure. Purification by flash column chromatography (10% to 30% ethyl acetate/hexane) provided the title compound (86 mg, 0.33 mmol, 66%) as a white solid.

The compound matched previously reported characterization data.[v]

^{1}H NMR (400 MHz, $CDCl_3$) δ 7.65 (d, *J* = 7.7 Hz, 2H), 7.39 (t, *J* = 7.3 Hz, 1H), 7.33 – 7.23 (m, 3H), 6.91 (d, *J* = 8.8 Hz, 2H), 6.62 (d, *J* = 8.7 Hz, 2H), 3.60 (s, 3H); ^{13}C NMR (101 MHz, $CDCl_3$) δ 157.8, 138.8, 132.9, 129.0, 127.3, 125.3, 114.4, 55.4.

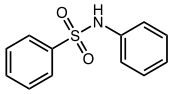

***N*-phenylbenzenesulfonamide (4.26)**

Procedure A: Prepared following the general procedure outlined above using bromobenzene (79 mg, 0.50 mmol, 1.0 equiv.), benzenesulfonamide (118 mg, 0.75 mmol, 1.50 equiv.), $Ir(ppy)_2(bpy)PF_6$ (0.2 mg, 0.25 μmol, 0.0005 equiv.), $NiCl_2$·glyme (5.5 mg, 25 μmol, 0.05 equiv.), TMG (86 mg, 0.75 mmol, 1.5 equiv.), and MeCN (1.3 mL). After 10 hours of blue LED irradiation at 68 ℃, the reaction mixture was subjected to the workup procedure outlined in the general procedure. Purification by flash column chromatography (ethyl acetate/hexane) provided the title compound (96 mg, 0.41 mmol, 82%) as a white solid.

Procedure B: Prepared following the general procedure outlined above using bromobenzene (79 mg, 0.50 mmol, 1.0 equiv.), benzenesulfonamide (118 mg, 0.75 mmol, 1.50 equiv.), $Ir(ppy)_2(dtbbpy)PF_6$ (2.3 mg, 2.5 μmol, 0.005 equiv.), $NiCl_2$·glyme (5.5 mg, 25 μmol, 0.05 equiv.), dtbbpy (1.3 mg, 5 μmol, 0.01 equiv.), TMG (86 mg, 0.75 mmol, 1.5 equiv.), and MeCN (2.0 mL). After 24 hours of blue LED irradiation at 55 ℃, the reaction mixture was subjected to the workup procedure outlined in the general procedure. Purification by flash column chromatography (10% to 30% ethyl acetate/hexane) provided the title compound (112 mg, 0.48 mmol, 96%) as a white solid.

The compound matched previously reported characterization data.[iii]

^{1}H NMR (400 MHz, $CDCl_3$) δ 7.80 (d, *J* = 8.0 Hz, 2H), 7.53 (t, *J* = 7.4 Hz, 1H), 7.43 (t, *J* = 7.7 Hz, 2H), 7.23 (t, *J* = 7.7 Hz, 2H), 7.10 (m, *J* = 8.8 Hz, 4H); ^{13}C NMR (101 MHz, $CDCl_3$) δ 138.9, 136.5, 133.1, 129.4, 129.1, 127.3, 125.4, 121.6.

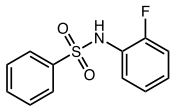

***N*-(2-fluorophenyl)benzenesulfonamide (4.27)**

Procedure A: Prepared following the general procedure outlined above using 1-bromo-2-fluorobenzene (88 mg, 0.50 mmol, 1.0 equiv.), benzenesulfonamide (118 mg, 0.75 mmol, 1.50 equiv.), $Ir(ppy)_2(bpy)PF_6$ (0.2 mg, 0.25 μmol, 0.0005 equiv.), $NiCl_2$·glyme (5.5 mg, 25 μmol, 0.05 equiv.), TMG (86 mg, 0.75 mmol, 1.5 equiv.), and MeCN (1.3 mL). After 24 hours of blue LED irradiation at 68 ℃, the reaction mixture was subjected to the workup procedure outlined in the general procedure. Purification by flash column chromatography (ethyl acetate/hexane) provided the title compound (68 mg, 0.27 mmol, 54%) as a white solid.

Procedure B: Prepared following the general procedure outlined above using 1-bromo-2-fluorobenzene (88 mg, 0.50 mmol, 1.0 equiv.), benzenesulfonamide (118 mg, 0.75 mmol, 1.50 equiv.), $Ir(ppy)_2(dtbbpy)PF_6$ (2.3 mg, 2.5 μmol, 0.005 equiv.), $Ni(cod)_2$ (6.9 mg, 25 μmol, 0.05 equiv.), dtbbpy (1.3 mg, 5 μmol, 0.01 equiv.), TMG (86 mg, 0.75 mmol, 1.5 equiv.), and DMSO (2.0 mL). After 48 hours of blue LED irradiation at 55 ℃, the reaction mixture was subjected to the workup procedure outlined in the general procedure. Purification by flash column chromatography (10% to 25% ethyl acetate/hexane) provided the title compound (91 mg, 0.36 mmol, 72%) as a white solid.

IR (neat) 3259, 1501, 1335, 1166, 921 cm^{-1}; H NMR (500 MHz, $CDCl_3$) δ 7.77 (d, *J* = 7.4 Hz, 2H), 7.60 (td, *J* = 7.9, 2.0 Hz, 1H), 7.55 (t, *J* = 7.5 Hz, 1H), 7.44 (t, *J* = 7.8 Hz, 2H), 7.13 – 7.03 (m, 2H), 6.98 – 6.91 (m, 1H), 6.67 (s, 1H); ^{13}C NMR (100 MHz, $CDCl_3$) δ 154.2 (d, *J* = 244.8 Hz), 133.4, 129.2, 127.3, 126.5 (d, *J* = 7.5 Hz), 124.9 (d, *J* = 4.0 Hz), 124.7, 124.6, 123.7, 115.6 (d, *J* = 19.5 Hz); ^{19}F NMR (376 MHz, $CDCl_3$) δ -129.8 (m, 1H); HRMS (ESI) calcd. for $C_{12}H_{10}FNNaO_2S$ [$(M+Na)^+$]: 274.0308, found 274.0312.

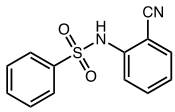

_N_-(2-cyanophenyl)benzenesulfonamide (4.28)

Procedure A: Prepared following the general procedure outlined above using 2-bromobenzonitrile (91 mg, 0.50 mmol, 1.0 equiv.), benzenesulfonamide (118 mg, 0.75 mmol, 1.50 equiv.), $Ir(ppy)_2(bpy)PF_6$ (0.2 mg, 0.25 μmol, 0.0005 equiv.), $NiCl_2$·glyme (5.5 mg, 25 μmol, 0.05 equiv.), TMG (86 mg, 0.75 mmol, 1.5 equiv.), and MeCN (1.3 mL). After 24 hours of blue LED irradiation at 68 ℃, the reaction mixture was subjected to the workup procedure outlined in the general procedure. Purification by flash column chromatography (ethyl acetate/hexane) provided the title compound (65 mg, 0.25 mmol, 50%) as a white solid.

Procedure B: Prepared following the general procedure outlined above using 2-bromobenzonitrile (91 mg, 0.50 mmol, 1.0 equiv.), benzenesulfonamide (118 mg, 0.75 mmol, 1.50 equiv.), $Ir(ppy)_2(dtbbpy)PF_6$ (2.3 mg, 2.5 μmol, 0.005 equiv.), $Ni(cod)_2$ (6.9 mg, 25 μmol, 0.05 equiv.), dtbbpy (1.3 mg, 5 μmol, 0.01 equiv.), TMG (86 mg, 0.75 mmol, 1.5 equiv.), and MeCN (2.0 mL). After 24 hours of blue LED irradiation at 25 ℃, the reaction mixture was subjected to the workup procedure outlined in the general procedure. Purification by flash column chromatography (20% to 30% ethyl acetate/hexane) provided the title compound (108 mg, 0.42 mmol, 83%) as a white solid.

IR (neat) ν_{max} 3252, 2229, 1492, 1335, 1162, 1090, 901 cm^{-1}; ^1H NMR (400 MHz, $CDCl_3$) δ 7.82 (d, J = 7.4 Hz, 2H), 7.74 (d, J = 8.4 Hz, 1H), 7.57 (ddd, J = 12.3, 9.0, 4.0 Hz, 2H), 7.48 (t, J = 7.3 Hz, 3H), 7.19 (t, J = 7.6 Hz, 1H), 7.07 (s, 1H); ^{13}C NMR (101 MHz, $CDCl_3$) δ 139.3, 138.5, 134.4, 133.9, 132.9, 129.5, 127.5, 125.5, 122.1, 115.7, 104.6. *m*/*z* calcd. for $C_{13}H_{10}N_2NaO_2S$ ($[M+Na]^+$) 281.0355, found 281.0356.

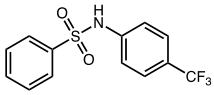

***N*-(4-(trifluoromethyl)phenyl)benzenesulfonamide (4.30)**

Procedure A: Prepared following the general procedure outlined above using 4-bromobenzotrifluoride (113 mg, 0.50 mmol, 1.0 equiv.), benzenesulfonamide (118 mg, 0.75 mmol, 1.50 equiv.), $Ir(ppy)_2(bpy)PF_6$ (0.2 mg, 0.25 μmol, 0.0005 equiv.), $NiCl_2$·glyme (5.5 mg, 25 μmol, 0.05 equiv.), TMG (86 mg, 0.75 mmol, 1.5 equiv.), and MeCN (1.3 mL). After 12 hours of blue LED irradiation at 35 ℃, the reaction mixture was subjected to the workup procedure outlined in the general procedure. Purification by flash column chromatography (ethyl acetate/hexane) provided the title compound (127 mg, 0.42 mmol, 84%) as a white solid.

Procedure B: Prepared following the general procedure outlined above using 4-bromobenzotrifluoride (113 mg, 0.50 mmol, 1.0 equiv.), benzenesulfonamide (118 mg, 0.75 mmol, 1.50 equiv.), $Ir(ppy)_2(dtbbpy)PF_6$ (2.3 mg, 2.5 μmol, 0.005 equiv.), $NiCl_2$·glyme (5.5 mg, 25 μmol, 0.05 equiv.), dtbbpy (1.3 mg, 5 μmol, 0.01 equiv.), TMG (86 mg, 0.75 mmol, 1.5 equiv.), and MeCN (2.0 mL). After 24 hours of blue LED irradiation at 25 ℃, the reaction mixture was subjected to the workup procedure outlined in the general procedure. Purification by flash column chromatography (10% to 30% ethyl acetate/hexane) provided the title compound (140 mg, 0.47 mmol, 93%) as a white solid.

The compound matched previously reported characterization data.[v]

^{1}H NMR (400 MHz, $CDCl_3$) δ 7.99 (s, 1H), 7.81 (d, *J* = 7.2 Hz, 2H), 7.45 (t, *J* = 6.9 Hz, 1H), 7.40 – 7.32 (m, 4H), 7.14 (d, *J* = 8.4 Hz, 2H). ^{13}C NMR (101 MHz, $CDCl_3$) δ 140.0, 138.6, 133.7, 124.0 (q, *J* = 271.8 Hz), 129.5, 127.3, 127.0, 126.7 (q, *J* = 3.7 Hz), 126.6, 126.3, 119.9; ^{19}F NMR (376 MHz, $CDCl_3$) δ -62.3 (s, 3H).

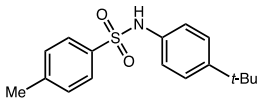

***N*-(4-(*tert*-butyl)phenyl)-4-methylbenzenesulfonamide (4.31)**

Procedure A: Prepared following the general procedure outlined above using 1-bromo-4-*tert*-butylbenzene (107 mg, 0.50 mmol, 1.0 equiv.), *p*-toluenesulfonamide (128 mg, 0.75 mmol, 1.50 equiv.), $Ir[dF(CF_3)ppy]_2(dtbbpy)PF_6$ (0.28 mg, 0.25 μmol, 0.0005 equiv.), $NiCl_2$·glyme (5.5 mg, 25 μmol, 0.05 equiv.), TMG (86 mg, 0.75 mmol, 1.5 equiv.), and MeCN (1.3 mL). After 24 hours of blue LED irradiation at 68 ℃, the reaction mixture was subjected to the workup procedure outlined in the general procedure. Purification by flash column chromatography (ethyl acetate/hexane) provided the title compound (130 mg, 0.43 mmol, 86%) as a white solid.

Procedure B: Prepared following the general procedure outlined above using 1-bromo-4-*tert*-butylbenzene (107 mg, 0.50 mmol, 1.0 equiv.), *p*-toluenesulfonamide (128 mg, 0.75 mmol, 1.50 equiv.), $Ir(ppy)_2(dtbbpy)PF_6$ (2.3 mg, 2.5 μmol, 0.005 equiv.), $NiCl_2$·glyme (5.5 mg, 25 μmol, 0.05 equiv.), dtbbpy (1.3 mg, 5 μmol, 0.01 equiv.), TMG (86 mg, 0.75 mmol, 1.50 equiv.), and MeCN (2.0 mL). After 48 hours of blue LED irradiation at 25 ℃, the reaction mixture was subjected to the workup procedure outlined in the general procedure. Purification by flash column chromatography (10% to 30% ethyl acetate/hexane) provided the title compound (149 mg, 0.49 mmol, 98%) as a white solid.

The compound matched previously reported characterization data.[vi]

^{1}H NMR (400 MHz, $CDCl_3$) δ 7.65 (d, *J* = 8.2 Hz, 2H), 7.24 (m, 3H), 6.97 (d, *J* = 8.6 Hz, 2H), 6.50 (d, *J* = 7.6 Hz, 1H), 2.39 (s, 3H), 1.26 (s, 9H); ^{13}C NMR (101 MHz, $CDCl_3$) δ 148.6, 143.8, 136.5, 133.8, 129.7, 127.4, 126.3, 121.7, 34.5, 31.4, 21.7.

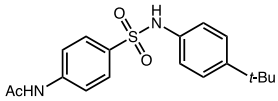

***N*-(4-(N-(4-(*tert*-butyl)phenyl)sulfamoyl)phenyl)acetamide (4.32)**

Procedure A: Prepared following the general procedure outlined above using 1-bromo-4-*tert*-butylbenzene (107 mg, 0.50 mmol, 1.0 equiv.), 4-acetamidobenzenesulfonamide (161 mg, 0.75 mmol, 1.50 equiv.), $Ir[dF(CF_3)ppy]_2(dtbbpy)PF_6$ (0.28 mg, 0.25 μmol, 0.0005 equiv.), $NiCl_2$·glyme (5.5 mg, 25 μmol, 0.05 equiv.), TMG (86 mg, 0.75 mmol, 1.5 equiv.), and MeCN (1.3 mL). After 48 hours of blue LED irradiation at 68 ℃, the reaction mixture was subjected to the workup procedure outlined in the general procedure. Purification by flash column chromatography (ethyl acetate/hexane) provided the title compound (157 mg, 0.45 mmol, 91%) as a white solid.

Procedure B: Prepared following the general procedure outlined above using 1-bromo-4-*tert*-butylbenzene (107 mg, 0.50 mmol, 1.0 equiv.), 4-acetamidobenzenesulfonamide (161 mg, 0.75 mmol, 1.50 equiv.), $Ir(ppy)_2(dtbbpy)PF_6$ (2.3 mg, 2.5 μmol, 0.005 equiv.), $NiCl_2$·glyme (5.5 mg, 25 μmol, 0.05 equiv.), dtbbpy (1.3 mg, 5 μmol, 0.01 equiv.), TMG (86 mg, 0.75 mmol, 1.50 equiv.), and MeCN (2.0 mL). After 48 hours of blue LED irradiation at 55 ℃, the reaction mixture was subjected to the workup procedure outlined in the general procedure. Purification by flash column chromatography (30% to 80% ethyl acetate/hexane) provided the title compound (172 mg, 0.50 mmol, > 99%) as a white solid.

IR (neat) ν_{max} 3257, 2964, 1680, 1592, 1514, 1401, 1327, 1156, 1093, 837 cm^{-1}; ^1H NMR (400 MHz, $(CD_3)_2SO$) δ 10.28 (s, 1H), 10.05 (s, 1H), 7.69 (s, 4H), 7.23 (d, J = 8.6 Hz, 2H), 6.99 (d, J = 8.6 Hz, 2H), 2.05 (s, 3H), 1.19 (s, 9H); ^{13}C NMR (101 MHz, $(CD_3)_2SO$) δ 169.0, 146.2, 143.0, 135.1, 133.4, 127.9, 125.8, 119.8, 118.5, 33.9, 31.1, 24.1; HRMS $C_{18}H_{22}N_2NaO_3S$ ($[M+Na]^+$) m/z calcd. for 369.1243, found 369.1245.

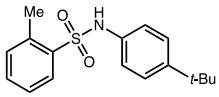

***N*-(4-(*tert*-butyl)phenyl)-2-methylbenzenesulfonamide (4.33)**

Procedure A: Prepared following the general procedure outlined above using 1-bromo-4-*tert*-butylbenzene (107 mg, 0.50 mmol, 1.0 equiv.), *o*-toluenesulfonamide (128 mg, 0.75 mmol, 1.50 equiv.), $Ir[dF(CF_3)ppy]_2(dtbbpy)PF_6$ (0.28 mg, 0.25 μmol, 0.0005 equiv.), $NiCl_2$·glyme (5.5 mg, 25 μmol, 0.05 equiv.), TMG (86 mg, 0.75 mmol, 1.5 equiv.), and MeCN (1.3 mL). After 24 hours of blue LED irradiation at 68 ℃, the reaction mixture was subjected to the workup procedure outlined in the general procedure. Purification by flash column chromatography (ethyl acetate/hexane) provided the title compound (125 mg, 0.41 mmol, 82%) as a white solid.

Procedure B: Prepared following the general procedure outlined above using 1-bromo-4-*tert*-butylbenzene (107 mg, 0.50 mmol, 1.0 equiv.), *o*-toluenenesulfonamide (128 mg, 0.75 mmol, 1.50 equiv.), $Ir(ppy)_2(dtbbpy)PF_6$ (2.3 mg, 2.5 μmol, 0.005 equiv.), $NiCl_2$·glyme (5.5 mg, 25 μmol, 0.05 equiv.), dtbbpy (1.3 mg, 5 μmol, 0.01 equiv.), TMG (86 mg, 0.75 mmol, 1.50 equiv.), and MeCN (2.0 mL). After 48 hours of blue LED irradiation at 55 ℃, the reaction mixture was subjected to the workup procedure outlined in the general procedure. Purification by flash column chromatography (15% ethyl acetate/hexane) provided the title compound (148 mg, 0.49 mmol, 97%) as a white solid.

IR (neat) ν_{max} 3273, 2963, 1515, 1328, 1158, 926, 833 cm^{-1}; ^1H NMR (400 MHz, $CDCl_3$) δ 7.97 (d, *J* = 8.0 Hz, 1H), 7.43 (t, *J* = 7.4 Hz, 1H), 7.28 (d, *J* = 7.3 Hz, 2H), 7.22 (d, *J* = 8.4 Hz, 2H), 6.93 (d, *J* = 8.5 Hz, 2H), 6.68 (s, 1H), 2.65 (s, 3H), 1.24 (s, 9H); ^{13}C NMR (101 MHz, $CDCl_3$) δ 137.9, 137.4, 133.8, 133.2, 132.7, 130.0, 126.4, 126.3, 120.9, 120.8, 34.5, 31.4, 20.6; HRMS $C_{17}H_{21}NNaO_2S$ ($[M+Na]^+$) *m*/*z* calcd. for 326.1185, found 326.1185.

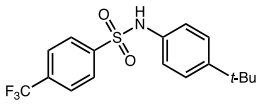

***N*-(4-(*tert*-butyl)phenyl)-4-(trifluoromethyl)benzenesulfonamide (4.34)**

Procedure A: Prepared following the general procedure outlined above using 1-bromo-4-*tert*-butylbenzene (107 mg, 0.50 mmol, 1.0 equiv.), 4-(trifluoromethyl)benzenesulfonamide (225 mg, 1.0 mmol, 2.0 equiv.), $Ir[dF(CF_3)ppy]_2(dtbbpy)PF_6$ (0.28 mg, 0.25 μmol, 0.0005 equiv.), $NiCl_2$·glyme (5.5 mg, 25 μmol, 0.05 equiv.), TMG (115 mg, 1.0 mmol, 2.0 equiv.), and MeCN (1.3 mL). After 24 hours of blue LED irradiation at 68 ºC, the reaction mixture was subjected to the workup procedure outlined in the general procedure. Purification by flash column chromatography (ethyl acetate/hexane) provided the title compound (118 mg, 0.33 mmol, 66%) as a white solid.

Procedure B: Prepared following the general procedure outlined above using 1-bromo-4-*tert*-butylbenzene (107 mg, 0.50 mmol, 1.0 equiv.), 4-(trifluoromethyl)benzenesulfonamide (169 mg, 0.75 mmol, 1.50 equiv.), $Ir(ppy)_2(dtbbpy)PF_6$ (2.3 mg, 2.5 μmol, 0.005 equiv.), $NiCl_2$·glyme (5.5 mg, 25 μmol, 0.05 equiv.), dtbbpy (1.3 mg, 5 μmol, 0.01 equiv.), TMG (86 mg, 0.75 mmol, 1.50 equiv.), and MeCN (2.0 mL). After 48 hours of blue LED irradiation at 55 ºC, the reaction mixture was subjected to the workup procedure outlined in the general procedure. Purification by flash column chromatography (10% to 30% ethyl acetate/hexane) provided the title compound (176 mg, 0.49 mmol, 99%) as a white solid.

IR (neat) ν_{max} 3262, 2966, 1516, 1323, 1167, 1063, 840 cm^{-1}; ^1H NMR (400 MHz, $CDCl_3$) δ 7.90 (d, *J* = 8.2 Hz, 2H), 7.70 (d, *J* = 8.2 Hz, 2H), 7.27 (d, *J* = 8.4 Hz, 2H), 7.00 (d, *J* = 8.5 Hz, 2H), 6.89 (s, 1H), 1.26 (s, 9H); ^{13}C NMR (101 MHz, $CDCl_3$) δ 149.5, 142.9, 134.5 (q, *J* = 33.1 Hz), 133.0, 127.9, 126.6, 126.1 (q, *J* = 3.7 Hz), 123.1 (q, *J* = 272.9 Hz), 122.3, 34.6, 31.4; ^{19}F NMR (376 MHz, $CDCl_3$) δ -63.2 (s, 3H); HRMS $C_{17}H_{18}F_3NNaO_2S$ ($[M+Na]^+$) *m*/*z* calcd. for 380.0903, found 380.0904.

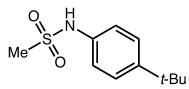

***N*-(4-(*tert*-butyl)phenyl)methanesulfonamide (4.35)**

Procedure A: Prepared following the general procedure outlined above using 1-bromo-4-*tert*-butylbenzene (107 mg, 0.50 mmol, 1.0 equiv.), methanesulfonamide (136 mg, 0.75 mmol, 1.50 equiv.), $Ir[dF(CF_3)ppy]_2(dtbbpy)PF_6$ (0.28 mg, 0.25 μmol, 0.0005 equiv.), $NiCl_2$·glyme (5.5 mg, 25 μmol, 0.05 equiv.), TMG (86 mg, 0.75 mmol, 1.5 equiv.), and MeCN (1.3 mL). After 14 hours of blue LED irradiation at 68 ℃, the reaction mixture was subjected to the workup procedure outlined in the general procedure. Purification by flash column chromatography (ethyl acetate/hexane) provided the title compound (102 mg, 0.45 mmol, 90%) as a white solid.

Procedure B: Prepared following the general procedure outlined above using 1-bromo-4-*tert*-butylbenzene (107 mg, 0.50 mmol, 1.0 equiv.), methanesulfonamide (71 mg, 0.75 mmol, 1.50 equiv.), $Ir(ppy)_2(dtbbpy)PF_6$ (2.3 mg, 2.5 μmol, 0.005 equiv.), $NiCl_2$·glyme (5.5 mg, 25 μmol, 0.05 equiv.), dtbbpy (1.3 mg, 5 μmol, 0.01 equiv.), TMG (86 mg, 0.75 mmol, 1.50 equiv.), and MeCN (2.0 mL). After 48 hours of blue LED irradiation at 55 ℃, the reaction mixture was subjected to the workup procedure outlined in the general procedure. Purification by flash column chromatography (10% to 30% ethyl acetate/hexane) provided the title compound (111 mg, 0.49 mmol, 97%) as a white solid.

The compound matched previously reported characterization data.[vi]

^{1}H NMR (400 MHz, $CDCl_3$) δ 7.36 (d, *J* = 8.3 Hz, 2H), 7.20 (d, *J* = 8.5 Hz, 2H), 7.06 (d, *J* = 19.5 Hz, 1H), 3.00 (s, 3H), 1.30 (s, 9H); ^{13}C NMR (101 MHz, $CDCl_3$) δ 148.8, 134.1, 126.6, 121.2, 39.2, 34.5, 31.4.

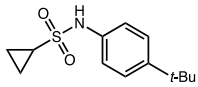

***N*-(4-(*tert*-butyl)phenyl)cyclopropanesulfonamide (4.36)**

Procedure A: Prepared following the general procedure outlined above using 1-bromo-4-*tert*-butylbenzene (107 mg, 0.50 mmol, 1.0 equiv.), cyclopropanesulfonamide (91 mg, 0.75 mmol, 1.50 equiv.), $Ir[dF(CF_3)ppy]_2(dtbbpy)PF_6$ (0.28 mg, 0.25 μmol, 0.0005 equiv.), $NiCl_2$·glyme (5.5 mg, 25 μmol, 0.05 equiv.), TMG (86 mg, 0.75 mmol, 1.5 equiv.), and MeCN (1.3 mL). After 14 hours of blue LED irradiation at 68 ℃, the reaction mixture was subjected to the workup procedure outlined in the general procedure. Purification by flash column chromatography (ethyl acetate/hexane) provided the title compound (96 mg, 0.38 mmol, 76%) as a white solid.

Procedure B: Prepared following the general procedure outlined above using 1-bromo-4-*tert*-butylbenzene (107 mg, 0.50 mmol, 1.0 equiv.), cyclopropanesulfonamide (91 mg, 0.75 mmol, 1.50 equiv.), $Ir(ppy)_2(dtbbpy)PF_6$ (2.3 mg, 2.5 μmol, 0.005 equiv.), $NiCl_2$·glyme (5.5 mg, 25 μmol, 0.05 equiv.), dtbbpy (1.3 mg, 5 μmol, 0.01 equiv.), TMG (86 mg, 0.75 mmol, 1.50 equiv.), and MeCN (2.0 mL). After 48 hours of blue LED irradiation at 55 ℃, the reaction mixture was subjected to the workup procedure outlined in the general procedure. Purification by flash column chromatography (10% to 30% ethyl acetate/hexane) provided the title compound (125 mg, 0.49 mmol, 98%) as a white solid.

IR (neat) ν_{max} 3259, 2963, 1514, 1331, 1150, 918, 838 cm^{-1}; ^1H NMR (500 MHz, $CDCl_3$) δ 7.35 (d, *J* = 8.6 Hz, 2H), 7.19 (d, *J* = 8.6 Hz, 2H), 6.53 (s, 1H), 2.53 – 2.45 (m, 1H), 1.31 (s, 9H), 1.20 – 1.14 (m, 2H), 0.99 – 0.91 (m, 2H); ^{13}C NMR (101 MHz, $CDCl_3$) δ 148.9, 134.1, 126.5, 122.1, 34.6, 31.5, 29.9, 5.8; HRMS $C_{13}H_{19}NNaO_2S$ ($[M+Na]^+$) *m*/*z* calcd. for 276.1029, found 276.1031.

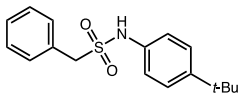

***N*-(4-(*tert*-butyl)phenyl)-1-phenylmethanesulfonamide (4.37)**

Procedure A: Prepared following the general procedure outlined above using 1-bromo-4-*tert*-butylbenzene (107 mg, 0.50 mmol, 1.0 equiv.), benzylsulfonamide (128 mg, 0.75 mmol, 1.50 equiv.), $Ir[dF(CF_3)ppy]_2(dtbbpy)PF_6$ (0.28 mg, 0.25 μmol, 0.0005 equiv.), $NiCl_2$·glyme (5.5 mg, 25 μmol, 0.05 equiv.), TMG (86 mg, 0.75 mmol, 1.5 equiv.), and MeCN (1.3 mL). After 14 hours of blue LED irradiation at 68 ℃, the reaction mixture was subjected to the workup procedure outlined in the general procedure. Purification by flash column chromatography (ethyl acetate/hexane) provided the title compound (110 mg, 0.36 mmol, 73%) as a white solid.

Procedure B: Prepared following the general procedure outlined above using 1-bromo-4-*tert*-butylbenzene (107 mg, 0.50 mmol, 1.0 equiv.), benzylsulfonamide (128 mg, 0.75 mmol, 1.50 equiv.), $Ir(ppy)_2(dtbbpy)PF_6$ (2.3 mg, 2.5 μmol, 0.005 equiv.), $NiCl_2$·glyme (5.5 mg, 25 μmol, 0.05 equiv.), dtbbpy (1.3 mg, 5 μmol, 0.01 equiv.), TMG (86 mg, 0.75 mmol, 1.50 equiv.), and MeCN (2.0 mL). After 48 hours of blue LED irradiation at 55 ℃, the reaction mixture was subjected to the workup procedure outlined in the general procedure. Purification by flash column chromatography (10% to 30% ethyl acetate/hexane) provided the title compound (152 mg, 0.50 mmol, > 99%) as a white solid.

IR (neat) ν_{max} 3259, 2962, 1515, 1333, 1155, 929 cm^{-1}; ^1H NMR (400 MHz, $CDCl_3$) δ 7.34 (M *J* = 10.2, 5H), 7.31 – 7.26 (m, 2H), 7.10 (d, *J* = 8.6 Hz, 2H), 6.63 (s, 1H), 4.30 (s, 2H), 1.33 (s, 9H); ^{13}C NMR (101 MHz, $CDCl_3$) δ 148.2, 134.2, 131.0, 129.0, 128.9, 128.8, 126.5, 120.4, 57.5, 34.5, 31.5; HRMS $C_{17}H_{21}NNaO_2S$ ($[M+Na]^+$) *m*/*z* calcd. for 326.1185, found 326.1185.

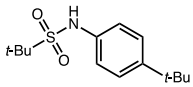

***N*-(4-(*tert*-butyl)phenyl)-2-methylpropane-2-sulfonamide (4.38)**

Procedure A: Prepared following the general procedure outlined above using 1-bromo-4-*tert*-butylbenzene (107 mg, 0.50 mmol, 1.0 equiv.), *tert*-butylsulfonamide (137 mg, 1.0 mmol, 2.0 equiv.), $Ir[dF(CF_3)ppy]_2(dtbbpy)PF_6$ (0.28 mg, 0.25 μmol, 0.0005 equiv.), $NiCl_2$·glyme (5.5 mg, 25 μmol, 0.05 equiv.), TMG (115 mg, 1.0 mmol, 2.0 equiv.), and MeCN (1.3 mL). After 24 hours of blue LED irradiation at 68 ℃, the reaction mixture was subjected to the workup procedure outlined in the general procedure. Purification by flash column chromatography (ethyl acetate/hexane) provided the title compound (55 mg, 0.20 mmol, 41%) as a white solid.

Procedure B: Prepared following the general procedure outlined above using 1-bromo-4-*tert*-butylbenzene (107 mg, 0.50 mmol, 1.0 equiv.), *tert*-butylsulfonamide (103 mg, 0.75 mmol, 1.50 equiv.), $Ir(ppy)_2(dtbbpy)PF_6$ (2.3 mg, 2.5 μmol, 0.005 equiv.), $NiCl_2$·glyme (5.5 mg, 25 μmol, 0.05 equiv.), dtbbpy (1.3 mg, 5 μmol, 0.01 equiv.), TMG (86 mg, 0.75 mmol, 1.50 equiv.), and MeCN (2.0 mL). After 48 hours of blue LED irradiation at 55 ℃, the reaction mixture was subjected to the workup procedure outlined in the general procedure. Purification by flash column chromatography (10% to 30% ethyl acetate/hexane) provided the title compound (132 mg, 0.49 mmol, 98%) as a white solid.

IR (neat) ν_{max} 3257, 2964, 1515, 1323, 1290, 1131, 924 cm^{-1}; ^1H NMR (500 MHz, $CDCl_3$) δ 7.30 (d, *J* = 8.7 Hz, 2H), 7.21 (d, *J* = 8.6 Hz, 2H), 6.80 (s, 1H), 1.41 (s, 9H), 1.29 (s, 9H); ^{13}C NMR (101 MHz, $CDCl_3$) δ 147.7, 135.9, 126.3, 120.4, 61.9, 34.4, 31.5, 25.0; HRMS $C_{14}H_{23}NNaO_2S$ ($[M+Na]^+$) *m*/*z* calcd. for 292.1342, found 292.1344.

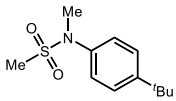

***N*-(4-(*tert*-butyl)phenyl)-*N*-methylmethanesulfonamide (4.39)**

Prepared following the general procedure B outlined above using 1-bromo-4-*tert*-butylbenzene (107 mg, 0.50 mmol, 1.0 equiv.), *N*-methylmethanesulfonamide (136 mg, 1.25 mmol, 2.50 equiv.), $Ir(ppy)_2(dtbbpy)PF_6$ (2.3 mg, 2.5 μmol, 0.005 equiv.), $NiCl_2$·glyme (5.5 mg, 25 μmol, 0.05 equiv.), dtbbpy (1.3 mg, 5 μmol, 0.01 equiv.), TMG (115 mg, 1.0 mmol, 2.0 equiv.), and MeCN (2.0 mL). After 48 h without fan cooling, the reaction mixture was subjected to the workup protocol outlined in the general procedure. Purification by flash column chromatography (5% to 15% ethyl acetate/hexane) provided the title compound (81 mg, 0.34 mmol, 67%) as a white solid.

IR (neat) ν_{max} 2961, 1506, 1340, 1149, 1070, 964, 877, 838 cm^{-1}; ^1H NMR (400 MHz, $CDCl_3$) δ 7.39 (d, *J* = 8.6 Hz, 2H), 7.29 (d, *J* = 8.6 Hz, 2H), 3.31 (s, 3H), 2.84 (s, 3H), 1.32 (s, 9H). ^{13}C NMR (101 MHz, $CDCl_3$) δ 150.7, 138.8, 126.4, 126.0, 38.3, 35.3, 34.7, 31.4. HRMS $C_{12}H_{19}NNaO_2S$ ($[M+Na]^+$) *m*/*z* calcd. for 264.1029, found 264.1030.

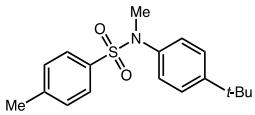

***N*-(4-(*tert*-butyl)phenyl)-*N*,4-dimethylbenzenesulfonamide (4.40)**

Procedure A: Prepared following the general procedure outlined above using 1-bromo-4-*tert*-butylbenzene (107 mg, 0.50 mmol, 1.0 equiv.), *N*-methyl-*p*-toluenesulfonamide (187 mg, 1.0 mmol, 2.0 equiv.), $Ir[dF(CF_3)ppy]_2(dtbbpy)PF_6$ (0.28 mg, 0.25 μmol, 0.0005 equiv.), $NiCl_2$·glyme (5.5 mg, 25 μmol, 0.05 equiv.), TMG (115 mg, 1.0 mmol, 2.0 equiv.), 4-methylstyrene (5.9 mg, 50 mol, 0.10 equiv.) and MeCN (1.3 mL). After 24 hours of blue LED irradiation at 68 ℃, the reaction mixture was analyzed by NMR. The reaction yield was determined to be 19%.

Procedure B: Prepared following the general procedure outlined above using 1-bromo-4-*tert*-butylbenzene (107 mg, 0.50 mmol, 1.0 equiv.), *N*-methyl-*p*-toluenesulfonamide (231 mg, 1.25 mmol, 2.50 equiv.), $Ir(ppy)_2(dtbbpy)PF_6$ (2.3 mg, 2.5 μmol, 0.005 equiv.), $NiCl_2$·glyme (5.5 mg, 25 μmol, 0.05 equiv.), dtbbpy (1.3 mg, 5 μmol, 0.01 equiv.), TMG (115 mg, 1.0 mmol, 2.0 equiv.), and MeCN (2.0 mL). After 48 hours of blue LED irradiation at 55 ℃, the reaction mixture was subjected to the workup procedure outlined in the general procedure. Purification by flash column chromatography (5% to 15% ethyl acetate/hexane) provided the title compound (100 mg, 0.32 mmol, 63%) as an orange solid. IR (neat) ν_{max} 2963, 1508, 1349, 1173, 1156, 873 cm^{-1}; ^1H NMR (500 MHz, $CDCl_3$) δ 7.45 (d, *J* = 8.1 Hz, 2H), 7.30 (d, *J* = 8.6 Hz, 2H), 7.25 (d, *J* = 8.2 Hz, 2H), 7.01 (d, *J* = 8.5 Hz, 2H), 3.14 (s, 3H), 2.42 (s, 3H), 1.30 (s, 9H); ^{13}C NMR (101 MHz, $CDCl_3$) δ 150.4, 143.5, 139.0, 133.8, 129.4, 128.0, 126.3, 125.8, 38.2, 34.6, 31.4, 21.6; HRMS $C_{18}H_{23}NNaO_2S$ ($[M+Na]^+$) *m*/*z* calcd. for 340.1342, found 340.1342.

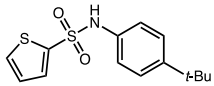

***N*-(4-(*tert*-butyl)phenyl)thiophene-2-sulfonamide (4.41)**

Procedure A: Prepared following the general procedure outlined above using 1-bromo-4-*tert*-butylbenzene (107 mg, 0.50 mmol, 1.0 equiv.), 2-thiophenesulfonamide (122 mg, 0.75 mmol, 1.50 equiv.), $Ir[dF(CF_3)ppy]_2(dtbbpy)PF_6$ (0.28 mg, 0.25 μmol, 0.0005 equiv.), $NiCl_2$·glyme (5.5 mg, 25 μmol, 0.05 equiv.), TMG (86 mg, 0.75 mmol, 1.5 equiv.), and MeCN (1.3 mL). After 24 hours of blue LED irradiation at 68 ℃, the reaction mixture was subjected to the workup procedure outlined in the general procedure. Purification by flash column chromatography (ethyl acetate/hexane) provided the title compound (109 mg, 0.37 mmol, 74%) as a white solid.

Procedure B: Prepared following the general procedure outlined above using 1-bromo-4-*tert*-butylbenzene (107 mg, 0.50 mmol, 1.0 equiv.), 2-thiophenesulfonamide (122 mg, 0.75 mmol, 1.50 equiv.), $Ir(ppy)_2(dtbbpy)PF_6$ (2.3 mg, 2.5 μmol, 0.005 equiv.), $NiCl_2$·glyme (5.5 mg, 25 μmol, 0.05 equiv.), dtbbpy (1.3 mg, 5 μmol, 0.01 equiv.), TMG (86 mg, 0.75 mmol, 1.50 equiv.), and MeCN (2.0 mL). After 48 hours of blue LED irradiation at 55 ℃, the reaction mixture was subjected to the workup procedure outlined in the general procedure. Purification by flash column chromatography (10% to 30% ethyl acetate/hexane) provided the title compound (141 mg, 0.48 mmol, 96%) as a white solid.

IR (neat) ν_{max} 3257, 2963, 1514, 1335, 1158, 1017, 923 cm^{-1}; ^1H NMR (400 MHz, $CDCl_3$) δ 7.53 (d, *J* = 5.0 Hz, 1H), 7.51 – 7.49 (m, 1H), 7.29 (d, *J* = 8.6 Hz, 2H), 7.06 (d, *J* = 8.6 Hz, 2H), 7.00 (t, *J* = 4.4 Hz, 1H), 6.85 (s, 1H), 1.27 (s, 9H); ^{13}C NMR (101 MHz, $CDCl_3$) δ 149.1, 139.8, 133.4, 132.9, 132.4, 127.4, 126.4, 122.1, 34.6, 31.4; HRMS $C_{14}H_{17}NNaO_2S_2$ ($[M+Na]^+$) *m*/*z* calcd. for 318.0593, found 318.0595.

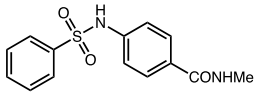

***N*-methyl-4-(phenylsulfonamido)benzamide (4.48)**

Procedure A: Prepared following the general procedure outlined above using *N*-methyl 4-bromobenzamide (107 mg, 0.50 mmol, 1.0 equiv.), benzenesulfonamide (118 mg, 0.75 mmol, 1.50 equiv.), $Ir(ppy)_2(bpy)PF_6$ (0.2 mg, 0.25 μmol, 0.0005 equiv.), $NiCl_2$·glyme (5.5 mg, 25 μmol, 0.05 equiv.), TMG (86 mg, 0.75 mmol, 1.5 equiv.), and MeCN (1.3 mL). After 8 hours of blue LED irradiation at 35 ℃, the reaction mixture was subjected to the workup procedure outlined in the general procedure. Purification by flash column chromatography (ethyl acetate/hexane) provided the title compound (128 mg, 0.44 mmol, 88%) as a white solid.

Procedure B: Prepared following the general procedure outlined above using *N*-methyl 4-bromobenzamide (107 mg, 0.50 mmol, 1.0 equiv.), benzenesulfonamide (118 mg, 0.75 mmol, 1.50 equiv.), $Ir(ppy)_2(dtbbpy)PF_6$ (2.3 mg, 2.5 μmol, 0.005 equiv.), $NiCl_2$·glyme (5.5 mg, 25 μmol, 0.05 equiv.), dtbbpy (1.3 mg, 5 μmol, 0.01 equiv.), TMG (86 mg, 0.75 mmol, 1.5 equiv.), and MeCN (2.0 mL). After 24 hours of blue LED irradiation at 25 ℃, the reaction mixture was subjected to the workup procedure outlined in the general procedure. Purification by flash column chromatography (30% to 80% ethyl acetate/hexane) provided the title compound (139 mg, 0.48 mmol, 96%) as a white solid.

IR (neat) ν_{max} 3412, 3108, 1609, 1558, 1505, 1332, 1158, 1091, 923 cm^{-1}; ^1H NMR (400 MHz, $(CD_3)_2SO$) δ 10.62 (s, 1H), 8.25 (d, *J* = 4.4 Hz, 1H), 7.80 (d, *J* = 7.3 Hz, 2H), 7.68 (d, *J* = 8.6 Hz, 2H), 7.62 (t, *J* = 7.3 Hz, 1H), 7.55 (t, *J* = 7.4 Hz, 2H), 7.14 (d, *J* = 8.5 Hz, 2H), 2.72 (d, *J* = 4.5 Hz, 3H). ^{13}C NMR (101 MHz, $(CD_3)_2SO$) δ 165.9, 140.2, 139.3, 133.1, 129.8, 129.4, 128.3, 126.7, 118.5, 26.2. *m*/*z* calcd. For $C_{14}H_{14}N_2NaO_3S$ ($[M+Na]^+$) 313.0617, found 313.0618.

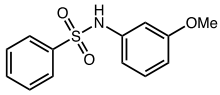

***N*-(3-methoxyphenyl)benzenesulfonamide (4.49)**

Procedure A: Prepared following the general procedure outlined above using 3-bromoanisole (94 mg, 0.50 mmol, 1.0 equiv.), benzenesulfonamide (118 mg, 0.75 mmol, 1.50 equiv.), $Ir[dF(CF_3)ppy]_2(dtbbpy)PF_6$ (0.28 mg, 0.25 μmol, 0.0005 equiv.), $NiCl_2$·glyme (5.5 mg, 25 μmol, 0.05 equiv.), TMG (86 mg, 0.75 mmol, 1.5 equiv.), and MeCN (1.3 mL). After 24 hours of blue LED irradiation at 68 ℃, the reaction mixture was subjected to the workup procedure outlined in the general procedure. Purification by flash column chromatography (ethyl acetate/hexane) provided the title compound (100 mg, 0.38 mmol, 76%) as a white solid.

Procedure B: Prepared following the general procedure outlined above using 3-bromoanisole (94 mg, 0.50 mmol, 1.0 equiv.), benzenesulfonamide (118 mg, 0.75 mmol, 1.50 equiv.), $Ir(ppy)_2(dtbbpy)PF_6$ (2.3 mg, 2.5 μmol, 0.005 equiv.), $NiCl_2$·glyme (5.5 mg, 25 μmol, 0.05 equiv.), dtbbpy (1.3 mg, 5 μmol, 0.01 equiv.), TMG (86 mg, 0.75 mmol, 1.5 equiv.), and DMSO (2.0 mL). After 48 hours of blue LED irradiation at 55 ℃, the reaction mixture was subjected to the workup procedure outlined in the general procedure. Purification by flash column chromatography (10% to 30% ethyl acetate/hexane) provided the title compound (127 mg, 0.48 mmol, 96%) as a white solid.

The compound matched previously reported characterization data.[iv]

^{1}H NMR (400 MHz, $CDCl_3$) δ 7.85 (d, *J* = 7.6 Hz, 2H), 7.63 (s, 1H), 7.50 (t, *J* = 7.4 Hz, 1H), 7.41 (t, *J* = 7.7 Hz, 2H), 7.09 (t, *J* = 8.1 Hz, 1H), 6.73 (s, 1H), 6.68 (d, *J* = 7.9 Hz, 1H), 6.62 (d, *J* = 8.3 Hz, 1H), 3.70 (s, 3H). ^{13}C NMR (101 MHz, $CDCl_3$) δ 160.3, 138.9, 137.8, 133.1, 130.1, 129.1, 127.3, 113.4, 111.0, 106.9, 55.3.

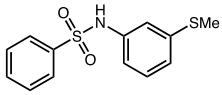

***N*-(3-(methylthio)phenyl)benzenesulfonamide (4.50)**

Procedure A: Prepared following the general procedure outlined above using 3-bromothioanisole (102 mg, 0.50 mmol, 1.0 equiv.), benzenesulfonamide (118 mg, 0.75 mmol, 1.50 equiv.), $Ir[dF(CF_3)ppy]_2(dtbbpy)PF_6$ (0.28 mg, 0.25 μmol, 0.0005 equiv.), $NiCl_2$·glyme (5.5 mg, 25 μmol, 0.05 equiv.), TMG (86 mg, 0.75 mmol, 1.5 equiv.), and MeCN (1.3 mL). After 24 hours of blue LED irradiation at 68 ℃, the reaction mixture was subjected to the workup procedure outlined in the general procedure. Purification by flash column chromatography (ethyl acetate/hexane) provided the title compound (112 mg, 0.40 mmol, 80%) as a beige solid.

Procedure B: Prepared following the general procedure outlined above using 3-bromothioanisole (102 mg, 0.50 mmol, 1.0 equiv.), benzenesulfonamide (118 mg, 0.75 mmol, 1.50 equiv.), $Ir(ppy)_2(dtbbpy)PF_6$ (2.3 mg, 2.5 μmol, 0.005 equiv.), $NiCl_2$·glyme (5.5 mg, 25 μmol, 0.05 equiv.), dtbbpy (1.3 mg, 5 μmol, 0.01 equiv.), TMG (86 mg, 0.75 mmol, 1.5 equiv.), and DMSO (2.0 mL). After 48 hours of blue LED irradiation at 55 ℃, the reaction mixture was subjected to the workup procedure outlined in the general procedure. Purification by flash column chromatography (10% to 30% ethyl acetate/hexane) provided the title compound (136 mg, 0.49 mmol, 97%) as a beige solid.

IR (neat) ν_{max} 3257, 1592, 1319, 1159, 1091, 940 cm^{-1}; ^1H NMR (400 MHz, $CDCl_3$) δ 7.79 (d, *J* = 8.1 Hz, 2H), 7.55 (t, *J* = 7.4 Hz, 1H), 7.45 (t, *J* = 7.6 Hz, 2H), 7.13 (t, *J* = 7.9 Hz, 1H), 6.98 (d, *J* = 7.9 Hz, 1H), 6.94 (s, 1H), 6.81 (d, *J* = 7.9 Hz, 1H), 6.68 (s, 1H), 2.40 (s, 3H); ^{13}C NMR (101 MHz, $CDCl_3$) δ 140.1, 138.8, 137.1, 133.2, 129.6, 129.2, 127.3, 123.1, 118.6, 117.7, 15.5. HRMS calcd. for $C_{13}H_{13}NNaO_2S_2$ ($[M+Na]^+$) 302.0280, found 302.0282.

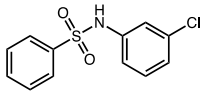

***N*-(3-chlorophenyl)benzenesulfonamide (4.51)**

Procedure A: Prepared following the general procedure outlined above using 1-bromo-3-chlorobenzene (96 mg, 0.50 mmol, 1.0 equiv.), benzenesulfonamide (118 mg, 0.75 mmol, 1.50 equiv.), $Ir[dF(CF_3)ppy]_2(dtbbpy)PF_6$ (0.28 mg, 0.25 μmol, 0.0005 equiv.), $NiCl_2$·glyme (5.5 mg, 25 μmol, 0.05 equiv.), TMG (86 mg, 0.75 mmol, 1.5 equiv.), and MeCN (1.3 mL). After 24 hours of blue LED irradiation at 68 ℃, the reaction mixture was subjected to the workup procedure outlined in the general procedure. Purification by flash column chromatography (ethyl acetate/hexane) provided the title compound (112 mg, 0.42 mmol, 84%) as a white solid.

Procedure B: Prepared following the general procedure outlined above using 1-bromo-3-chlorobenzene (96 mg, 0.50 mmol, 1.0 equiv.), benzenesulfonamide (118 mg, 0.75 mmol, 1.50 equiv.), $Ir(ppy)_2(dtbbpy)PF_6$ (2.3 mg, 2.5 μmol, 0.005 equiv.), $NiCl_2$·glyme (5.5 mg, 25 μmol, 0.05 equiv.), dtbbpy (1.3 mg, 5 μmol, 0.01 equiv.), TMG (86 mg, 0.75 mmol, 1.5 equiv.), and MeCN (2.0 mL). After 24 hours of blue LED irradiation at 55 ℃, the reaction mixture was subjected to the workup procedure outlined in the general procedure. Purification by flash column chromatography (10% to 30% ethyl acetate/hexane) provided the title compound (126 mg, 0.47 mmol, 94%) as a white solid.

The compound matched previously reported characterization data.[vi]

^{1}H NMR (400 MHz, $CDCl_3$) δ 7.83 (d, *J* = 8.0 Hz, 2H), 7.57 (t, *J* = 7.4 Hz, 1H), 7.47 (t, *J* = 7.6 Hz, 2H), 7.22 (s, 1H), 7.18 – 7.11 (m, 2H), 7.07 (d, *J* = 7.9 Hz, 1H), 6.98 (d, *J* = 8.0 Hz, 1H); ^{13}C NMR (101 MHz, $CDCl_3$) δ 138.8, 137.8, 135.1, 133.5, 130.5, 129.4, 127.3, 125.6, 121.3, 119.3.

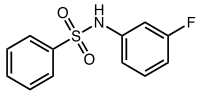

***N*-(3-fluorophenyl)benzenesulfonamide (4.52)**

Procedure A: Prepared following the general procedure outlined above using 1-bromo-3-fluorobenzene (88 mg, 0.50 mmol, 1.0 equiv.), benzenesulfonamide (118 mg, 0.75 mmol, 1.50 equiv.), $Ir(ppy)_2(bpy)PF_6$ (0.2 mg, 0.25 μmol, 0.0005 equiv.), $NiCl_2$·glyme (5.5 mg, 25 μmol, 0.05 equiv.), TMG (86 mg, 0.75 mmol, 1.5 equiv.), and MeCN (1.3 mL). After 24 hours of blue LED irradiation at 68 ℃, the reaction mixture was subjected to the workup procedure outlined in the general procedure. Purification by flash column chromatography (ethyl acetate/hexane) provided the title compound (102 mg, 0.41 mmol, 81%) as a white solid.

Procedure B: Prepared following the general procedure outlined above using 1-bromo-3-fluorobenzene (88 mg, 0.50 mmol, 1.0 equiv.), benzenesulfonamide (118 mg, 0.75 mmol, 1.50 equiv.), $Ir(ppy)_2(dtbbpy)PF_6$ (2.3 mg, 2.5 μmol, 0.005 equiv.), $NiCl_2$·glyme (5.5 mg, 25 μmol, 0.05 equiv.), dtbbpy (1.3 mg, 5 μmol, 0.01 equiv.), TMG (86 mg, 0.75 mmol, 1.5 equiv.), and MeCN (2.0 mL). After 24 hours of blue LED irradiation at 55 ℃, the reaction mixture was subjected to the workup procedure outlined in the general procedure. Purification by flash column chromatography (10% to 25% ethyl acetate/hexane) provided the title compound (118 mg, 0.47 mmol, 94%) as a white solid.

IR (neat) ν_{max} 3257, 1614, 1494, 1327, 1140, 974 cm^{-1}; ^1H NMR (500 MHz, $CDCl_3$) δ 7.82 (d, *J* = 7.3 Hz, 2H), 7.56 (t, *J* = 7.5 Hz, 1H), 7.47 (t, *J* = 7.8 Hz, 2H), 7.18 (td, *J* = 8.2, 6.5 Hz, 1H), 7.02 (s, 1H), 6.91 (t, *J* = 2.2 Hz, 1H), 6.84 – 6.77 (m, 2H); ^{13}C NMR (100 MHz, $CDCl_3$) δ 163.1 (d, *J* = 246.6 Hz), 138.7, 138.2 (d, *J* = 10.4 Hz), 133.5, 130.7 (d, *J* = 9.3 Hz), 129.3, 127.3, 116.4 (d, *J* = 3.0 Hz), 112.0 (d, *J* = 21.1 Hz), 108.2 (d, *J* = 25.4 Hz); ^{19}F NMR (376 MHz, $CDCl_3$) δ -110.9 (dd, *J* = 16.3, 8.4 Hz, 1H); HRMS (ESI) calcd. for $C_{12}H_{10}FNNaO_2S$ [$(M+Na)^+$]: 274.0308, found 274.0311.

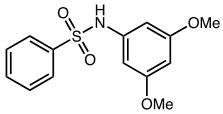

***N*-(3,5-dimethoxyphenyl)benzenesulfonamide (4.53)**

Procedure A: Prepared following the general procedure outlined above using 1-bromo-3,5-dimethoxybenzene (109 mg, 0.50 mmol, 1.0 equiv.), benzenesulfonamide (118 mg, 0.75 mmol, 1.50 equiv.), $Ir[dF(CF_3)ppy]_2(dtbbpy)PF_6$ (0.28 mg, 0.25 μmol, 0.0005 equiv.), $NiCl_2$·glyme (5.5 mg, 25 μmol, 0.05 equiv.), TMG (86 mg, 0.75 mmol, 1.5 equiv.), and MeCN (1.3 mL). After 18 hours of blue LED irradiation at 68 ℃, the reaction mixture was subjected to the workup procedure outlined in the general procedure. Purification by flash column chromatography (ethyl acetate/hexane) provided the title compound (82 mg, 0.28 mmol, 56%) as a white solid.

Procedure B: Prepared following the general procedure outlined above using 1-bromo-3,5-dimethoxybenzene (109 mg, 0.50 mmol, 1.0 equiv.), benzenesulfonamide (118 mg, 0.75 mmol, 1.50 equiv.), $Ir(ppy)_2(dtbbpy)PF_6$ (2.3 mg, 2.5 μmol, 0.005 equiv.), $NiCl_2$·glyme (5.5 mg, 25 μmol, 0.05 equiv.), dtbbpy (1.3 mg, 5 μmol, 0.01 equiv.), TMG (86 mg, 0.75 mmol, 1.5 equiv.), and DMSO (2.0 mL). After 48 hours of blue LED irradiation at 55 ℃, the reaction mixture was subjected to the workup procedure outlined in the general procedure. Purification by flash column chromatography (10% to 30% ethyl acetate/hexane) provided the title compound (135 mg, 0.46 mmol, 92%) as a white solid.

IR (neat) ν_{max} 3258, 1602, 1448, 1326, 1148, 1064 cm^{-1}; ^1H NMR (400 MHz, $CDCl_3$) δ 7.84 (d, *J* = 7.7 Hz, 2H), 7.54 (t, *J* = 7.4 Hz, 1H), 7.45 (t, *J* = 7.7 Hz, 2H), 7.05 (s, 1H), 6.27 (d, *J* = 1.8 Hz, 2H), 6.18 (s, 1H), 3.69 (s, 6H); ^{13}C NMR (101 MHz, $CDCl_3$) δ 161.3, 139.0, 138.3, 133.2, 129.2, 127.4, 99.4, 97.4, 55.5; HRMS calcd. for $C_{14}H_{15}NNaO_4S$ ($[M+Na]^+$) 316.0614, found 316.0617.

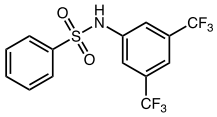

_N_-(3,5-bis(trifluoromethyl)phenyl)benzenesulfonamide (4.54)

Procedure A: Prepared following the general procedure outlined above using 1,3-bis(trifluoromethyl)-5-bromobenzene (147 mg, 0.50 mmol, 1.0 equiv.), benzenesulfonamide (118 mg, 0.75 mmol, 1.50 equiv.), $Ir(ppy)_2(bpy)PF_6$ (0.2 mg, 0.25 μmol, 0.0005 equiv.), $NiCl_2$·glyme (5.5 mg, 25 μmol, 0.05 equiv.), TMG (86 mg, 0.75 mmol, 1.5 equiv.), and MeCN (1.3 mL). After 20 hours of blue LED irradiation at 35 ℃, the reaction mixture was subjected to the workup procedure outlined in the general procedure. Purification by flash column chromatography (ethyl acetate/hexane) provided the title compound (157 mg, 0.43 mmol, 85%) as a white solid.

Procedure B: Prepared following the general procedure outlined above using 1,3-bis(trifluoromethyl)-5-bromobenzene (147 mg, 0.50 mmol, 1.0 equiv.), benzenesulfonamide (118 mg, 0.75 mmol, 1.50 equiv.), $Ir(ppy)_2(dtbbpy)PF_6$ (2.3 mg, 2.5 μmol, 0.005 equiv.), $NiCl_2$·glyme (5.5 mg, 25 μmol, 0.05 equiv.), dtbbpy (1.3 mg, 5 μmol, 0.01 equiv.), TMG (86 mg, 0.75 mmol, 1.5 equiv.), and MeCN (2.0 mL). After 24 hours of blue LED irradiation at 25 ℃, the reaction mixture was subjected to the workup procedure outlined in the general procedure. Purification by flash column chromatography (10% to 25% ethyl acetate/hexane) provided the title compound (160 mg, 0.43 mmol, 87%) as a white solid.

IR (neat) ν_{max} 3272, 1621, 1416, 1334, 1280, 1140 cm^{-1}; ^1H NMR (400 MHz, $CDCl_3$) δ 8.09 (s, 1H), 7.90 (d, J = 7.2 Hz, 2H), 7.61 (t, J = 8.0 Hz, 1H), 7.57 (s, 3H), 7.51 (t, J = 7.7 Hz, 2H); ^{13}C NMR (100 MHz, $CDCl_3$) δ 138.4, 138.1, 134.1, 133.0 (q, J = 33.8 Hz), 129.7, 127.4, 122.9 (q, J = 273.1 Hz). 120.1, 118.5; ^{19}F NMR (376 MHz, $CDCl_3$) δ -63.3 (s, 6H); HRMS (ESI) calcd. for $C_{14}H_{19}F_6NNaO_2S$ [$(M+Na)^+$]: 392.0150, found 392.0153.

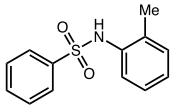

***N*-(*o*-tolyl)benzenesulfonamide (4.55)**

Procedure A: Prepared following the general procedure outlined above using 2-bromotoluene (86 mg, 0.50 mmol, 1.0 equiv.), benzenesulfonamide (118 mg, 0.75 mmol, 1.50 equiv.), $Ir[dF(CF_3)ppy]_2(dtbbpy)PF_6$ (0.28 mg, 0.25 μmol, 0.0005 equiv.), $NiCl_2$·glyme (5.5 mg, 25 μmol, 0.05 equiv.), TMG (86 mg, 0.75 mmol, 1.5 equiv.), and MeCN (1.3 mL). After 24 hours of blue LED irradiation at 68 ℃, the reaction mixture was subjected to the workup procedure outlined in the general procedure. Purification by flash column chromatography (ethyl acetate/hexane) provided the title compound (75 mg, 0.30 mmol, 61%) as a white solid.

Procedure B: Prepared following the general procedure outlined above using 2-bromotoluene (86 mg, 0.50 mmol, 1.0 equiv.), benzenesulfonamide (118 mg, 0.75 mmol, 1.50 equiv.), $Ir(ppy)_2(dtbbpy)PF_6$ (2.3 mg, 2.5 μmol, 0.005 equiv.), $NiCl_2$·glyme (5.5 mg, 25 μmol, 0.05 equiv.), dtbbpy (1.3 mg, 5 μmol, 0.01 equiv.), TMG (86 mg, 0.75 mmol, 1.5 equiv.), and DMSO (2.0 mL). After 72 hours of blue LED irradiation at 55 ℃, the reaction mixture was subjected to the workup procedure outlined in the general procedure. Purification by flash column chromatography (10% to 30% ethyl acetate/hexane) provided the title compound (91 mg, 0.37 mmol, 74%) as a white solid.

The compound matched previously reported characterization data.[v]

^{1}H NMR (400 MHz, $CDCl_3$) δ 7.79 (d, *J* = 8.1 Hz, 2H), 7.55 (t, *J* = 7.4 Hz, 1H), 7.45 (t, *J* = 7.6 Hz, 2H), 7.13 (t, *J* = 7.9 Hz, 1H), 6.98 (d, *J* = 7.9 Hz, 1H), 6.94 (s, 1H), 6.81 (d, *J* = 7.9 Hz, 1H), 6.68 (s, 1H), 2.40 (s, 3H); ^{13}C NMR (101 MHz, $CDCl_3$) δ 139.7, 134.4, 133.0, 131.9, 130.9, 129.1, 127.2, 127.0, 126.5, 124.8, 17.6.

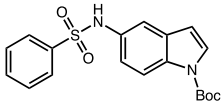

***tert*-butyl 5-(phenylsulfonamido)-1H-indole-1-carboxylate (4.56)**

Procedure A: Prepared following the general procedure outlined above using *N*-Boc-5-bromoindole (148 mg, 0.50 mmol, 1.0 equiv.), benzenesulfonamide (118 mg, 0.75 mmol, 1.50 equiv.), $Ir[dF(CF_3)ppy]_2(dtbbpy)PF_6$ (0.28 mg, 0.25 μmol, 0.0005 equiv.), $NiCl_2$·glyme (5.5 mg, 25 μmol, 0.05 equiv.), MTBD (115 mg, 0.75 mmol, 1.5 equiv.), and MeCN (1.3 mL). After 24 hours of blue LED irradiation at 68 ℃, the reaction mixture was subjected to the workup procedure outlined in the general procedure. Purification by flash column chromatography (ethyl acetate/hexane) provided the title compound (89 mg, 0.24 mmol, 48%) as a colorless oil.

Procedure B: Prepared following the general procedure outlined above using *N*-Boc-5-bromoindole (148 mg, 0.50 mmol, 1.0 equiv.), benzenesulfonamide (118 mg, 0.75 mmol, 1.50 equiv.), $Ir(ppy)_2(dtbbpy)PF_6$ (2.3 mg, 2.5 μmol, 0.005 equiv.), $NiCl_2$·glyme (5.5 mg, 25 μmol, 0.05 equiv.), dtbbpy (1.3 mg, 5 μmol, 0.01 equiv.), TMG (86 mg, 0.75 mmol, 1.5 equiv.), and DMSO (2.0 mL). After 48 hours of blue LED irradiation at 55 ℃, the reaction mixture was subjected to the workup procedure outlined in the general procedure. Purification by flash column chromatography (20% to 30% ethyl acetate/hexane) provided the title compound (178 mg, 0.47 mmol, 95%) as a colorless oil.

IR (neat) ν_{max} 3261, 2985, 2890, 1734, 1457, 1373, 1165, 1131, 1085 cm^{-1}; ^1H NMR (400 MHz, $CDCl_3$) δ 7.97 (d, *J* = 8.1 Hz, 1H), 7.77 (d, *J* = 8.4 Hz, 2H), 7.56 (s, 1H), 7.48 (t, *J* = 6.8 Hz, 1H), 7.37 (d, *J* = 8.2 Hz, 4H), 7.01 (d, *J* = 8.8 Hz, 1H), 6.45 (s, 1H), 1.64 (s, 9H). ^{13}C NMR (101 MHz, $CDCl_3$) δ 149.6, 138.9, 132.9, 131.3, 131.2, 129.0, 127.4, 127.0, 120.0, 115.7, 115.5, 107.2, 84.1, 28.2; HRMS (ESI-TOF) calcd. for $C_{19}H_{20}N_2NaO_4S$ [$(M+Na)^+$]: 395.1036, found 395.1033.

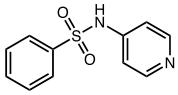

***N*-(pyridin-4-yl)benzenesulfonamide (4.62)**

Procedure A: Prepared following the general procedure outlined above using 4-bromopyridine•HCl (97 mg, 0.50 mmol, 1.0 equiv.), benzenesulfonamide (118 mg, 0.75 mmol, 1.50 equiv.), $Ir(ppy)_2(bpy)PF_6$ (0.2 mg, 0.25 μmol, 0.0005 equiv.), $NiCl_2$·glyme (5.5 mg, 25 μmol, 0.05 equiv.), TMG (144 mg, 1.25 mmol, 2.5 equiv.), and MeCN (1.3 mL). After 8 hours of blue LED irradiation at 35 ℃, the reaction mixture was subjected to the workup procedure outlined in the general procedure. Purification by flash column chromatography (isopropanol/acetone) provided the title compound (106 mg, 0.45 mmol, 90%) as a white solid.

Procedure B: Prepared following the general procedure outlined above using 4-bromopyridine•HCl (97 mg, 0.50 mmol, 1.0 equiv.), benzenesulfonamide (118 mg, 0.75 mmol, 1.50 equiv.), $Ir(ppy)_2(dtbbpy)PF_6$ (2.3 mg, 2.5 μmol, 0.005 equiv.), $NiCl_2$·glyme (5.5 mg, 25 μmol, 0.05 equiv.), dtbbpy (1.3 mg, 5 μmol, 0.01 equiv.), TMG (144 mg, 1.25 mmol, 2.5 equiv.), and MeCN (2.0 mL). After 48 hours of blue LED irradiation at 25 ℃, the reaction mixture was analyzed by NMR. No product formation was detected.

IR (neat) ν_{max} 1634, 1475, 1334, 1136, 1081, 940, 781, 685 cm^{-1} ^1H NMR (500 MHz, $(CD_3)_2SO$) δ 8.00 (d, J = 8.1 Hz, 2H), 7.86 – 7.74 (m, 2H), 7.57 – 7.43 (m, 3H), 6.92 (d, J = 6.5 Hz, 2H); ^{13}C NMR (126 MHz, $(CD_3)_2SO$) δ 160.9, 143.2, 140.0, 131.4, 128.8, 126.1, 114.4. *m*/*z* calcd. For $C_{11}H_{10}N_2O_2S$ ($[M+H]^+$) 235.05357, found 235.05352.

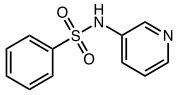

***N*-(pyridin-3-yl)benzenesulfonamide (4.63)**

Procedure A: Prepared following the general procedure outlined above using 3-bromopyridine (79 mg, 0.50 mmol, 1.0 equiv.), benzenesulfonamide (118 mg, 0.75 mmol, 1.50 equiv.), $Ir(ppy)_2(bpy)PF_6$ (0.2 mg, 0.25 μmol, 0.0005 equiv.), $NiCl_2$·glyme (5.5 mg, 25 μmol, 0.05 equiv.), TMG (86 mg, 0.75 mmol, 1.5 equiv.), and MeCN (1.3 mL). After 8 hours of blue LED irradiation at 35 ºC, the reaction mixture was subjected to the workup procedure outlined in the general procedure. Purification by flash column chromatography (ethyl acetate/hexane) provided the title compound (104 mg, 0.44 mmol, 89%) as a white solid.

Procedure B: Prepared following the general procedure outlined above using 3-bromopyridine (79 mg, 0.50 mmol, 1.0 equiv.), benzenesulfonamide (118 mg, 0.75 mmol, 1.50 equiv.), $Ir(ppy)_2(dtbbpy)PF_6$ (2.3 mg, 2.5 μmol, 0.005 equiv.), $NiCl_2$·glyme (5.5 mg, 25 μmol, 0.05 equiv.), dtbbpy (1.3 mg, 5 μmol, 0.01 equiv.), TMG (86 mg, 0.75 mmol, 1.5 equiv.), and MeCN (2.0 mL). After 48 hours of blue LED irradiation at 25 ºC, the reaction mixture was subjected to the workup procedure outlined in the general procedure. Purification by flash column chromatography (30% to 90% ethyl acetate/hexane) provided the title compound (85 mg, 0.36 mmol, 73%) as a beige solid.

The compound matched previously reported data.[vii]

^{1}H NMR (500 MHz, $(CD_3)_2SO$) δ 10.57 (s, 1H), 8.27 (d, *J* = 2.3 Hz, 1H), 8.24 (d, *J* = 3.8 Hz, 1H), 7.76 (d, *J* = 7.4 Hz, 2H), 7.63 (t, *J* = 7.4 Hz, 1H), 7.56 (t, *J* = 7.6 Hz, 2H), 7.50 (ddd, *J* = 8.3, 2.4, 1.4 Hz, 1H), 7.27 (dd, *J* = 8.3, 4.7 Hz, 1H); ^{13}C NMR (101 MHz, $(CD_3)_2SO$) δ 145.4, 141.8, 139.0, 134.3, 133.2, 129.4, 127.4, 126.7, 124.0.

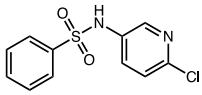

***N*-(6-chloropyridin-3-yl)benzenesulfonamide (4.64)**

Procedure A: Prepared following the general procedure outlined above using 5-bromo-2-chloropyridine (96 mg, 0.50 mmol, 1.0 equiv.), benzenesulfonamide (157 mg, 1.0 mmol, 2.0 equiv.), $Ir(ppy)_2(bpy)PF_6$ (0.2 mg, 0.25 μmol, 0.0005 equiv.), $NiCl_2$·glyme (5.5 mg, 25 μmol, 0.05 equiv.), DBU (152 mg, 1.0 mmol, 2.0 equiv.), and MeCN (1.3 mL). After 18 hours of blue LED irradiation at 68 ℃, the reaction mixture was subjected to the workup procedure outlined in the general procedure. Purification by flash column chromatography (ethyl acetate/hexane) provided the title compound (108 mg, 0.40 mmol, 80%) as a white solid.

Procedure B: Prepared following the general procedure outlined above using 5-bromo-2-chloropyridine (96 mg, 0.50 mmol, 1.0 equiv.), benzenesulfonamide (118 mg, 0.75 mmol, 1.50 equiv.), $Ir(ppy)_2(dtbbpy)PF_6$ (2.3 mg, 2.5 μmol, 0.005 equiv.), $NiCl_2$·glyme (5.5 mg, 25 μmol, 0.05 equiv.), dtbbpy (1.3 mg, 5 μmol, 0.01 equiv.), TMG (86 mg, 0.75 mmol, 1.5 equiv.), and MeCN (2.0 mL). After 48 hours of blue LED irradiation at 25 ℃, the reaction mixture was subjected to the workup procedure outlined in the general procedure. Purification by flash column chromatography (20% to 60% ethyl acetate/hexane) provided the title compound (95 mg, 0.35 mmol, 71%) as a white solid.

The compound matched previously reported characterization data.[v]

^{1}H NMR (400 MHz, $CDCl_3$) δ 8.06 (d, *J* = 2.7 Hz, 1H), 7.78 (d, *J* = 7.7 Hz, 2H), 7.63 – 7.55 (m, 2H), 7.49 (t, *J* = 7.7 Hz, 2H), 7.41 (s, 1H), 7.25 (d, *J* = 8.7 Hz, 1H); ^{13}C NMR (101 MHz, $CDCl_3$) δ 147.5, 142.7, 138.4, 133.7, 132.9, 132.3, 129.5, 127.2, 124.8.

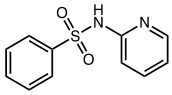

***N*-(pyridin-2-yl)benzenesulfonamide (4.65)**

Procedure A: Prepared following the general procedure outlined above using 2-bromopyridine (79 mg, 0.50 mmol, 1.0 equiv.), benzenesulfonamide (157 mg, 1.0 mmol, 2.0 equiv.), $Ir[dF(CF_3)ppy]_2(dtbbpy)PF_6$ (0.28 mg, 0.25 μmol, 0.0005 equiv.), $NiCl_2$·glyme (5.5 mg, 25 μmol, 0.05 equiv.), TMG (115 mg, 1.0 mmol, 2.0 equiv.), and MeCN (1.3 mL). After 8 hours of blue LED irradiation at 35 ℃, the reaction mixture was subjected to the workup procedure outlined in the general procedure. Purification by flash column chromatography (ethyl acetate/hexane) provided the title compound (65 mg, 0.28 mmol, 56%) and *N*,*N*-di(pyridin-2-yl)benzenesulfonamide (9 mg, 0.03 mmol, 6%) as a white solid.

Procedure B: Prepared following the general procedure outlined above using 2-bromopyridine (79 mg, 0.50 mmol, 1.0 equiv.), benzenesulfonamide (118 mg, 0.75 mmol, 1.50 equiv.), $Ir(ppy)_2(dtbbpy)PF_6$ (2.3 mg, 2.5 μmol, 0.005 equiv.), $NiCl_2$·glyme (5.5 mg, 25 μmol, 0.05 equiv.), dtbbpy (1.3 mg, 5 μmol, 0.01 equiv.), TMG (86 mg, 0.75 mmol, 1.5 equiv.), and MeCN (2.0 mL). After 48 hours of blue LED irradiation at 25 ℃, the reaction mixture was analyzed by NMR. The reaction yield was determined to be 20%.

The compound matched previously reported data.[viii]

^{1}H NMR (500 MHz, $(CD_3)_2SO$) monoarylation: δ 7.99 (dd, *J* = 5.6, 1.9 Hz, 1H), 7.87 (d, *J* = 6.9 Hz, 2H), 7.72 (ddd, *J* = 8.9, 7.2, 1.9 Hz, 1H), 7.58 – 7.50 (m, 3H), 7.17 (d, *J* = 8.7 Hz, 1H), 6.86 (s, 1H) diarylation: δ 8.38 (dd, J = 4.9, 1.8 Hz, 1H), 8.04 (dd, *J* = 7.3, 1.7 Hz, 1H), 7.85 – 7.80 (m, 1H), 7.68 (d, *J* = 7.3 Hz, 1H), 7.64 – 7.60 (m, 1H), 7.59 – 7.56 (m, 13H), 7.36 (s, 1H), 7.31 (dd, *J* = 7.5, 4.9 Hz, 1H), 7.25 (d, J = 8.2 Hz, 1H).; ^{13}C NMR (126 MHz, $(CD_3)_2SO$) δ 153.3, 152.6, 148.8, 143.0, 142.0, 140.6, 138.9, 133.3, 132.1, 131.8, 129.0, 128.0, 126.5, 125.6, 122.2, 120.7, 115.4, 113.9. *m*/*z* calcd. For $C_{11}H_{10}N_2O_2S$ ($[M+H]^+$) 235.05357, found 235.05379.

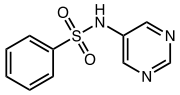

***N*-(pyrimidin-5-yl)benzenesulfonamide (4.66)**

Procedure A: Prepared following the general procedure outlined above using 5-bromopyrimidine (79 mg, 0.50 mmol, 1.0 equiv.), benzenesulfonamide (118 mg, 0.75 mmol, 1.5 equiv.), $Ir(ppy)_2(bpy)PF_6$ (0.2 mg, 0.25 μmol, 0.0005 equiv.), $NiCl_2$·glyme (5.5 mg, 25 μmol, 0.05 equiv.), TMG (86 mg, 0.75 mmol, 1.5 equiv.), and MeCN (1.3 mL). After 8 hours of blue LED irradiation at 35 ℃, the reaction mixture was subjected to the workup procedure outlined in the general procedure. Purification by flash column chromatography (ethyl acetate/hexane) provided the title compound (98 mg, 0.42 mmol, 83%) as a white solid.

Procedure B: Prepared following the general procedure outlined above using 5-bromopyrimidine (79 mg, 0.50 mmol, 1.0 equiv.), benzenesulfonamide (118 mg, 0.75 mmol, 1.50 equiv.), $Ir(ppy)_2(dtbbpy)PF_6$ (2.3 mg, 2.5 μmol, 0.005 equiv.), $NiCl_2$·glyme (5.5 mg, 25 μmol, 0.05 equiv.), dtbbpy (1.3 mg, 5 μmol, 0.01 equiv.), TMG (86 mg, 0.75 mmol, 1.5 equiv.), and MeCN (2.0 mL). After 48 hours of blue LED irradiation at 25 ℃, the reaction mixture was analyzed by NMR. The reaction yield was determined to be 15%.

IR (neat) ν_{max} 2803, 1568, 1426, 1324, 1166, 1090, 909, 760, 687 cm^{-1}; ^1H NMR (500 MHz, $(CD_3)_2SO$) δ 10.88 (s, 1H), 8.90 (s, 1H), 8.52 (s, 2H), 7.85 – 7.76 (m, 2H), 7.71 – 7.63 (m, 1H), 7.60 (dd, *J* = 8.5, 7.0 Hz, 2H); ^{13}C NMR (126 MHz, $(CD_3)_2SO$) δ 154.2, 148.3, 138.6, 133.6, 133.1, 129.6, 126.7. *m/z* calcd. for $C_{10}H_9N_3O_2S$ ($[M+H]^+$) 236.04882, found 236.04878.

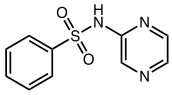

***N*-(pyrazin-2-yl)benzenesulfonamide (4.67)**

Procedure A: Prepared following the general procedure outlined above using 2-bromopyrazine (79 mg, 0.50 mmol, 1.0 equiv.), benzenesulfonamide (157 mg, 1.0 mmol, 2.0 equiv.), $Ir[dF(CF_3)ppy]_2(dtbbpy)PF_6$ (0.28 mg, 0.25 μmol, 0.0005 equiv.), $NiCl_2$·glyme (5.5 mg, 25 μmol, 0.05 equiv.), TMG (115 mg, 1.0 mmol, 2.0 equiv.), and MeCN (1.3 mL). After 8 hours of blue LED irradiation at 35 ℃, the reaction mixture was subjected to the workup procedure outlined in the general procedure. Purification by flash column chromatography (ethyl acetate/hexane) provided the title compound (65 mg, 0.28 mmol, 55%) as a white solid.

Procedure B: Prepared following the general procedure outlined above using 2-bromopyridine (79 mg, 0.50 mmol, 1.0 equiv.), benzenesulfonamide (118 mg, 0.75 mmol, 1.50 equiv.), $Ir(ppy)_2(dtbbpy)PF_6$ (2.3 mg, 2.5 μmol, 0.005 equiv.), $NiCl_2$·glyme (5.5 mg, 25 μmol, 0.05 equiv.), dtbbpy (1.3 mg, 5 μmol, 0.01 equiv.), TMG (86 mg, 0.75 mmol, 1.5 equiv.), and MeCN (2.0 mL). After 48 hours of blue LED irradiation at 25 ℃, the reaction mixture was analyzed by NMR. The reaction yield was determined to be <5%.

The compound matched previously reported data.[ix]

^{1}H NMR (500 MHz, $(CD_3)_2SO$) δ 11.59 (s, 1H), 8.36 (s, 1H), 8.28 – 8.15 (m, 2H), 8.04 – 7.87 (m, 2H), 7.74 – 7.50 (m, 3H); ^{13}C NMR (126 MHz, $(CD_3)_2SO$) δ 148.1, 142.1, 140.0, 138.9, 134.9, 133.3, 129.3, 127.1.

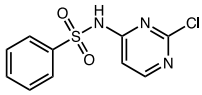

***N*-(2-chloropyrimidin-4-yl)benzenesulfonamide (4.68)**

Procedure A: Prepared following the general procedure outlined above using 2,4-dichloropyrimidine (74 mg, 0.50 mmol, 1.0 equiv.), benzenesulfonamide (157 mg, 1.0 mmol, 2.0 equiv.), $Ir(ppy)_2(bpy)PF_6$ (0.2 mg, 0.25 μmol, 0.0005 equiv.), $NiCl_2$·glyme (5.5 mg, 25 μmol, 0.05 equiv.), DBU (152 mg, 1.0 mmol, 2.0 equiv.), and MeCN (1.3 mL). After 24 hours of blue LED irradiation at 35 ℃, the reaction mixture was subjected to the workup procedure outlined in the general procedure. Purification by flash column chromatography (ethyl acetate/hexane) provided the title compound (66 mg, 0.25 mmol, 49%) as a white solid.

Procedure B: Prepared following the general procedure outlined above using 2,4-dichloropyrimidine (74 mg, 0.50 mmol, 1.0 equiv.), benzenesulfonamide (118 mg, 0.75 mmol, 1.50 equiv.), $Ir(ppy)_2(dtbbpy)PF_6$ (2.3 mg, 2.5 μmol, 0.005 equiv.), $NiCl_2$·glyme (5.5 mg, 25 μmol, 0.05 equiv.), dtbbpy (1.3 mg, 5 μmol, 0.01 equiv.), TMG (86 mg, 0.75 mmol, 1.5 equiv.), and MeCN (2.0 mL). After 48 hours of blue LED irradiation at 25 ℃, the reaction mixture was analyzed by NMR. The reaction yield was determined to be <10%.

IR (neat) ν_{max} 3074, 1570, 1366, 1159, 967, 757, 689 cm^{-1} ^1H NMR (500 MHz, $(CD_3)_2CO$) δ 8.43 (d, *J* = 5.7 Hz, 1H), 8.12 (d, *J* = 7.3 Hz, 2H), 7.77 – 7.71 (m, 1H), 7.66 (dd, *J* = 8.6, 7.0 Hz, 2H), 7.23 (d, *J* = 5.7 Hz, 1H).; ^{13}C NMR (126 MHz, $(CD_3)_2SO$) δ 160.2, 159.4, 159.1, 139.0, 133.9, 129.3, 127.5, 106.7. *m*/*z* calcd. for $C_{10}H_8ClN_3O_2S$ ($[M+H]^+$) 270.00985, found 270.01007.

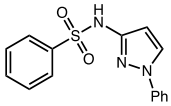

_N_-(1-phenyl-1_H_-pyrazol-3-yl)benzenesulfonamide (4.69)

Procedure A: Prepared following the general procedure outlined above using 3-bromo-1-phenyl-1*H*-pyrazole (112 mg, 0.50 mmol, 1.0 equiv.), benzenesulfonamide (157 mg, 1.0 mmol, 2.0 equiv.), $Ir(ppy)_2(bpy)PF_6$ (0.2 mg, 0.25 μmol, 0.0005 equiv.), $NiCl_2$·glyme (5.5 mg, 25 μmol, 0.05 equiv.), TMG (115 mg, 1.0 mmol, 2.0 equiv.), and MeCN (1.3 mL). After 24 hours of blue LED irradiation at 68 ℃, the reaction mixture was subjected to the workup procedure outlined in the general procedure. Purification by flash column chromatography (ethyl acetate/hexane) provided the title compound (92 mg, 0.31 mmol, 62%) as an off-white oil.

Procedure B: Prepared following the general procedure outlined above using 3-bromo-1-phenyl-1*H*-pyrazole (112 mg, 0.50 mmol, 1.0 equiv.), benzenesulfonamide (118 mg, 0.75 mmol, 1.50 equiv.), $Ir(ppy)_2(dtbbpy)PF_6$ (2.3 mg, 2.5 μmol, 0.005 equiv.), $NiCl_2$·glyme (5.5 mg, 25 μmol, 0.05 equiv.), dtbbpy (1.3 mg, 5 μmol, 0.01 equiv.), TMG (86 mg, 0.75 mmol, 1.5 equiv.), and MeCN (2.0 mL). After 48 hours of blue LED irradiation at 25 ℃, the reaction mixture was analyzed by NMR. The reaction yield was determined to be <5%.

IR (neat) ν_{max} 1547, 1477, 1360, 1167, 754, 689 cm^{-1} ^1H NMR (500 MHz, $(CD_3)_2CO$) δ 9.57 (s, 1H), 8.19 (d, *J* = 2.6 Hz, 1H), 7.99 – 7.90 (m, 2H), 7.69 – 7.64 (m, 2H), 7.64 – 7.59 (m, 1H), 7.56 (tt, *J* = 7.0, 1.7 Hz, 2H), 7.46 – 7.39 (m, 2H), 7.27 – 7.20 (m, 1H), 6.43 (d, *J* = 2.6 Hz, 1H); ^{13}C NMR (126 MHz, $(CD_3)_2CO$) δ 148.9, 141.4, 140.7, 133.8, 130.3, 129.9, 129.0, 128.1, 126.8, 118.7, 100.7. *m/z* calcd. for $C_{15}H_{14}N_3O_2S$ ($[M+H]^+$) 300.08012, found 300.07994.

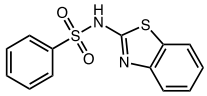

***N*-(benzo[d]thiazol-2-yl)benzenesulfonamide (4.70)**

Procedure A: Prepared following the general procedure outlined above using 2-bromobenzo[d]thiazole (107 mg, 0.50 mmol, 1.0 equiv.), benzenesulfonamide (157 mg, 1.0 mmol, 2.0 equiv.), $Ir(ppy)_2(bpy)PF_6$ (0.2 mg, 0.25 μmol, 0.0005 equiv.), $NiCl_2$·glyme (5.5 mg, 25 μmol, 0.05 equiv.), TMG (115 mg, 1.0 mmol, 2.0 equiv.), and MeCN (1.3 mL). After 18 hours of blue LED irradiation at 68 ℃, the reaction mixture was subjected to the workup procedure outlined in the general procedure. Purification by flash column chromatography (ethyl acetate/dichloromethane) followed by trituration in EtOAc provided the title compound (80 mg, 0.28 mmol, 55%) as a tan solid.

Procedure B: Prepared following the general procedure outlined above using 2-bromobenzo[d]thiazole (107 mg, 0.50 mmol, 1.0 equiv.), benzenesulfonamide (118 mg, 0.75 mmol, 1.50 equiv.), $Ir(ppy)_2(dtbbpy)PF_6$ (2.3 mg, 2.5 μmol, 0.005 equiv.), $NiCl_2$·glyme (5.5 mg, 25 μmol, 0.05 equiv.), dtbbpy (1.3 mg, 5 μmol, 0.01 equiv.), TMG (86 mg, 0.75 mmol, 1.5 equiv.), and MeCN (2.0 mL). After 48 hours of blue LED irradiation at 25 ℃, the reaction mixture was analyzed by NMR. The reaction yield was determined to be 16%.

The compound matched previously reported data.[x]

^{1}H NMR (500 MHz, $(CD_3)_2SO$) δ 13.23 (s, 1H), 7.87 (d, *J* = 7.5 Hz, 2H), 7.80 (d, *J* = 8.0 Hz, 1H), 7.66 – 7.51 (m, 3H), 7.38 (t, *J* = 7.7 Hz, 1H), 7.30 (d, *J* = 8.0 Hz, 1H), 7.25 (t, *J* = 7.8 Hz, 1H); ^{13}C NMR (126 MHz, $(CD_3)_2SO$) δ 167.1, 142.0, 136.2, 132.4, 129.1, 127.3, 125.8, 124.7, 123.7, 122.8, 112.8.

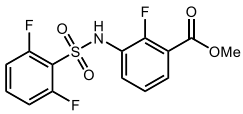

Methyl 3-((2,6-difluorophenyl)sulfonamido)-2-fluorobenzoate (4.74)

Prepared following the general procedure outlined above using methyl 3-bromo-2-fluorobenzoate (117 mg, 0.50 mmol, 1.0 equiv.), 2,6-difluorobenzenesulfonamide (145 mg, 0.75 mmol, 1.50 equiv.), $Ir(ppy)_2(dtbbpy)PF_6$ (2.3 mg, 2.5 μmol, 0.005 equiv.), $Ni(cod)_2$ (6.9 mg, 25 μmol, 0.05 equiv.), dtbbpy (1.3 mg, 5 μmol, 0.01 equiv.), TMG (86 mg, 0.75 mmol, 1.5 equiv.), and DMSO (2.0 mL). After 48 h without fan cooling, the reaction mixture was subjected to the workup protocol outlined in the general procedure. Purification by flash column chromatography (15% to 25% ethyl acetate/hexane) provided the title compound (144 mg, 0.42 mmol, 83%) as a white solid.

IR (neat) ν_{max} 3264, 1723, 1612, 1470, 1172, 1005 cm^{-1}; ^1H NMR (400 MHz, $CDCl_3$) δ 7.90 – 7.80 (m, 1H), 7.75 – 7.61 (m, 1H), 7.51 (tt, *J* = 8.4, 6.0 Hz, 1H), 7.32 (s, 1H), 7.17 (t, *J* = 7.6 Hz, 1H), 7.00 (t, *J* = 8.7 Hz, 2H), 3.90 (s, 3H); ^{13}C NMR (100 MHz, $CDCl_3$) δ 164.1 (d, *J* = 3.5 Hz), 159.8 (dd, *J* = 260.1, 3.5 Hz), 152.9 (d, *J* = 258.8 Hz), 135.6 (t, *J* = 11.2 Hz), 128.5, 126.7, 125.3 (d, *J* = 12.5 Hz), 124.6 (d, *J* = 5.0 Hz), 119.3 (d, *J* = 8.9 Hz), 116.7, 113.4 (dd, *J* = 23.1, 3.7 Hz), 52.7; ^{19}F NMR (376 MHz, $CDCl_3$) δ -105.9 (m, 2H), -128.0 (s, 1H); HRMS (ESI) calcd. for $C_{14}H_{10}F_3NNaO_4S$ $[(M+Na)^+]$: 368.0175, found 392.0178.

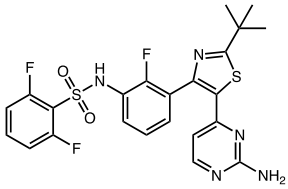

***N*-(3-(5-(2-aminopyrimidin-4-yl)-2-(tert-butyl)thiazol-4-yl)-2-fluorophenyl)-2,6-difluorobenzenesulfonamide (4.77)**

A stock solution of $NiBr_2$·glyme (1.25 mM, 1.25 μmol, 0.05 equiv.) and dtbbpy (0.5 mM, 0.50 μmol, 0.02 equiv.) was prepared in acetonitrile. The catalyst stock solution was added to an 8 mL vial and the solvent removed. To the reaction vial was added 4-(4-(3-Bromo-2-fluorophenyl)-2-(*tert*-butyl)thiazol-5-yl)pyrimidin-2-amine (102 mg, 0.25 mmol, 1.0 equiv.), 2,6-difluorobenzenesulfonamide (97 mg, 0.50 mmol, 2.0 equiv.), $Ir(ppy)_2(dtbbpy)PF_6$ (4.6 mg, 5.0 μmol, 0.02 equiv.). The vial was purged with N_2 and then TMG (86 mg, 0.75 mmol, 3.0 equiv.) and degassed DMSO (2.0 mL) were added in an N_2-filled glovebox. After 40 hours of blue LED irradiation at 55 ºC, sat'd $NaHCO_3$ was added to the reaction mixture and the resulting solution extracted with CH_2Cl_2 (4x). The combined organic layers were dried with Na_2SO_4, filtered, and concentrated. Purification by flash column chromatography (40% to 70% ethyl acetate/hexane) provided the title compound (74 mg, 0.14 mmol, 57%) as an off-white solid.

The compound matched previously reported characterization data.[xi]

^{1}H NMR (400 MHz, $CDCl_3$) δ 1H NMR (500 MHz, DMSO-d6) δ 10.88 (s, 1H), 7.98 (d, *J* = 5.3 Hz, 1H), 7.68 (tt, *J* = 8.4, 5.9 Hz, 1H), 7.43 (td, *J* = 7.7, 1.8 Hz, 1H), 7.36 (ddd, *J* = 8.0, 6.4, 1.8 Hz, 1H), 7.32 – 7.13 (m, 3H), 6.78 (s, 2H), 5.84 (d, *J* = 5.1 Hz, 1H), 1.40 (s, 9H); ^{13}C NMR (101 MHz, $CDCl_3$) δ 13C NMR (126 MHz, DMSO-d6) δ 182.0, 163.8, 160.2, 159.2, 157.9, 154.5, 152.5, 145.6, 136.5, 134.9, 129.8, 128.2, 125.5, 124.6, 113.9, 113.6, 105.5, 38.1, 30.8.

4.5.5. Stoichiometric Ligated Nickel Reductive Elimination

Methyl 4-iodobenzoate (13.1 mg, 0.05 mmol), phenanthroline (10.8 mg, 0.06 mmol), and 4-toluenesulfonamide potassium salt (10.5 mg, 0.05 mmol) were weighed on bench and the reaction flask was placed in an Ar filled glove box. $Ni(cod)_2$ (16.5 mg, 0.06 mmol) was added to the reaction flask and dissolved in MeCN (20 ml, 0.0025 M). The reaction was stirred on bench under Ar atmosphere for 45 minutes forming deep brown liquid. The complete consumption of iodoarene was confirmed by ^1H NMR analysis. The reaction mixture was stirred for additional 2 hours, and the stirring stopped. The supernatant was used directly.

To the reaction vials were added the indicated reagents, and the solution (4 ml) prepared from the above procedure (the solution rapidly turned partially green during the transfer). After 24 hours of stirring, 1,3,5-trimethoxybenzene (1.68 mg, dissolved in 1 ml of DCM) was added to each vial. The resulting solution was filtered through a short plug of silica gel and washed with eluent (50 ml, hexane/EtOAc = 3:1). The resulting solutions were evaporated under reduced pressure, and the yields were determined by ^1H NMR analysis.

4.5.6. Photocatalyst Decomposition Studies

Samples were prepared by eluting a crude reaction mixture through a short plug of silica gel using MeCN as the eluent. Samples were bubbled with argon for 5 min before the analysis. Temperature was maintained at 20 ℃ during the measurement. Emission correction curve in reference to the spectral radiance was applied to the all fluorescent spectra. Samples were excited at 460 nm and emission spectra were collected.

4.5.7. Oxidative Addition Rates

A solution of 1-bromo-4-*tert*-butylbenzene (0.1 mmol, 17.3 µl) in MeCN (10 ml) was prepared and bubbled with argon for about 30 minutes. To a reaction tube with pre-weighed reagents as indicated was added $Ni(cod)_2$ (0.012 mmol, 3.3 mg), and MeCN (4 ml). The resulting mixture were stirred for 20 minutes for the ligand exchange, and 1 ml solution of 1-Bromo-4-*tert*-butylbenzene (0.01 mmol) was added. After 5 minutes stirring, dimethyl terephthalate (0.01 mmol, dissolved in 1 ml of DCM) was added, and the reaction mixture was rapidly filtered through a short plug of silica gel and washed with eluent (50 ml, hexane/EtOAc = 3:1). The resulting crude mixture was directly analyzed by ^1H NMR analysis.

entry	1	2	3	4	5	6	7
reagents (µmol)	control (no Ni)	-	dtbbpy (12)	phen (12)	phen (12)	phen (12)	phen (12)
	-	-	-	-	TBAI (10)	K_2CO_3 (10)	DBU (10)
intensity	1.46	1.2	0.72	0.96	0.76	1.02	1.39
Conv.	0%	18%	51%	34%	48%	30%	0.5%

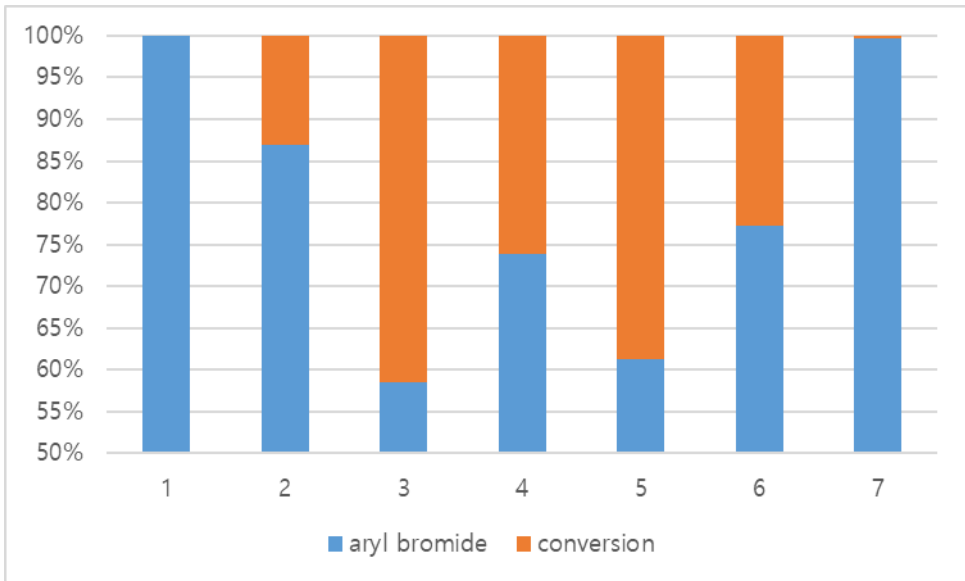

4.5.8. References Cited

[i] (a) Lowry, M. S.; Goldsmith, J. I.; Slinker, J. D.; Rohl, R.; Pascal, Jr., R. A.; Malliaras, G. G.; Bernhard, S. *Chem. Mater.* **2005**, *17*, 5712. (b) Ladouceur, S.; Fortin, D.; Zysman-Colman, E. *Inorg. Chem.* **2011**, *50*, 11514.

[ii] Pangborn, A. B.; Giardello, M. A.; Grubbs, R. H.; Rosen, R. K.; Timmers, F. J. *Organometallics* **1996**, *15*, 1518.

[iii] Buckingham, F.; Calderwood, S.; Checa, B.; Keller, T.; Tredwell, M.; Collier, T. L.; Newington, I. M.; Bhalla, R.; Glaser, M.; Gouverneur, V. *J. Fluorine Chem.* **2015,** *180*, 33.

[iv] Zhang, W.; Xie, J.; Rao, B.; Luo, M. *J. Org. Chem.* **2015,** *80*, 3504.

[v] Lee, D.; Chang, S. *Chem. A Eur. J.* **2015,** *21*, 5364.

[vi] Wang, X.; Guram, A.; Ronk, M.; Milne, J. E.; Tedrow, J. S.; Faul, M. M. *Tetrahedron Lett.* **2012,** *53*, 7.

[vii] Yang, K.; Ke, M.; Lin, Y.; Song, Q. *Green Chemistry* **2015,** *17*, 1395.

[viii] Wei, W.; Liu, C.; Yang, D.; Wen, J.; You, J.; Wang, H. *Adv. Synth. Catal.* **2015**, *357*, 987.

[ix] Dea-Ayuela, A.; Castillo, E.; Gonzalez-Alvarez, M.; Vega, C.; Rolon, M.; Bolas-Fernandez, F.; Borras, J.; Gonzalez-Rosende, E. *Bioorg. Med. Chem.* **2009**, *17*, 7449.

[x] Galiana-Roselló, C.; Bilbao-Ramos, P.; Dea-Ayuela, M. A.; Rolón, M.; Vega, C.; Bolás-Fernández, F.; García-España, E.; Alfonso, J.; Coronel, C.; and González-Rosende, M. E. *J. Med. Chem.* **2013**, *56*, 8984.

[xi] Rheault, T. R.; Stellwagen, J. C.; Adjabeng, G. M; Hornberger, K. R.; Petrov, K. G.; Waterson, A. G.; Dickerson, S. H.; Mook, R. A. Jr.; Laquerre, S. G.; King, A. J.; Rossanese, O. W.; Arnone, M. R.; Smitheman, K. N.; Kane-Carson, L. S.; Han, C.; Moorthy, G. S.; Moss, K. G.; Uehling, D. E. *ACS Med. Chem. Lett.* **2013**, *4*, 358.

Chapter 5. Transition Metal-Catalyzed C–S Bond Formation

5.1. Transition Metal-Catalyzed Sulfonylation of Aryl Halides

Sulfone is an important structural unit widely found in medicinal compounds, agrochemicals and organic materials.[1] Serving as a ketone bioisostere, the sulfone group can enhance the metabolic stability of bioactive molecules. The fine-tuning of electronics in aromatics is a useful tactic for tailoring chemical materials based on aryl sulfones,[1b,1d] which constitute a broad range of biologically active compounds, such as antibacterial, antitumors and HIV agents.[1e-g] A great deal of efforts from many research groups have recently been devoted to the development of SO_2 surrogates such as DABSO and $K_2S_2O_5$ capable of fixing SO_2 for the synthesis of sulfinate intermediates en route to sulfonyl compounds.[2]

Despite the remarkable advance in the transition metal catalyzed cross-coupling chemistry, sulfone synthesis via C-S bond formation using cross-coupling of aryl halides, however, has seen little progress since the initial report based on copper and palladium catalysis.[3] Most of the methods for sulfone synthesis still relies on the oxidation of sulfides after the formation of C–S bonds while the metal-catalyzed cross-coupling approaches typically employ substrates with an electrophilic sulfur center such as sulfonyl chlorides.[4] In the sulfide to sulfone approach, the extra steps needed for S-oxidation sometimes can be complicated by the presence of a functional group susceptible to oxidative conditions. Given the importance of the sulfone as a structural unit in biological and materials sciences, together with its versatility as a functional group in organic synthesis, and given the inefficiency of current methods for sulfone synthesis, development of an efficient catalytic protocol that allows for selective C-S bond formation under mild conditions would be of great value. In particular, the approach based on the cross-coupling of readily available aryl halides with sulfinates as S-nucleophiles would provide a mild and sustainable method for synthesis of aromatic sulfones that are broadly applied in many areas.[2]

5.1.1. Palladium-, and Copper-Catalyzed Sulfone Synthesis

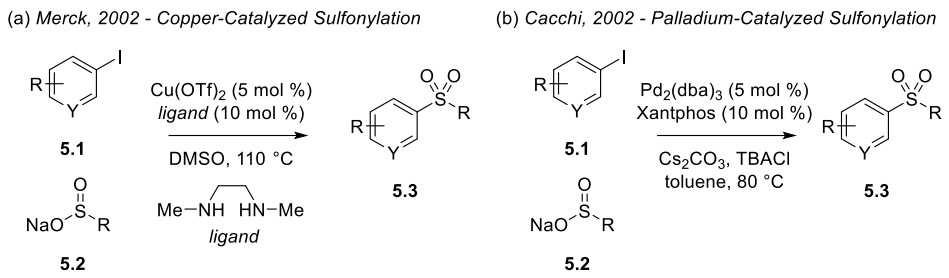

Scheme 5.1. Seminal Reports in Sulfonylation of Aryl Halides

The seminal work on the metal-catalyzed sulfone formation was reported in 2002 based on the cross-coupling aryl halides **5.1** with sulfinates **5.2** (**Scheme 5.1**). A research group at Merck disclosed a copper-catalyzed method for aryl sulfone synthesis employing the reaction conditions analogous to those of the Buchwald's C–O and C–N bond formation (**Figure 5.1a**).[3a] The Cacchi group concurrently reported an alternative palladium-catalyzed method using Xantphos as an ancillary ligand (**Figure 5.1b**),[3b] and later extended the scope of the reaction to include other electrophiles.[3c] Interestingly, the dramatic advance made in the palladium catalyzed cross-coupling with heteroatom nucleophiles was not translated to C-S bond formations. There have been only a few reports describing sulfone synthesis under palladium catalysis since Cacchi's work, probably due to the high reaction temperature required for the reaction, at which a number of processes are known for sulfinate decomposition such as oxidation to sulfonates, redox disproportionation and extrusion of SO_2.[5] In general, the alkyl sulfinates are not efficient partners in these cross-coupling reactions. An additional complication arises from the amphiphilic nucleophilicity of the sulfinate anion, which often results in *O*-arylation.[3c] Copper catalysis, on the other hand, has been used in developing milder protocols, as exemplified by the work of the Ma group utilizing tailored ligands.[6] However, even with the fine-tuned ligands, the copper-catalyzed sulfonylation still is not free from the problems associated with slow oxidative addition and high reaction temperatures.

5.1.2. Photoredox/Nickel-Catalyzed Sulfone Synthesis

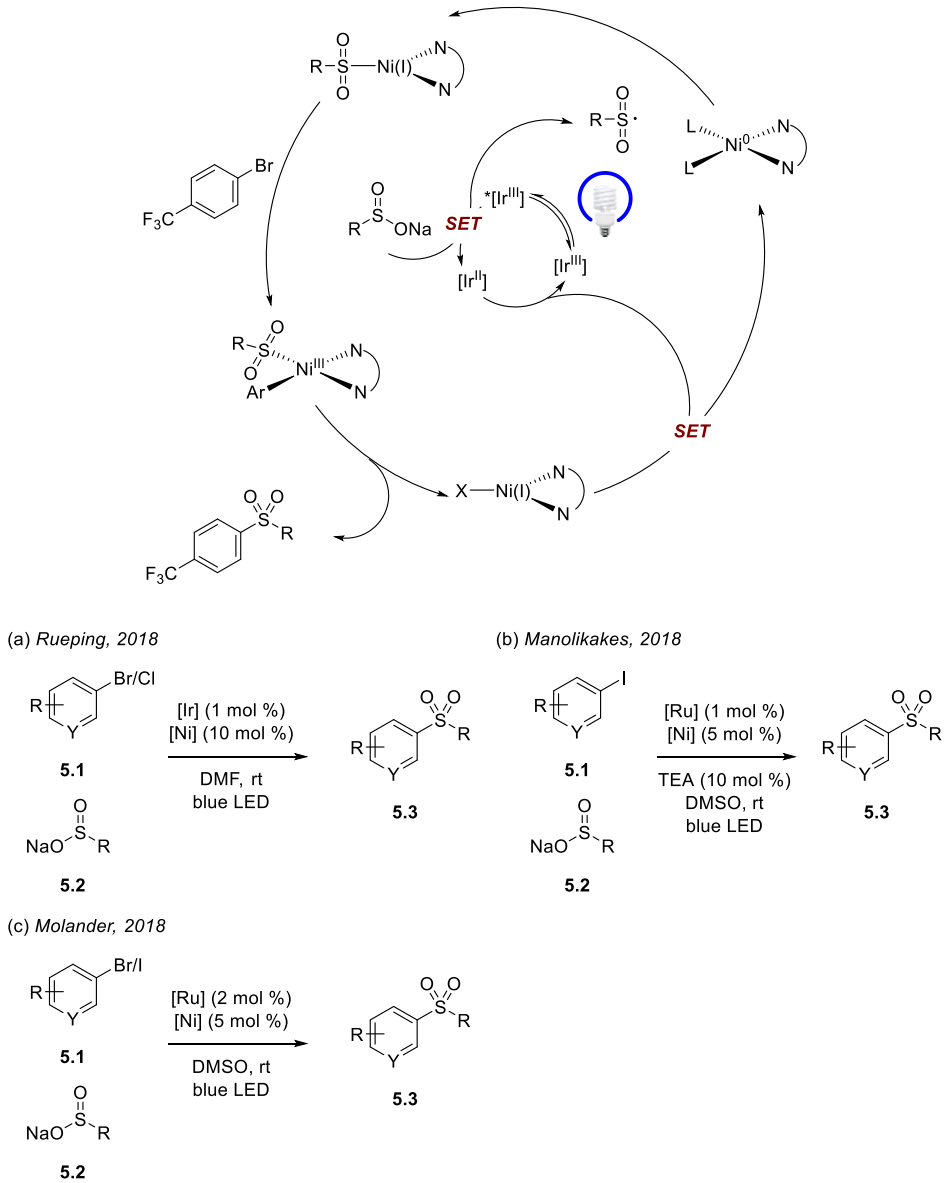

Figure 5.1. Photoredox/Nickel-Catalyzed Sulfonylation

The sulfonyl radical-mediated nickel-catalyzed strategy is also viable for the synthesis of sulfones (**Figure 5.1**). The Rueping, Molander, and Manolikakes groups

independently published new sulfonylation methods making use of photoredox/nickel dual-catalysis.[7] In these studies, the ^{3}MLCT iridium or ruthenium complexes oxidized the sulfinate anion affording a sulfonyl radical, which added to the low valent Ni^0 center to form a Ni^I intermediate. Subsequent oxidative addition of the Ni^I sulfinato complex to an aryl halide and reductive elimination of the resulting Ni^{III} intermediate provided the desired sulfone. While the reaction conditions were milder as compared with the previous approaches, the intermediacy of reactive sulfonyl radicals often resulted in sulfide byproduct formation presumably via disproportionation to sulfonates and thiols. Also, the radical desulfination of alkyl sulfonyl radicals was problematic, hampering the formation of desired sulfone products. While the rate of S to C radical translocation via SO_2 extrusion is slow for many alkyl sulfinates derived radicals, the desulfination can be the drawback of this photoredox/Ni dual-catalytic approach.[8]

5.2. Visible-Light-Activated Palladium Catalysis

Changing the reactivity of transition metals via photochemical excitation has long been an interest to chemists. Palladium, as one of the most common metal catalysts, has also been a subject of this line of study especially in addressing problems associated with the reaction with alkyl halides.[9] Alkyl halides are among the most unreactive electrophiles for oxidative addition of palladium complexes, along with the rapid β-hydride elimination of palladium alkyl complexes.[10] However, palladium complexes, upon light irradiation, are capable of entering the cross-coupling pathway involving a radical intermediate generated through electron transfer or dissociation of Pd–C bonds, as demonstrated by the successful light-excited palladium catalysis.[11] In particular, the palladium catalysis mediated by an SET process, instead of η^2-coordination or S_N2 initiated oxidative addition, may bypass the high-energy barrier for Pd-C bond formation and deleterious reaction pathways associated with alkyl substrates. Despite the success of early approaches, the necessity of a strong UV light source limits their broad utility in organic chemistry laboratories.

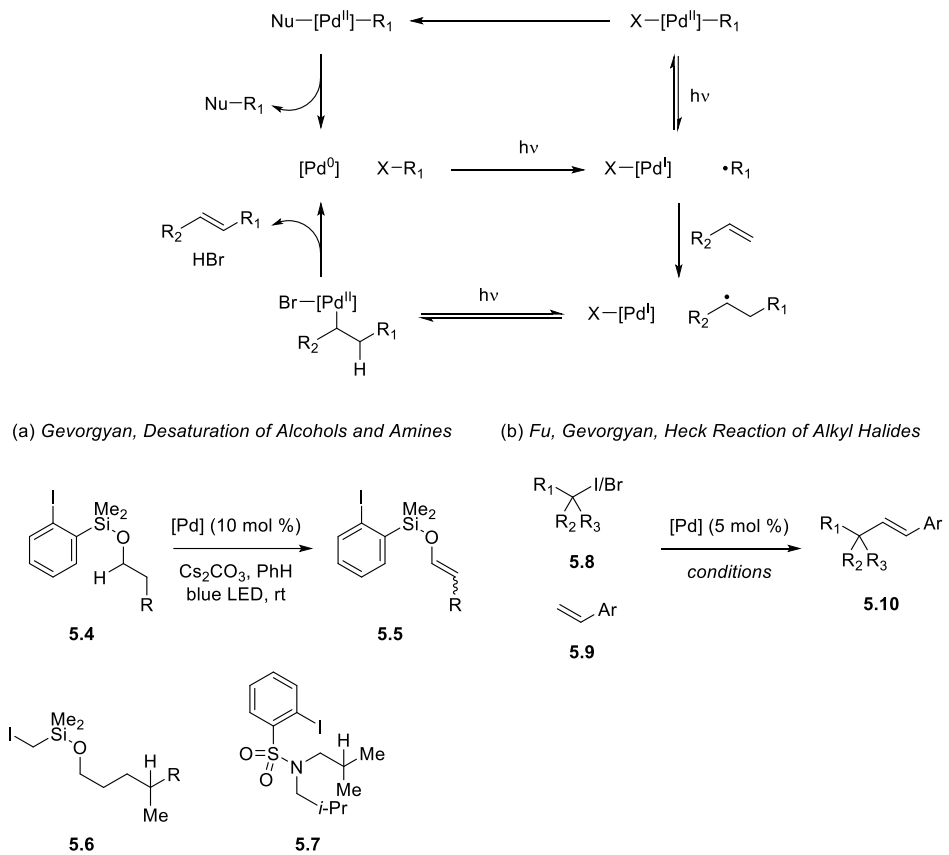

Figure 5.2. Visible-Light-Activated Palladium Catalysis

The recent approach of using photonic energy of visible light in transition metal catalysis has also made its way to palladium-catalyzed reactions.[12] Although the reaction mechanism remains to be established, a proposal has been put forward in which visible light irradiation generates an excited state palladium complex capable of forming carbon-centered radicals from organohalides via single electron transfer as an alternative mode of oxidative addition (**Figure 5.2**). After activation of a chemical bond that might lead to C–C bond formation, the radical is recombined with the Pd^{I} to form a Pd^{II} intermediate poised for reductive elimination or β-hydride elimination. Current approaches based on visible-light-mediated palladium catalysis include selective desaturation of aliphatic alkane chains directed by the pendent radical tethered through alcohol or amine groups (**5.4**, **5.6** and **5.7**), and the alkyl Heck reaction of **5.8**. The Gevorgyan group utilized the aryl and alkyl radicals

generated via light-activated palladium catalysis for selective activation of C_{sp}^3–H bonds by hydrogen atom abstraction, from which a Pd^{II} intermediate arose through rebound of the translocated radical and underwent β-hydride elimination to afford alkene **5.5** (**Figure 5.2a**).[12a,b,g] The regioselectivity of this method was superior to the previous free radical desaturation protocol which involved a carbocation intermediate.[13] Fu and coworkers also established a radical-mediated Heck reaction that worked with tertiary and secondary alkyl halides, in which the β-hydride elimination was proposed as a critical step. In a similar vein, the Gevorgyan group proposed a radical polar crossover mechanism involving the formation of a carbocationic intermediate during the catalysis (**Figure 5.2b**).[12c,d,e,f]

5.3. Visible-Light-Activated Palladium-Catalyzed Sulfonylation of Aryl Halides

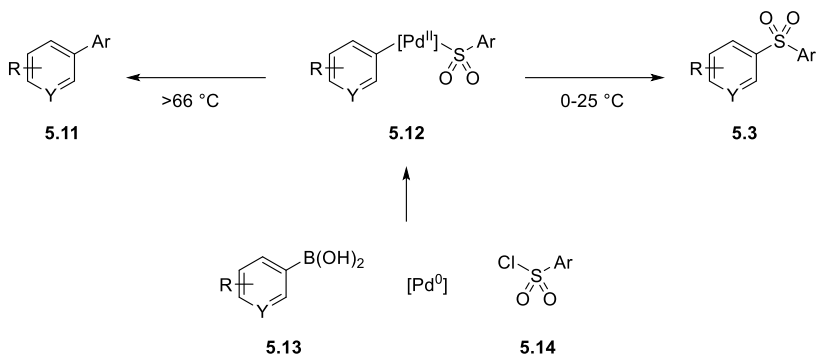

Scheme 5.2. Desulfinylation and Sulfonylation in Palladium Complex

It is a nontrivial task to pinpoint which step is responsible for the inefficiency of the current cross-coupling methods for sulfonylation. Nevertheless, we surmised that the sulfinate might impede one of the elementary steps of the catalytic cycle, most likely the oxidative addition step. The reductive elimination of the palladium sulfinato complex seems to be a fast process, as noted in the previous studies by the Vogel group who detected rapid sulfone bond formation from **5.12** at a low temperature (**Scheme 5.2**).[5b] Also, in the studies of sulfone synthesis using sulfinato palladium complexes, the sulfone linkage was generated at low temperatures to indicate the facility of C-S bond formation via reductive elimination.[4,5] Along the same line, it is worthy of note that the palladium-catalyzed reaction between sulfonyl chlorides and boronic acids did not require specially designed ligands for efficient sulfone generation at room temperature. While other factors might be responsible for the inefficiency of the palladium-catalyzed sulfonylation of aromatic halides, we postulated that the change of the oxidative addition step to a different reaction pathway could lead to the development of new sulfonylation reaction.

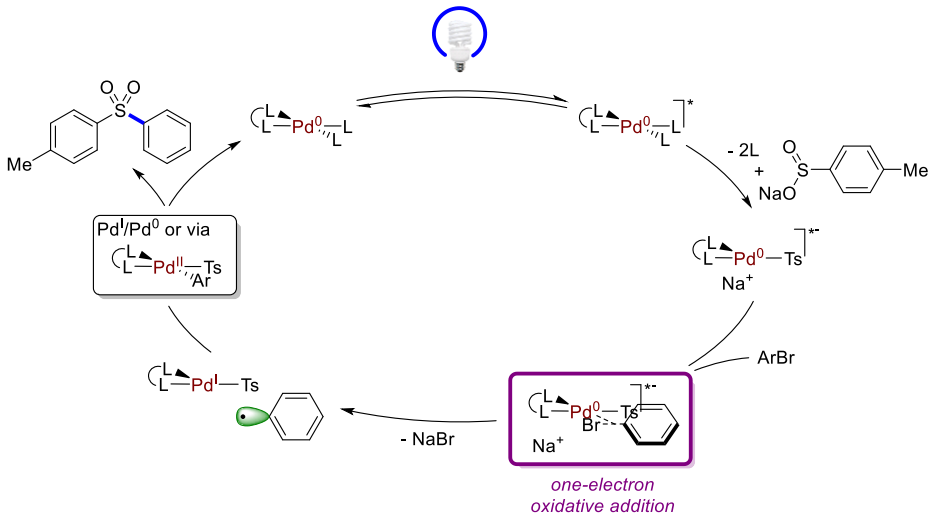

Figure 5.3. Visible-Light-Excited Palladium-Catalyzed Sulfonylation

Our proposition is schematically outlined in Figure 5.3, in which photo-excitation of the low-valent palladium intermediate unlocks a new mechanistic pathway for activating the aryl bromide (**Figure 5.3**). More specifically, the excited palladium is proposed to activate the aryl halides in a mesolytic fashion, rather than through direct insertion into the C-Br σ-bond, giving rise to a Pd^{I} sulfinato complex and an aryl radical. The aryl radical would then forge a sulfonyl bond via a Pd^{II} intermediate or a Pd^{I}/Pd^{0} bond-making process. While it remains to be established if photoexcitation can be achieved selectively for the targeted low-valent palladium, the strategy to split a two-electron step into multiple stages involving odd-electron species may enable facile activation of aryl halide substrates.

5.3.1 Discovery and Optimization of Sulfonylation

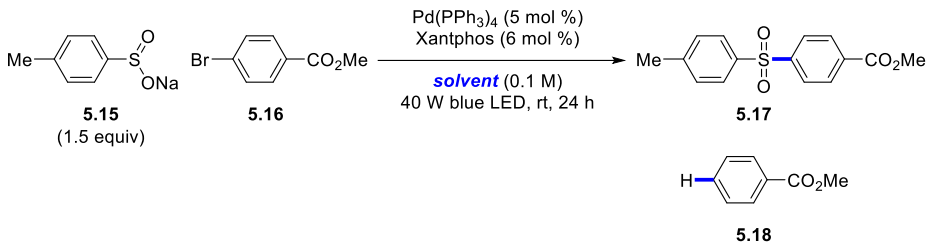

entry	*solvent*	5.16 (%)	5.17 (%)	5.18 (%)
1[b]	DMSO	96	0	0
2[c]	DMSO	98	0	0
3	DMSO	62	32	0
4	DMA	45	19	35
5	DMF	82	7	10
6	MeCN	96	0	0
7	DMSO/toluene (4:1)	80	8	0
8	DMSO/toluene (1:1)	66	9	0

[a]Yields are determined by NMR analysis with an internal standard using ArBr **5.16** (0.2 mmol). [b]Without Pd. [c]without light.

Table 5.1. Initial Discovery of Sulfonylation[a]

Using sulfinate **5.15** and aryl bromide **5.16**, we explored the feasibility of the visible-light-activated palladium-catalyzed sulfonylation (**Table 5.1**). The formation of bis-arylsulfone **5.17** took place when the reaction using the modified Cacchi protocol was carried out with blue LED irradiation (*entries* 1-3).[3c] The use of polar solvents was crucial presumably due to the poor solubility of sulfinates (*entries* 4-6). Also, the reaction in solvents with a hydridic C-H bond gave a significant amount of the debromohydrogenated product **5.18** (*entries* 4, and 5), which arose potentially from hydrogen abstraction of the reactive aryl radical. Interestingly, the use of toluene as a cosolvent decreased the reaction efficiency and increased starting material decomposition (*entries* 7-8). Based on the appearance of multiple byproducts in small amounts, the Minisci-type interception of aryl radicals was speculated to take place in solvent systems containing toluene.

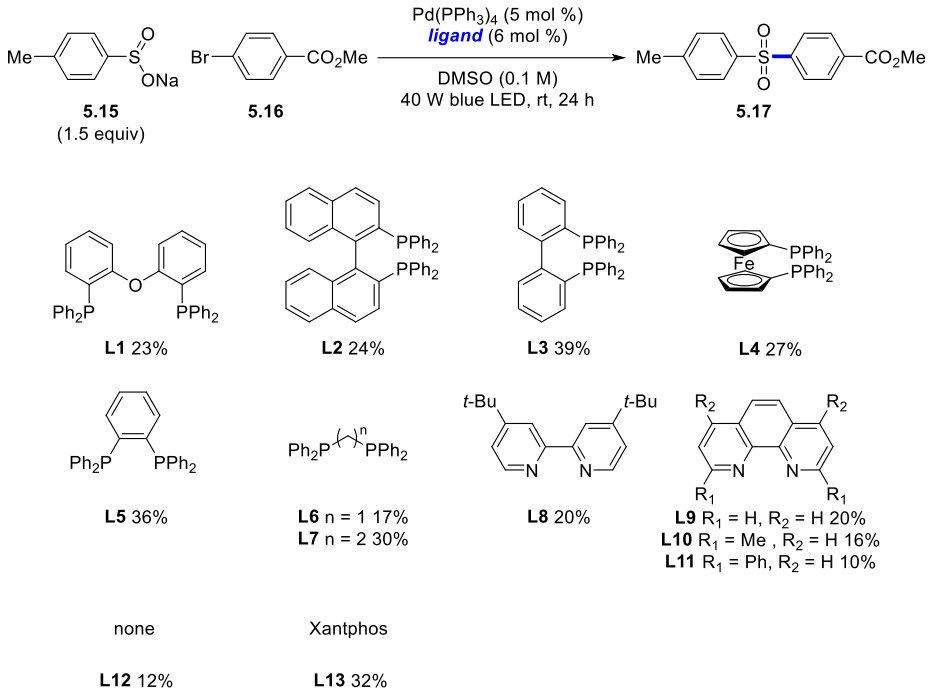

[a]Yields are determined by NMR analysis with an internal standard using ArBr **5.16** (0.2 mmol).

Table 5.2. Ligands Tested for Sulfonylation[a]

The initial ligand screening experiments using an assortment of bisphosphine and dinitrogen ligands suggested the prospect of improving the yield (**Table 5.2**). The bite angle of the ligand did not affect the reaction, as shown by the comparable results obtained with the ligands with a large bite angle (**L1**, **L4**, and **L13**) and those with a smaller bite angle (**L2**, **L3**, and **L7**). While the ligand scaffold exerted little effect (**L2** vs. **L7**), it was notable that the reaction with bipyridine ligands did produce the product albeit in low yields. BIPHEP (bis(diphenylphosphino)biphenyl, **L3**), a bisphosphine with a rotationally flexible backbone, was found to be optimal. However, a ligand with more conjugation such as BINAP (**L2**) gave inferior results, suggesting possible importance of the ligand backbone.

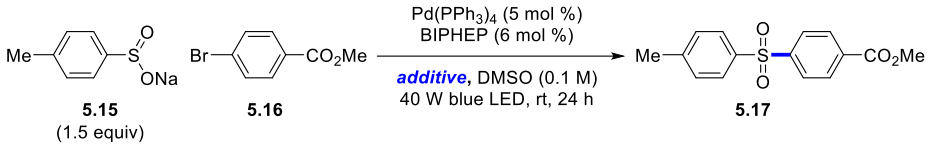

5.15 (1.5 equiv) **5.16** **5.17**

entry	*additive*	5.16 (%)	5.17 (%)
1	-	46	38
2	*fac*-Ir(ppy)$_3$ (1 mol %)	35	37
3	Ir(ppy)$_2$(dtbbpy)PF$_6$ (1 mol %)	41	38
4	Ir[dF(CF$_3$)ppy)$_2$(dtbbpy)PF$_6$ (1 mol %)	51	33
5	Ru(bpy)$_3$(PF$_6$)$_2$	51	31
6	Zn (0.5 equiv)	0	53
7	Zn (1.0 equiv)	0	53
8	Zn (1.5 equiv)	0	51
9	Mn (0.5 equiv)	28	39
10	Mn (1.5 equiv)	0	54

[a]Yields are determined by NMR analysis with an internal standard using ArBr **5.16** (0.2 mmol).

Table 5.3. Additives Tested for Sulfonylation[a]

In order to examine if direct excitation of palladium might not be efficient as noted in our studies on nickel catalysis, we tested dual-catalytic systems (**Table 5.3**). Photocatalysts in this reaction, however, did not seem to act as a photosensitizer, providing similar (*entries* 2 and 3) or worse results (*entries* 4 and 5). In contrast to the photocatalysts that showed little to no effect, the addition of Zn and Mn led to increase in yields of sulfone formation (*entries* 6-10). The addition of 1.0 equivalent of Zn allowed reduction of the catalyst loading to 1 mol % in the reaction conducted at a higher concentration. It was suspected, however, that the Zn^{2+} ion formed in the reaction mixture might suppress the reaction by weakening the nucleophilicity of the sulfinate. The addition of a Zn^{2+} salt (e.g. zinc diacetate) to the reaction mixture decreased catalytic efficiency. The reaction with Langlois's reagent (CF_3SO_2Na), a known coupling partner even with its low nucleophilicity, under the reductive reaction conditions gave no sulfone product. While the exact role of Zn and Mn is unclear, these metallic reductants may help maintain the concentration of the potentially unstable odd-electron palladium species in the reaction mixture by preventing

disproportionation.

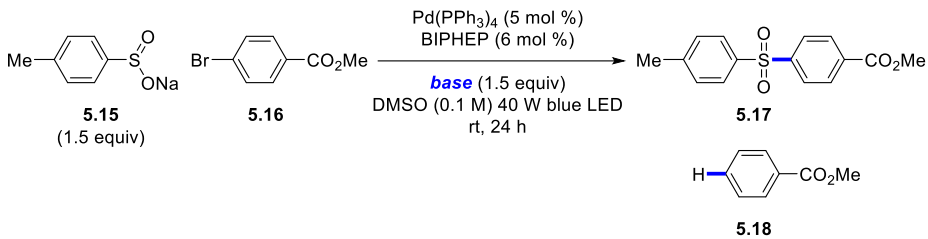

entry	*base*	5.16 (%)	5.17 (%)	5.18 (%)
1	-	44	39	<5
2	K_2CO_3	23	52	<5
3	Cs_2CO_3	0	70	<5
4	K_3PO_4	52	34	<5
5	K_2HPO_4	55	40	<5
6	KOAc	20	54	<5
7	*t*-BuOK	0	0	0
8	TEA	0	33	37
9	DBU	25	41	25
10	TMG	29	41	25

[a]Yields are determined by NMR analysis with an internal standard using ArBr **5.16** (0.2 mmol).

Table 5.4. Base Effects in Sulfonylation[a]

Unexpectedly, inorganic bases promoted the conversion of this reaction (**Table 5.4**). The incorporation of carbonate and acetate bases increased the yields of the product (*entries* 2, 3, and 6) while phosphate bases showed little effect (*entries* 4 and 5*)*. Among the bases tested, Cs_2CO_3 provided the best result (*entry* 3) whereas the use of more nucleophilic *t*-BuOK led to complete decomposition of aryl halide **5.16** (*entry* 7). Amine bases also increased conversion (*entries* 8-10), although formation of the hydrodebromination product **5.18** became more pronounced. It was unclear whether **5.18** came from radical reduction or transfer hydrogenation via β-hydride and reductive eliminations. The effect of a base might also arise from the increase in the concentration of an anionic Pd^0 species (ate complex) derived from complexation of the base with Pd^0. The decomposition of the aryl halide substrate induced by *t*-BuOK might be caused by the strong complex formation between the alkoxide and the Pd^0 center that hampered the sulfinate coordination.[14]

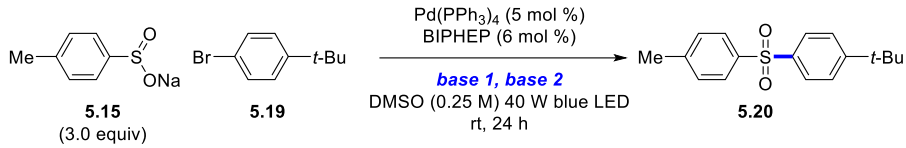

5.15 (3.0 equiv) **5.19** **5.20**

entry	*base 1*	*equiv*	*base 2*	*equiv*	5.15 (%)	5,20 (%)
1	*t*-BuOK	0.5	-	-	46	10
2	*t*-BuOK	1.5	-	-	54	13
3	*t*-BuOK	3	-	-	44	12
4	*t*-BuOK	5	-	-	45	7
5	*t*-BuOK	0.5	Cs_2CO_3	1.5	58	27
6[b]	*t*-BuOK	0.5	Cs_2CO_3	1.5	50	34
7	*t*-BuOK	1.5	Cs_2CO_3	1.5	42	30
8	*t*-BuOK	3.0	Cs_2CO_3	1.5	42	27

[a]Yields are determined by NMR analysis with an internal standard using ArBr **5.19** (0.2 mmol). [b]55 °C

Table 5.5. Base Effects in Sulfonylation with Electron Neutral Aryl Halide[a]

In sharp contrast to the reactions with the electron-poor aryl bromide **5.16**, aryl bromide **5.19** did not decompose in the reaction using *t*-BuOK base (**Table 5.5**). In these experiments, the conversion of **5.19** was found to be similar regardless of the equivalent of the *t*-BuOK added (*entries* 1-4). The generally low level of the yield was enhanced upon the addition of cesium carbonate (*entries* 5-8). The ameliorating effect of Cs_2CO_3 addition, however, could not render further improvement, as screening reaction temperatures and base equivalents did not lead to higher yields of the product. Also conducted was a radical mediated reduction of the same substrate **5.19** using Hantzsch ester, which provided good yields of the reduction product. It appeared that base is essential for the higher conversion of aryl halides while at the same time the bases might be impeding the sulfinate coordination hampering the catalyst turnover and C–S bond formation.

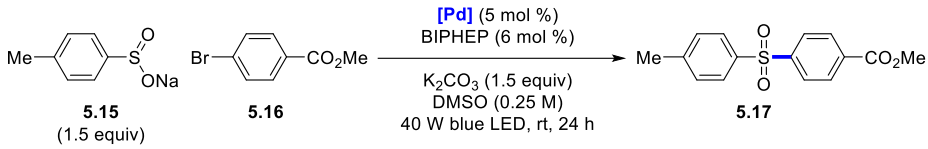

5.15 (1.5 equiv) **5.16** **5.17**

entry	[Pd]	*x*	5.16 (%)	5.17 (%)
1	$Pd(OAc)_2$	6	62	32
2	$Pd(OAc)_2$	10	51	44
3	$Pd(dba)_2$	6	64	34
4	$Pd(dba)_2$	10	33	49
5	$Pd(PPh_3)_4$	6	32	46
6	$Pd(PPh_3)_4$	10	0	54
7	$Pd(BIPHEP)_2$, without ligand	0	24	54

[a]Yields are determined by NMR analysis with an internal standard using ArBr **5.16** (0.2 mmol).

Table 5.6. Phosphine Equivalent Effects in Sulfonylation[a]

The involvement of a base in this reaction prompted us to examine various palladium precatalysts (**Table 5.6**). In the absence of a base, the reactions using $Pd(OAc)_2$ and $Pd(dba)_2$ showed almost no conversion of aryl halide **5.16**. In the reactions using a base (K_2CO_3, 1.5 equiv), $Pd(OAc)_2$ and $Pd(dba)_2$ showed significant catalytic reactivity to give the product in 32% and 34% yield, respectively (*entries* 1 and 3), with $Pd(PPh_3)_4$ being the most efficient (*entry* 5). The effect of the precatalyst, however, was negligible when the amount of BIPHEP was increased, and the reaction using $Pd(PPh_3)_4$ led to significant decomposition of the starting aryl bromide (*entries* 2, 4, and 6). Based on the hypothesis that $Pd(BIPHEP)_2$ or $Pd(BIPHEP)L_2$ might absorb light to initiate the catalytic cycle, we synthesized $Pd(BIPHEP)_2$ and tested it in our reaction conditions to find a result similar to those obtained with precatalysts (*entry* 7). This observation is in line with the notion that phosphine saturated Pd^0 complexes are capable of harvesting photonic energy as supported by a report on the photochemical property of the $Pd(BIPHEP)_2$, where a unique MLCT process was claimed to be feasible by d^8 metal phosphine saturation.[15] Also proposed was a distortion of the complex structure from tetrahedral to square planar after light absorption. It is possible that the structural change facilitates coordination of sulfinates to the palladium

center by an associative mechanism. The excess phosphine (*entry* 6) might also have deleterious effects on this ligand exchange process and be responsible for decomposition of the aryl halide.

5.3.2. Reaction Scope

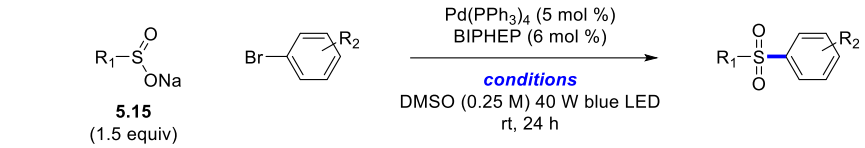

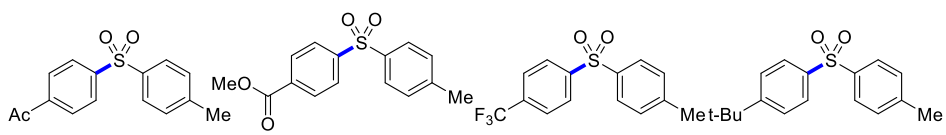

5.21 62% **5.17** 67% **5.22** 72% **5.20** 34%

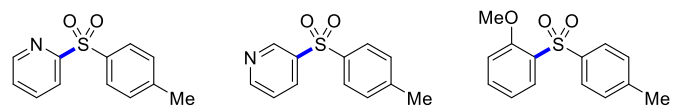

5.23 19% **5.24** 80% **5.25** 23%

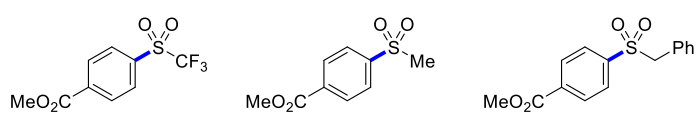

5.26 21% **5.27** 42% **5.28** 18%

[a]See experimental section for more details

Table 5.7. Scope of Sulfonylation[a]

The limitations of our method at the current state were evident (**Table 5.7**). The reaction showed high conversion with electron-deficient aryl bromides, but it was not translated into the yields of the products (**5.17**, **5.21**, **5.22,** and **5.24**). Also problematic was substitution on 2-position of pyridine (**5.23**). The byproducts isolated from this reaction were mostly the dimer and simple reduction products from aryl halides. The yields of these compounds did

not amount to the high conversions of aromatic halides, and additional intractable byproducts were also observed. The electron-neutral aryl halides required additional reagents for the reaction, which still gave lower than 40% yield (**5.20**, and **5.23**). The slow activation of aryl halides might be responsible for the poor performance of the substrates with electron donating groups. In case the C–S bond formation via reductive elimination is a turnover-limiting step, electron-donating groups would impede this process.

A potentially attractive feature of the present catalytic method is the viability of forming sulfones from various alkyl sulfinates. For instance, the sulfinates with high propensity of radical SO_2 extrusion, such as trifluoromethyl and benzyl sulfinates, showed some reactivity in this sulfonylation reaction, suggesting that sulfonyl radicals may not be involved in the C–S bond making step (**5.26**-**5.28**).[8a]

5.3.3. Mechanistic Studies

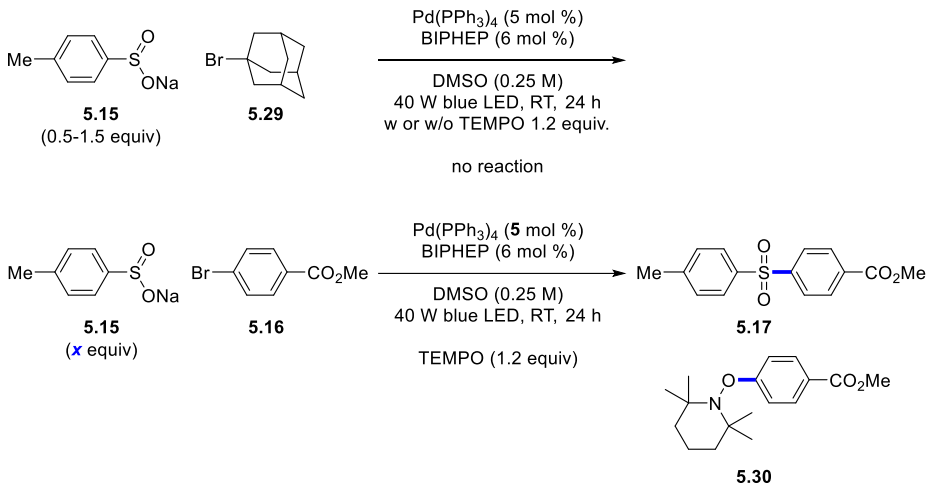

entry	*x*	5.17 (%)	5.30 (%)
1	0	0	0
2	0.5	22	0
3	1	23	24
4	1.5	21	21
5	Cs_2CO_3 (1.5 equiv) instead of 5.15	-	10

Table 5.8. Radical Trapping Experiments in Sulfonylation

Despite the similarity of the reaction conditions with those of Fu and Gevorgyan systems in terms of using SET for initiation, we could not detect carbon-centered radical formation from aliphatic halide **5.29**, a surprising observation given the facile formation of carbon-centered radicals from alkyl halides by SET (**Table 5.8**). However, the formation of aryl ether **5.30** took place when the reaction of aryl halide **5.16** with sulfinate **5.15** was performed in the presence of TEMPO. The formation of the TEMPO adduct depended on the added anionic nucleophile and base. For instance, running the reaction without the sulfinate did form **5.30** whereas the addition of Cs_2CO_3 instead of sulfinate provided a significant amount of the TEMPO adduct. While the base might act as an alternative nucleophile making an anionic palladium species, more studies are necessary. It can be speculated that formation of a carbon-centered radical might occur through a different

mechanism, rather than the SET process, in which the two-stage oxidative addition effected by a photoexcited palladium complex renders a carbon-centered radical and a Pd^{I} complex.

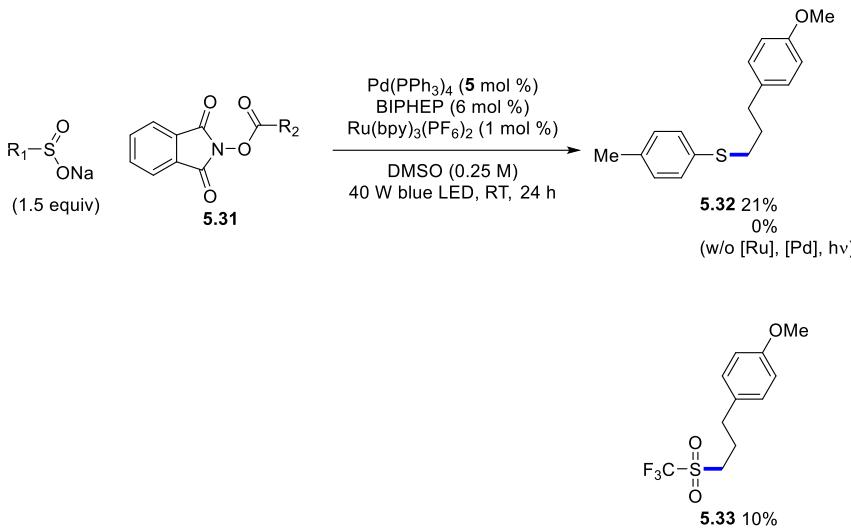

Scheme 5.3. Redox-Active Ester in Sulfonylation

To further exclude the possibility of SET, we set up a reaction using an Okada's redox-active ester instead of aryl bromides and detected formation of sulfide **5.32** under photoredox/palladium dual-catalysis (**Scheme 5.3**).[16] As expected, no detectable formation of a C–S bond-containing compound occurred without $Ru(bpy)_3(PF_6)_2$, and a background reaction between the sulfinate and ester **5.31** resulted in the formation of the carboxylic acid after hydrolysis. When the Langlois reagent was employed, the corresponding sulfone **5.33** was obtained 10% yield.[8a] From the results of these experiments, it was concluded that the sulfide formation also took place through the same mechanism as the sulfonylation.

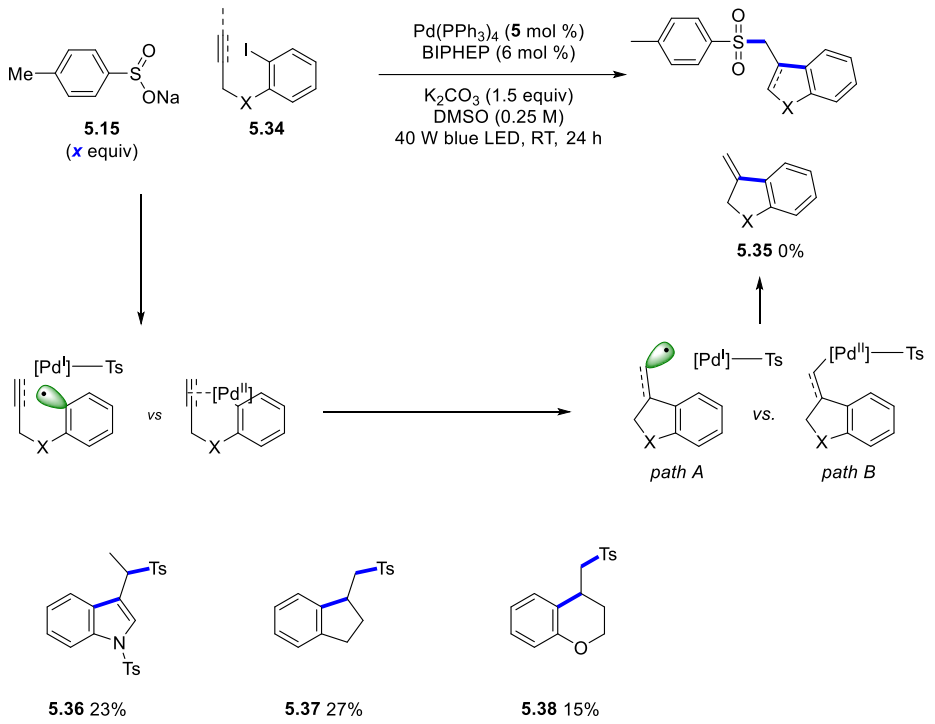

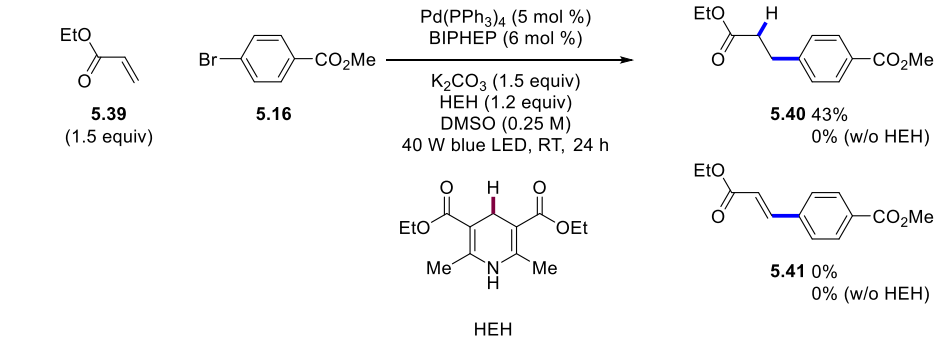

Table 5.9. Radical Addition using Visible-Light-Activated Palladium Catalysis

It was of interest to see whether the palladium and carbon-centered radicals recombine to give the organometallic palladium intermediate as proposed by Fu in their palladium-catalyzed Heck reaction (**Table 5.9**).[12d] No formation of Heck products (**5.35** and **5.41**), which should come from β-hydride elimination of the palladium intermediate, was observed during our investigation. Instead, the products derived from carbosulfonylation and aryl radical addition (**5.36**-**5.38** and **4.30**) were obtained. The exclusion of sulfinates in these cyclization experiments resulted in almost no conversion of the starting material, indicating that the C–S bond-making step was requisite for the catalyst turnover. In addition, the Hantzsch ester was an essential component in the intermolecular Giese addition, suggesting the hydrogen atom transfer was driving the catalytic cycle forward. Although the detailed mechanism awaits more experimentation, it appears that the C–S bond-forming step might occur through a common reductive elimination pathway. Similar to the recent proposal by Fu and Peters in their visible-light activated amination under copper catalysis, the sulfur center might act as a persistent radical when ligated to the Pd^{I} intermediate, thus capable of undergoing pseudo-radical-radical coupling to form a sulfone linkage.[17] Another possible explanation is that the reductive elimination was rapid enough to avoid the β-hydride elimination.

5.4. Conclusion

Herein we report our initial efforts to develop a new strategy for efficient sulfone synthesis by using visible-light irradiation as an initiation tool for the palladium-catalyzed cross-coupling of sulfinates and aryl halides. The use of a Pd^0 precatalyst with the bidentate BIPHEP ligand was effective to provide moderate yields of the sulfone products from electron-deficient aryl halides. Aryl and alkylsulfinates also participated in the reaction to furnish the corresponding coupling products without byproducts. Preliminary mechanistic studies suggested that the activation of aryl halides might occur through a carbon-centered radical pathway that did not involve a SET process. It was also shown that the putative Pd^I sulfinato intermediate could form the C–S bonds, albeit with low yields, from both C_{sp}^3 and C_{sp}^2 radicals.

5.5. References

1) (a) Craig, C. R.; Stitzel, R. E. *Modern pharmacology with clinical applications*. Lippincott Williams & Wilkins: Philadelphia, **2004**. (b) Fink, J. K. *High performance polymers*. William Andrew: Oxford, UK; Waltham, MA, **2014**. (c) Minghao, F.; Bingqing, T.; Steven, H. L.; Xuefeng, J. *Curr. Top. Med. Chem.* **2016,** *16*, 1200. (d) Patani, G. A.; LaVoie, E. J. *Chem. Rev.* **1996,** *96*, 3147. (e) Jones, T. R.; Webber, S. E.; Varney, M. D.; Reddy, M. R.; Lewis, K. K.; Kathardekar, V.; Mazdiyasni, H.; Deal, J.; Nguyen, D.; Welsh, K. M.; Webber, S.; Johnston, A.; Matthews, D. A.; Smith, W. W.; Janson, C. A.; Bacquet, R. J.; Howland, E. F.; Booth, C. L. J.; Herrmann, S. M.; Ward, R. W.; White, J.; Bartlett, C. A.; Morse, C. A. *J. Med. Chem.* **1997,** *40*, 677. (f) Dinsmore, C. J.; Williams, T. M.; O'Neill, T. J.; Liu, D.; Rands, E.; Culberson, J. C.; Lobell, R. B.; Koblan, K. S.; Kohl, N. E.; Gibbs, J. B.; Oliff, A. I.; Graham, S. L.; Hartman, G. D. *Bioorg. Med. Chem. Lett.* **1999,** *9*, 3301. (g) Neamati, N.; Mazumder, A.; Zhao, H.; Sunder, S.; Burke, T. R.; Schultz, R. J.; Pommier, Y. *Antimicrob. Agents Chemother.* **1997,** *41*, 385.

2) Emmett, E. J.; Willis, M. C. *Asian J. Org. Chem.* **2015,** *4*, 602.

3) (a) Baskin, J. M.; Wang, Z. *Org. Lett.* **2002,** *4*, 4423. (b) Cacchi, S.; Fabrizi, G.; Goggiamani, A.; Parisi, L. M. *Org. Lett.* **2002,** *4*, 4719. (c) Cacchi, S.; Fabrizi, G.; Goggiamani, A.; Parisi, L. M.; Bernini, R. *J. Org. Chem* **2004,** *69*, 5608.

4) Bandgar, B. P.; Bettigeri, S. V.; Phopase, J. *Org. Lett.* **2004,** *6*, 2105.

5) (a) Dubbaka, S. R.; Vogel, P. *J. Am. Chem. Soc.* **2003,** *125*, 15292. (b) Dubbaka, S. R.; Vogel, P. *Angew. Chem. Int. Ed.* **2005,** *44*, 7674. (c) Yuan, K.; Soulé, J.-F.; Doucet, H. *ACS Catalysis* **2015,** *5*, 978.

6) Zhao, J.; Niu, S.; Jiang, X.; Jiang, Y.; Zhang, X.; Sun, T.; Ma, D. *J. Org. Chem* **2018,** *83*, 6589.

7) (a) Yue, H.; Zhu, C.; Rueping, M. *Angew. Chem. Int. Ed.* **2018,** *57*, 1371. (b) Liu, N.-W.; Hofman, K.; Herbert, A.; Manolikakes, G. *Org. Lett.* **2018,** *20*, 760. (c) Cabrera-Afonso, M. J.; Lu, Z.-P.; Kelly, C. B.; Lang, S. B.; Dykstra, R.; Gutierrez, O.; Molander, G. A. *Chem.*

Sci. **2018,** *9*, 3186.

8) (a) Bertrand, F.; Le Guyader, F.; Liguori, L.; Ouvry, G.; Quiclet-Sire, B.; Seguin, S.; Zard, S. Z. *Comptes Rendus de l'Académie des Sciences - Series IIC - Chemistry* **2001,** *4*, 547. (b) Knauber, T.; Chandrasekaran, R.; Tucker, J. W.; Chen, J. M.; Reese, M.; Rankic, D. A.; Sach, N.; Helal, C. *Org. Lett.* **2017,** *19*, 6566.

9) Sumino, S.; Fusano, A.; Fukuyama, T.; Ryu, I. *Acc. Chem. Res.* **2014,** *47*, 1563.

10) Netherton, M. R.; Fu, G. C. Palladium-Catalyzed Cross-Coupling Reactions of Unactivated Alkyl Electrophiles with Organometallic Compounds. In *Palladium in Organic Synthesis*, Tsuji, J., Ed. Springer Berlin Heidelberg: Berlin, Heidelberg, **2005**; pp 85.

11) Van Leeuwen, P. W. N. M.; Roobeek, C. F.; Huis, R. *J. Organomet. Chem.* **1977,** *142*, 233.

12) For selected examples of visible-light activated palladium catalysis see (a) Parasram, M.; Chuentragool, P.; Sarkar, D.; Gevorgyan, V. *J. Am. Chem. Soc.* **2016,** *138*, 6340. (b) Parasram, M.; Chuentragool, P.; Wang, Y.; Shi, Y.; Gevorgyan, V. *J. Am. Chem. Soc.* **2017,** *139*, 14857. (c) Kurandina, D.; Parasram, M.; Gevorgyan, V. *Angew. Chem. Int. Ed.* **2017,** *56*, 14212. (d) Wang, G.-Z.; Shang, R.; Cheng, W.-M.; Fu, Y. *J. Am. Chem. Soc.* **2017,** *139*, 18307. (e) Wang, G.-Z.; Shang, R.; Fu, Y. *Org. Lett.* **2018,** *20*, 888. (f) Kurandina, D.; Rivas, M.; Radzhabov, M.; Gevorgyan, V. *Org. Lett.* **2018,** *20*, 357. (g) Chuentragool, P.; Parasram, M.; Shi, Y.; Gevorgyan, V. *J. Am. Chem. Soc.* **2018,** *140*, 2465.

13) Voica, A.-F.; Mendoza, A.; Gutekunst, W. R.; Fraga, J. O.; Baran, P. S. *Nat. Chem.* **2012,** *4*, 629.

14) (a) Alcazar-Roman, L. M.; Hartwig, J. F. *J. Am. Chem. Soc.* **2001,** *123*, 12905. (b) Shekhar, S.; Hartwig, J. F. *Organometallics* **2007,** *26*, 340.

15) Tsubomura, T.; Ito, Y.; Inoue, S.; Tanaka, Y.; Matsumoto, K.; Tsukuda, T. *Inorg. Chem.* **2008,** *47*, 481.

16) Okada, K.; Okamoto, K.; Morita, N.; Okubo, K.; Oda, M. *J. Am. Chem. Soc.* **1991,** *113*, 9401.

17) Ahn, J. M.; Ratani, T. S.; Hannoun, K. I.; Fu, G. C.; Peters, J. C. *J. Am. Chem. Soc.* **2017,** *139*, 12716.

5.6. Experimental Section

5.6.1. General Information

Aryl Halides and sulfinates were purchased from commercial sources and used as received unless otherwise noticed. All solvents were purified according to the method of Grubbs.[i] Non-aqueous reagents were transferred under nitrogen or argon via syringe or cannula. Organic solutions were concentrated under reduced pressure on a Büchi rotary evaporator using a water bath. Chromatographic purification of products was accomplished using forced-flow chromatography on silica gel (Merck 9385 Kiesel gel 60). Thin-layer chromatography (TLC) was performed on Silicycle 0.25 mm silica gel F-254 plates. Visualization of the developed chromatogram was performed by fluorescence quenching or $KMnO_4$ stain. ^1H NMR spectra were recorded on an Agilent 400-MR DD2 400 MHz, and Varian/Oxford As-500 500 MHz are internally referenced to residual protio $CDCl_3$ signal (7.26 ppm). Data for ^1H NMR are reported as follows: chemical shift (δ ppm), integration, multiplicity (s = singlet, d = doublet, t = triplet, q = quartet, m = multiplet, dd = doublet of doublets, dt = doublet of triplets, br = broad), coupling constant (Hz), and assignment. ^{13}C NMR spectra were recorded on an Agilent 400-MR DD2 400 MHz, and Varian/Oxford As-500 500 MHz, and data are reported in terms of chemical shift relative to $CDCl_3$ (77.0 ppm).

5.6.2. Preparation of Substrates

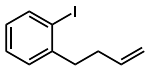

1-(but-3-en-1-yl)-2-iodobenzene[ii]

To a solution of 2-iodobenzyl bromide (297 mg, 1.0 mmol, 1.0 equiv.) dissolved in THF (2 ml), allylmagnesium bromide (1.0 M solution in Et_2O, 2.0 ml, 2.0 mmol, 2.0 equiv.) was slowly added at 0 °C. The reaction mixture was warmed to room temperature and stirred overnight. The reaction was quenched using aq. NH_4Cl and the aqueous layer was extracted with 3x with DCM. The combined organic layer was concentrated *in vacuo*. Purification by flash column chromatography provided the title compound (165 mg, 0.64 mmol, 64%) as a colorless oil.

^{1}H NMR (400 MHz, $CDCl_3$) δ 7.82 (dd, *J* = 7.9, 0.9 Hz, 1H), 7.27 (td, *J* = 7.5, 1.1 Hz, 1H), 7.21 (dd, *J* = 7.6, 1.6 Hz, 1H), 6.88 (td, *J* = 7.7, 1.7 Hz, 1H), 5.89 (ddt, *J* = 16.9, 10.2, 6.6 Hz, 1H), 5.14 – 4.95 (m, 1H), 2.85 – 2.76 (m, 1H), 2.35 (dt, *J* = 7.8, 6.6 Hz, 1H).

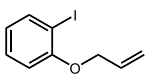

1-(allyloxy)-2-iodobenzene[iii]

To a solution of 2-iodophenol (660 mg, 3 mmol, 1.0 equiv.), and K_2CO_3 (1.24 g, 9.0 mmol, 3.0 equiv) in DMF was added allyl bromide (0.31 ml, 3.6 mmol, 1.2 equiv.), and the resulting reaction mixture was stirred overnight. The reaction mixture was diluted with hexane and washed 3x with brine. The combined organic layer was dried ($MgSO_4$). Concentration and purification by flash column chromatography provided the title compound (721 mg, 2.8 mmol, 92%) as a colorless oil.

^{1}H NMR (400 MHz, $CDCl_3$) δ 7.78 (dd, *J* = 7.8, 1.5 Hz, 1H), 7.33 – 7.23 (m, 1H), 6.81 (dd, *J* = 8.2, 0.9 Hz, 1H), 6.71 (td, *J* = 7.6, 1.1 Hz, 1H), 6.13 – 5.99 (m, 1H), 5.53 (dd, *J* = 17.3, 1.6 Hz, 1H), 5.32 (dd, *J* = 10.6, 1.4 Hz, 1H), 4.66 – 4.56 (m, 2H).

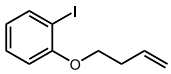

1-(but-3-en-1-yloxy)-2-iodobenzene[iv]

To a solution of 2-iodophenol (1.10 g, 5 mmol, 1.0 equiv.) in DMF (10 ml) was added NaH (220 mg, 60% dispersion in mineral oil, 5.5 mol, 1.1 equiv.) portionwise at 0 ℃. The resulting suspension was stirred for 30 minutes and 4-bromo-1-butene (0.76 ml,7.5 mmol, 1.5 equiv.) was added dropwise. The reaction mixture was warmed up to room temperature and stirred for additional 2 hours. The reaction was quenched using aq. NH_4Cl and the organic layer was washed 2x with brine. The organic layer was dried ($MgSO_4$) and concentrated *in vacuo*. Purification by flash column chromatography provided the title compound (416 mg, 1.5 mmol, 30%) as a colorless oil.

^{1}H NMR (400 MHz, $CDCl_3$) δ 7.77 (dd, *J* = 7.8, 1.6 Hz, 1H), 7.31 – 7.23 (m, 1H), 6.80 (dd, *J* = 8.2, 1.2 Hz, 1H), 6.70 (td, *J* = 7.6, 1.3 Hz, 1H), 5.98 (ddt, *J* = 17.1, 10.2, 6.8 Hz, 1H), 4.06 (t, *J* = 6.6 Hz, 3H), 2.60 (dt, *J* = 6.7, 6.1 Hz, 3H).

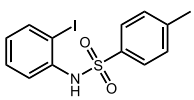

***N*-(2-iodophenyl)-4-methylbenzenesulfonamide**[v]

A flask charged with 2-iodoaniline (1.0 g, 4.6 mmol, 1.0 equiv.), and *p*-toluenesulfonyl chloride (915 mg, 4.8 mmol, 1.05 equiv.) was added pyridine (10 ml). The resulting reaction mixture was stirred for 4 hours. The reaction was concentrated *in vacuo*. Purification by flash column chromatography provided the title compound (1.68 g, 4.6 mmol, 99%) as a beige solid.

^{1}H NMR (400 MHz, $CDCl_3$) δ 7.69 – 7.60 (m, 4H), 7.31 (t, *J* = 7.7 Hz, 1H), 7.22 (d, *J* = 8.1 Hz, 2H), 6.83 (t, *J* = 7.7 Hz, 1H), 6.79 (s, 1H), 2.38 (s, 3H).

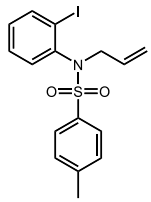

_N_-allyl-_N_-(2-iodophenyl)-4-methylbenzenesulfonamide[vi]

To a solution of *N*-(2-iodophenyl)-4-methylbenzenesulfonamide (413 mg, 1.0 mmol, 1.0 equiv.), and K_2CO_3 (138 mg, 1.0 mmol, 1.0 equiv.) in THF (7 ml) was added allyl bromide (0.35 ml, 4.0 mmol, 4.0 equiv.). The reaction flask was placed on the preheated oil bath (60 ℃) and stirred for 24 hours. The reaction mixture was cooled down to room temperature and concentrated *in vacuo*. Purification by flash column chromatography provided the title compound (413 mg, 1.0 mmol, 99%) as a yellow oil.

^{1}H NMR (400 MHz, $CDCl_3$) δ 7.90 (dd, *J* = 7.9, 1.2 Hz, 1H), 7.67 (d, *J* = 8.2 Hz, 2H), 7.29 (d, *J* = 8.1 Hz, 2H), 7.27 – 7.23 (m, 1H), 7.01 (td, *J* = 7.8, 1.5 Hz, 1H), 6.93 (dd, *J* = 7.9, 1.3 Hz, 1H), 5.86 (ddt, *J* = 16.9, 10.1, 6.9 Hz, 1H), 5.07 – 4.90 (m, 2H), 4.15 (qd, *J* = 14.7, 6.9 Hz, 3H), 2.44 (s, 3H).

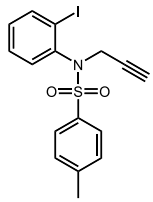

_N_-(2-iodophenyl)-4-methyl-_N_-(prop-2-yn-1-yl)benzenesulfonamide[vii]

To a solution of *N*-(2-iodophenyl)-4-methylbenzenesulfonamide (413 mg, 1.0 mmol, 1.0 equiv.), and K_2CO_3 (691 mg, 5.0 mmol, 5.0 equiv.) in acetone (8 ml) was added propargyl bromide (0.27 ml, 2.5 mmol, 2.5 equiv.). The reaction flash was place on the preheated oil bath (60 ℃) and stirred for 24 hours. The reaction mixture was concentrated *in vacuo*. Purification by flash column chromatography provided the title compound (411 mg, 1.0 mmol, 99%) as an off-white solid.

^{1}H NMR (400 MHz, $CDCl_3$) δ 7.91 (d, *J* = 7.9 Hz, 1H), 7.72 (d, *J* = 8.2 Hz, 2H), 7.29 (d, *J* = 7.9 Hz, 2H), 7.14 (d, *J* = 7.9 Hz, 1H), 7.06 (t, *J* = 7.7 Hz, 1H), 4.76 (d, *J* = 18.1 Hz, 1H), 4.16 – 4.07 (m, 2H), 2.45 (s, 3H), 2.16 (dd, *J* = 4.9, 2.4 Hz, 1H).

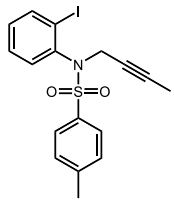

_N_-(but-2-yn-1-yl)-_N_-(2-iodophenyl)-4-methylbenzenesulfonamide

To a solution of _N_-(2-iodophenyl)-4-methylbenzenesulfonamide (413 mg, 1.0 mmol, 1.0 equiv.), and K_2CO_3 (276 mg, 2.0 mmol, 2.0 equiv.) in DMF (2.5 ml) was added 1-bromo-2-butyne (0.11 ml, 1.3 mmol, 1.3 equiv.). The resulting reaction mixture was stirred for 24 hours. The reaction was diluted with EtOAc and washed 2x with brine. The organic layer was dried ($MgSO_4$) and concentrated *in vacuo*. Purification by flash column chromatography provided the title compound (424 mg, 1.0 mmol, 99%) as a pale yellow oil. ^{1}H NMR (400 MHz, $CDCl_3$) δ 7.91 (d, *J* = 7.9 Hz, 1H), 7.72 (d, *J* = 8.0 Hz, 2H), 7.27 (dd, *J* = 10.9, 4.3 Hz, 4H), 7.06 (dd, *J* = 17.5, 8.5 Hz, 2H), 4.68 (d, *J* = 17.7 Hz, 1H), 4.05 (d, *J* = 17.0 Hz, 1H), 2.45 (s, 3H).

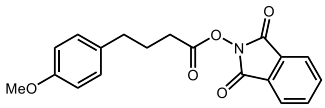

1,3-dioxoisoindolin-2-yl 4-(4-methoxyphenyl)butanoate (5.31)

To a solution of 4-(4-methoxyphenyl)butyric acid (1.94 g, 10.00 mmol, 1 equiv.), *N*-hydroxyphthalimide (2.77 g, 17 mmol, 1.7 equiv.), and DMAP (61.0 g, 0.5 mmol, 0.05 equiv.) dissolved in THF (50 ml) was added *N,N'*-diisopropylcarbodiimide (2.3 ml, 15 mmol, 1.5 equiv.) dropwise and the reaction mixture was stirred overnight. The mixture was concentrated *in vacuo*. Purification of the crude mixture provided the title compound as a white solid.

^{1}H NMR (400 MHz, $CDCl_3$) δ 7.89 (dt, *J* = 7.2, 3.6 Hz, 2H), 7.82 – 7.76 (m, 2H), 7.14 (d, *J* = 8.6 Hz, 2H), 6.86 (d, *J* = 8.6 Hz, 2H), 3.80 (s, 3H), 2.72 (t, *J* = 7.5 Hz, 2H), 2.66 (t, *J* = 7.3 Hz, 2H), 2.08 (p, *J* = 7.4 Hz, 2H).

5.6.3. General Sulfonylation Procedure

To an oven dried 4 ml vial equipped with a stir bar was added $Pd(PPh_3)_4$ (0.05 equiv), BIPHEP (0.06 equiv), aryl halide (1.0 equiv), sodium sulfinate (1.5-3.0 equiv), Cs_2CO_3 (0-1.5 equiv), KO^{t}Bu (0-0.5 equiv) and DMSO (0.25 M). The reaction was sparged with N_2 for 15 minutes, after which the cap was sealed with parafilm. The reaction was stirred and irradiated with 40 W blue LED lamp with fan cooling to maintain the reaction under the ambient temperature (< 32 ℃). The reaction was quenched with saturated NaCl and diluted with EtOAc. The organic layer was washed with water and NaCl solution. Combined organic extracts were dried ($MgSO_4$), and concentrated *in vacuo*. Purification by flash column chromatography yielded the sulfonylated product.

Reaction Apparatus

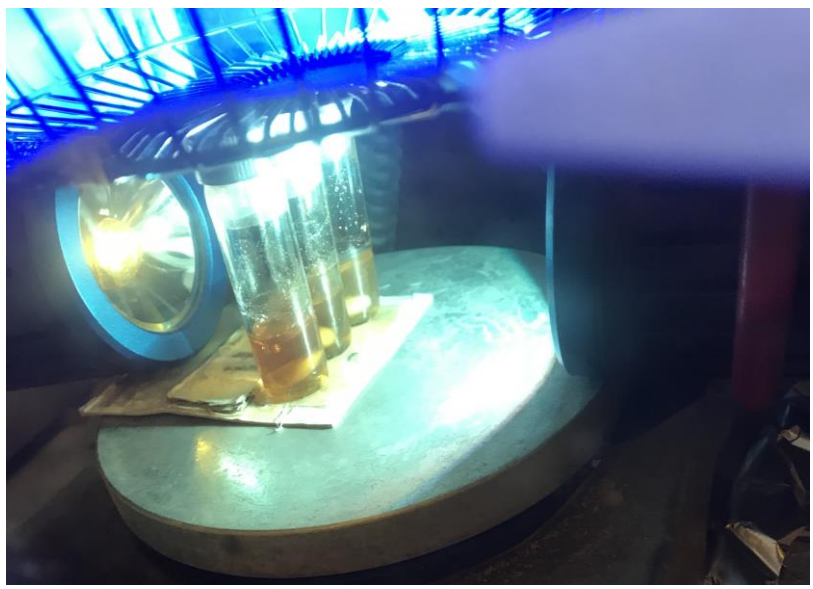

5.6.4. Experimental Data for Sulfonylation Products

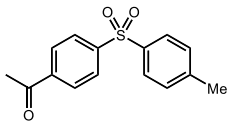

1-(4-tosylphenyl)ethan-1-one (5.21)[viii]

Prepared following the general procedure outlined above using $Pd(PPh_3)_4$ (28.9 mg, 0.025 mmol, 0.05 equiv), BIPHEP (15.7 mg, 0.03 mmol, 0.06 equiv), 4'-bromoacetophenone (100 mg, 0.5 mmol, 1.0 equiv), sodium *p*-toluenesulfinate (267 mg, 1.5 mmol, 3.0 equiv), Cs_2CO_3 (244 mg, 0.75 mmol, 1.5 equiv), and DMSO (2 ml). After 24 hours blue LED irradiation with fan cooling, the reaction mixture was subjected to the work up procedure outlined in the general procedure. Purification by flash column chromatography (ethyl acetate/hexane) provided the title compound (96.8 mg) as a white solid.

^{1}H NMR (400 MHz, $CDCl_3$) δ 8.08 – 7.98 (m, 4H), 7.82 (t, *J* = 10.0 Hz, 2H), 7.31 (d, *J* = 8.1 Hz, 2H), 2.61 (s, 3H), 2.40 (s, 3H); ^{13}C NMR (101 MHz, $cdcl_3$) δ 196.6, 145.8, 144.7, 140.1, 137.8, 130.1, 129.0, 127.9, 127.8, 26.9, 21.6.

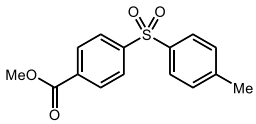

methyl 4-tosylbenzoate (5.17)[viii]

Prepared following the general procedure outlined above using $Pd(PPh_3)_4$ (28.9 mg, 0.025 mmol, 0.05 equiv), BIPHEP (15.7 mg, 0.03 mmol, 0.06 equiv), methyl 4-bromobenzoate (108 mg, 0.5 mmol, 1.0 equiv), sodium *p*-toluenesulfinate (267 mg, 1.5 mmol, 3.0 equiv), Cs_2CO_3 (244 mg, 0.75 mmol, 1.5 equiv), and DMSO (2 ml). After 24 hours blue LED irradiation with fan cooling, the reaction mixture was subjected to the work up procedure outlined in the general procedure. Purification by flash column chromatography (ethyl acetate/hexane) provided the title compound (108 mg) as a white solid.

^{1}H NMR (400 MHz, $CDCl_3$) δ 8.13 (d, *J* = 8.4 Hz, 2H), 7.98 (d, *J* = 8.5 Hz, 2H), 7.83 (d, *J* = 8.2 Hz, 2H), 7.31 (d, *J* = 8.1 Hz, 2H), 3.92 (s, 3H), 2.40 (s, 3H); ^{13}C NMR (101 MHz, $CDCl_3$) δ 165.5, 145.8, 144.7, 137.8, 134.1, 130.4, 130.1, 127.9, 127.5, 52.6, 21.6.

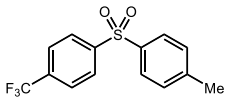

1-methyl-4-((4-(trifluoromethyl)phenyl)sulfonyl)benzene (5.22)[viii]

Prepared following the general procedure outlined above using $Pd(PPh_3)_4$ (28.9 mg, 0.025 mmol, 0.05 equiv), BIPHEP (15.7 mg, 0.03 mmol, 0.06 equiv), 4-bromobenzotrifluoride (113 mg, 0.5 mmol, 1.0 equiv), sodium *p*-toluenesulfinate (267 mg, 1.5 mmol, 3.0 equiv), Cs_2CO_3 (244 mg, 0.75 mmol, 1.5 equiv), and DMSO (2 ml). After 24 hours blue LED irradiation with fan cooling, the reaction mixture was subjected to the work up procedure outlined in the general procedure. Purification by flash column chromatography (ethyl acetate/hexane) provided the title compound (96.8 mg) as a white solid.

^{1}H NMR (400 MHz, $CDCl_3$) δ 8.05 (d, *J* = 8.2 Hz, 2H), 7.84 (d, *J* = 8.3 Hz, 2H), 7.75 (d, *J* = 8.3 Hz, 2H), 7.33 (d, *J* = 8.1 Hz, 2H), 2.41 (s, 3H).

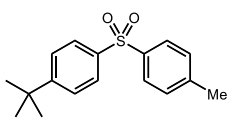

1-(tert-butyl)-4-tosylbenzene (5.20)

Prepared following the general procedure outlined above using $Pd(PPh_3)_4$ (28.9 mg, 0.025 mmol, 0.05 equiv), BIPHEP (15.7 mg, 0.03 mmol, 0.06 equiv), 1-bromo-4-tert-butylbenzene (107 mg, 0.5 mmol, 1.0 equiv), sodium *p*-toluenesulfinate (267 mg, 1.5 mmol, 3.0 equiv), Cs_2CO_3 (244 mg, 0.75 mmol, 1.5 equiv), and DMSO (2 ml). After 24 hours blue LED irradiation with fan cooling, the reaction mixture was subjected to the work up procedure outlined in the general procedure. The yield was determined to be 34% by ^{1}H NMR analysis.

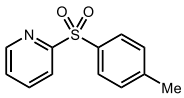

2-tosylpyridine (5.23)[ix]

Prepared following the general procedure outlined above using $Pd(PPh_3)_4$ (11.6 mg, 0.01 mmol, 0.05 equiv), BIPHEP (6.3 mg, 0.012 mmol, 0.06 equiv), 2-bromopyridine (32 mg, 0.2 mmol, 1.0 equiv), sodium *p*-toluenesulfinate (107 mg, 0.6 mmol, 3.0 equiv), Cs_2CO_3 (98 mg, 0.3 mmol, 1.5 equiv), and DMSO (0.8 ml). After 24 hours blue LED irradiation with fan cooling, the reaction mixture was subjected to the work up procedure outlined in the general procedure. The yield was determined to be 19% by ^{1}H NMR analysis.

^{1}H NMR (400 MHz, $CDCl_3$) δ 8.67 (dd, *J* = 4.7, 0.7 Hz, 1H), 8.19 (d, *J* = 7.9 Hz, 1H), 7.97 – 7.85 (m, 3H), 7.44 (ddd, *J* = 7.6, 4.7, 1.0 Hz, 1H), 7.33 (d, *J* = 8.0 Hz, 2H), 2.41 (s, 3H).

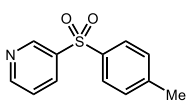

3-tosylpyridine (5.24)[ix]

Prepared following the general procedure outlined above using $Pd(PPh_3)_4$ (11.6 mg, 0.01 mmol, 0.05 equiv), BIPHEP (6.3 mg, 0.012 mmol, 0.06 equiv), 3-bromopyridine (32 mg, 0.2 mmol, 1.0 equiv), sodium *p*-toluenesulfinate (107 mg, 0.6 mmol, 3.0 equiv), Cs_2CO_3 (98 mg, 0.3 mmol, 1.5 equiv), and DMSO (0.8 ml). After 24 hours blue LED irradiation with fan cooling, the reaction mixture was subjected to the work up procedure outlined in the general procedure. The yield was determined to be 80% by ^{1}H NMR analysis.

^{1}H NMR (400 MHz, $CDCl_3$) δ 9.12 (d, *J* = 2.0 Hz, 1H), 8.77 (dd, *J* = 4.8, 1.5 Hz, 1H), 8.22 – 8.17 (m, 1H), 7.85 (d, *J* = 8.3 Hz, 2H), 7.43 (dd, *J* = 8.0, 4.9 Hz, 1H), 7.33 (d, *J* = 8.1 Hz, 2H), 2.42 (s, 3H).

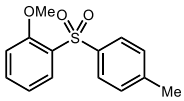

1-methoxy-2-tosylbenzene (5.25)

Prepared following the general procedure outlined above using $Pd(PPh_3)_4$ (11.6 mg, 0.01 mmol, 0.05 equiv), BIPHEP (6.3 mg, 0.012 mmol, 0.06 equiv), 2-iodoanisole (47 mg, 0.2 mmol, 1.0 equiv), sodium *p*-toluenesulfinate (107 mg, 0.6 mmol, 3.0 equiv), Cs_2CO_3 (98 mg, 0.3 mmol, 1.5 equiv), and DMSO (0.8 ml). After 24 hours blue LED irradiation with fan cooling, the reaction mixture was subjected to the work up procedure outlined in the general procedure. The yield was determined to be 23% by ^{1}H NMR analysis.

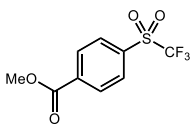

1-methoxy-4-((trifluoromethyl)sulfonyl)benzene (5.26)[x]

Prepared following the general procedure outlined above using $Pd(PPh_3)_4$ (11.6 mg, 0.01 mmol, 0.05 equiv), BIPHEP (6.3 mg, 0.012 mmol, 0.06 equiv), methyl 4-bromobenzoate (43 mg, 0.2 mmol, 1.0 equiv), sodium triflinate (47 mg, 0.3 mmol, 1.5 equiv), and DMSO (0.8 ml). After 24 hours blue LED irradiation with fan cooling, the reaction mixture was subjected to the work up procedure outlined in the general procedure. The yield was determined by ^{1}H NMR analysis.

^{1}H NMR (400 MHz, $CDCl_3$) δ 8.32 (d, *J* = 8.5 Hz, 2H), 8.13 (d, *J* = 8.4 Hz, 2H), 4.00 (s, 3H).

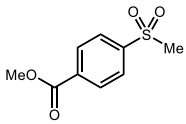

methyl 4-(methylsulfonyl)benzoate (5.27)

Prepared following the general procedure outlined above using $Pd(PPh_3)_4$ (11.6 mg, 0.01 mmol, 0.05 equiv), BIPHEP (6.3 mg, 0.012 mmol, 0.06 equiv), methyl 4-bromobenzoate (43 mg, 0.2 mmol, 1.0 equiv), sodium methanesulfinate (31 mg, 0.3 mmol, 1.5 equiv), and DMSO (0.8 ml). After 24 hours blue LED irradiation with fan cooling, the reaction mixture was subjected to the work up procedure outlined in the general procedure. The yield was determined to be 42% by ^{1}H NMR analysis.

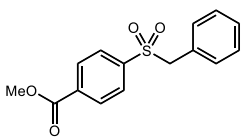

methyl 4-(benzylsulfonyl)benzoate (5.28)

Prepared following the general procedure outlined above using $Pd(PPh_3)_4$ (11.6 mg, 0.01 mmol, 0.05 equiv), BIPHEP (6.3 mg, 0.012 mmol, 0.06 equiv), 2-iodoanisole (47 mg, 0.2 mmol, 1.0 equiv), sodium benzylsulfinate (54 mg, 0.3 mmol, 1.5 equiv), Cs_2CO_3 (98 mg, 0.3 mmol, 1.5 equiv), and DMSO (0.8 ml). After 24 hours blue LED irradiation with fan cooling, the reaction mixture was subjected to the work up procedure outlined in the general procedure. The yield was determined to be 18% by ^{1}H NMR analysis.

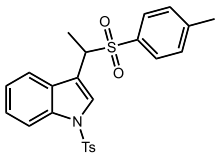

1-tosyl-3-(1-tosylethyl)-1*H*-indole (5.36)

Prepared following the general procedure outlined above using $Pd(PPh_3)_4$ (11.6 mg, 0.01 mmol, 0.05 equiv), BIPHEP (6.3 mg, 0.012 mmol, 0.06 equiv), *N*-(but-2-yn-1-yl)-*N*-(2-iodophenyl)-4-methylbenzenesulfonamide (85 mg, 0.2 mmol, 1.0 equiv), sodium *p*-toluenesulfinate (54 mg, 0.3 mmol, 1.5 equiv), K_2CO_3 (41 mg, 0.3 mmol, 1.5 equiv), and DMSO (0.8 ml). After 24 hours blue LED irradiation with fan cooling, the reaction mixture was subjected to the work up procedure outlined in the general procedure. The yield was determined to be 23% by ^{1}H NMR analysis.

^{1}H NMR (400 MHz, $CDCl_3$) δ 7.92 (d, *J* = 8.3 Hz, 1H), 7.75 (d, *J* = 8.3 Hz, 2H), 7.37 – 7.27 (m, 5H), 7.13 (t, *J* = 7.7 Hz, 1H), 7.01 (d, *J* = 8.0 Hz, 2H), 2.38 (s, 3H), 2.34 (s, 3H).

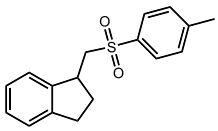

1-(tosylmethyl)-2,3-dihydro-1*H*-indene (5.37)

Prepared following the general procedure outlined above using $Pd(PPh_3)_4$ (11.6 mg, 0.01 mmol, 0.05 equiv), BIPHEP (6.3 mg, 0.012 mmol, 0.06 equiv), 1-(but-3-en-1-yl)-2-iodobenzene (52 mg, 0.2 mmol, 1.0 equiv), sodium *p*-toluenesulfinate (54 mg, 0.3 mmol, 1.5 equiv), K_2CO_3 (41 mg, 0.3 mmol, 1.5 equiv), and DMSO (0.8 ml). After 24 hours blue LED irradiation with fan cooling, the reaction mixture was subjected to the work up procedure outlined in the general procedure. The yield was determined to be 27% by ^{1}H NMR analysis.

^{1}H NMR (400 MHz, $CDCl_3$) δ 7.88 (d, *J* = 8.3 Hz, 2H), 7.40 (d, *J* = 8.1 Hz, 2H), 7.19 (m, *J* = 21.3, 16.5, 6.7 Hz, 5H), 3.71 – 3.61 (m, 1H), 3.57 (dd, *J* = 14.1, 3.1 Hz, 1H), 3.20 (dd, *J* = 14.0, 10.3 Hz, 1H), 3.02 – 2.82 (m, 2H), 2.53 – 2.40 (m, 4H), 1.96 (dt, *J* = 21.1, 8.1 Hz, 1H).

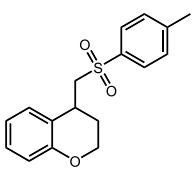

1-(but-3-en-1-yloxy)-2-iodobenzene (5.38)

Prepared following the general procedure outlined above using $Pd(PPh_3)_4$ (11.6 mg, 0.01 mmol, 0.05 equiv), BIPHEP (6.3 mg, 0.012 mmol, 0.06 equiv), 1-(but-3-en-1-yl)-2-iodobenzene (55 mg, 0.2 mmol, 1.0 equiv), sodium *p*-toluenesulfinate (54 mg, 0.3 mmol, 1.5 equiv), K_2CO_3 (41 mg, 0.3 mmol, 1.5 equiv), and DMSO (0.8 ml). After 24 hours blue LED irradiation with fan cooling, the reaction mixture was subjected to the work up procedure outlined in the general procedure. The yield was determined to be 15% by ^{1}H NMR analysis.

5.6.5. Additional Observations during Alkene Addition Studies

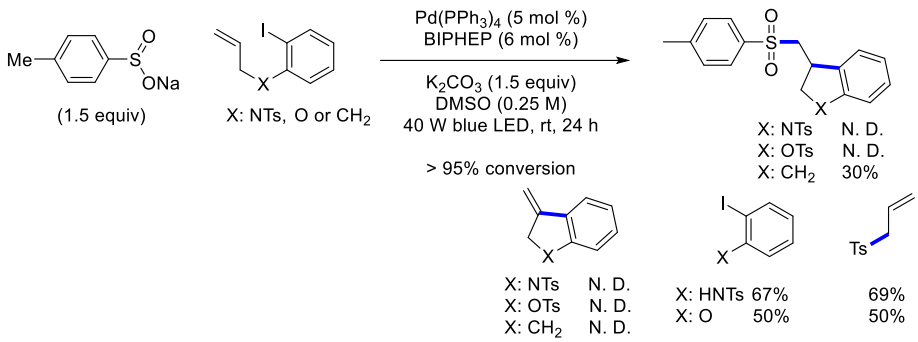

During the intramolecular cyclization studies, olefins containing allylic heteroatoms resulted in the formation of Tsuji-Trost type sulfonylation products. Notably, in the presence of the allyl group, which can potentially coordinate to the palladium, made the conversion of this reaction almost quantitative. The resulting crude mixture contained various byproducts which could not be identified at the current stage.

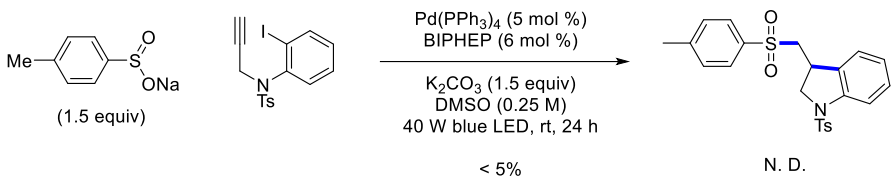

Terminal alkyne also quenched the palladium-catalyzed radical formation giving almost no conversion of the starting aryl iodide,

5.6.6. Radical Trapping Experiment

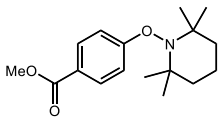

methyl 4-((2,2,6,6-tetramethylpiperidin-1-yl)oxy)benzoate (5.30)

Prepared following the general procedure outlined above using $Pd(PPh_3)_4$ (11.6 mg, 0.01 mmol, 0.05 equiv), BIPHEP (6.3 mg, 0.012 mmol, 0.06 equiv), methyl 4-bromobenzoate (43 mg, 0.2 mmol, 1.0 equiv), sodium *p*-toluenesulfinate (or Cs_2CO_3) (*x* mmol, *x* equiv), and DMSO (0.8 ml). After 24 hours blue LED irradiation with fan cooling, the reaction mixture was subjected to the work up procedure outlined in the general procedure. The yield was determined by ^{1}H NMR analysis.

^{1}H NMR (400 MHz, $CDCl_3$) δ 7.92 (d, *J* = 9.1 Hz, 2H), 7.35 – 7.16 (m, 2H), 3.86 (s, 3H), 1.69 – 1.53 (m, 4H), 1.29 – 1.21 (m, 8H), 0.99 (s, 6H).

5.6.7. Redox-Active Ester Experiements

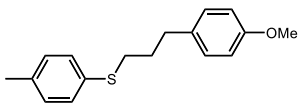

(3-(4-methoxyphenyl)propyl)(p-tolyl)sulfane (5.32)

Prepared following the general procedure outlined above using $Ru(bpy)_3(PF_6)_2$ (1.7 mg, 0.002 mmol, 0.01 equiv.), BIPHEP (6.3 mg, 0.012 mmol, 0.06 equiv), 1,3-dioxoisoindolin-2-yl 4-(4-methoxyphenyl)butanoate (68 mg, 0.2 mmol, 1.0 equiv), sodium *p*-toluenesulfinate (54 mg, 0.3 mmol, 1.5 equiv), and DMSO (0.8 ml). After 24 hours blue LED irradiation with fan cooling, the re68action mixture was subjected to the work up procedure outlined in the general procedure. The yield was determined to be 21% by ^{1}H NMR analysis.

^{1}H NMR (400 MHz, $CDCl_3$) δ 7.23 (d, *J* = 8.1 Hz, 2H), 7.08 (d, *J* = 8.6 Hz, 4H), 6.82 (d, *J* = 8.7 Hz, 2H), 3.79 (s, 3H), 2.87 (t, *J* = 7.3 Hz, 2H), 2.68 (t, *J* = 7.5 Hz, 2H), 2.32 (s, 3H), 1.96 – 1.84 (m, 2H).

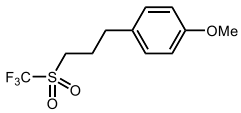

1-methoxy-4-(3-((trifluoromethyl)sulfonyl)propyl)benzene (5.33)

Prepared following the general procedure outlined above using $Ru(bpy)_3(PF_6)_2$ (1.7 mg, 0.002 mmol, 0.01 equiv.), $Pd(PPh_3)_4$ (11.6 mg, 0.01 mmol, 0.05 equiv), BIPHEP (6.3 mg, 0.012 mmol, 0.06 equiv), 1,3-dioxoisoindolin-2-yl 4-(4-methoxyphenyl)butanoate (68 mg, 0.2 mmol, 1.0 equiv), sodium triflinate (47 mg, 0.3 mmol, 1.5 equiv), and DMSO (0.8 ml). After 24 hours blue LED irradiation with fan cooling, the reaction mixture was subjected to the work up procedure outlined in the general procedure. The yield was determined to be 10% by ^{1}H NMR analysis.

^{1}H NMR (400 MHz, $CDCl_3$) δ 7.09 (d, *J* = 8.7 Hz, 2H), 6.84 (d, *J* = 8.4 Hz, 2H), 3.80 (s, 3H), 2.83 – 2.74 (m, 2H), 2.66 – 2.58 (m, 2H), 2.02 – 1.91 (m, 2H); ^{19}F NMR (376 MHz, $CDCl_3$) δ -62.38 (s, 3H).

5.6.8. Intermolecular Radical Addition Experiments

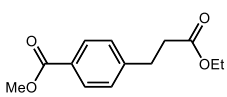

methyl 4-(3-ethoxy-3-oxopropyl)benzoate (5.40)

Prepared following the general procedure outlined above using $Pd(PPh_3)_4$ (11.6 mg, 0.01 mmol, 0.05 equiv), BIPHEP (6.3 mg, 0.012 mmol, 0.06 equiv), 1,3-dioxoisoindolin-2-yl 4-(4-methoxyphenyl)butanoate (68 mg, 0.2 mmol, 1.0 equiv), K_2CO_3 (41 mg, 0.3 mmol, 1.5 equiv), Hantzsch ester (61 mg, 0.24 mmol, 1.2 equiv.), ethyl acrylate (33 μl, 0.3 mmol, 1.5 equiv.) and DMSO (0.8 ml). After 24 hours blue LED irradiation with fan cooling, the reaction mixture was subjected to the work up procedure outlined in the general procedure. The yield was determined to be 43% by ^{1}H NMR analysis.

5.6.9. References Cited

[i] Pangborn, A. B.; Giardello, M. A.; Grubbs, R. H.; Rosen, R. K.; Timmers, F. J. *Organometallics* **1996**, *15*, 1518.

[ii] Zheng, H.-X.; Shan, X.-H.; Qu, J.-P.; Kang, Y.-B. *Org. Lett.* **2017,** *19*, 5114.

[iii] Zhang, H.; Huang, X. *Adv. Synth. Cat.* **2016,** *358*, 3736.

[iv] Kim, H.; Lee, C. *Angew. Chem. Int. Ed.* **2012,** *51*, 12303.

[v] Bressy, C.; Alberico, D.; Lautens, M. *J. Am. Chem. S.* **2005,** *127*, 13148.

[vi] Rixson, J. E.; Chaloner, T.; Heath, C. H.; Tietze, L. F.; Stewart, S. G. *Eur. J. Org. Chem.* **2012,** *2012*, 544.

[vii] He, S.; Hsung, R. P.; Presser, W. R.; Ma, Z.-X.; Haugen, B. J. *Org. Lett.* **2014,** *16*, 2180.

[viii] Yue, H.; Zhu, C.; Rueping, M. *Angew. Chem. Int. Ed.* **2018,** *57*, 1371.

[ix] Maloney, K. M.; Kuethe, J. T.; Linn, K. *Org. Lett.* **2011,** *13*, 102.

[x] Smyth, L. A.; Phillips, E. M.; Chan, V. S.; Napolitano, J. G.; Henry, R.; Shekhar, S. *J. Org. Chem.* **2016,** *81*, 1285.

국문초록

이리듐과 루테늄 폴리피리딜 복합체들은 유기화학반응에서 광자에너지를 사용할 수 있게 해주는 훌륭한 도구로 사용되어 왔다(**Chapter 1**). 빛을 받아 ^{3}MLCT 형태로 들뜬 이 복합체는 열적 활성방법으로 형성하기 어려운 전자구조의 중간체 형성을 용이하게 한다. 더 나아가 강한 산화제와 환원제로 동시에 작용할 수 있는 이 ^{3}MLCT 복합체로 인해 하나의 반응시스템에서 분자의 단전자 환원과 산화를 동시에 수행할 수 있다. 또한 이 들뜬 고리형 금속화합물의 덱스터 에너지전이(Dexter Energy Transfer) 기작은 대다수 유기분자들의 흡광 및 항간교차의 낮은 효율을 극복하고 새로운 삼중항 상태의 들뜬 분자 형성에 유용하게 사용될 수 있는 수단이다.

광촉매의 단전자 전달 기작을 이용, 우리는 방향족 탄소–수소 결합을 질소로 치환하는 방법론을 개발하였고 이를 통해 효율적으로 아닐린 유도체들을 합성할 수 있었다(**Chapter 2**). 우리는 전자가 부족한 질소 중심 라디칼을 광촉매를 사용한 질소–염소 결합의 활성화를 통해 형성하였고, 이 중간체를 이용해 활성화되지 않은 방향족화합물에 질소 치환기를 도입할 수 있었다.

전이금속 촉매를 사용한 방향족 할라이드와 아민의 짝지음 반응은 여러 분야에 유용하게 사용되는 방향족 아민의 합성에 주로 사용되는 방법이다(**Chapter 3**). 이에 대한 수년간의 연구는 정교한 금속촉매의 개발로 이어졌고, 이 촉매들은 효율적인 방향족 친전자체들의 아민화반응을 가능케 하였다. 최근 가시광선을 사용한 광촉매는 새로운 전자적 구조를 가지는 금속 중간체를 이전의 짝지음 촉매 순환에 도입, 이를 통해 새로운 개념의 아민화 반응의 가능성을 보였다. 이 전략의 중요점은 4주기 전이금속의 부족한

반응성을 전자적 구조 변환을 통해 극복할 수 있다는 것이다. 우리는 이를 활용해 니켈의 느린 환원적 탈리 기작을 전자적으로 들뜬 니켈 중간체를 형성해 해결하여서 방향족 친전자체에 설폰아미드기를 도입하는 방법론을 개발하였다(**Chapter 4**). 특히, 리간드의 존재에 따라 상호보완적인 반응성을 보이는 두개의 반응조건을 수립할 수 있었다. 이를 바탕으로 넓은 범위의 방향족 화합물로부터 2차 설폰아미드 화합물을 합성할 수 있음을 보였다. 초기 기작연구에서 삼중항 상태로 들뜬 니켈 중간체가 탄소–질소 결합의 환원적 탈리 과정을 촉진한다는 것을 확인할 수 있었다. 추가적으로 사용된 광촉매의 바이피리딘 리간드의 촉매 이탈을 관측하였고, 이를 통해 별도로 첨가된 리간드가 분해된 광촉매의 회복에 관여한다는 리간드의 새로운 역할 또한 제안하였다.

최근 설핀삼염의 합성을 위한 SO_2 대체화합물을 개발하고 이를 활용해 설폰과 설폰아미드 화합물을 합성하는 것이 각광을 받고 있다. 하지만 설핀산염으로부터 방향족 설폰 화합물을 합성하는 방법은 여전히 고전적 팔라듐 촉매 반응을 통해 수행되어 왔다. 방향족 설폰은 의약, 농약 그리고 재료 분야에서 널리 사용되는 중요한 구조이기 때문에 우리는 이 설폰 화합물의 합성을 위해 기존의 팔라듐 촉매 반응보다 더 효율적인 대안을 고안하였다. 우리는 이전의 팔라듐을 이용한 설폰 합성의 높은 반응온도 조건의 원인을 설핀삼염의 작용에 의한 산화적 첨가 기작의 저해일 것이라고 생각하였다. 따라서 가시광선을 이용해 팔라듐의 산화적 첨가 기작을 변환하여 아릴 라디칼 중간체를 형성하고 이를 통해 빠르게 유기금속 팔라듐 중간체를 형성한다면 보다 더 효율적인 설폰 합성법을 개발할 수 있을 것이라고 생각하였다. 이 제안을 바탕으로 우리는 가시광선에 의해 활성화되는 팔라듐 촉매 설폰 합성방법을 개발하였다(**Chapter 5**). 초기 기작연구를 통해 탄소

라디칼 중간체가 반응에 관여한다는 것을 확인할 수 있었다. 이 라디칼 중간체의 형성이 단전자의 전달이 아닌 단전자 산화적 첨가를 통한 탄소 라디칼의 형성이라는 새로운 반응 기작도 제안하였다.

주제어: 광촉매, 탄소–수소 결합 치환, 아닐린, 설폰아미드, 짝지음 반응, 니켈, 팔라듐, 설폰

학번: 2013-20261

Acknowledgments

저라는 한 사람이 박사학위를 받기 위해 정말 많은 분들의 도움을 받았습니다. 이 기회를 빌어 그동안 저를 도와주셨던 많은 분들에게 감사함을 전하려고 합니다.

먼저 지난 6년간 저를 지지해준 가족들에게 감사함을 전합니다. 특히, 어머니의 사랑과 격려는 저의 박사과정동안 훌륭한 버팀목이 되었습니다. 어머니는 저의 인생에서 항상 훌륭한 스승이셨으며 더 나아가 가장 든든한 조력자셨습니다. 아버지 또한 제가 선택한 이 길을 나아가는데 항상 든든한 지지를 보내주셨습니다.

저를 학부생때부터 지난 8년동안 지도해주신 이철범 지도교수님께 감사드립니다. 뛰어나다고 할 수 없었던 학부생을 기꺼이 거두어 주시고 지도해 주신 덕분에 제가 이런 과분한 박사라는 학위를 받을 수 있었습니다. 박사과정중 말씀해 주신 학문이라는 것은 외우는 것이 아닌 이해하는 것이다라는 조언은 평생 잊지 못할 훌륭한 조언으로 남을것입니다.

박사학위 심사위원이신 김병문 교수님, 조은진 교수님 그리고 이홍근 교수님께 감사의 마음을 전하고 싶습니다. 긴 시간동안 공부를 하였음에도 불구하고 부족했던 저를 위해 하나라도 더 가르침을 주시려고 훌륭한 지도를 해주셨습니다. 선배님들의 오랜 경험에서 나온 훌륭한 조언들을 항상 잊지 않겠습니다. 그동안 받아온 다른 많은 조언들 또한 제 인생에 큰 도움이 될 것임을 믿어 의심치 않습니다. 저에게 심사위원님들은 훌륭한 스승들이었습니다.

그동안 함께 일해왔던 동료들 모두에게 진심으로 고마운 마음을 전합니다. 특히, 연구를 시작할 수 있도록 지도해준 사수들인 김선우 박사, 노승주 박사 그리고 김혜진 박사에게 감사함을 표합니다. 고집이 강한 저를

포기하지 않고 가르치기 위해 기울인 이들의 노력은 저의 연구들에 훌륭한 밑거름이 되었습니다.

I sincerely appreciate Prof. David Y. Chen for his great advice during my Ph.D. life. He was willing to help me whenever I was in trouble as well. I could not have survived this Ph.D. course without his help. He is also one of the most brilliant chemists I have ever met. He shall be an unforgettable teacher in my life.

I appreciate Prof. David W. C. MacMillan for his helpful advice about the sulfonamidation collaboration as well as my life. We spent some time together while he was visiting SNU. During this time, he influenced me a lot in a good way when I was feeling desperate about academia. He made me determine to stay more in academia and was a true teacher in my life.

Thank you to all of the collaborators from Princeton University. Stefan McCarver was a great coworker, and it was a great pleasure to write a paper with him. We also spent a great time with his colleagues in Jeju and Seoul. Also, Thanks to Emily Corcoran for working with me and helping me at the beginning of the collaboration with the MacMillan group. I would not have made it without her assistance.

Thanks to my dear friend Felix de Courcy-Ireland from Imperial College London. We had a wonderful time together when he was staying at SNU as an exchange student. He was a great english teacher as well as a talented researcher. It was a fantastic opportunity for me to work with him during the summer vacation.

이외에도 서울대학교 화학부에서 저와 같이 박사과정을 밟은 많은 친구들의 도움 감사드립니다.

Appendix A

Chapter 4. NMR Spectra

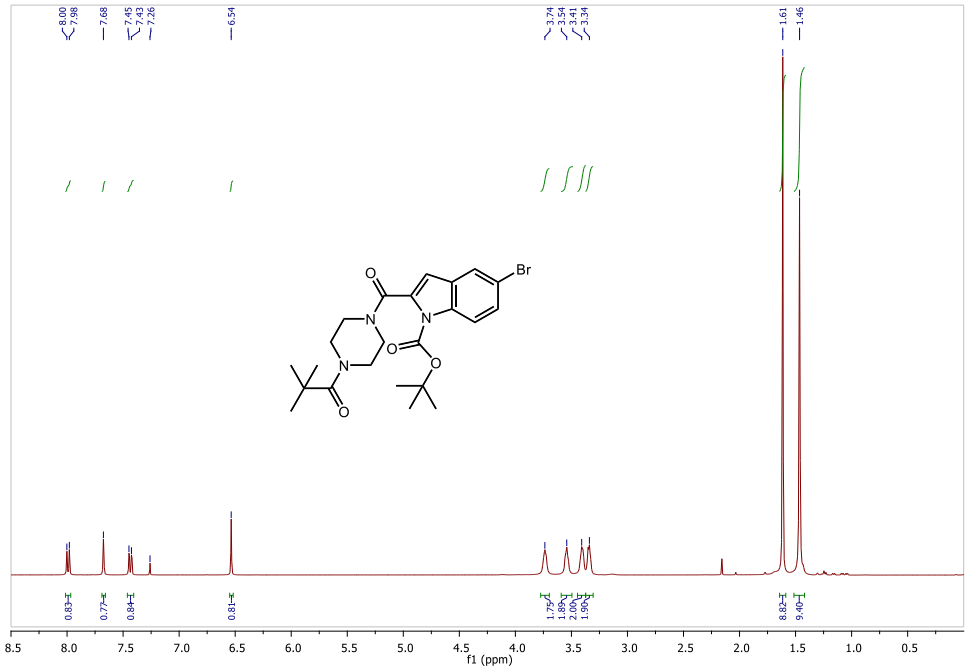
8.00
7.98
7.68
7.45
7.43
7.26
6.54
3.74
3.54
3.41
3.34
1.61
1.46
Br
0.83
0.77
0.84
0.81
1.75
1.89
2.06
1.90
8.82
9.40
f1 (ppm)

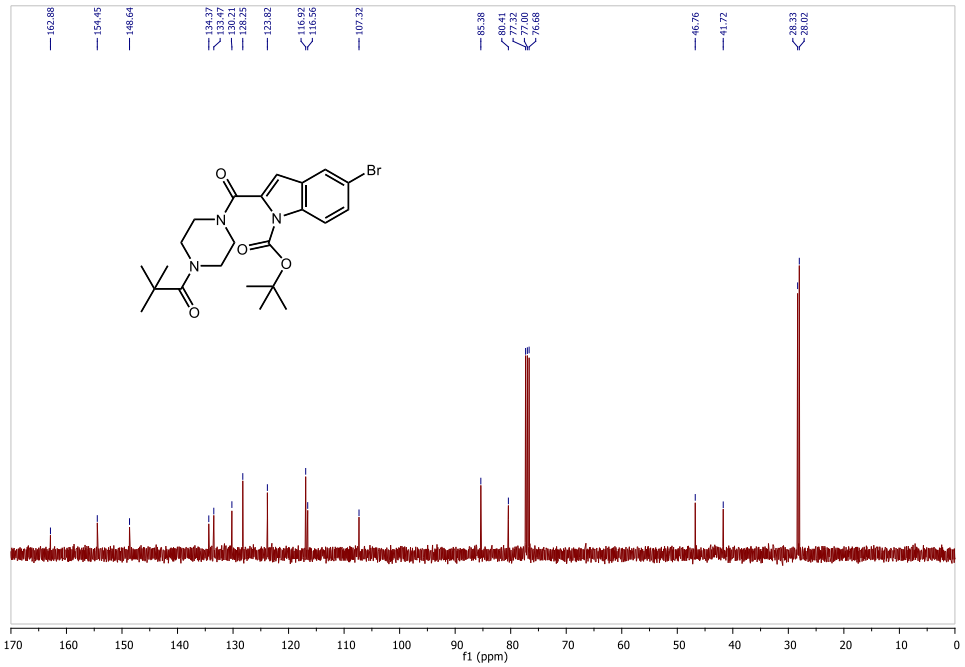
162.88
154.45
148.64
134.37
133.47
130.21
128.25
123.82
116.92
116.56
107.32
85.38
80.41
77.32
77.00
76.68
46.76
41.72
28.33
28.02
Br
f1 (ppm)

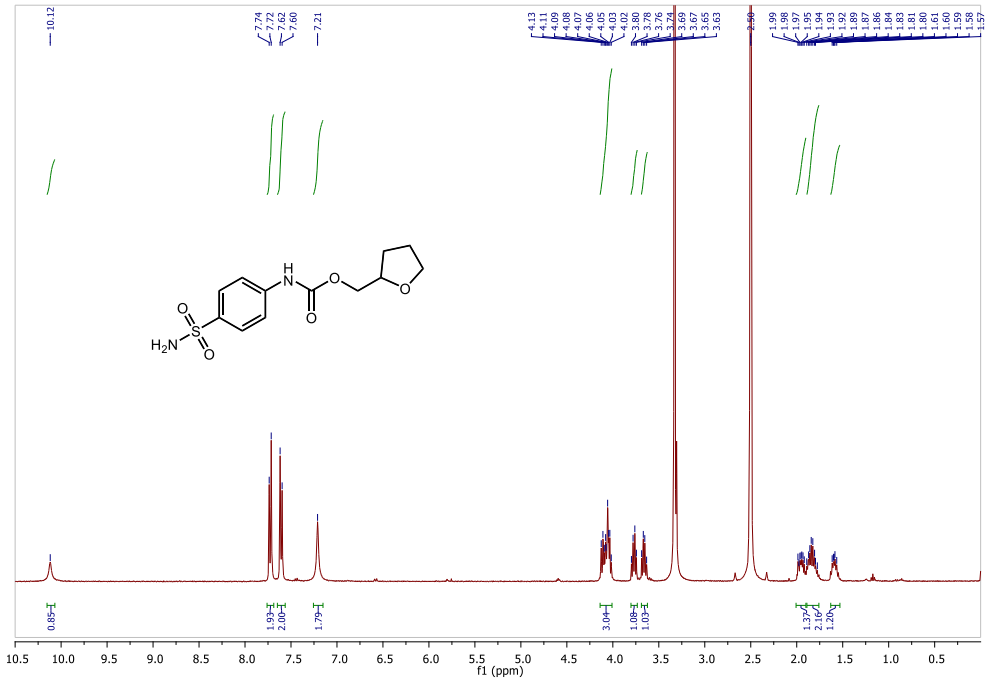
10.12
7.74
7.72
7.62
7.60
7.21
4.13
4.11
4.09
4.08
4.07
4.06
4.05
4.03
4.02
3.80
3.78
3.76
3.74
3.69
3.67
3.65
3.63
2.66
1.99
1.98
1.97
1.95
1.94
1.93
1.92
1.89
1.87
1.86
1.84
1.83
1.81
1.80
1.61
1.60
1.59
1.58
1.57
0.89
1.92
2.00
1.79
3.04
1.08
1.05
1.37
2.16
1.20
10.5
10.0
9.5
9.0
8.5
8.0
7.5
7.0
6.5
6.0
5.5
5.0
4.5
4.0
3.5
3.0
2.5
2.0
1.5
1.0
0.5
f1 (ppm)

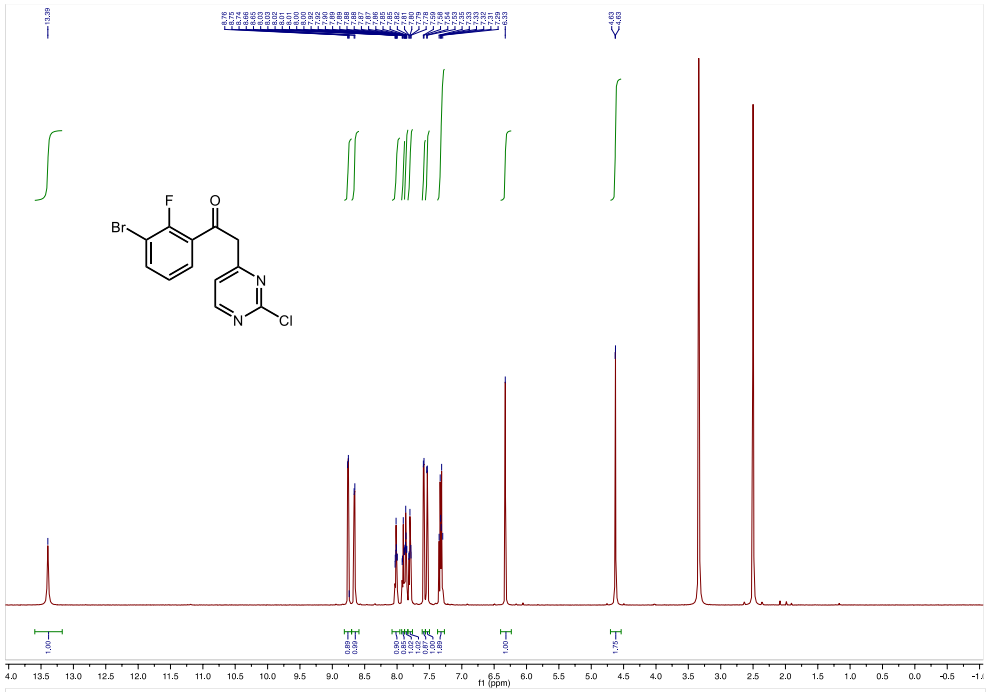
F
O
Br
N
N
Cl
f1 (ppm)

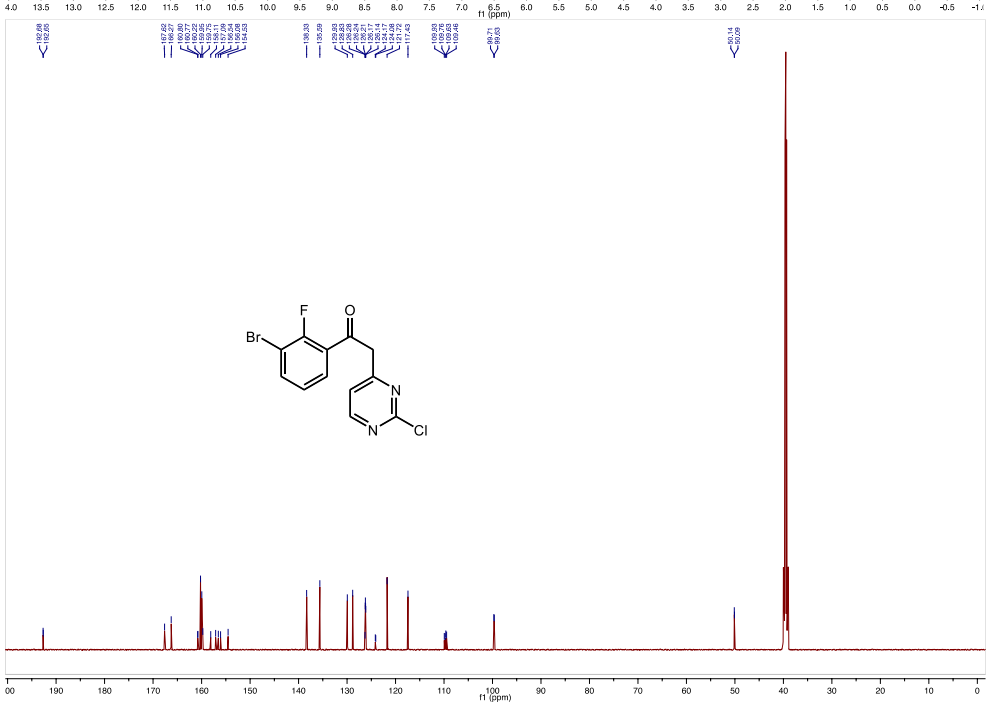
F
O
Br
N
N
Cl
f1 (ppm)

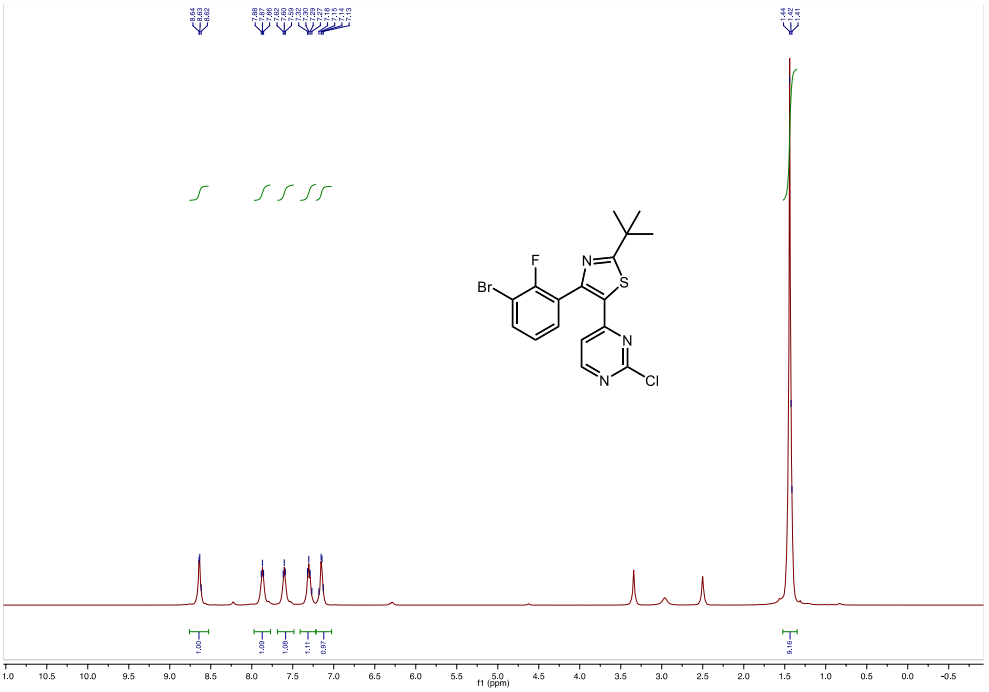
8.84
8.83
8.82
7.88
7.86
7.85
7.60
7.59
7.30
7.29
7.27
7.16
7.15
7.14
7.13
1.44
1.42
1.41
F
N
S
Br
N
N
Cl
1.00
1.09
1.08
1.11
0.97
9.16
f1 (ppm)

,

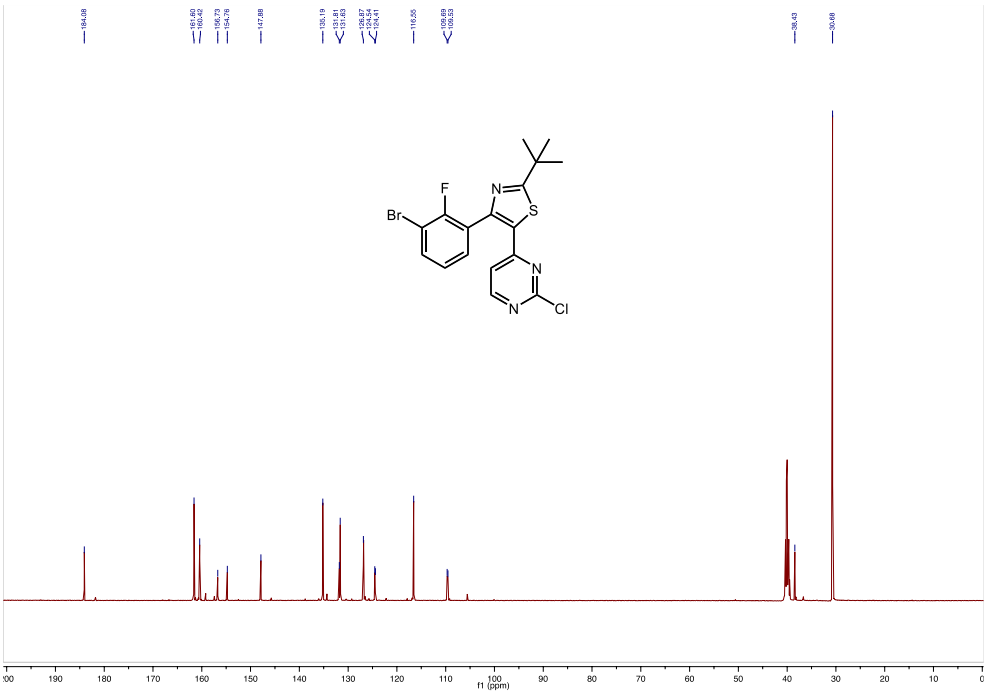
164.08
161.60
160.42
156.73
154.76
147.88
136.19
133.81
131.83
126.87
124.54
124.41
119.55
105.69
105.53
38.43
30.68
F
N
S
Br
N
N
Cl
f1 (ppm)

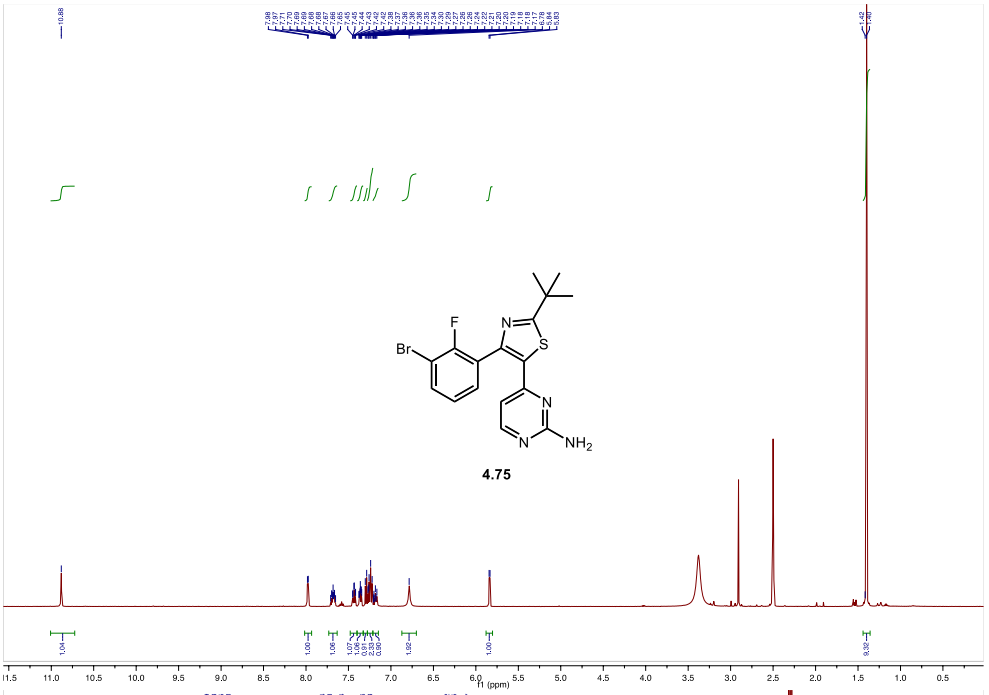
F
N
S
Br
N
N
NH2
4.75
f1 (ppm)

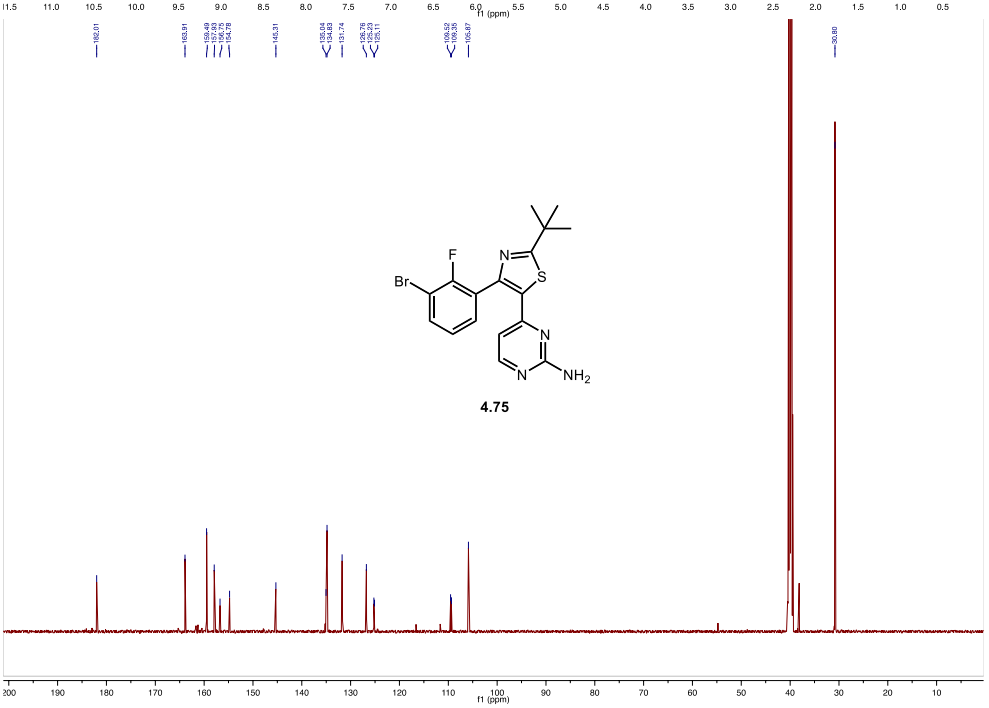
F
N
S
Br
N
N
NH2
4.75
f1 (ppm)

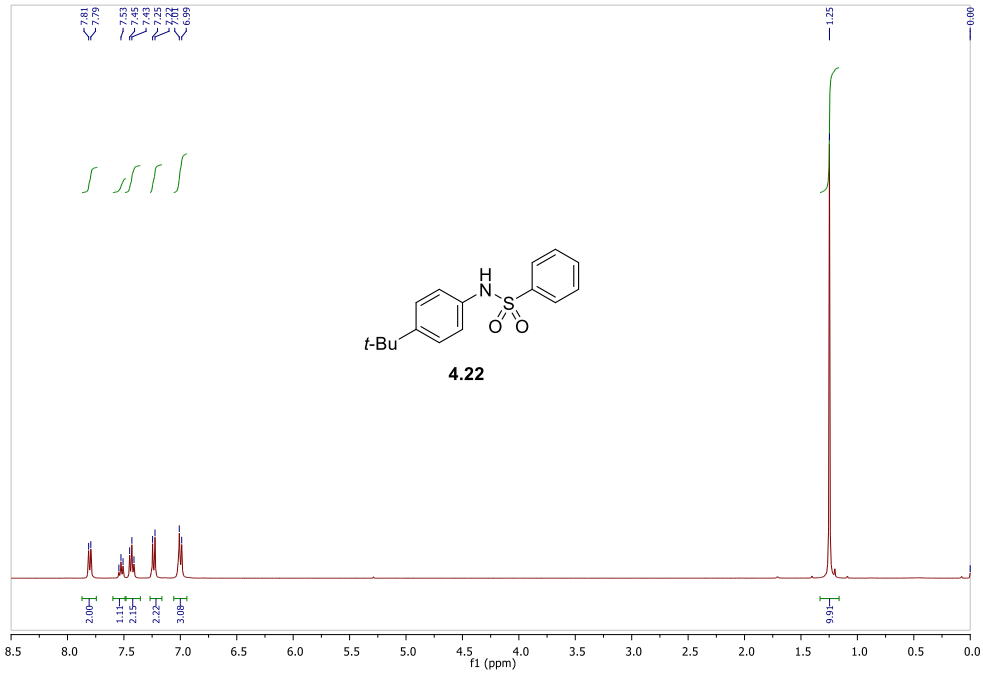
7.81
7.79
7.53
7.45
7.43
7.25
7.07
6.99
1.25
0.00
H
N
S
O
O
t-Bu
4.22
2.00
1.11
2.15
2.22
3.08
9.91
f1 (ppm)

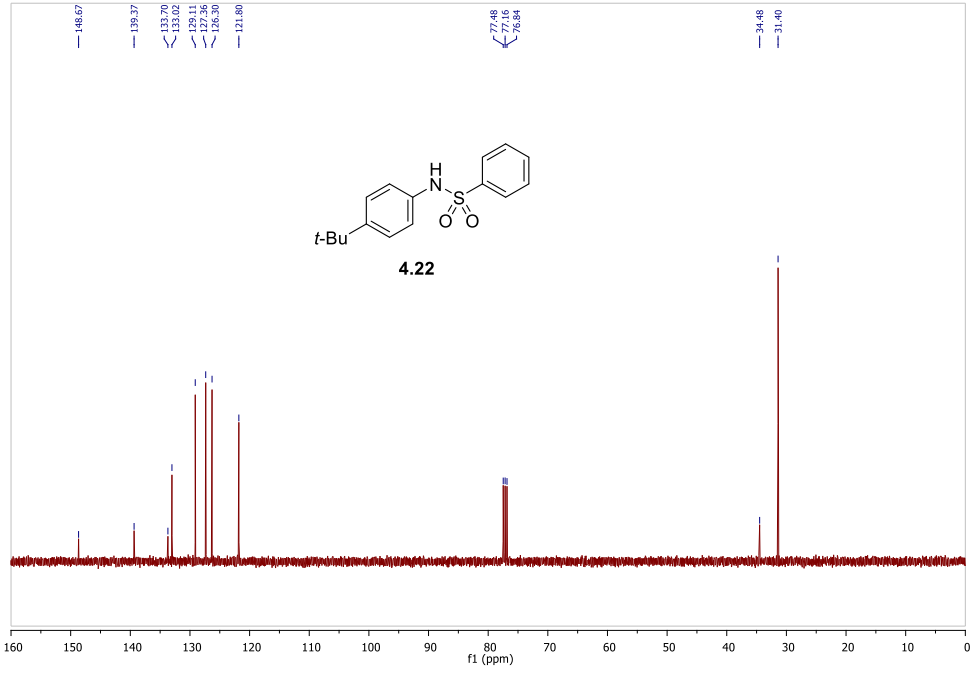
148.67
139.37
133.70
133.02
129.11
127.36
126.30
121.80
77.48
77.16
76.84
34.48
31.40
H
N
S
O
O
t-Bu
4.22
f1 (ppm)

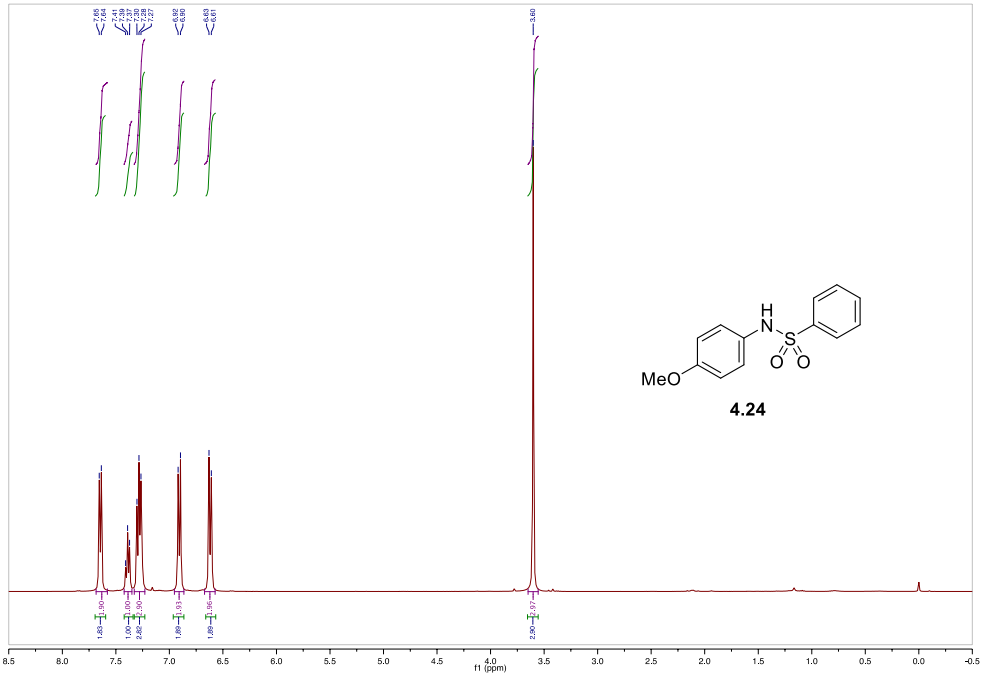
7.65
7.64
7.41
7.39
7.37
7.29
7.28
7.27
6.92
6.90
6.63
6.61
3.60
MeO
4.24
f1 (ppm)

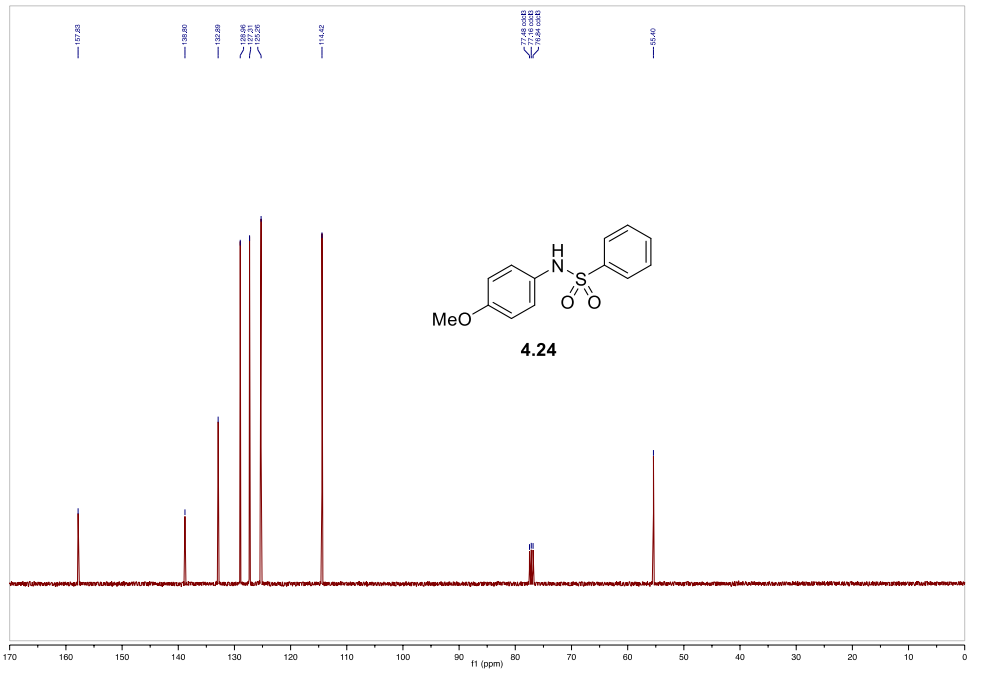
157.83
139.80
132.89
129.96
121.31
120.26
114.42
77.48
77.16
76.84
55.40
MeO
4.24
f1 (ppm)

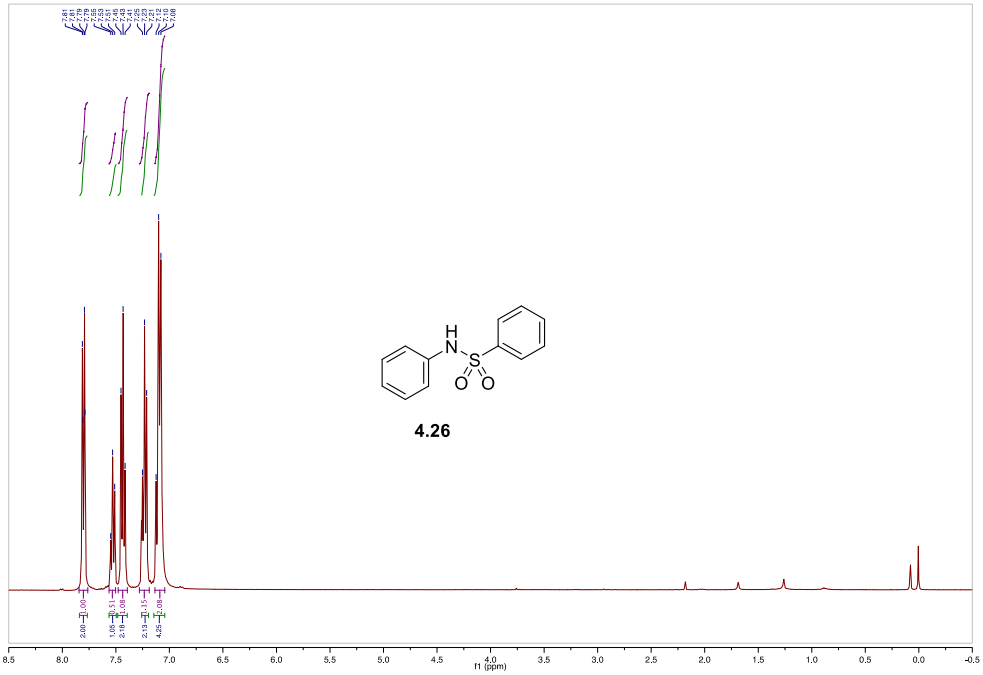
4.26
f1 (ppm)

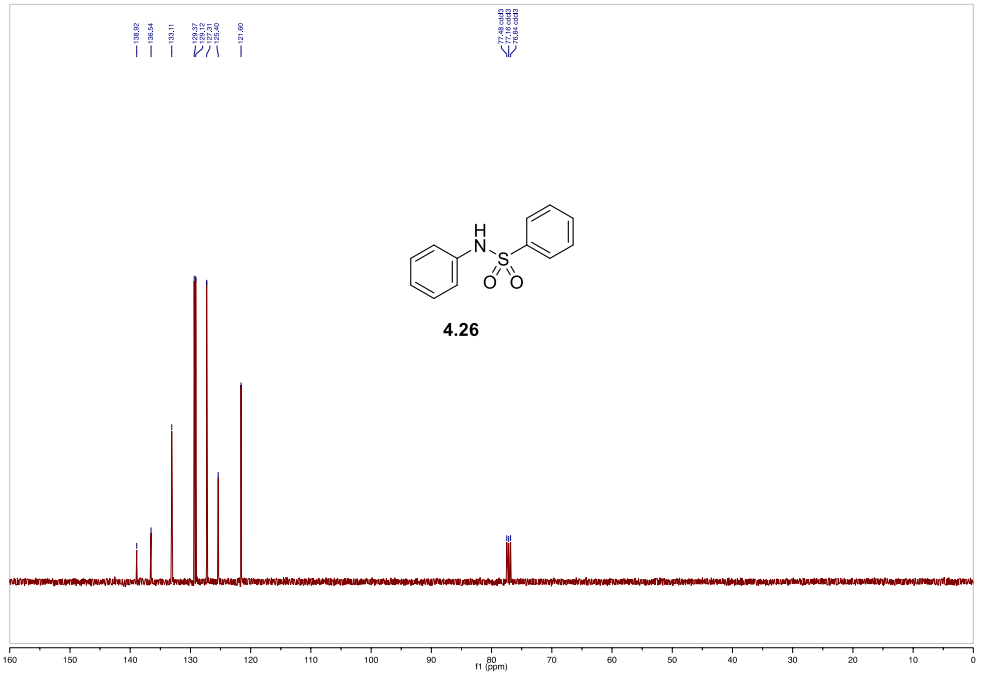
4.26
f1 (ppm)

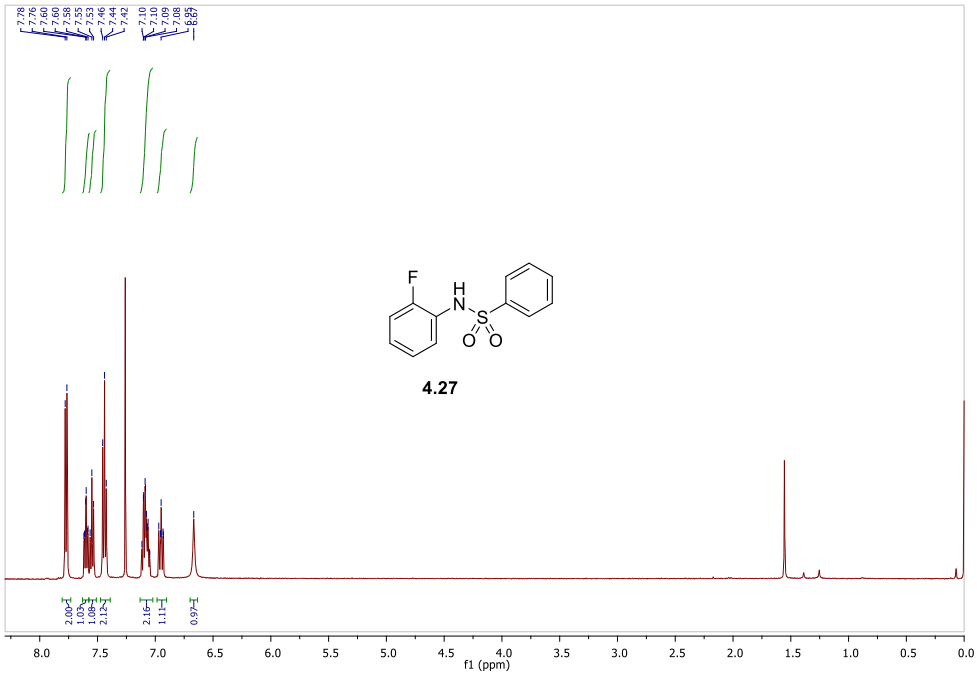
7.78
7.76
7.60
7.60
7.58
7.55
7.53
7.46
7.44
7.42
7.10
7.10
7.09
7.08
6.87
6.85
F
H
N
S
O
O
4.27
2.00
1.03
1.08
2.12
2.16
1.11
0.97
8.0
7.5
7.0
6.5
6.0
5.5
5.0
4.5
4.0
3.5
3.0
2.5
2.0
1.5
1.0
0.5
0.0
f1 (ppm)

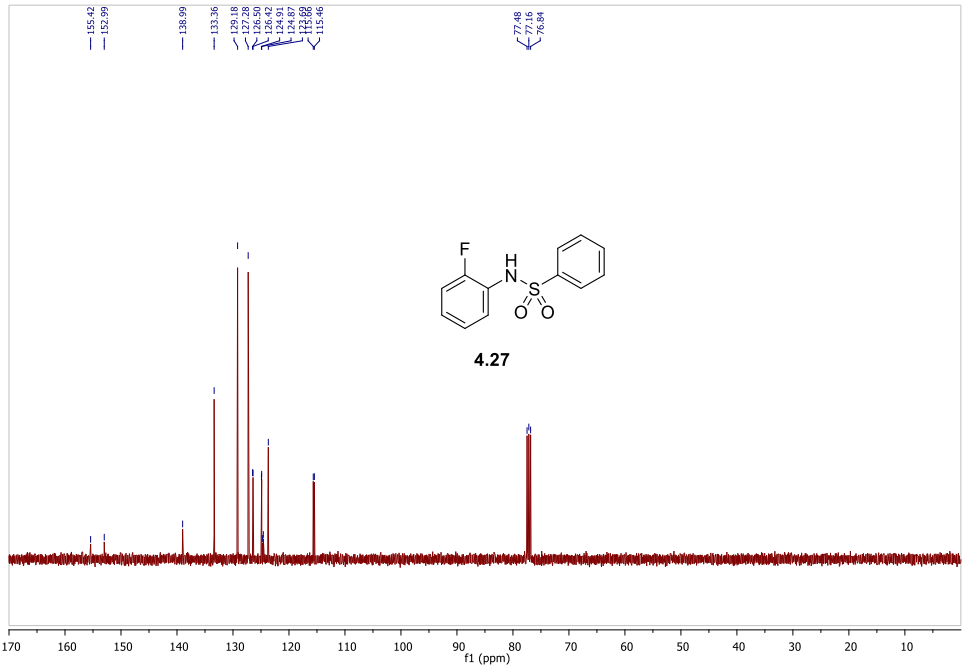
155.42
152.99
138.99
133.36
129.18
127.28
126.50
126.42
124.91
124.87
115.68
115.46
77.48
77.16
76.84
F
H
N
S
O
O
4.27
170
160
150
140
130
120
110
100
90
80
70
60
50
40
30
20
10
f1 (ppm)

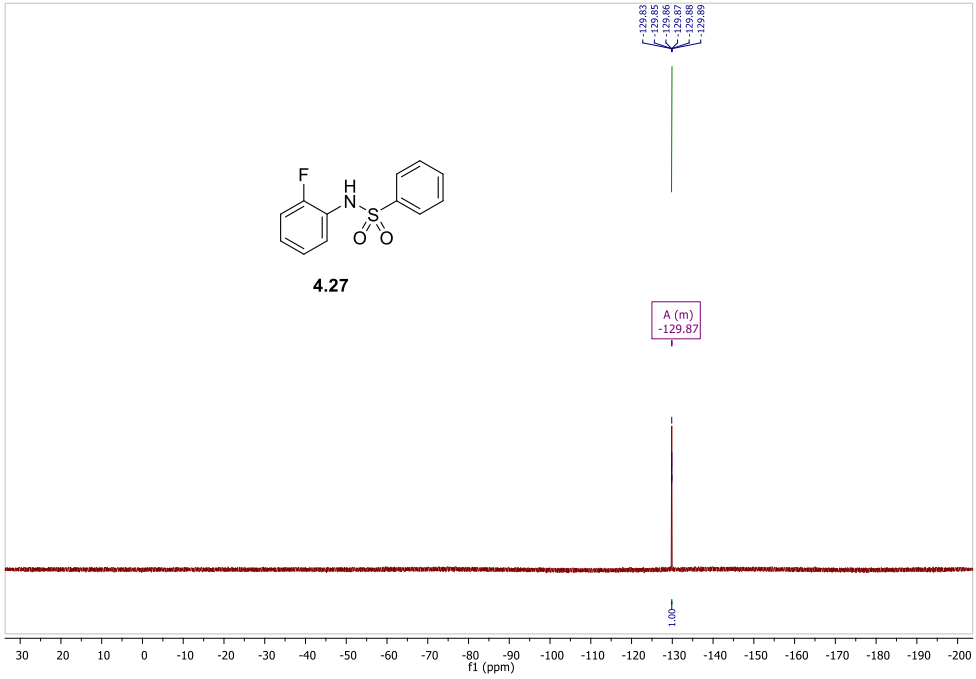
-129.83
-129.85
-129.86
-129.87
-129.88
-129.89
F
H
N
S
O
O
4.27
A (m)
-129.87
1.00
30 20 10 0 -10 -20 -30 -40 -50 -60 -70 -80 -90 -100 -110 -120 -130 -140 -150 -160 -170 -180 -190 -200
f1 (ppm)

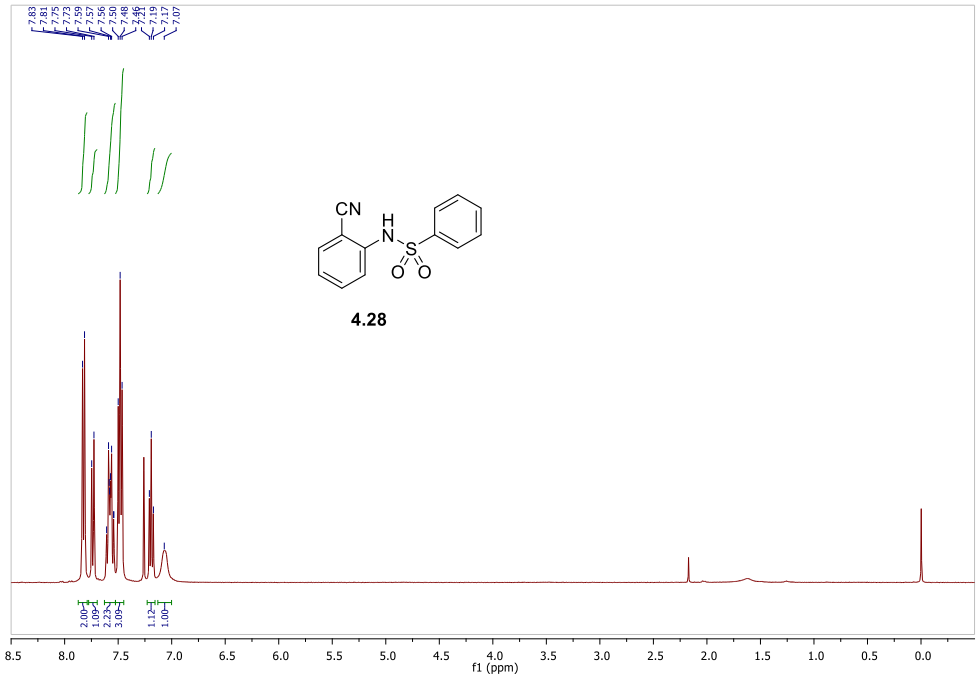
7.83
7.81
7.75
7.73
7.59
7.57
7.56
7.50
7.48
7.46
7.21
7.19
7.17
7.07
CN
H
N
S
O
O
4.28
2.00
1.04
2.23
3.05
1.12
1.00
8.5
8.0
7.5
7.0
6.5
6.0
5.5
5.0
4.5
4.0
3.5
3.0
2.5
2.0
1.5
1.0
0.5
0.0
f1 (ppm)

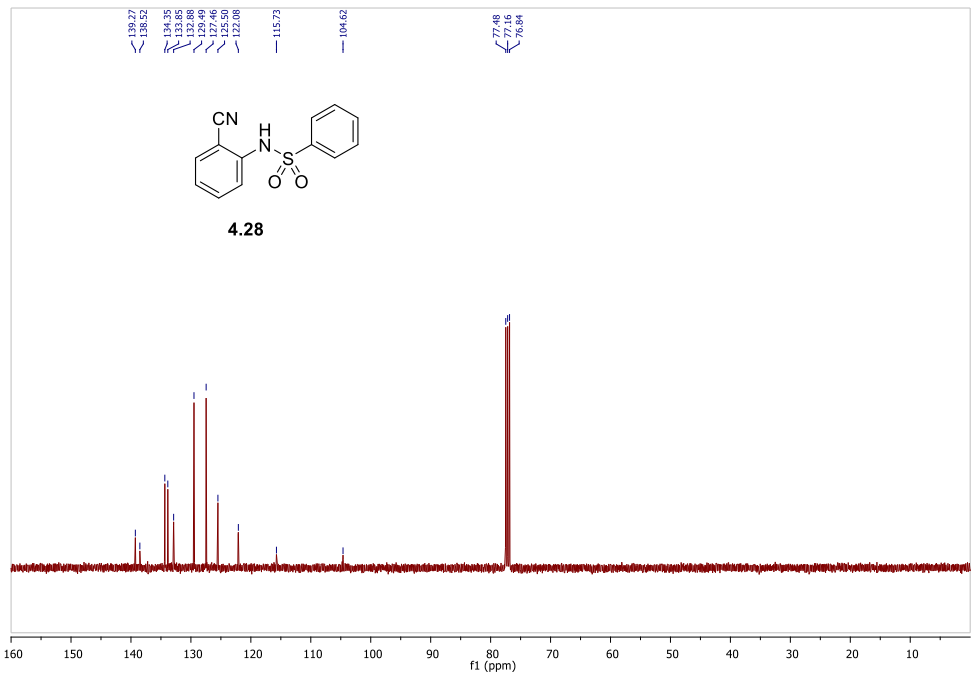
139.27
138.52
134.35
133.85
132.88
129.49
127.46
125.50
122.08
115.73
104.62
77.48
77.16
76.84
CN
H
N
S
O
O
4.28
160
150
140
130
120
110
100
90
80
70
60
50
40
30
20
10
f1 (ppm)

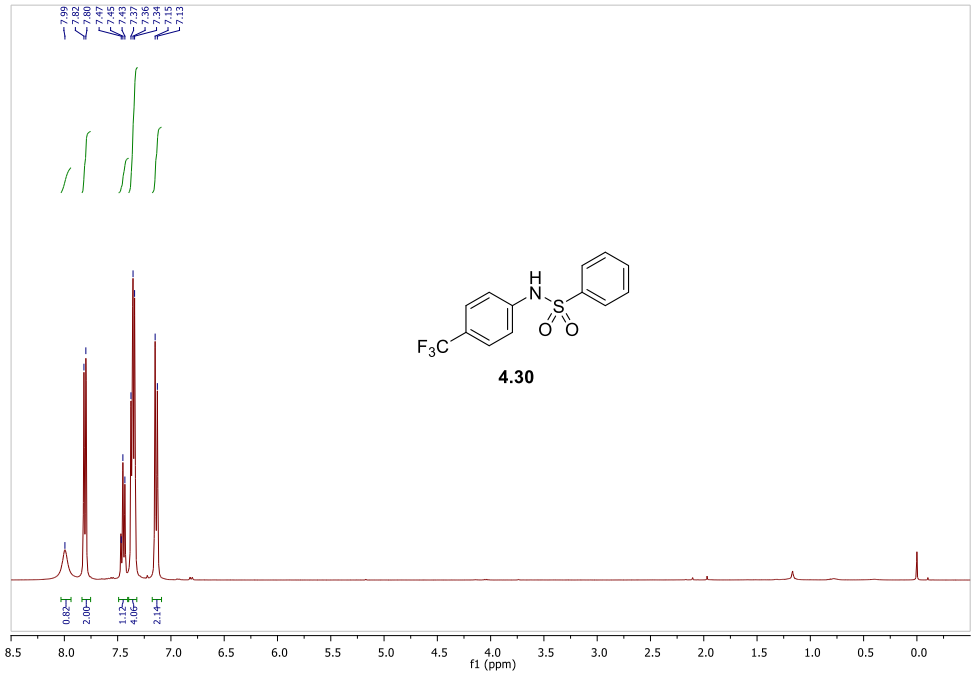
7.99
7.82
7.80
7.47
7.45
7.43
7.37
7.36
7.34
7.15
7.13
0.82
2.00
1.12
4.06
2.14
8.5
8.0
7.5
7.0
6.5
6.0
5.5
5.0
4.5
4.0
3.5
3.0
2.5
2.0
1.5
1.0
0.5
0.0
f1 (ppm)
H
N
S
O
O
F3C
4.30

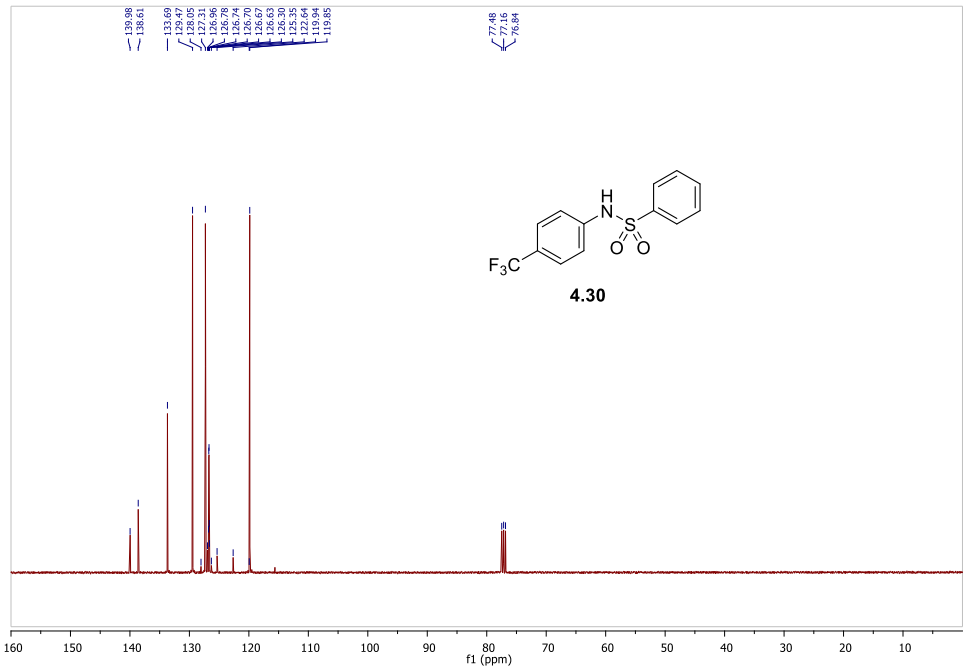
139.98
136.61
133.69
129.47
128.05
127.31
126.96
126.78
126.74
126.70
126.67
126.63
126.30
124.35
122.64
119.94
119.85
77.48
77.16
76.84
160
150
140
130
120
110
100
90
80
70
60
50
40
30
20
10
f1 (ppm)
H
N
S
O
O
F3C
4.30

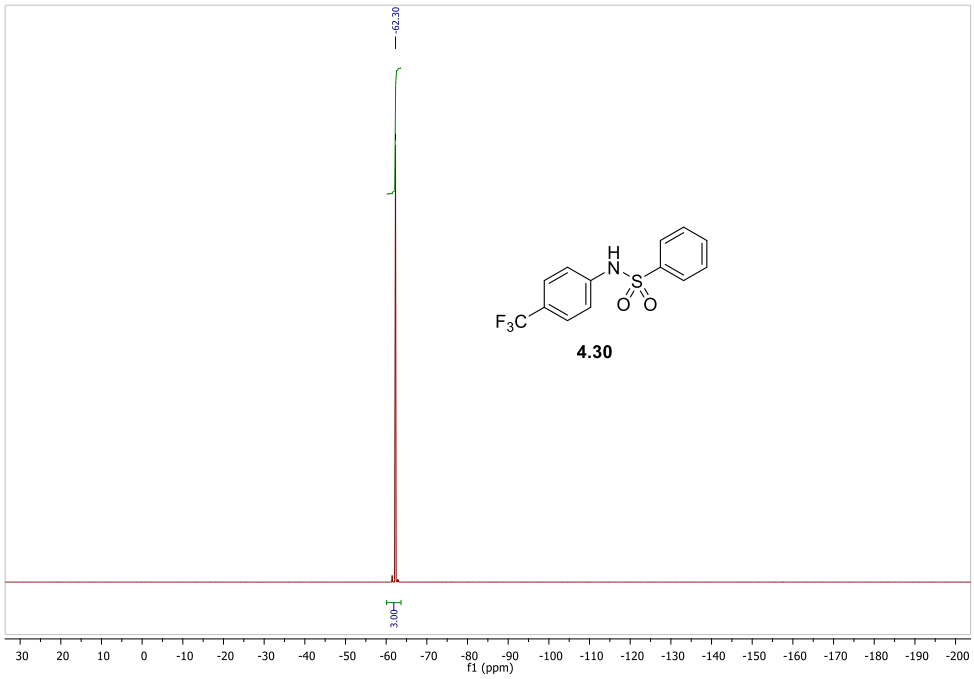
-62.30
3.00
30 20 10 0 -10 -20 -30 -40 -50 -60 -70 -80 -90 -100 -110 -120 -130 -140 -150 -160 -170 -180 -190 -200
f1 (ppm)

4.30

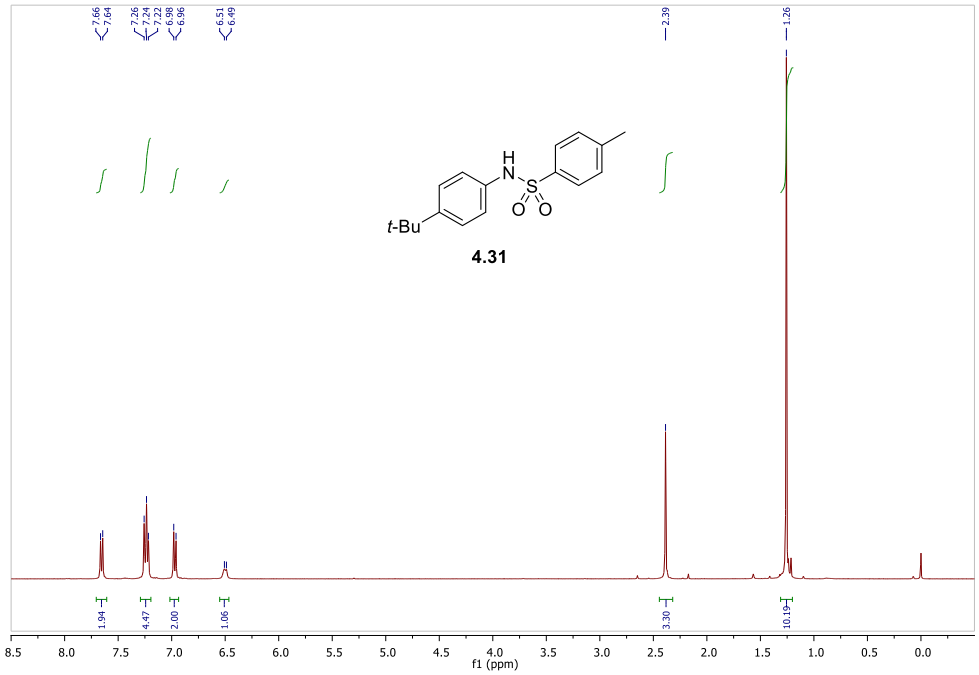
7.66
7.64
7.26
7.24
7.22
6.98
6.96
6.51
6.49
2.39
1.26
H
N
S
O
O
t-Bu
4.31
1.94
4.47
2.00
1.06
3.30
10.19
8.5
8.0
7.5
7.0
6.5
6.0
5.5
5.0
4.5
4.0
3.5
3.0
2.5
2.0
1.5
1.0
0.5
0.0
f1 (ppm)

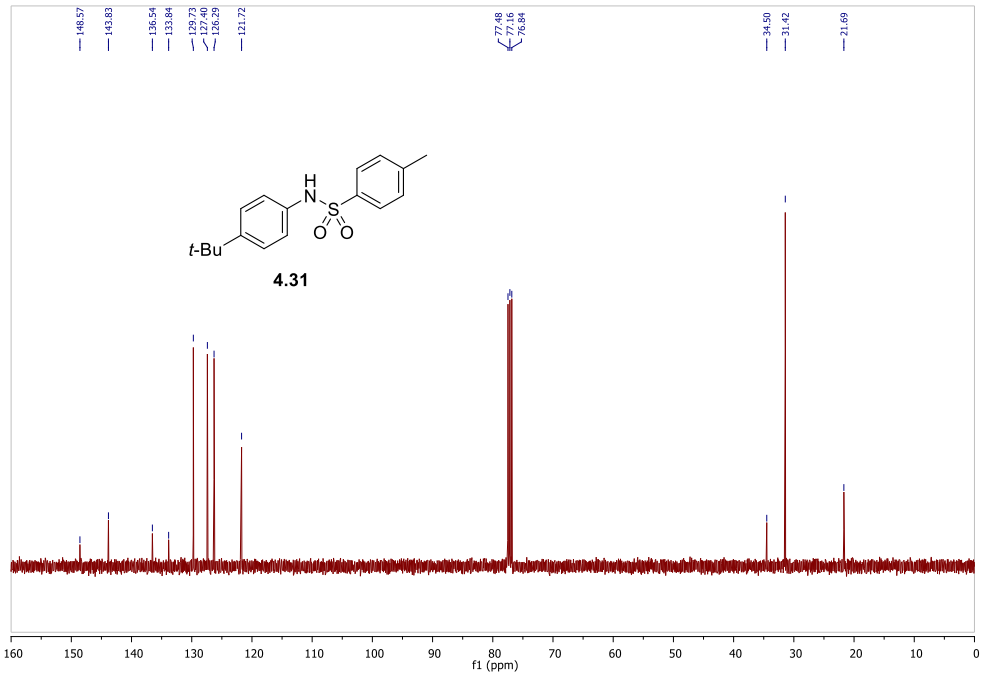
148.57
143.83
136.54
133.84
129.73
127.40
126.29
121.72
77.48
77.16
76.84
34.50
31.42
21.69
H
N
S
O
O
t-Bu
4.31
160
150
140
130
120
110
100
90
80
70
60
50
40
30
20
10
0
f1 (ppm)

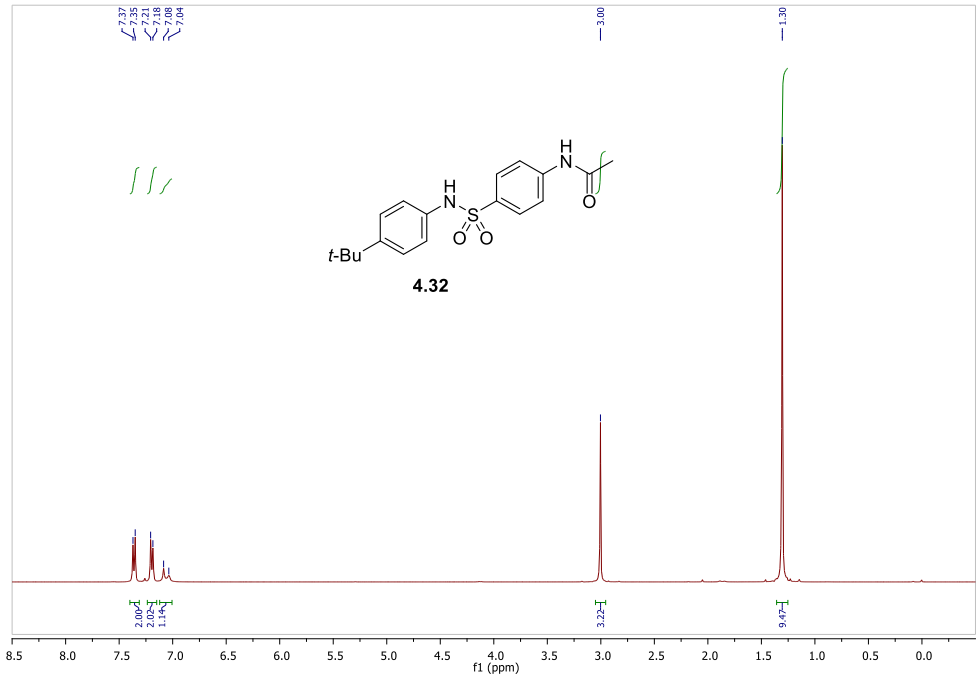
7.37
7.35
7.21
7.18
7.08
7.04
3.00
1.30
H
N
S
O
O
H
N
O
t-Bu
4.32
2.00
2.02
1.14
3.22
9.47
8.5
8.0
7.5
7.0
6.5
6.0
5.5
5.0
4.5
4.0
3.5
3.0
2.5
2.0
1.5
1.0
0.5
0.0
f1 (ppm)

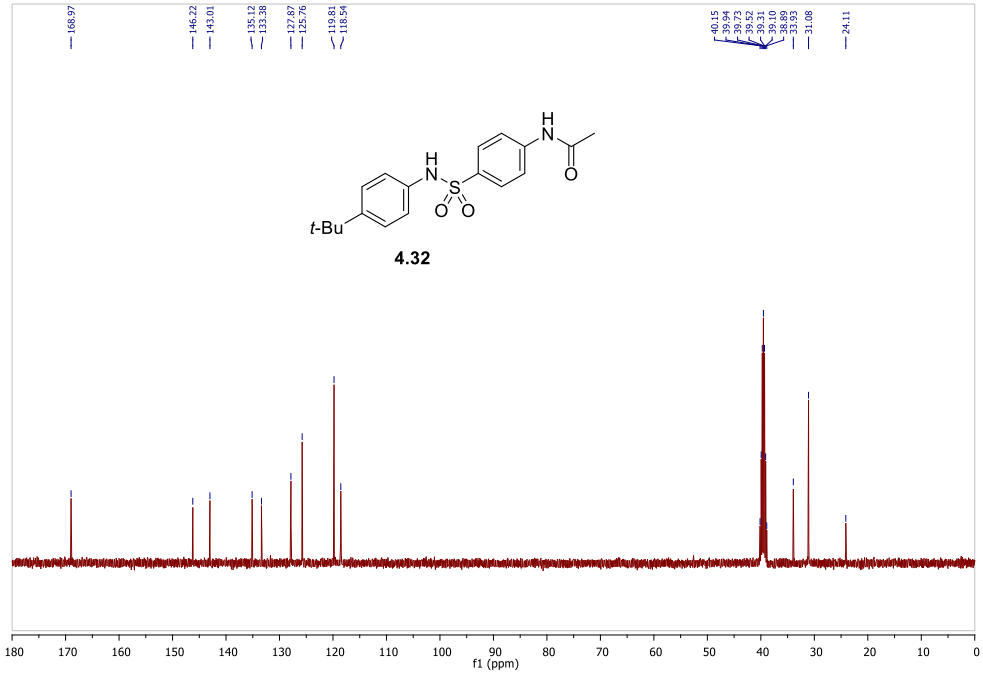
168.97
146.22
143.01
135.12
133.38
127.87
125.76
119.81
118.54
40.15
39.94
39.73
39.52
39.31
39.10
38.89
33.93
31.08
24.11
H
N
S
O
O
H
N
O
t-Bu
4.32
180
170
160
150
140
130
120
110
100
90
80
70
60
50
40
30
20
10
0
f1 (ppm)

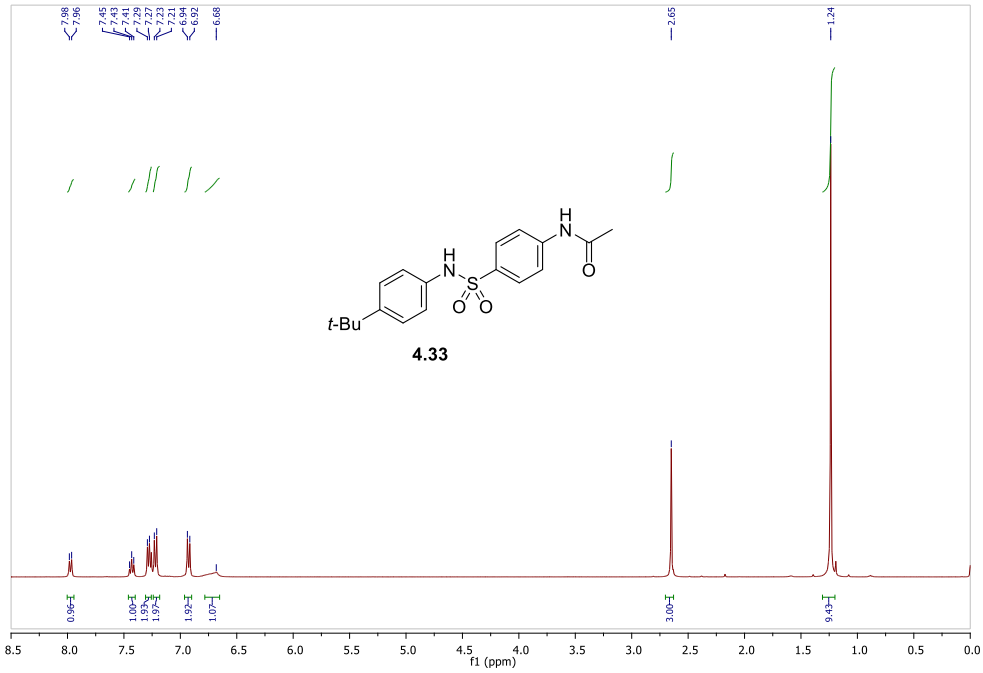
7.98
7.96
7.45
7.43
7.41
7.29
7.27
7.23
7.21
6.94
6.92
6.68
2.65
1.24
t-Bu
4.33
0.96
1.00
1.93
1.97
1.92
1.07
3.00
9.43
f1 (ppm)

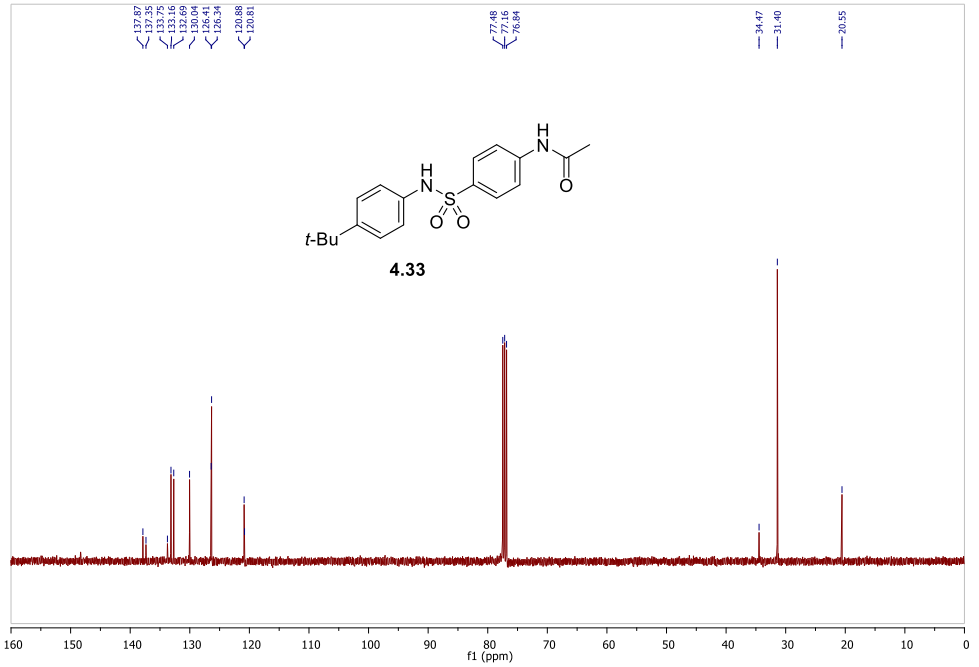
137.87
137.35
133.75
133.16
132.69
130.04
126.41
126.34
120.88
120.81
77.48
77.16
76.84
34.47
31.40
20.55
t-Bu
4.33
f1 (ppm)

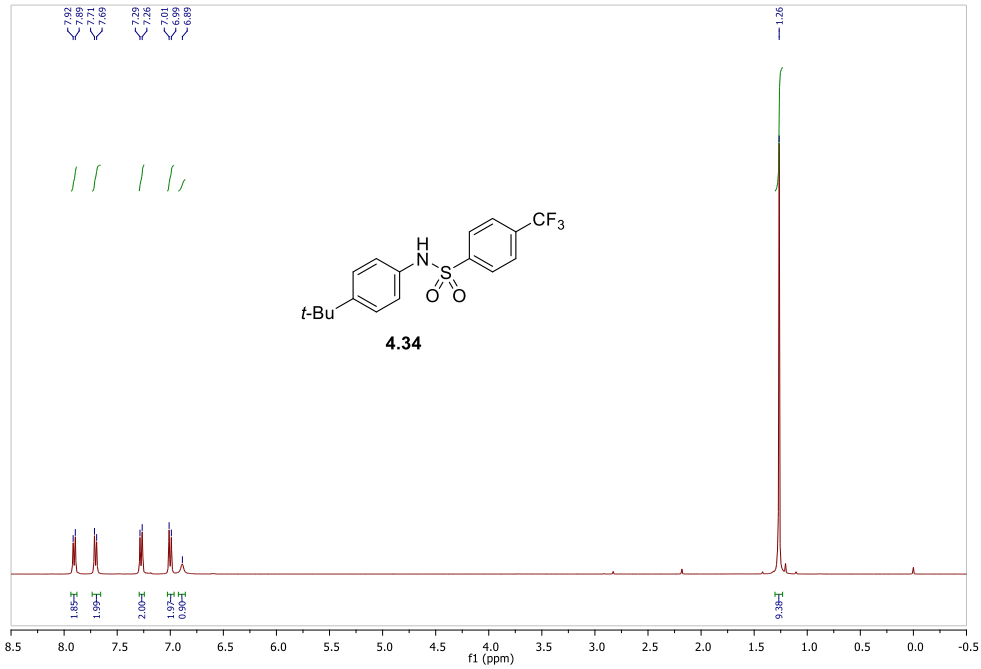
7.92
7.89
7.71
7.69
7.29
7.26
7.01
6.99
6.89
1.26
CF3
H
N
S
O
O
t-Bu
4.34
1.85
1.99
2.00
1.97
0.90
9.38
f1 (ppm)

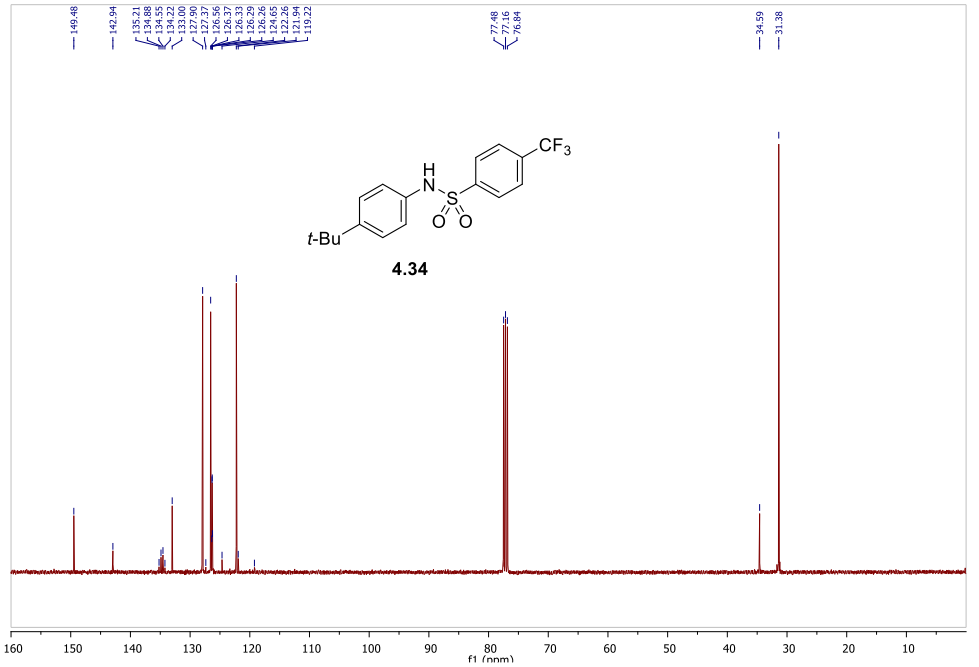
149.48
142.94
135.21
134.88
134.55
134.22
133.00
127.90
127.37
126.56
126.37
126.33
126.29
126.26
124.65
122.26
121.94
119.22
77.48
77.16
76.84
34.59
31.38
CF3
H
N
S
O
O
t-Bu
4.34
f1 (ppm)

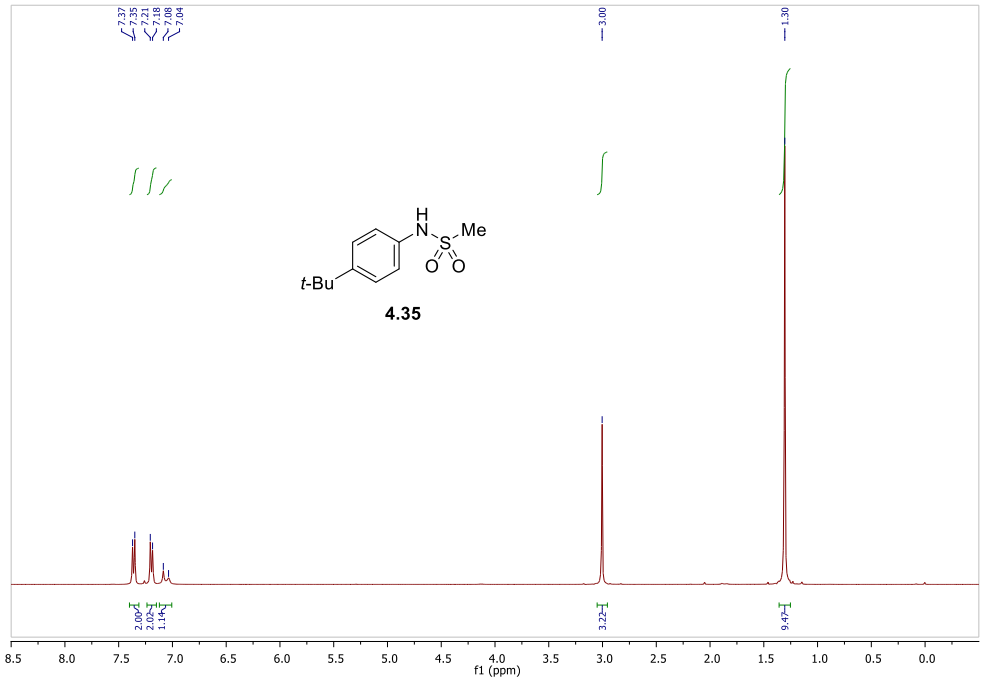
7.37
7.35
7.21
7.18
7.08
7.04
3.00
1.30
H
N
S
Me
O
O
t-Bu
4.35
2.00
2.03
1.14
3.22
9.47
f1 (ppm)

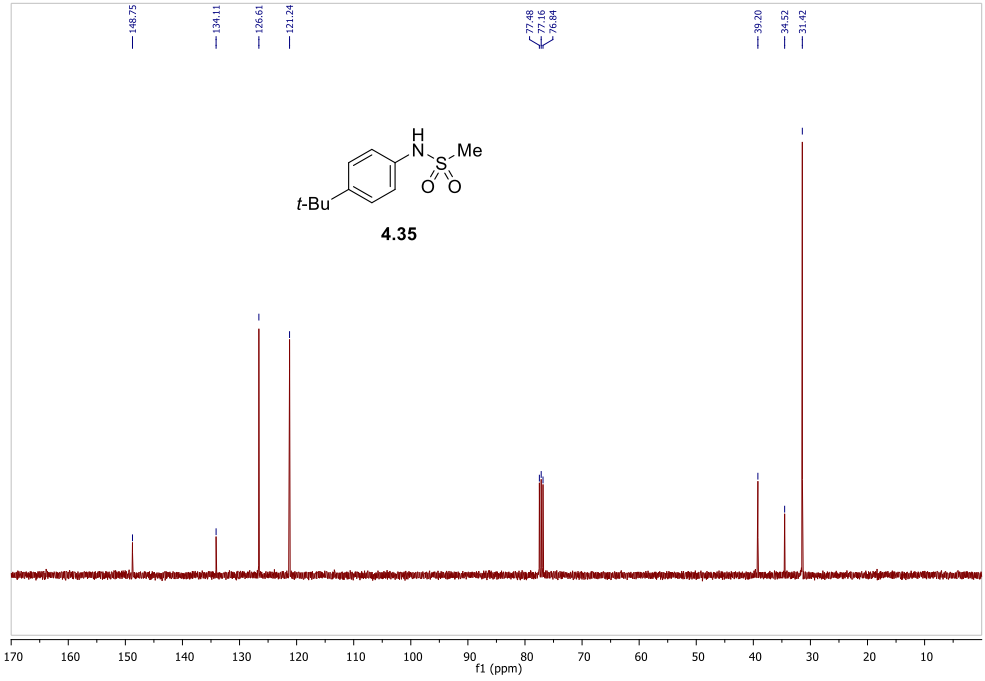
148.75
134.11
126.61
121.24
77.48
77.16
76.84
39.20
34.52
31.42
H
N
S
Me
O
O
t-Bu
4.35
f1 (ppm)

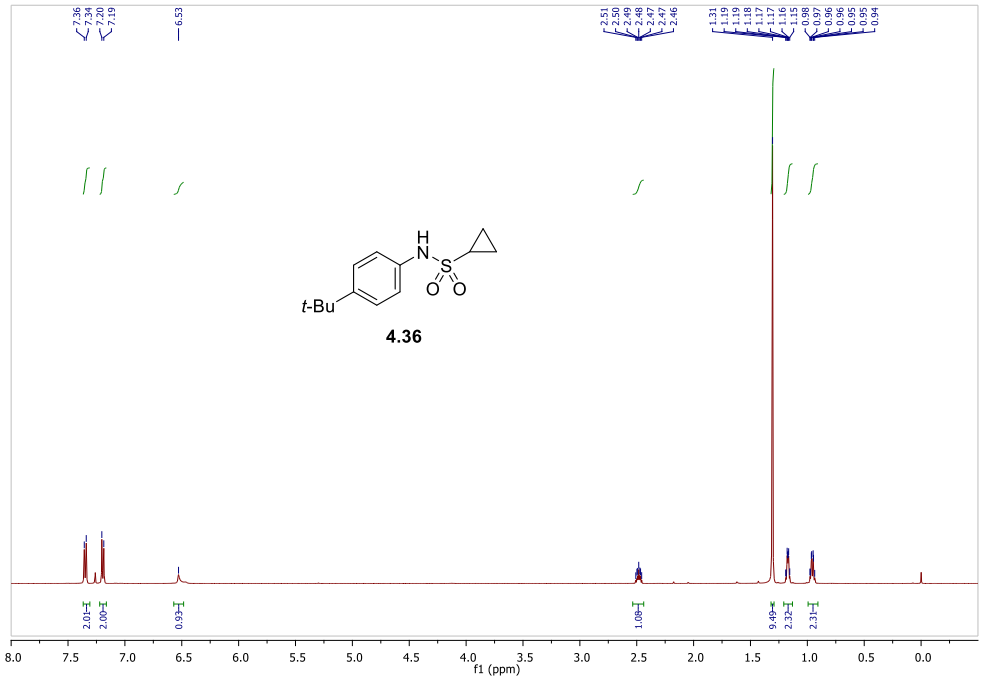
7.36
7.34
7.20
7.19
6.53
2.51
2.50
2.49
2.48
2.47
2.47
2.46
1.31
1.19
1.19
1.18
1.17
1.17
1.16
1.15
0.98
0.97
0.96
0.96
0.95
0.95
0.94
2.01
2.00
0.93
1.00
9.49
2.32
2.31
8.0
7.5
7.0
6.5
6.0
5.5
5.0
4.5
4.0
3.5
3.0
2.5
2.0
1.5
1.0
0.5
0.0
f1 (ppm)
H
N
S
O
O
t-Bu
4.36

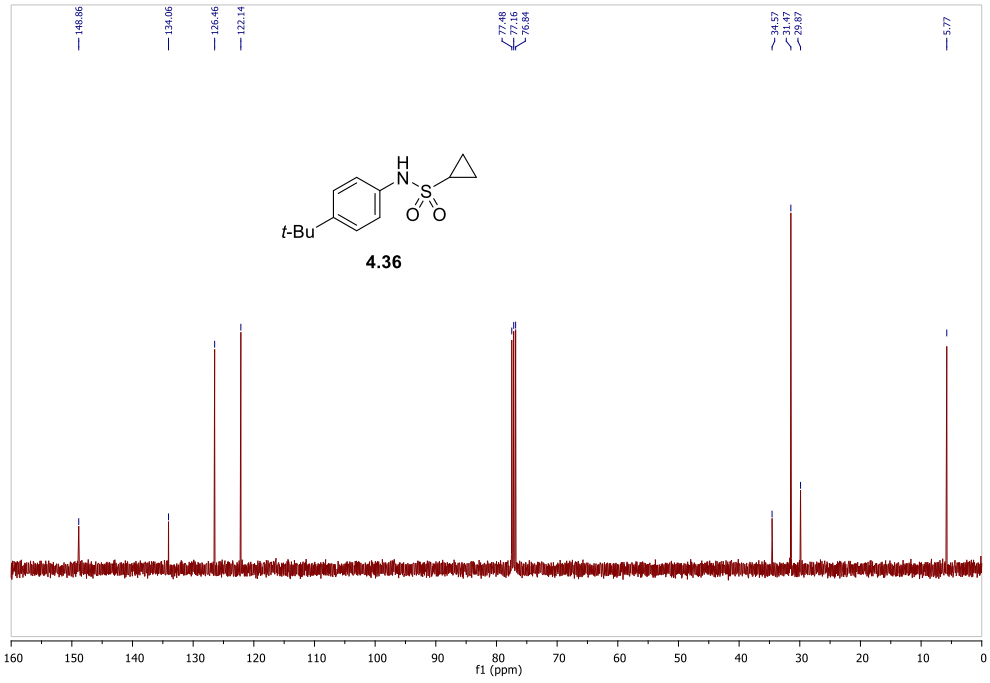
148.86
134.06
126.46
122.14
77.48
77.16
76.84
34.57
31.47
29.87
5.77
160
150
140
130
120
110
100
90
80
70
60
50
40
30
20
10
0
f1 (ppm)
H
N
S
O
O
t-Bu
4.36

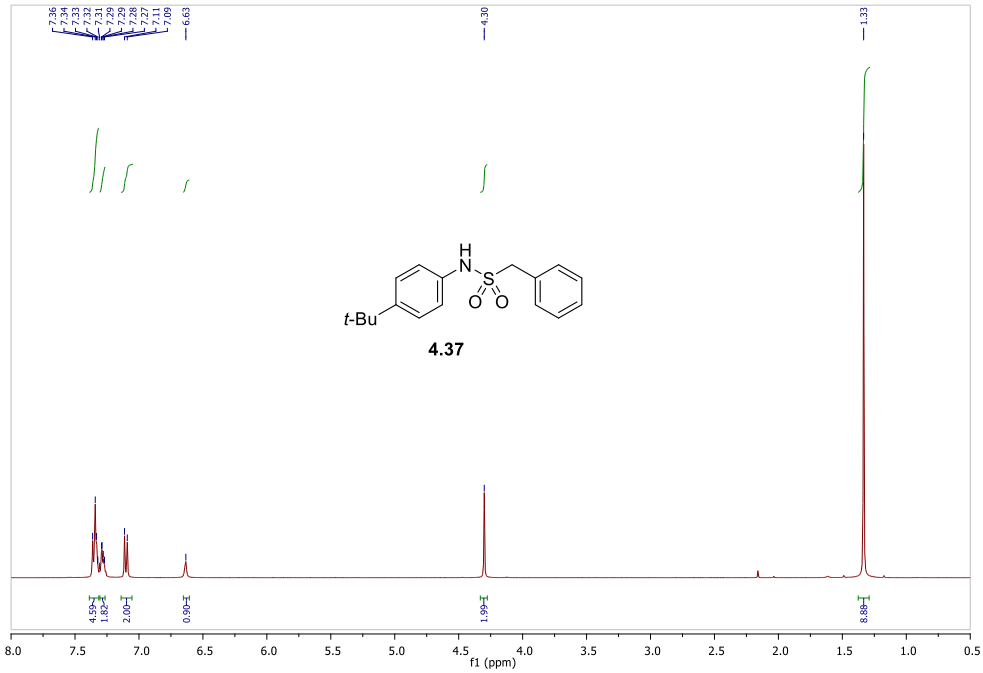
7.36
7.34
7.33
7.32
7.31
7.29
7.28
7.27
7.11
7.09
6.63
4.30
1.33
H
N
S
O
O
t-Bu
4.37
4.59
1.82
2.00
0.90
1.99
8.89
f1 (ppm)

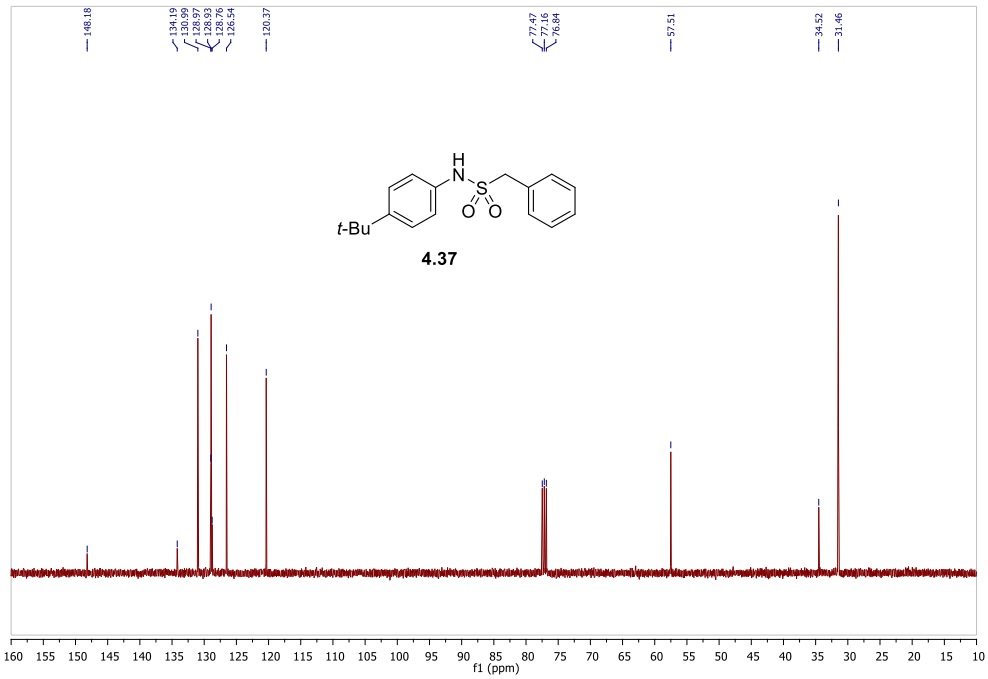
148.18
134.19
130.99
128.97
128.83
128.76
126.54
120.37
77.47
77.16
76.84
57.51
34.52
31.46
H
N
S
O
O
t-Bu
4.37
f1 (ppm)

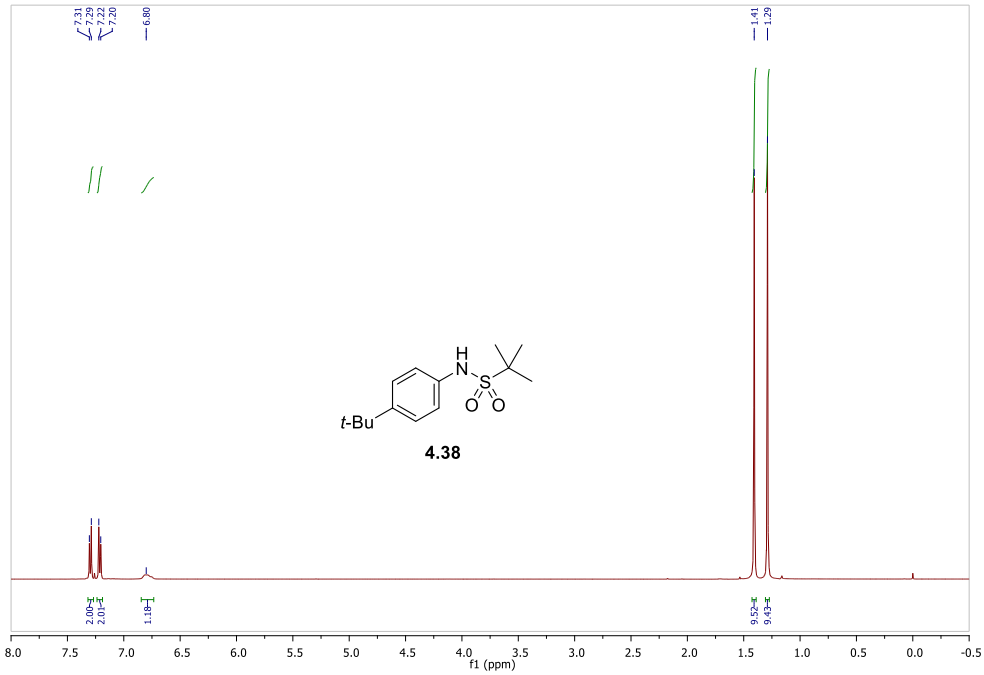
7.31
7.29
7.22
7.20
6.80
1.41
1.29
H
N
S
O
O
t-Bu
4.38
2.00
2.01
1.18
9.52
9.43
f1 (ppm)

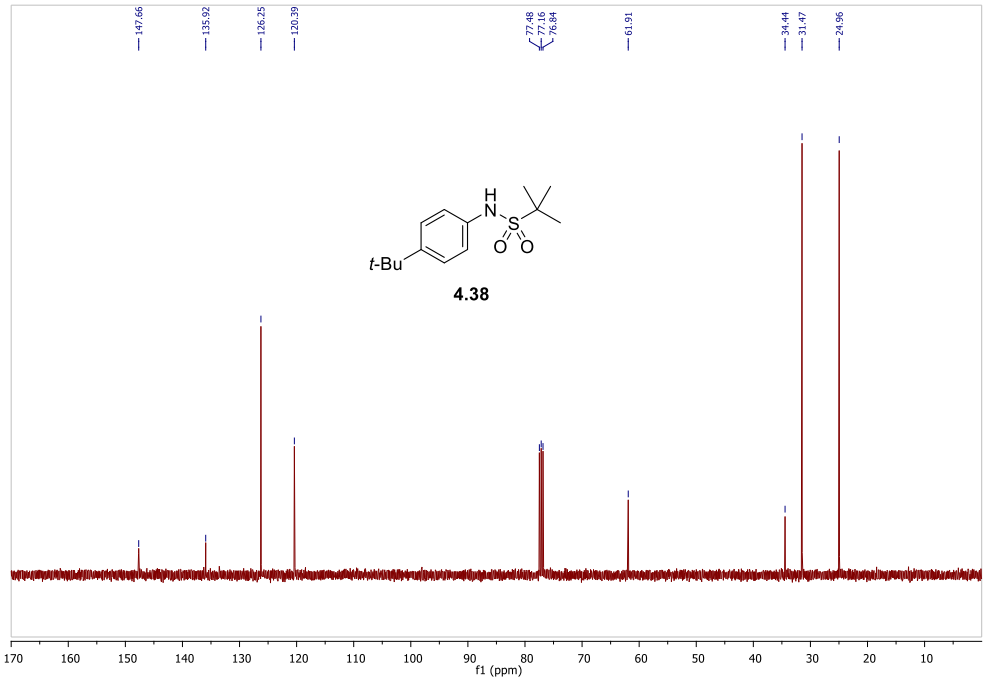
147.66
135.92
126.25
120.39
77.48
77.16
76.84
61.91
34.44
31.47
24.96
H
N
S
O
O
t-Bu
4.38
f1 (ppm)

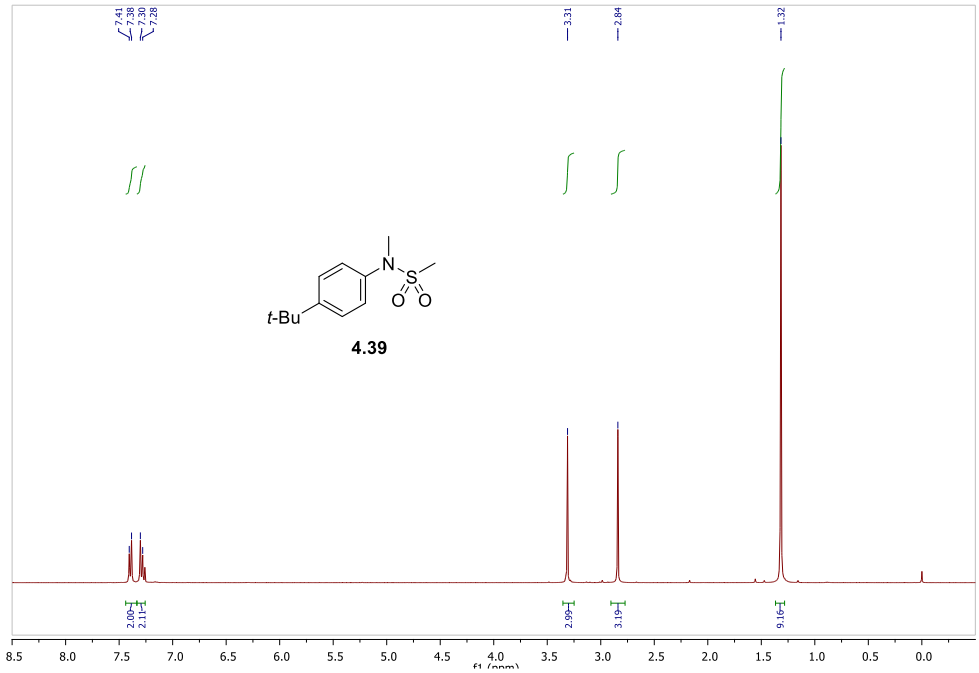
7.41
7.38
7.30
7.28
3.31
2.84
1.32
t-Bu
4.39
2.06
2.11
2.99
3.19
9.16
f1 (ppm)

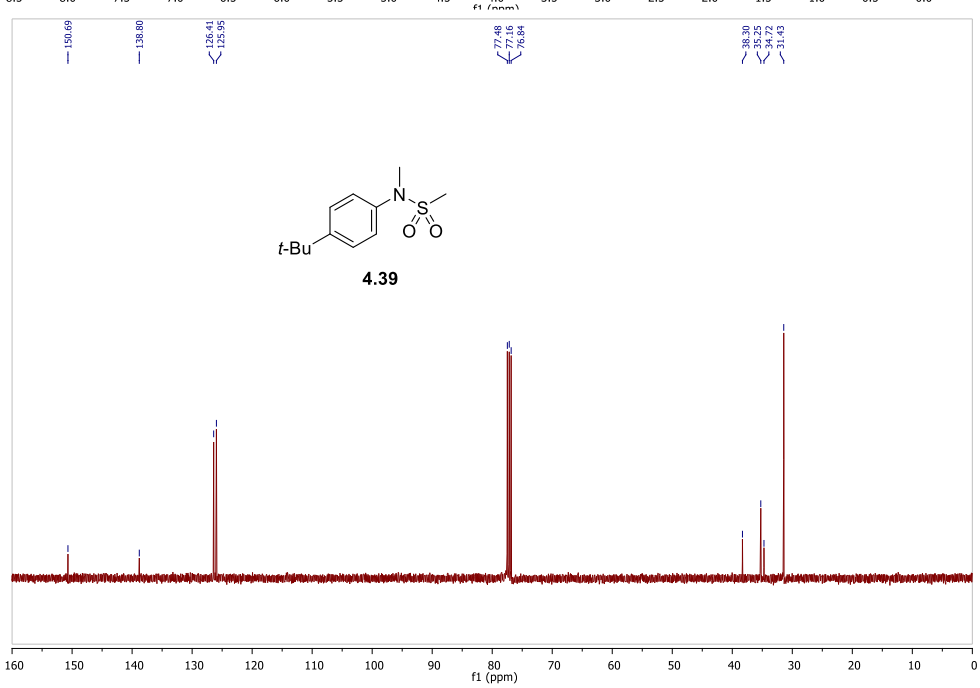
150.69
138.80
126.41
125.95
77.48
77.16
76.84
38.30
35.25
34.72
31.43
t-Bu
4.39
f1 (ppm)

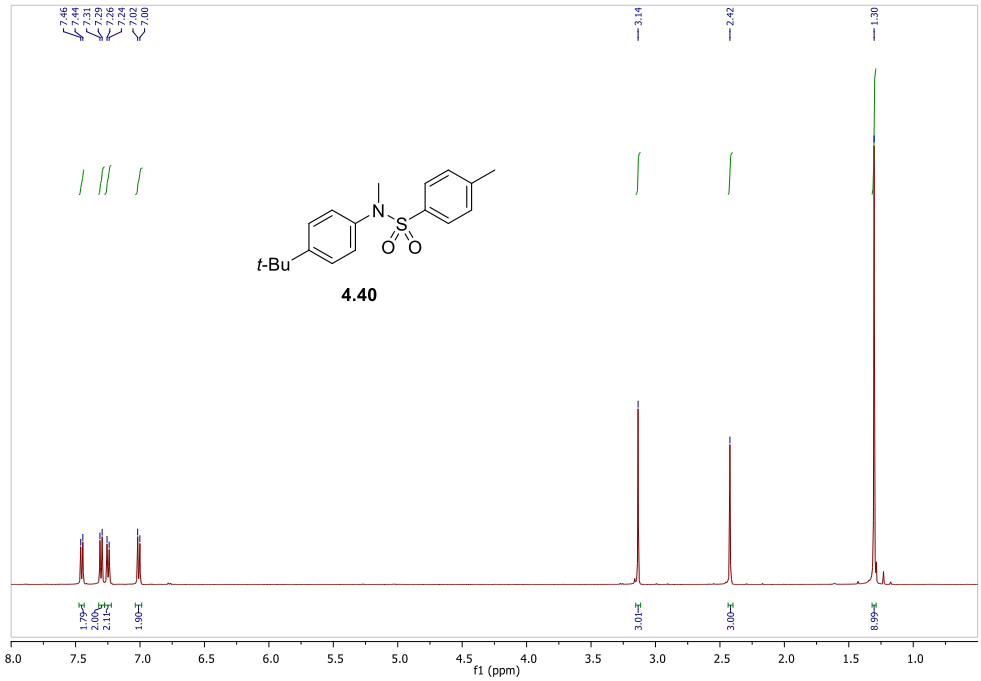
7.46
7.44
7.31
7.29
7.26
7.24
7.02
7.00
3.14
2.42
1.30
t-Bu
4.40
1.79
2.08
2.11
1.90
3.01
3.00
8.99
f1 (ppm)

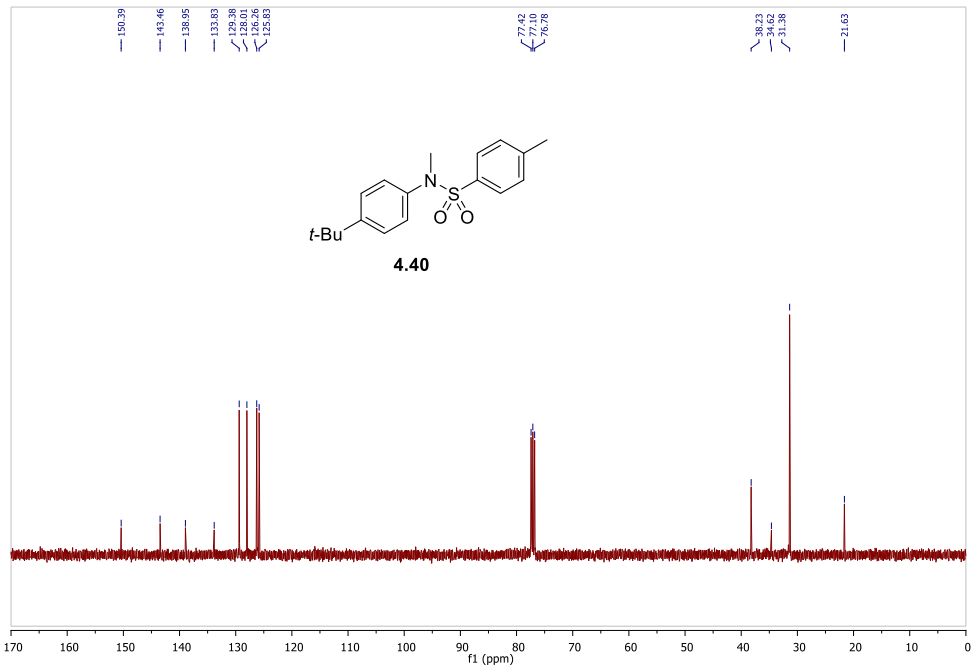
150.39
143.46
138.95
133.83
129.38
128.01
126.26
125.83
77.42
77.10
76.78
38.23
34.62
31.38
21.63
t-Bu
4.40
f1 (ppm)

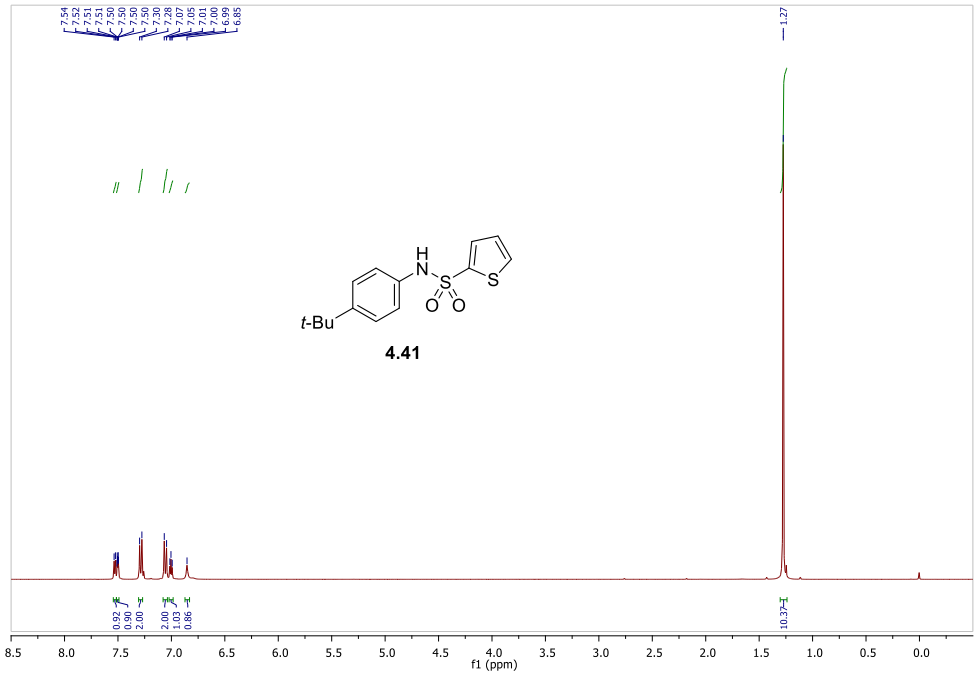
7.54
7.52
7.51
7.51
7.50
7.50
7.50
7.50
7.30
7.28
7.07
7.05
7.01
7.00
6.99
6.85
1.27
t-Bu
4.41
0.92
0.90
2.00
2.00
1.03
0.86
10.37
f1 (ppm)

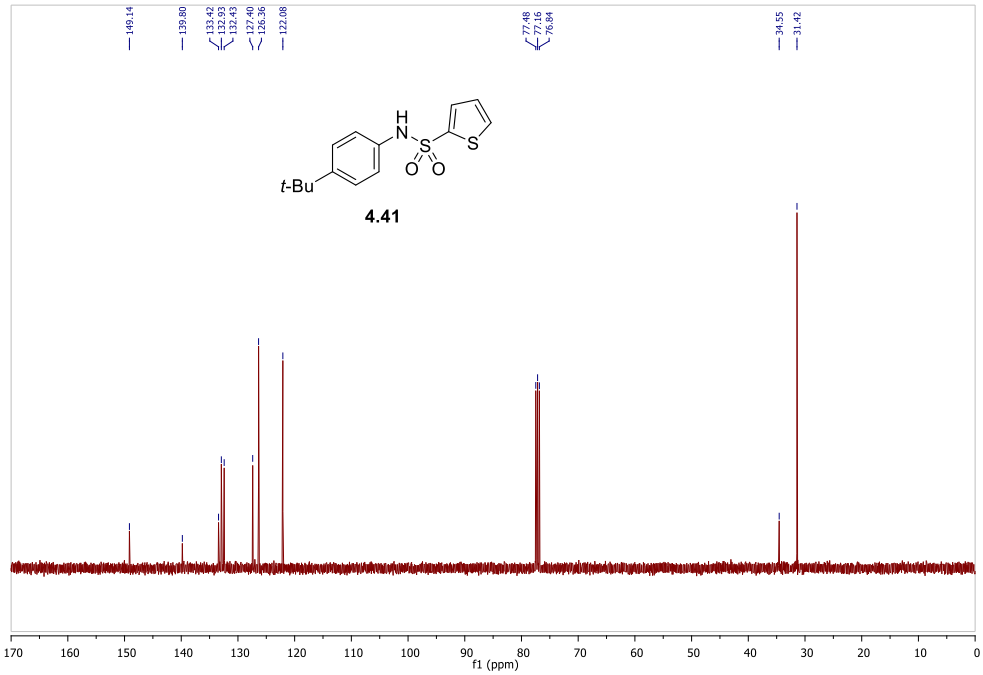
149.14
139.80
133.42
132.93
132.43
127.40
126.36
122.08
77.48
77.16
76.84
34.55
31.42
t-Bu
4.41
f1 (ppm)

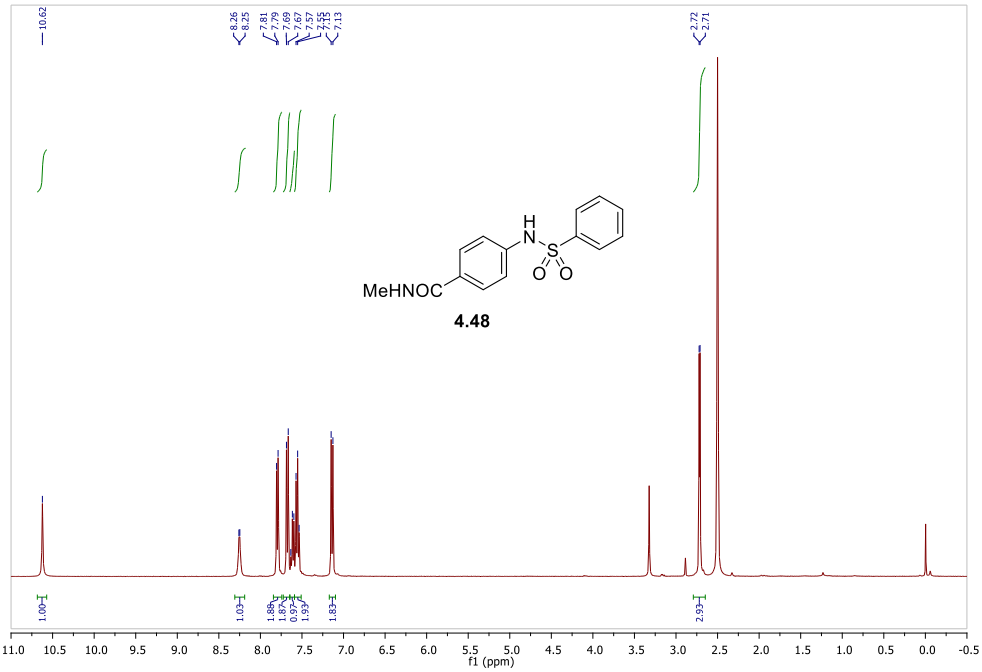
10.62
8.26
8.25
7.81
7.79
7.69
7.67
7.57
7.55
7.13
2.72
2.71
MeHNOC
4.48
1.00
1.03
1.88
1.87
0.97
1.93
1.83
2.93
f1 (ppm)

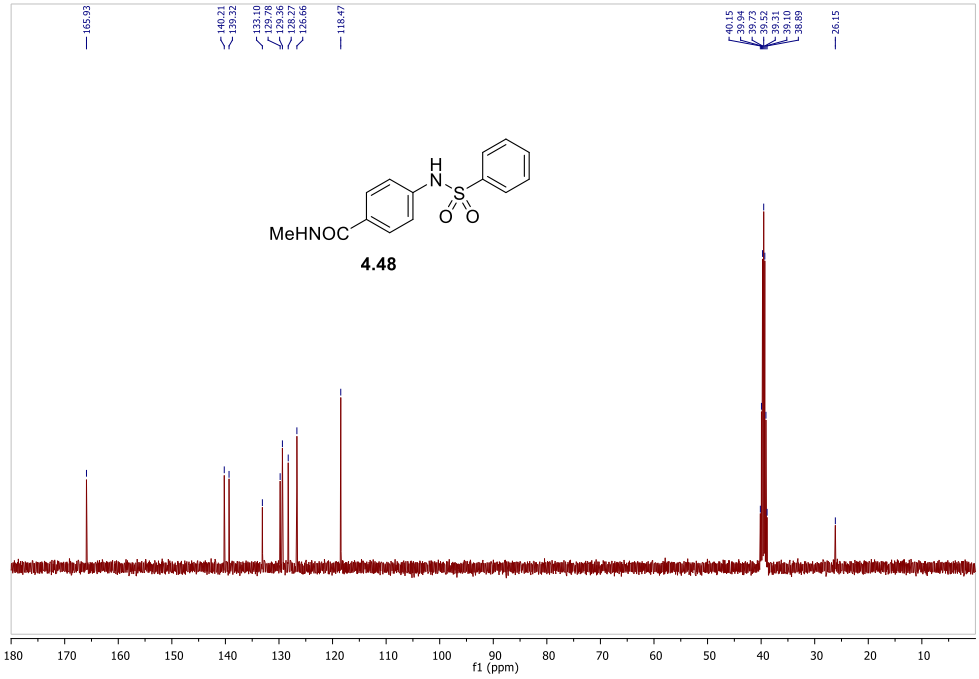
165.93
140.21
139.32
133.10
129.78
128.36
128.27
126.66
118.47
40.15
39.94
39.73
39.52
39.31
39.10
38.89
26.15
MeHNOC
4.48
f1 (ppm)

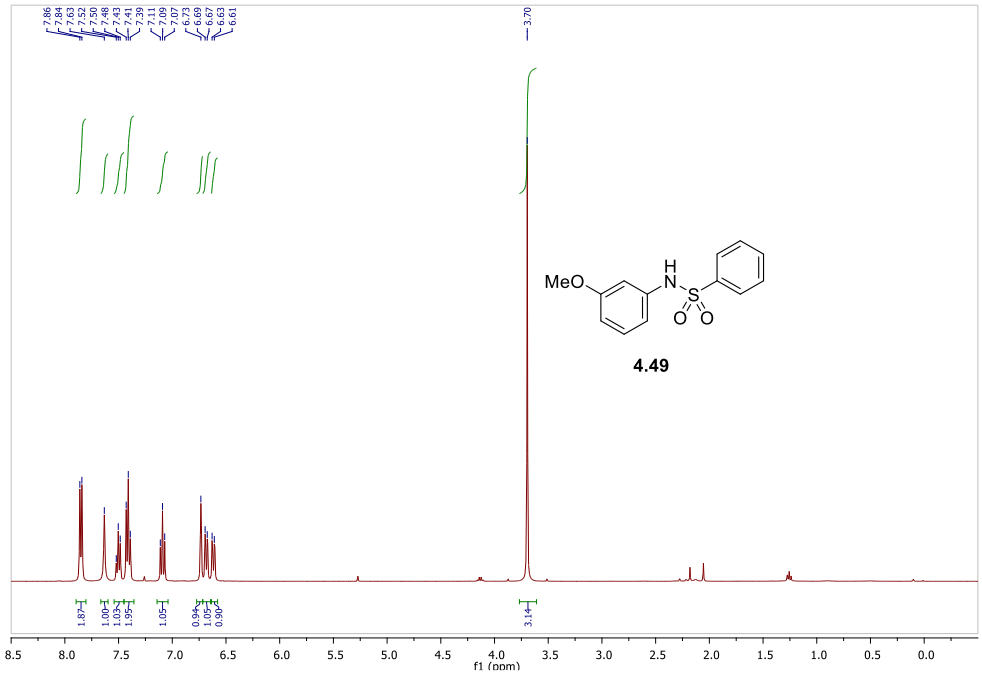
7.86
7.84
7.63
7.52
7.50
7.48
7.43
7.41
7.39
7.11
7.09
7.07
6.73
6.69
6.67
6.63
6.61
3.70
MeO
H
N
S
O
O
4.49
1.87
1.00
1.03
1.95
1.05
0.94
1.00
0.90
3.14
8.5
8.0
7.5
7.0
6.5
6.0
5.5
5.0
4.5
4.0
3.5
3.0
2.5
2.0
1.5
1.0
0.5
0.0
f1 (ppm)

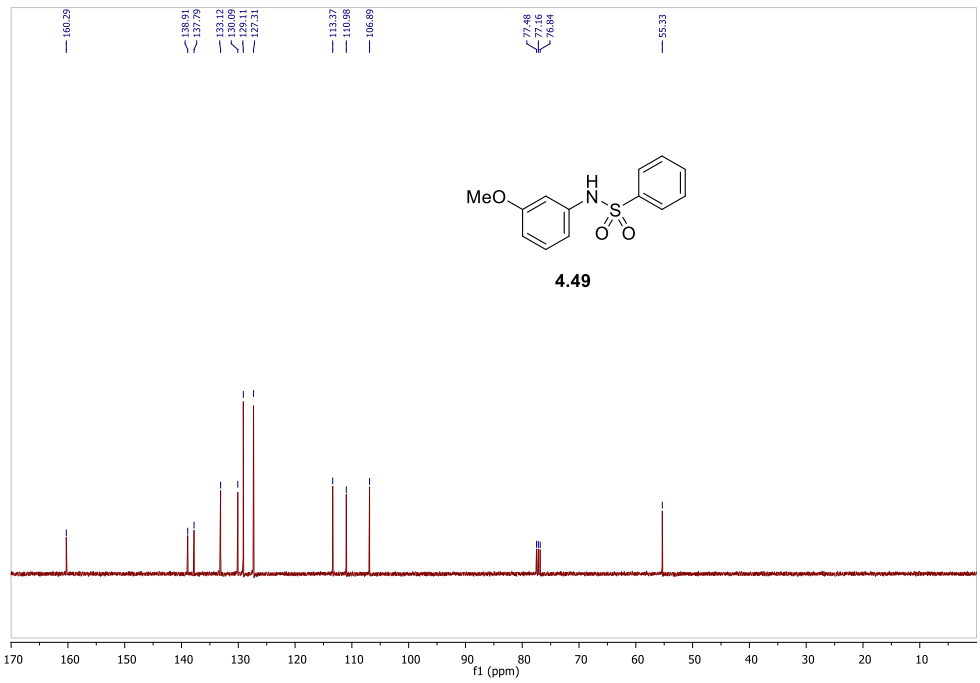
160.29
138.91
137.79
133.12
130.09
129.11
127.31
113.37
110.98
106.89
77.48
77.16
76.84
55.33
MeO
H
N
S
O
O
4.49
170
160
150
140
130
120
110
100
90
80
70
60
50
40
30
20
10
f1 (ppm)

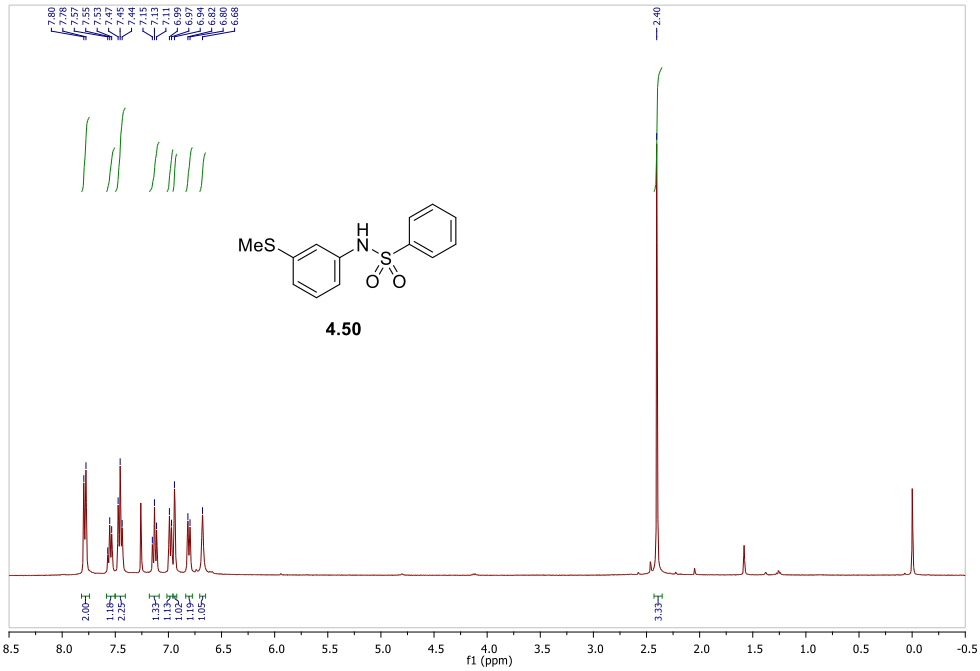
7.80
7.78
7.57
7.55
7.53
7.47
7.45
7.44
7.15
7.13
7.11
6.99
6.97
6.94
6.82
6.80
6.68
2.40
MeS
H
N
S
O
O
4.50
2.00
1.19
2.25
1.33
1.15
1.02
1.19
1.05
3.33
f1 (ppm)

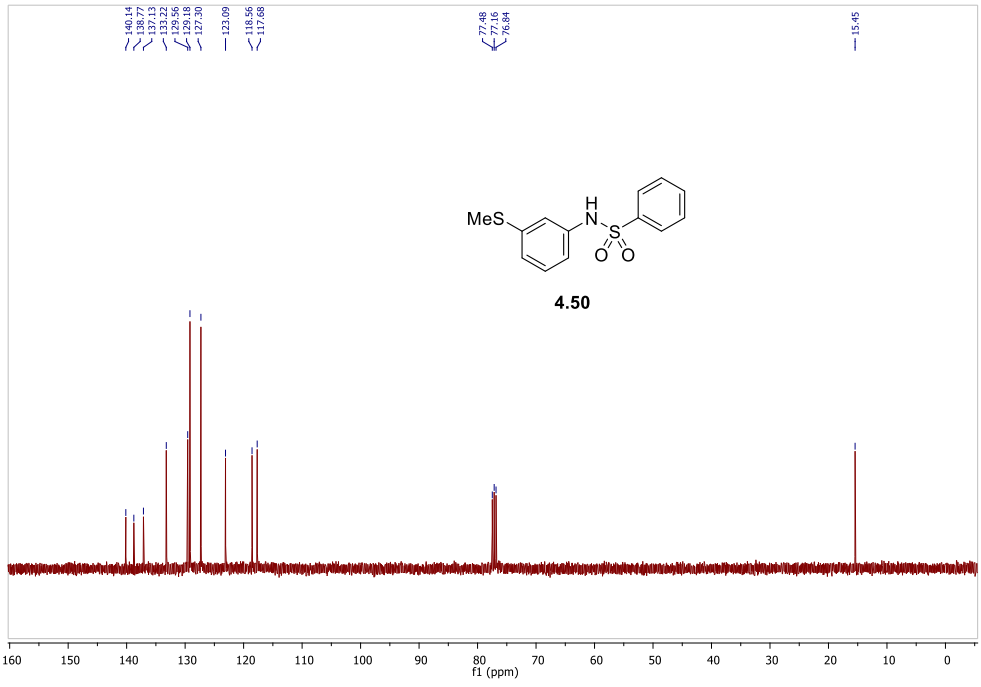
140.14
138.77
137.13
133.22
129.56
129.18
127.30
123.09
118.56
117.68
77.48
77.16
76.84
15.45
MeS
H
N
S
O
O
4.50
f1 (ppm)

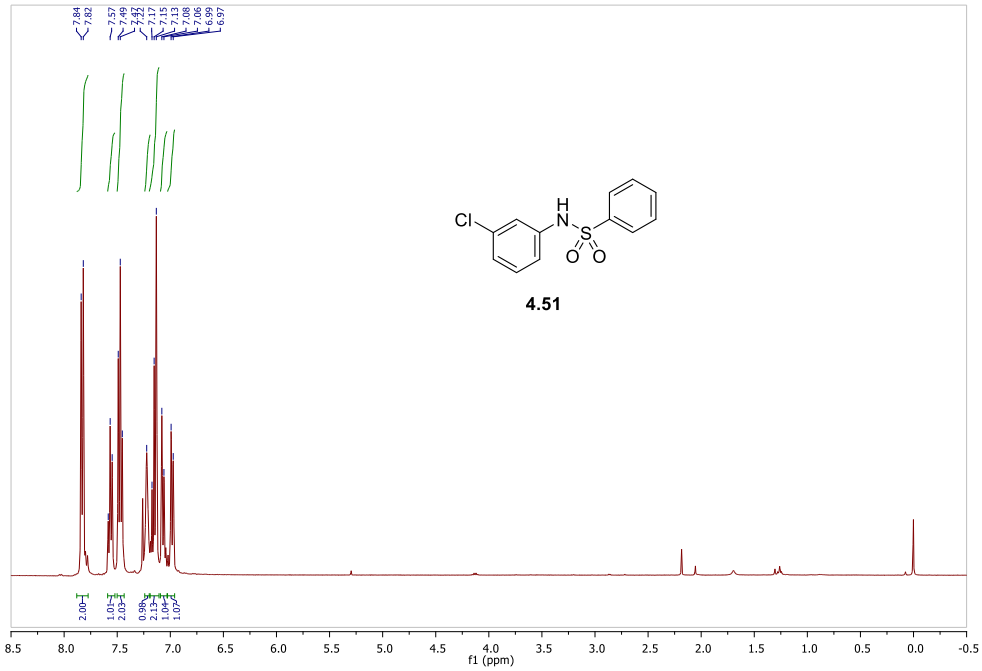
7.84
7.82
7.57
7.49
7.42
7.17
7.15
7.13
7.08
7.06
6.99
6.97
Cl
H
N
S
O
O
4.51
2.00
1.01
2.03
0.98
2.13
1.94
1.07
8.5
8.0
7.5
7.0
6.5
6.0
5.5
5.0
4.5
4.0
3.5
3.0
2.5
2.0
1.5
1.0
0.5
0.0
-0.5
f1 (ppm)

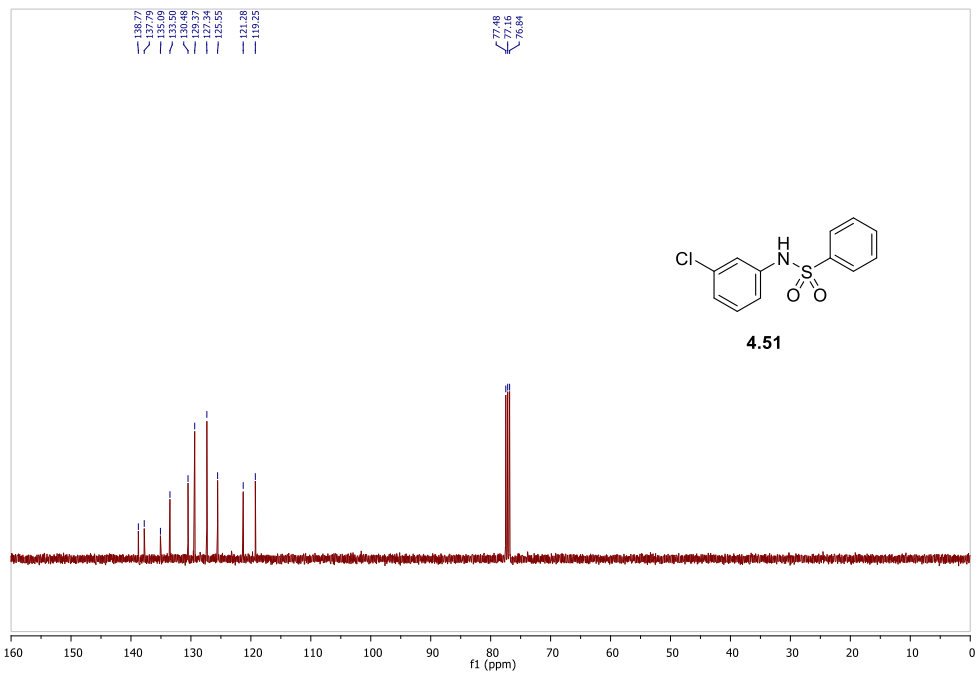
138.77
137.79
135.09
133.50
130.48
129.32
127.34
125.55
121.28
119.25
77.48
77.16
76.84
Cl
H
N
S
O
O
4.51
160
150
140
130
120
110
100
90
80
70
60
50
40
30
20
10
0
f1 (ppm)

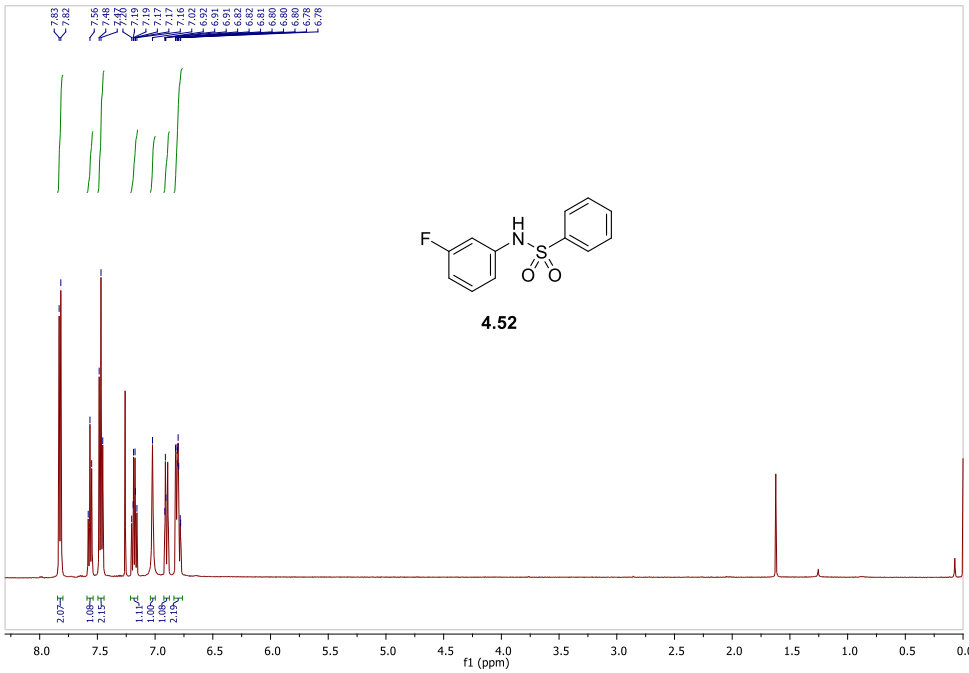
7.83
7.82
7.56
7.48
7.47
7.20
7.19
7.19
7.17
7.17
7.16
7.02
6.92
6.91
6.82
6.82
6.81
6.80
6.80
6.78
6.78
F
H
N
S
O
O
4.52
2.07
1.08
2.15
1.11
1.05
1.08
2.18
8.0
7.5
7.0
6.5
6.0
5.5
5.0
4.5
4.0
3.5
3.0
2.5
2.0
1.5
1.0
0.5
0.0
f1 (ppm)

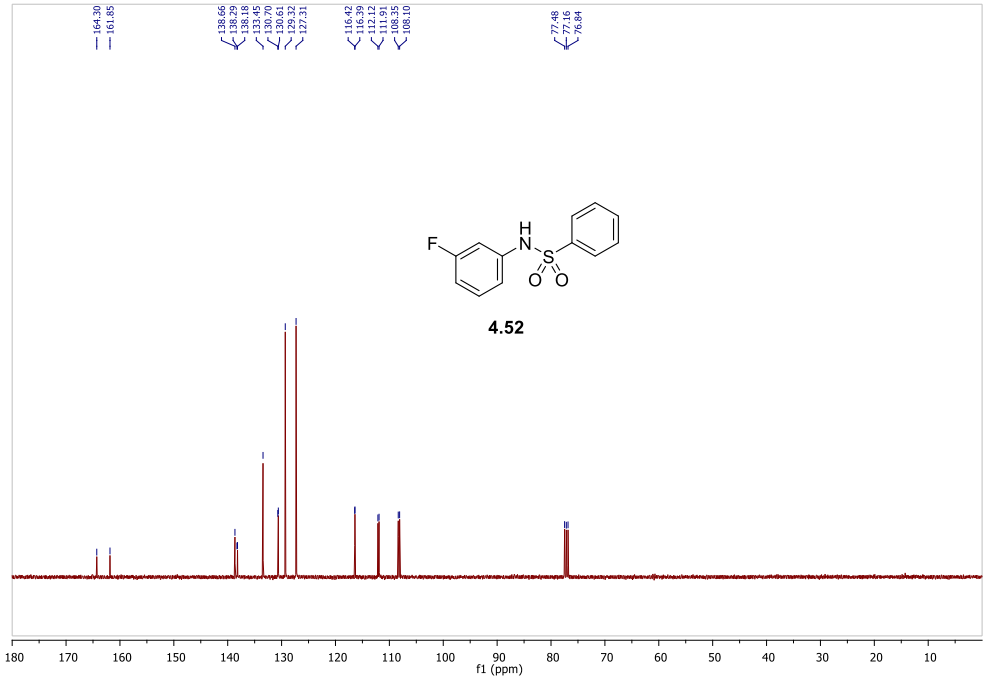
164.30
161.85
138.66
138.29
138.18
133.45
130.70
130.61
129.32
127.31
116.42
116.39
112.12
111.91
108.35
108.10
77.48
77.16
76.84
F
H
N
S
O
O
4.52
180
170
160
150
140
130
120
110
100
90
80
70
60
50
40
30
20
10
f1 (ppm)

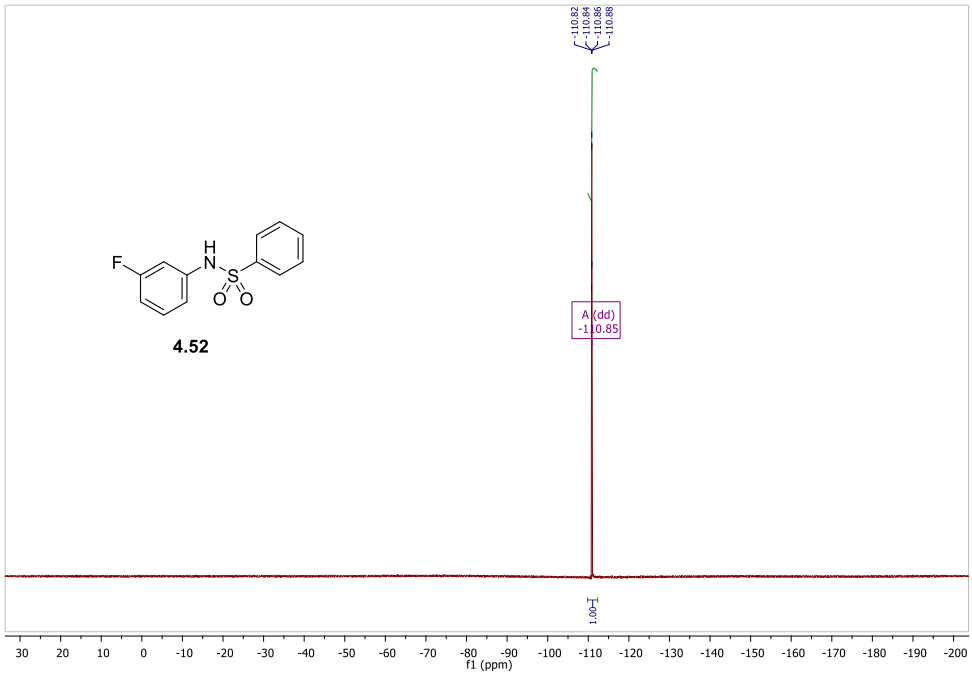
-110.82
-110.84
-110.86
-110.88
A (dd)
-110.85
1.00
30 20 10 0 -10 -20 -30 -40 -50 -60 -70 -80 -90 -100 -110 -120 -130 -140 -150 -160 -170 -180 -190 -200
f1 (ppm)

4.52

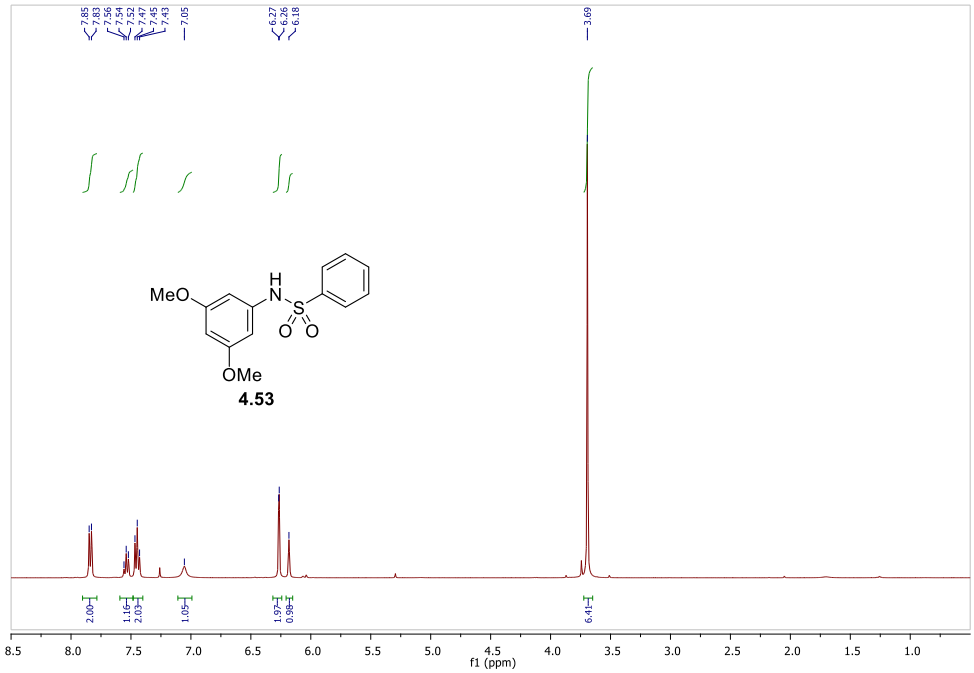
7.85
7.83
7.56
7.54
7.52
7.47
7.45
7.43
7.05
6.27
6.26
6.18
3.69
MeO
H
N
S
O
O
OMe
4.53
2.00
1.16
2.05
1.05
1.97
0.98
6.41
f1 (ppm)

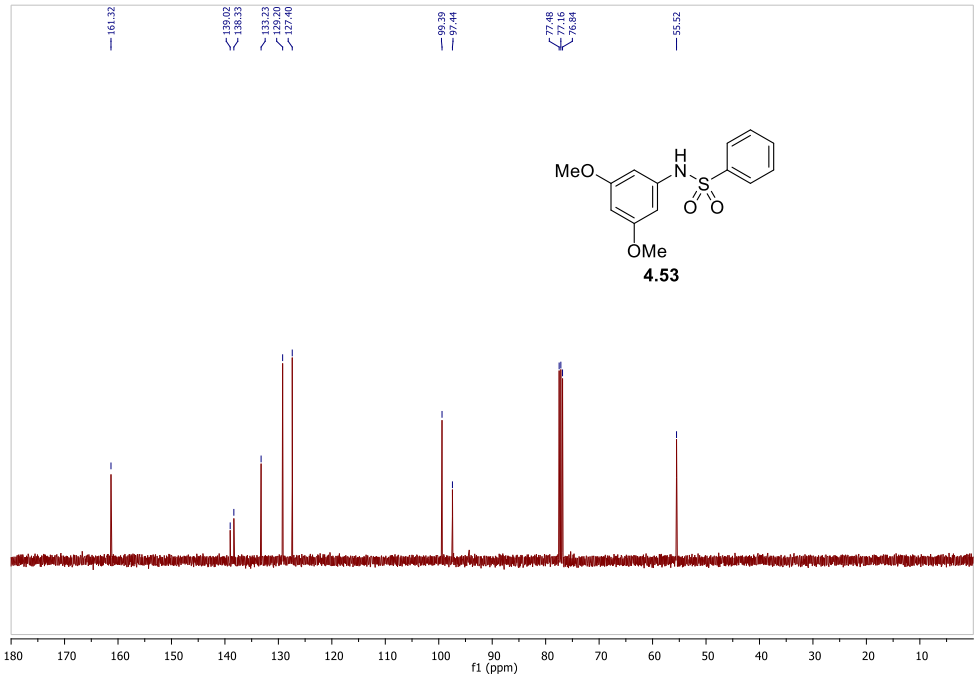
161.32
139.02
138.33
133.23
129.20
127.40
99.39
97.44
77.48
77.16
76.84
55.52
MeO
H
N
S
O
O
OMe
4.53
f1 (ppm)

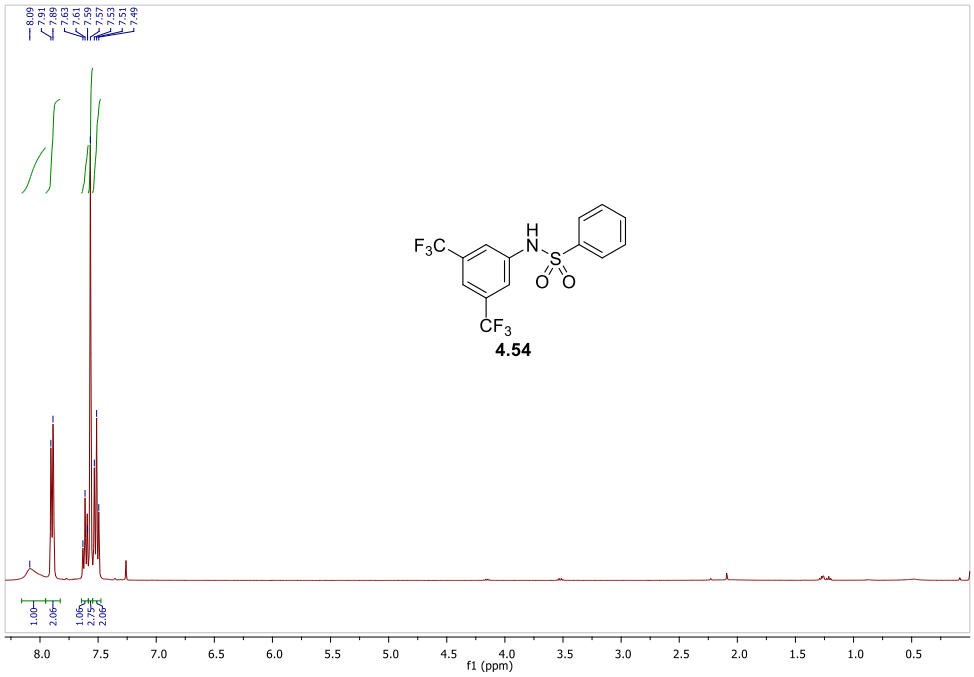
8.09
7.91
7.89
7.63
7.61
7.59
7.57
7.53
7.51
7.49
1.00
2.06
1.05
2.75
2.06
F3C
H
N
S
O
O
CF3
4.54
f1 (ppm)

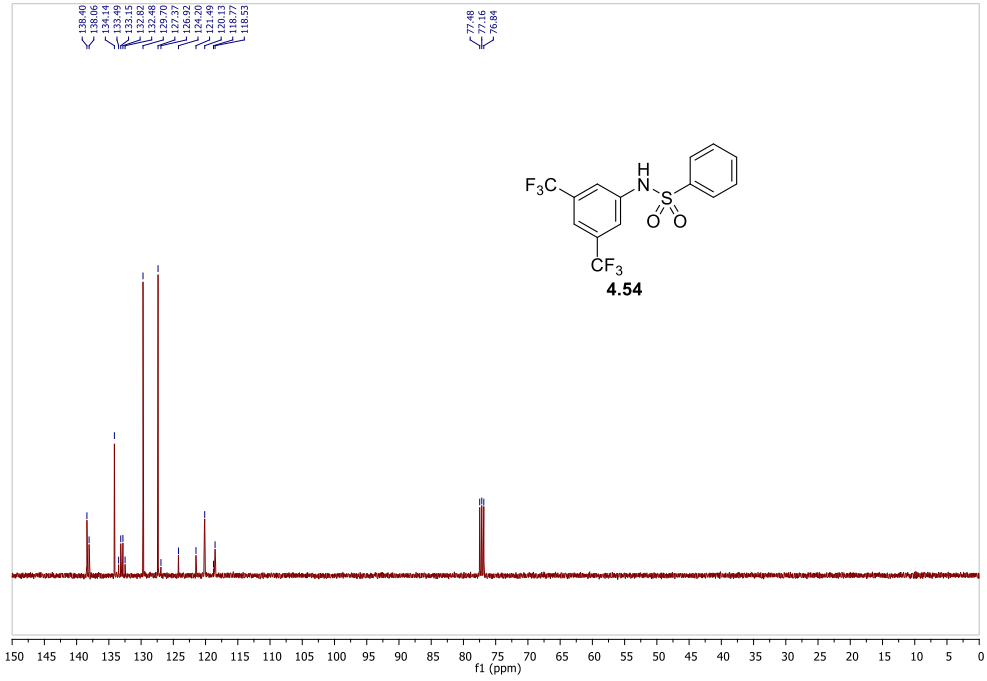
138.40
138.06
134.14
133.49
133.15
132.82
132.48
129.70
127.37
126.92
124.20
121.49
120.13
118.77
118.53
77.48
77.16
76.84
F3C
H
N
S
O
O
CF3
4.54
f1 (ppm)

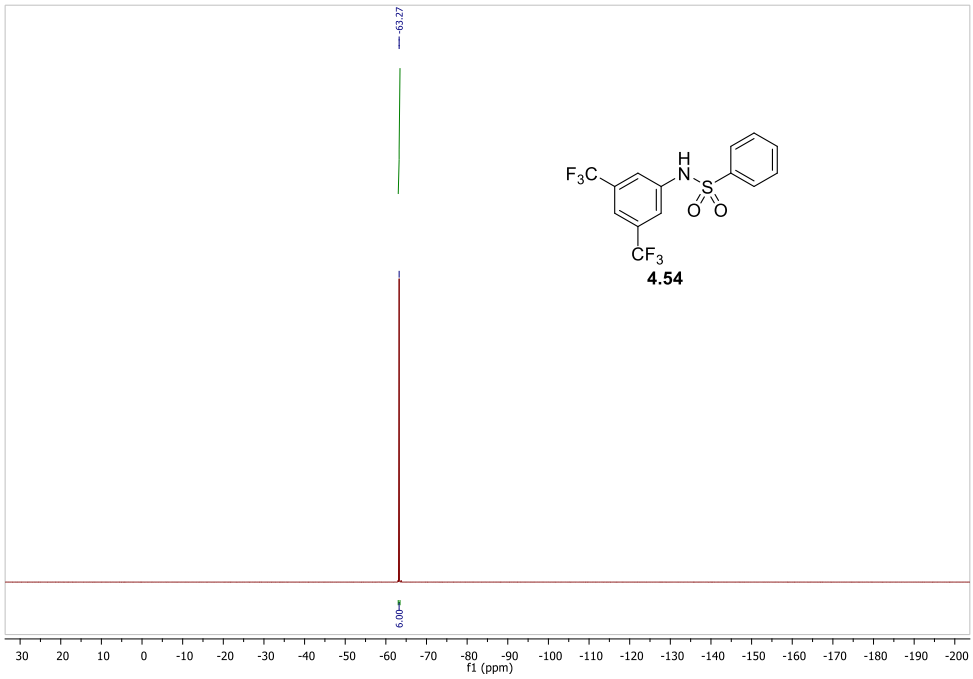
-63.27
6.00
30 20 10 0 -10 -20 -30 -40 -50 -60 -70 -80 -90 -100 -110 -120 -130 -140 -150 -160 -170 -180 -190 -200
f1 (ppm)
F3C
H
N
S
O
O
CF3
4.54

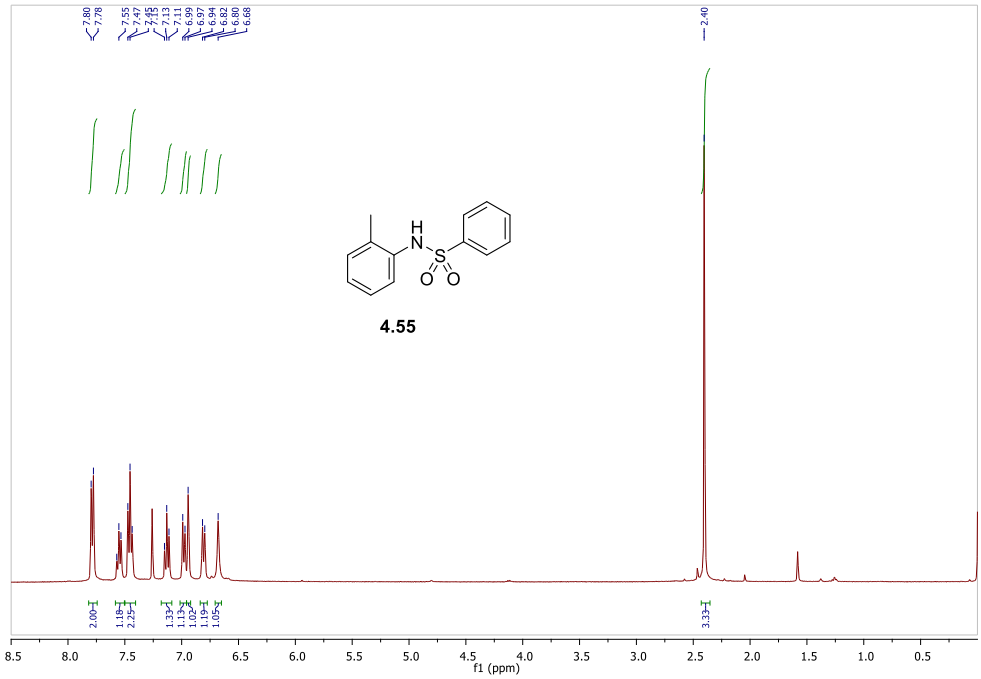
7.80
7.78
7.55
7.47
7.45
7.13
7.11
6.99
6.97
6.94
6.82
6.80
6.68
2.40
4.55
2.00
1.18
2.25
1.37
1.15
1.02
1.19
1.05
3.33
f1 (ppm)

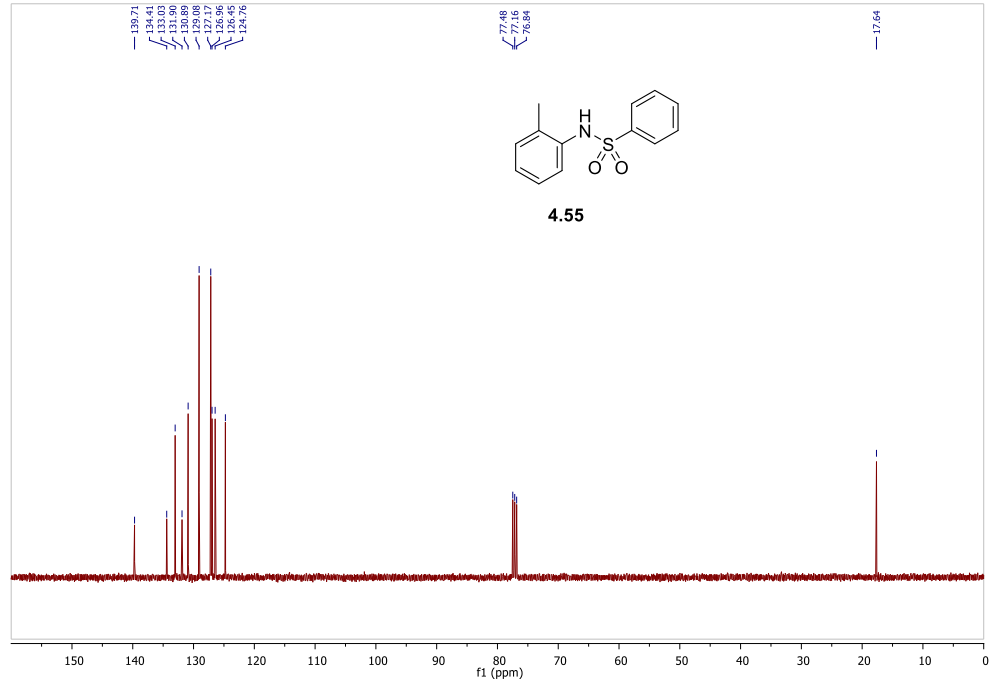
139.71
134.41
133.03
131.90
130.89
129.08
127.27
126.96
126.45
124.76
77.48
77.16
76.84
17.64
4.55
f1 (ppm)

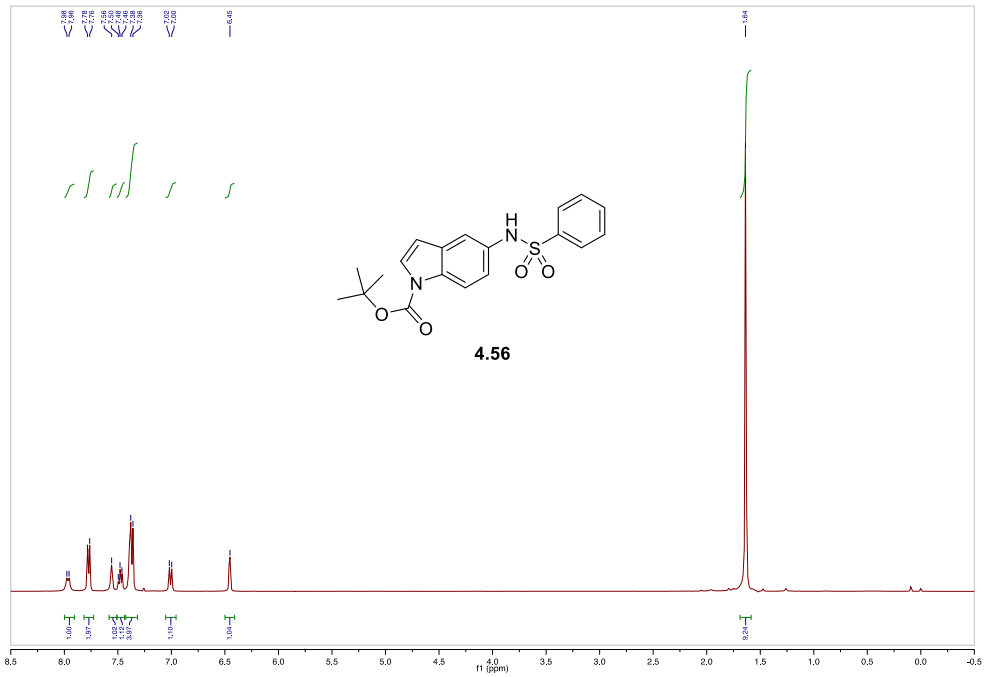
4.56
f1 (ppm)

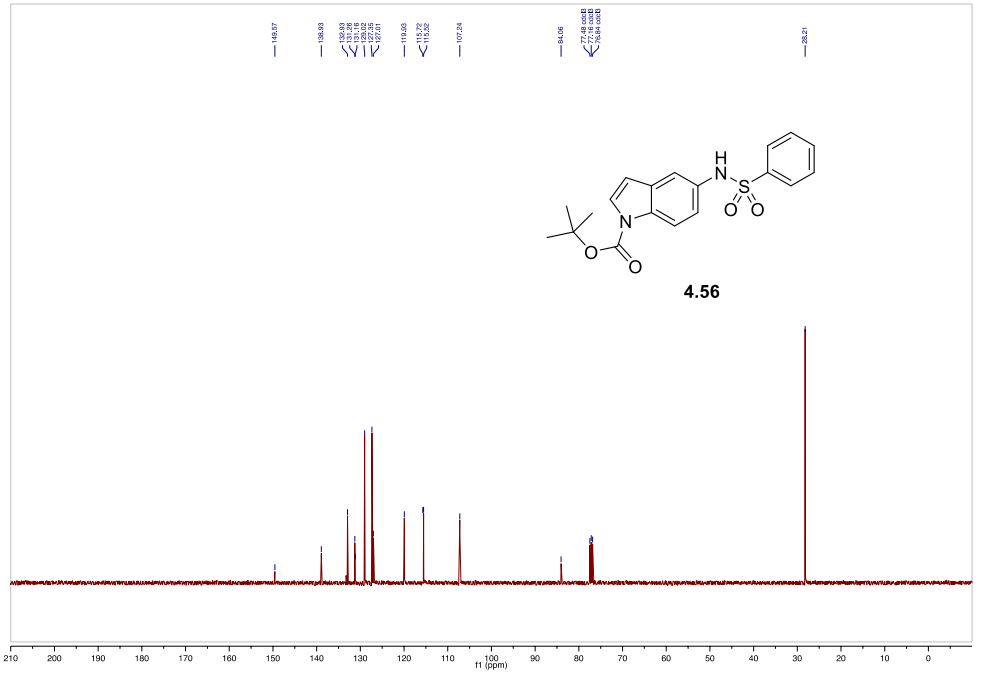
4.56
f1 (ppm)

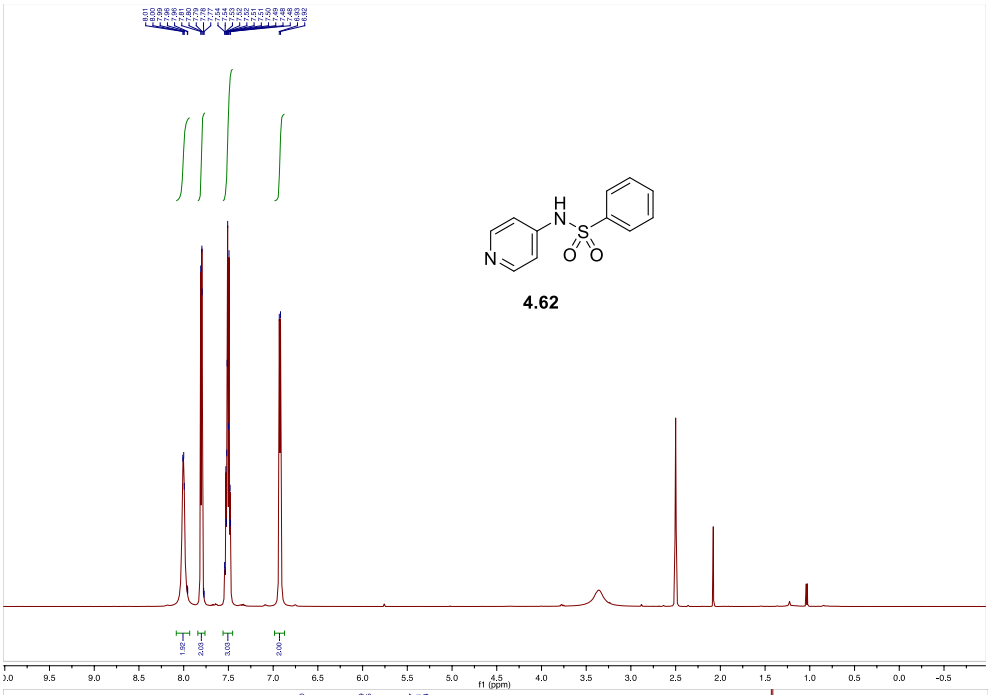
4.62

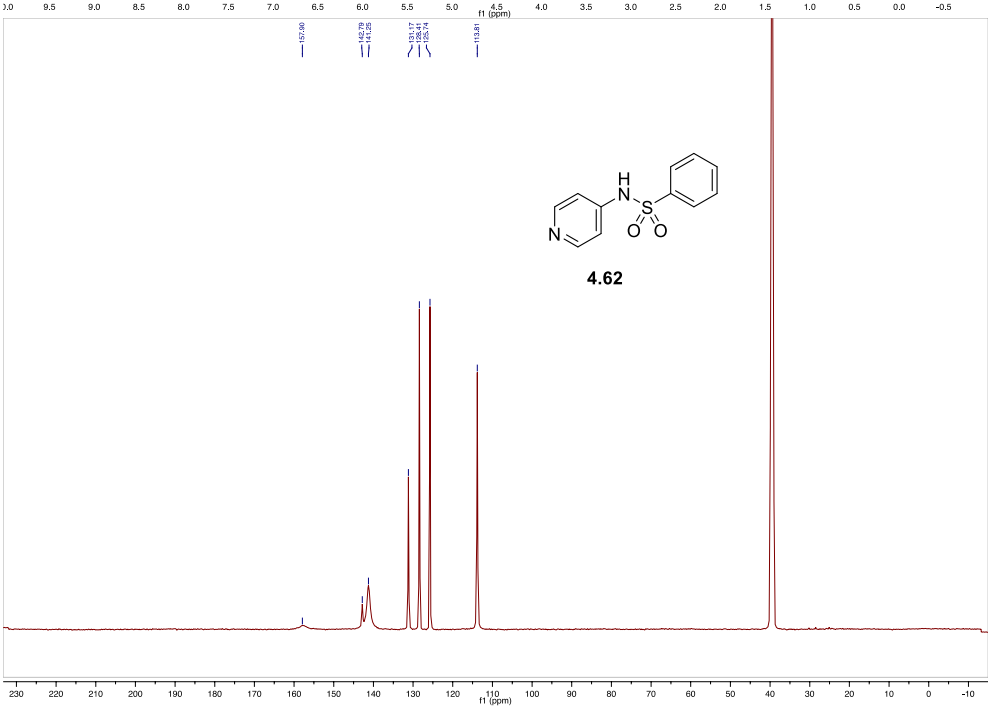
4.62

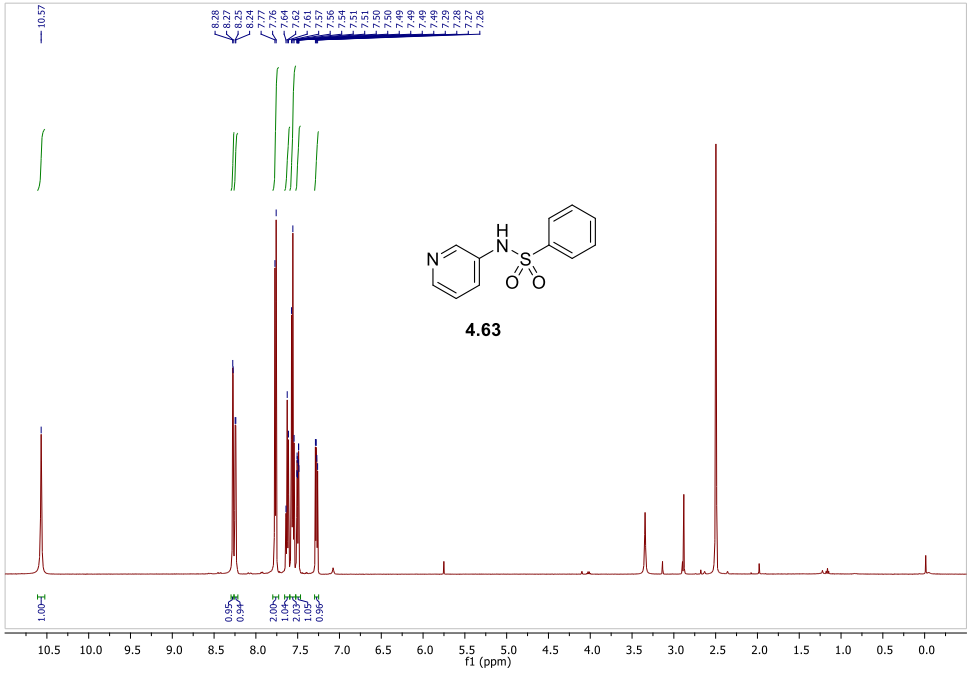
10.57
8.28
8.27
8.25
8.24
7.77
7.76
7.64
7.62
7.61
7.57
7.56
7.54
7.51
7.51
7.50
7.50
7.49
7.49
7.49
7.49
7.29
7.28
7.27
7.26
1.00
0.95
0.94
2.00
1.04
2.03
1.05
0.96
10.5 10.0 9.5 9.0 8.5 8.0 7.5 7.0 6.5 6.0 5.5 5.0 4.5 4.0 3.5 3.0 2.5 2.0 1.5 1.0 0.5 0.0
f1 (ppm)
4.63

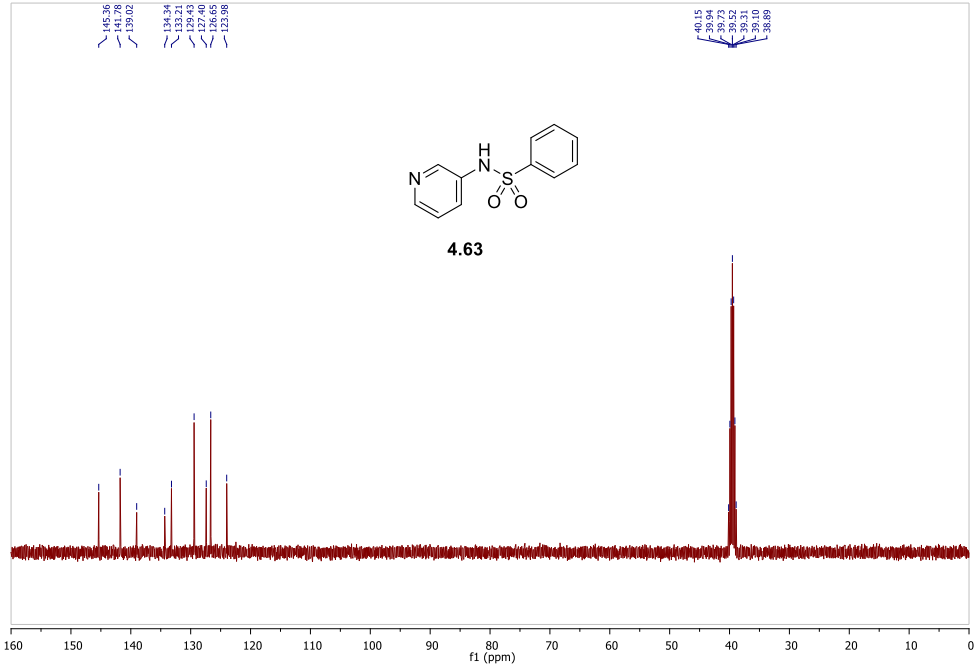
145.36
141.78
139.02
134.34
133.21
129.43
127.40
126.65
123.98
40.15
39.94
39.73
39.52
39.31
39.10
38.89
160 150 140 130 120 110 100 90 80 70 60 50 40 30 20 10 0
f1 (ppm)
4.63

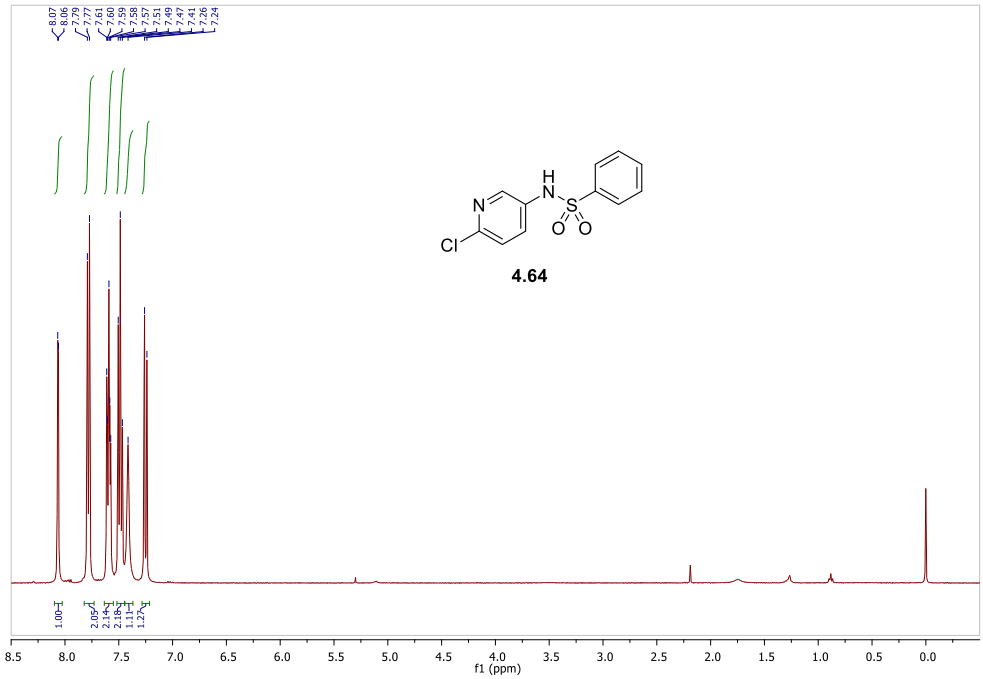
8.07
8.06
7.79
7.77
7.61
7.60
7.59
7.58
7.57
7.51
7.49
7.47
7.41
7.26
7.24
1.00
2.09
2.14
2.18
1.11
1.27
8.5
8.0
7.5
7.0
6.5
6.0
5.5
5.0
4.5
4.0
3.5
3.0
2.5
2.0
1.5
1.0
0.5
0.0
f1 (ppm)
H
N
S
O
O
N
Cl

4.64

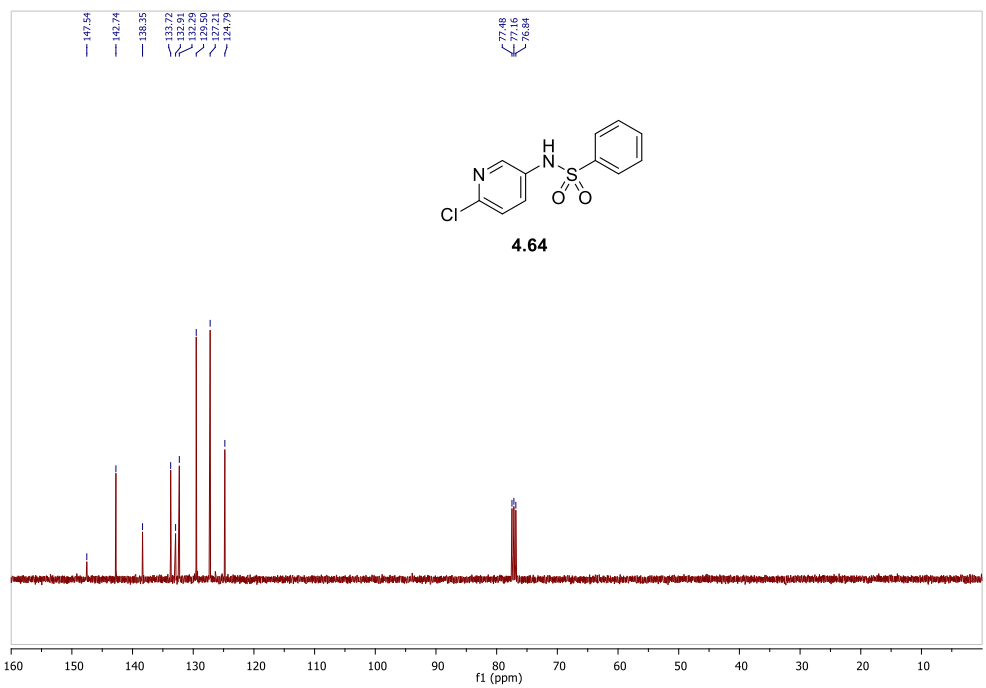
147.54
142.74
138.35
133.72
133.31
132.29
129.50
127.21
124.79
77.48
77.16
76.84
160
150
140
130
120
110
100
90
80
70
60
50
40
30
20
10
f1 (ppm)
H
N
S
O
O
N
Cl

4.64

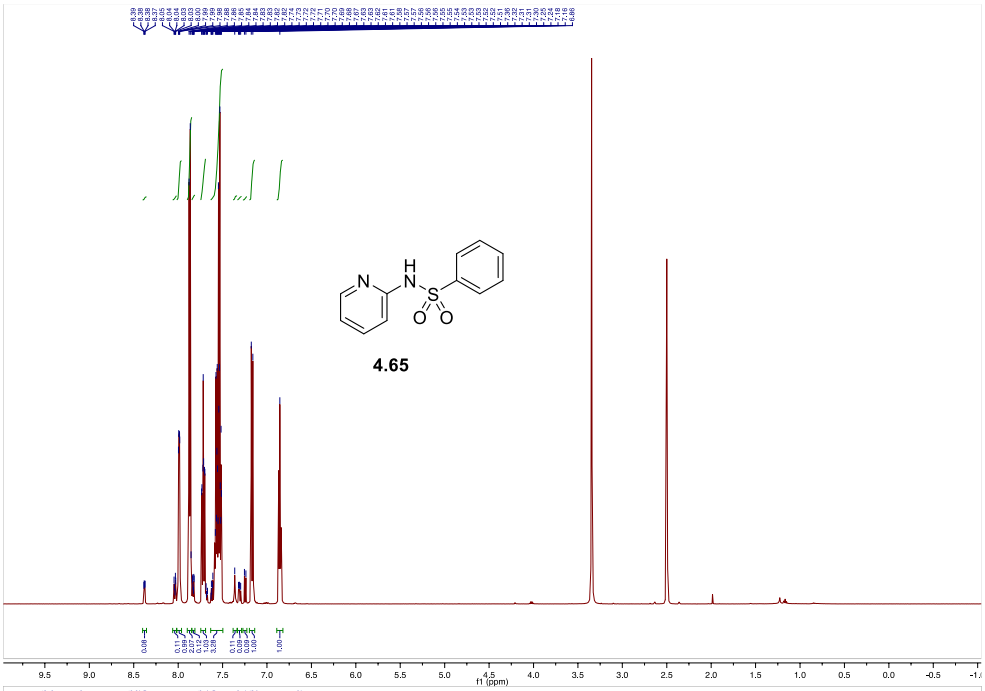
4.65

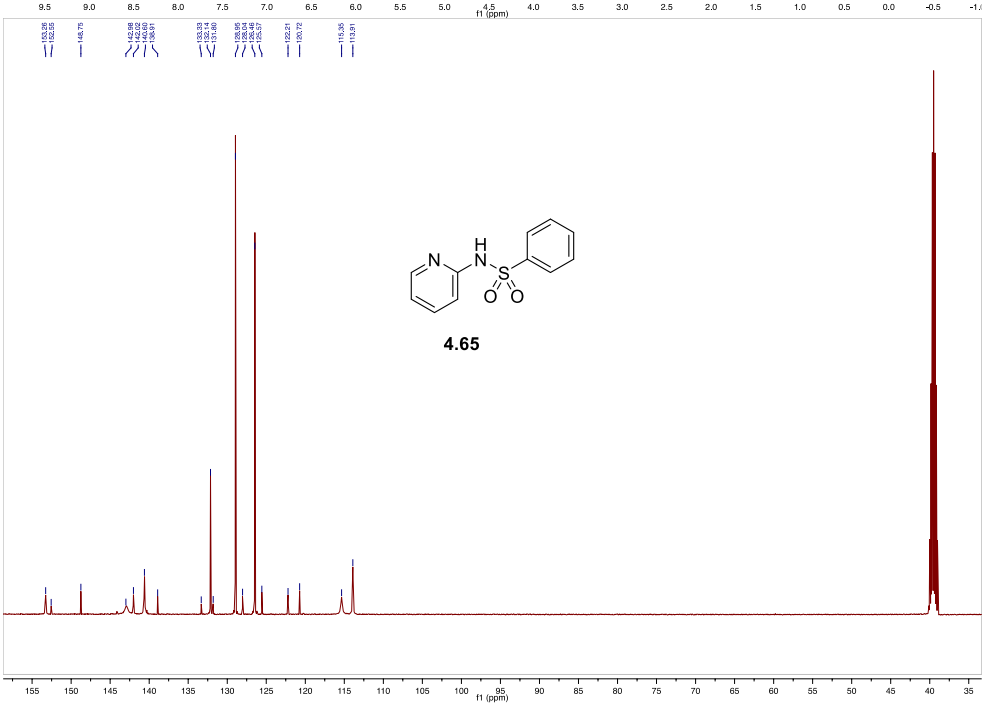
4.65

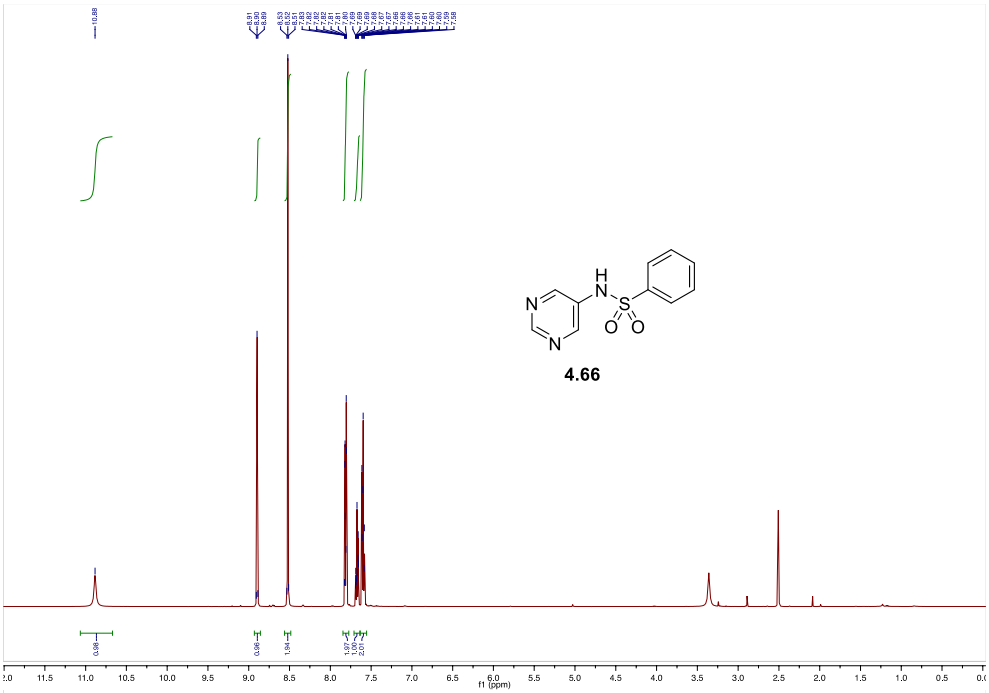
4.66

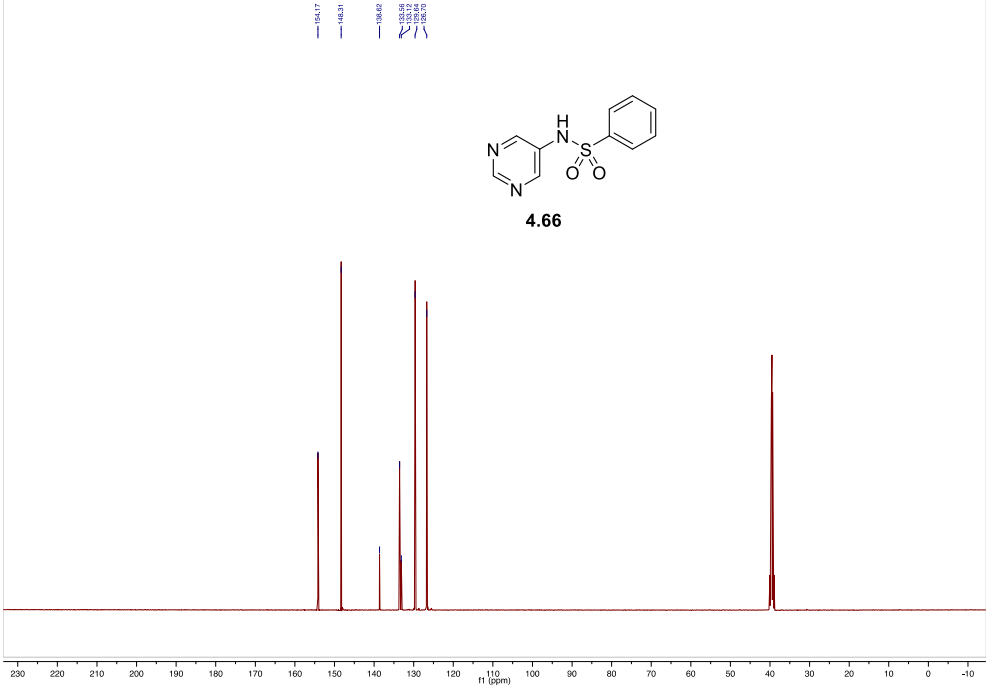
4.66

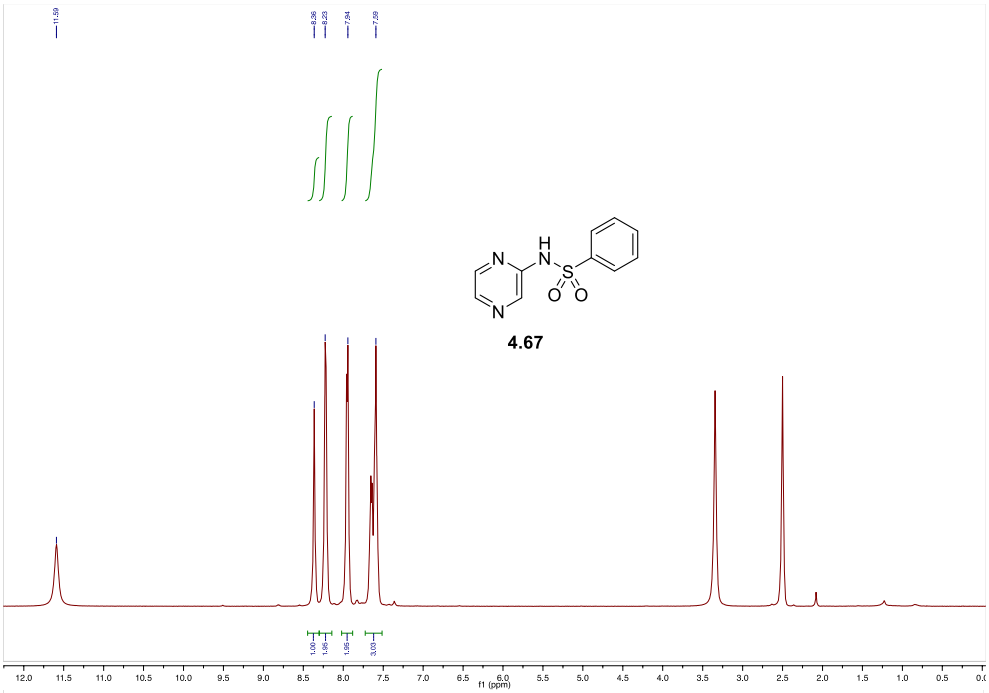
11.59
8.36
8.23
7.94
7.59
4.67
1.00
1.95
1.95
3.03
f1 (ppm)

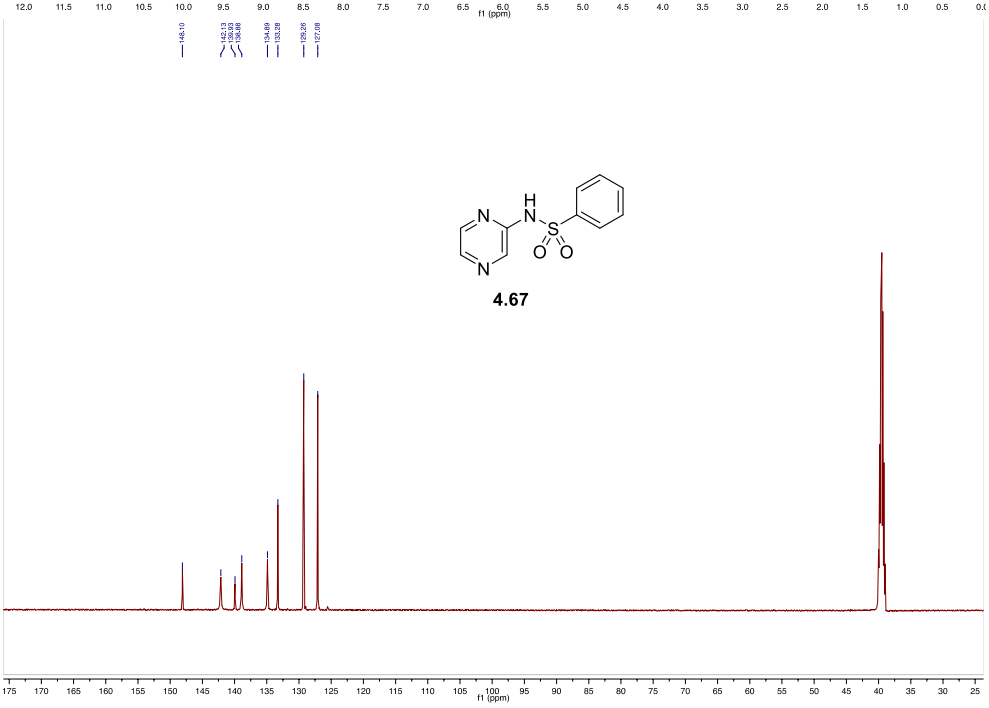
146.10
143.13
139.93
139.68
134.89
129.38
126.26
127.08
4.67
f1 (ppm)

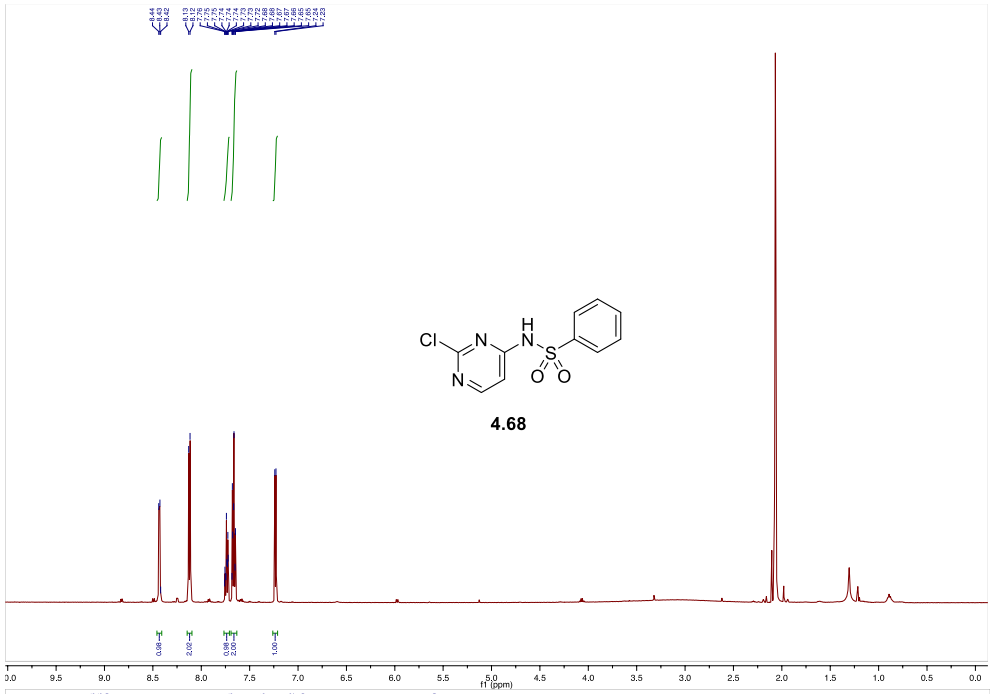
Cl
N
H
N
S
O
O
N
4.68
f1 (ppm)

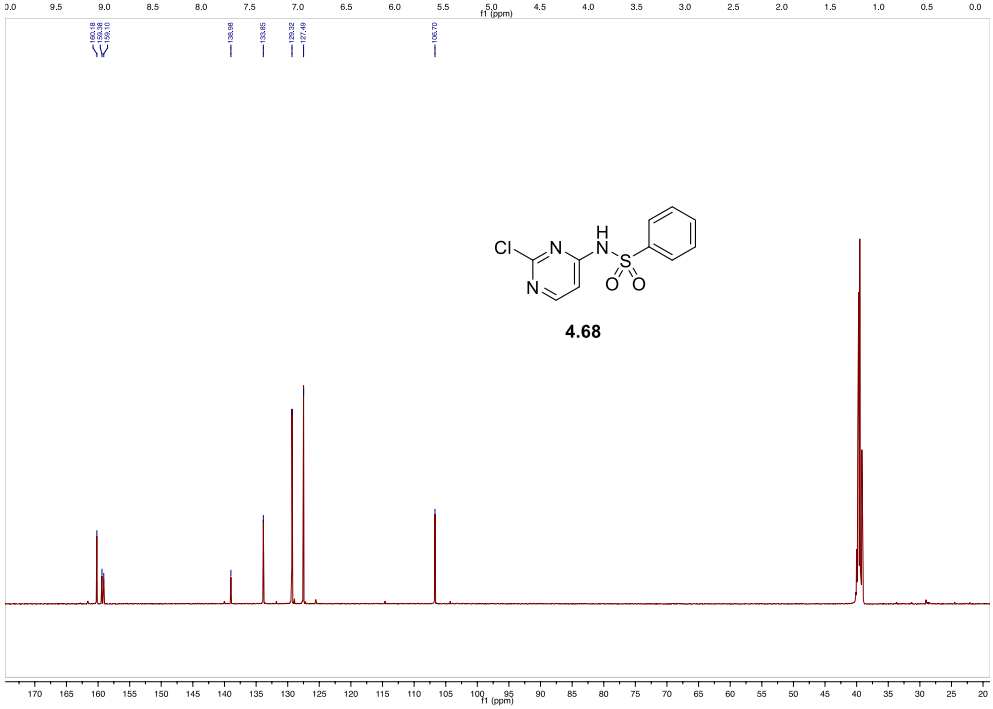
Cl
N
H
N
S
O
O
N
4.68
f1 (ppm)

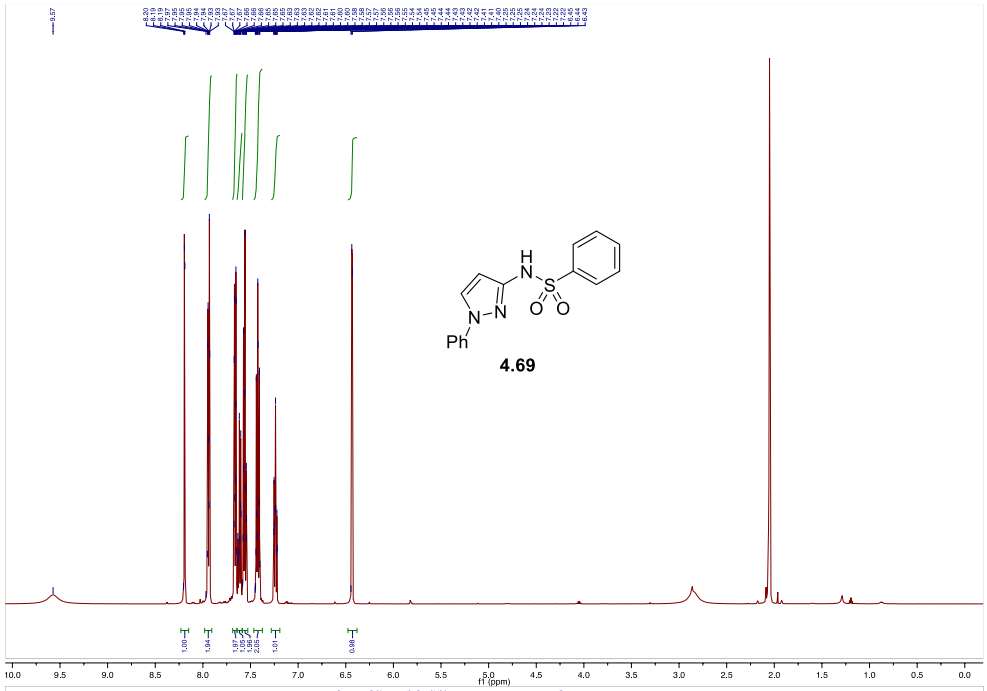
H
N
S
O
O
N
N
Ph
4.69

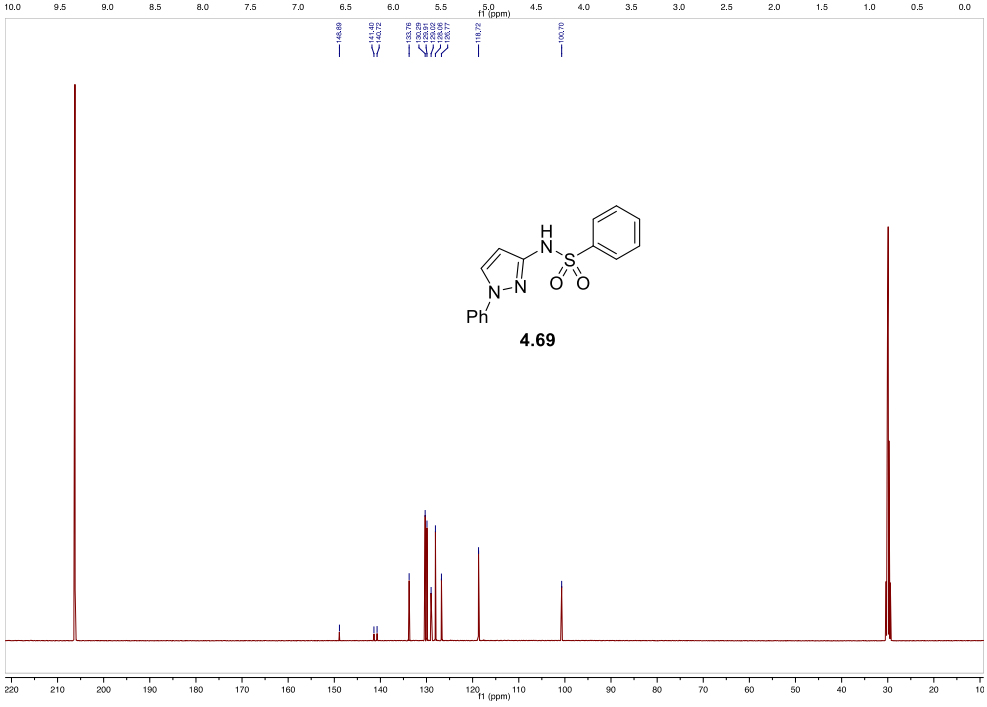
H
N
S
O
O
N
N
Ph
4.69

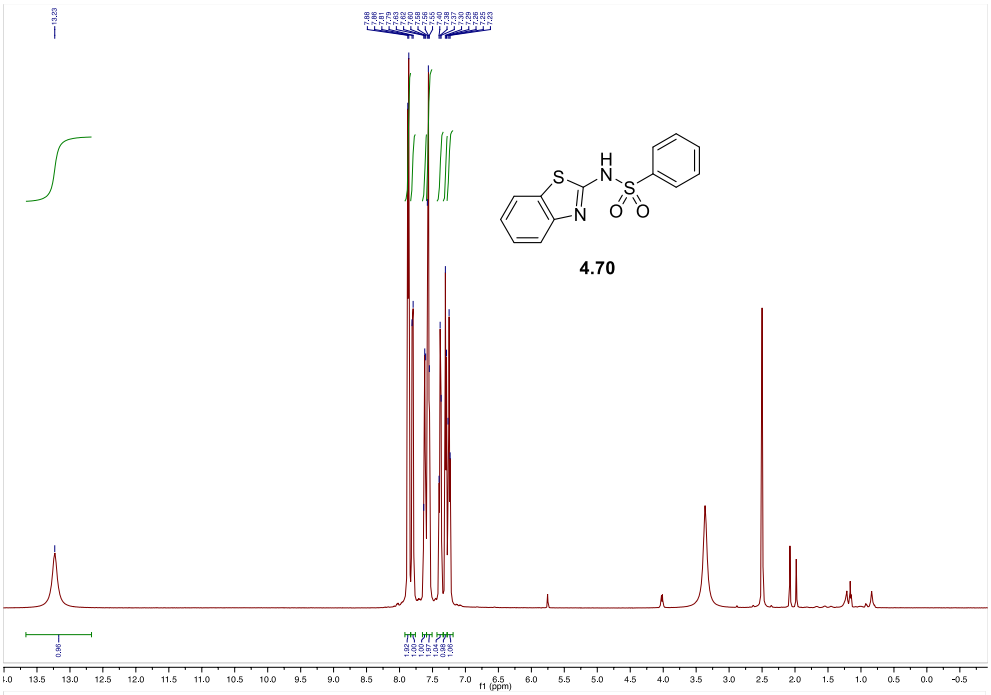
4.70
f1 (ppm)

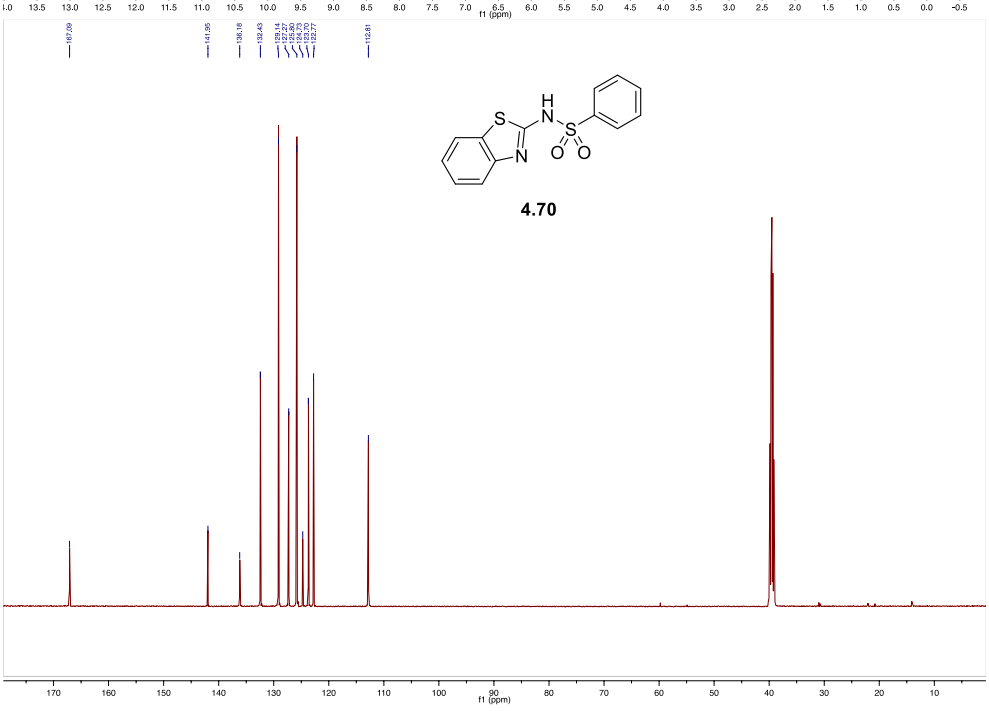
4.70
f1 (ppm)

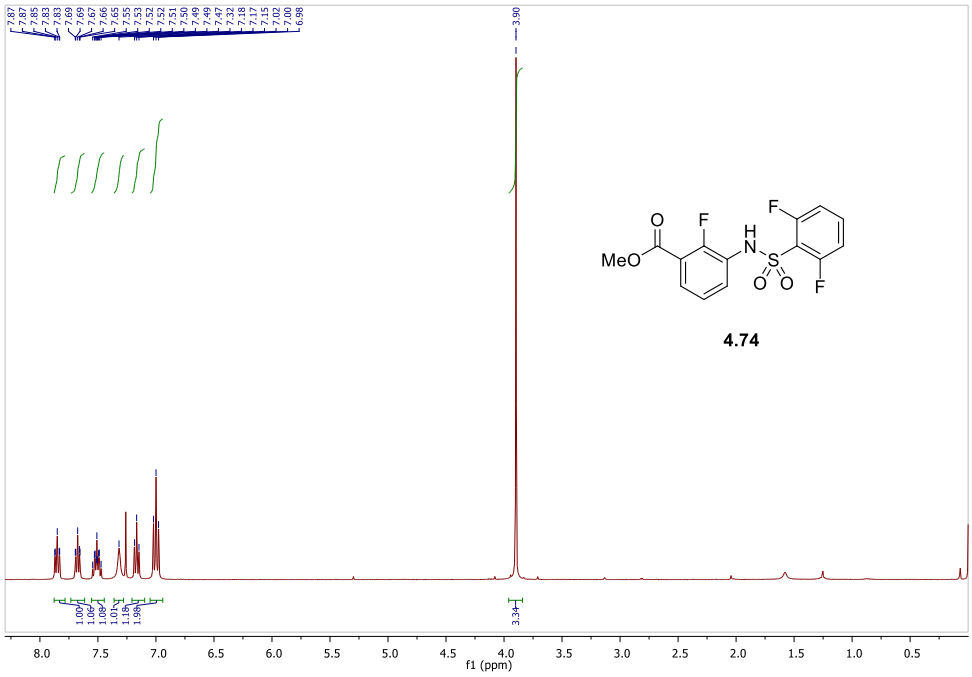
7.87
7.87
7.85
7.83
7.69
7.69
7.67
7.66
7.65
7.55
7.53
7.52
7.52
7.51
7.50
7.49
7.49
7.47
7.32
7.18
7.17
7.15
7.02
7.00
6.98
3.90
1.00
1.08
1.08
1.01
1.18
1.98
3.34
8.0
7.5
7.0
6.5
6.0
5.5
5.0
4.5
4.0
3.5
3.0
2.5
2.0
1.5
1.0
0.5
f1 (ppm)
O
F
H
N
F
MeO
S
O
O
F

4.74

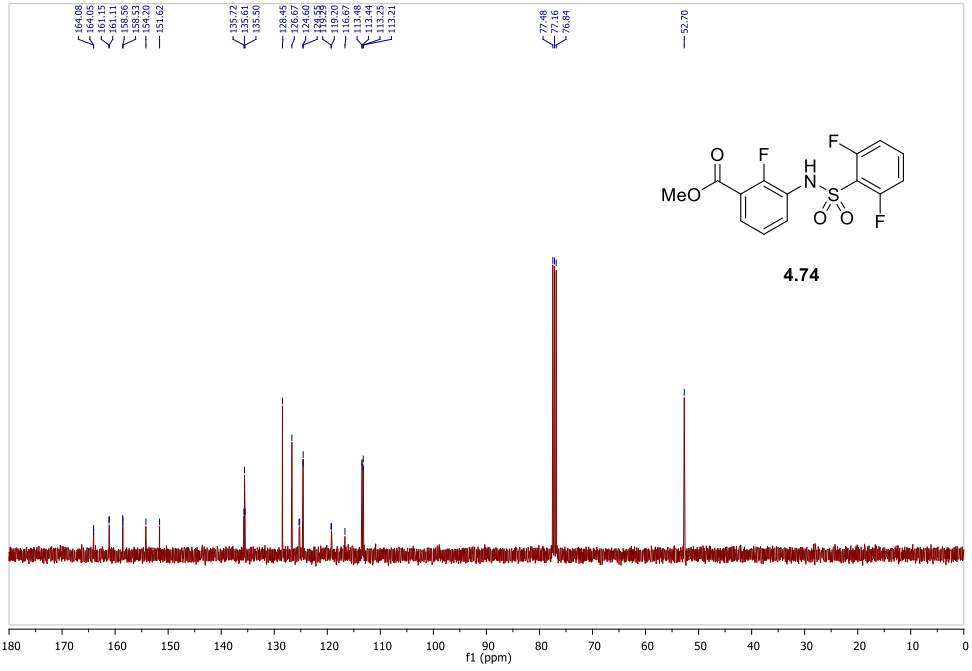
164.08
164.05
161.15
161.11
158.56
158.53
154.20
151.62
135.72
135.61
135.50
128.45
126.67
124.60
119.20
116.97
113.48
113.44
113.25
113.21
77.48
77.16
76.84
52.70
180
170
160
150
140
130
120
110
100
90
80
70
60
50
40
30
20
10
0
f1 (ppm)
O
F
H
N
F
MeO
S
O
O
F

4.74

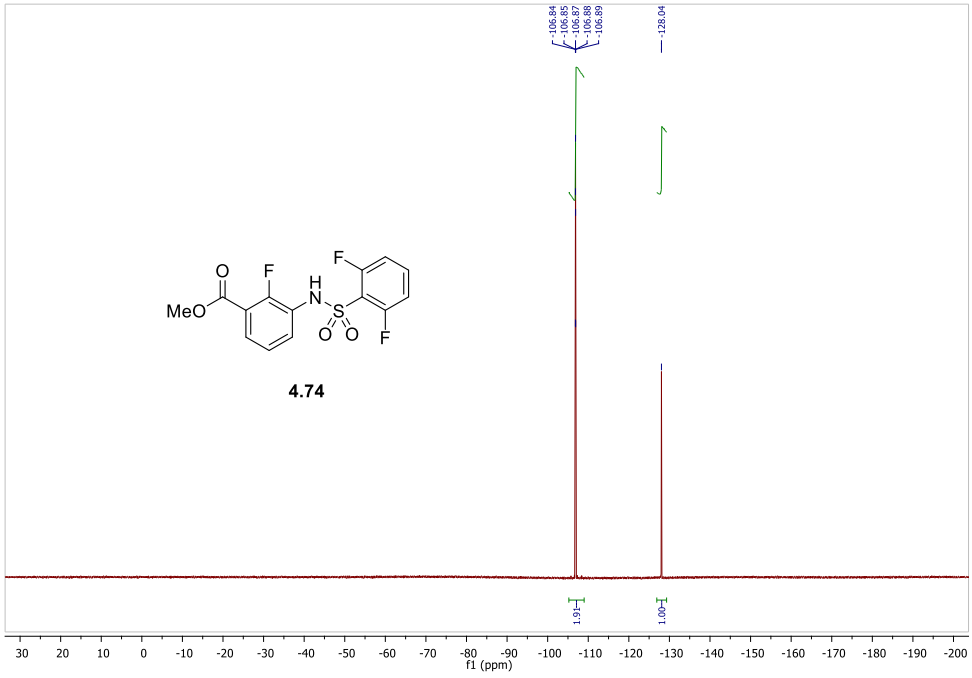
-106.84
-106.85
-106.87
-106.88
-106.89
-128.04
O
F
H
N
MeO
S
O
O
F
F
4.74
1.91
1.00
30 20 10 0 -10 -20 -30 -40 -50 -60 -70 -80 -90 -100 -110 -120 -130 -140 -150 -160 -170 -180 -190 -200
f1 (ppm)

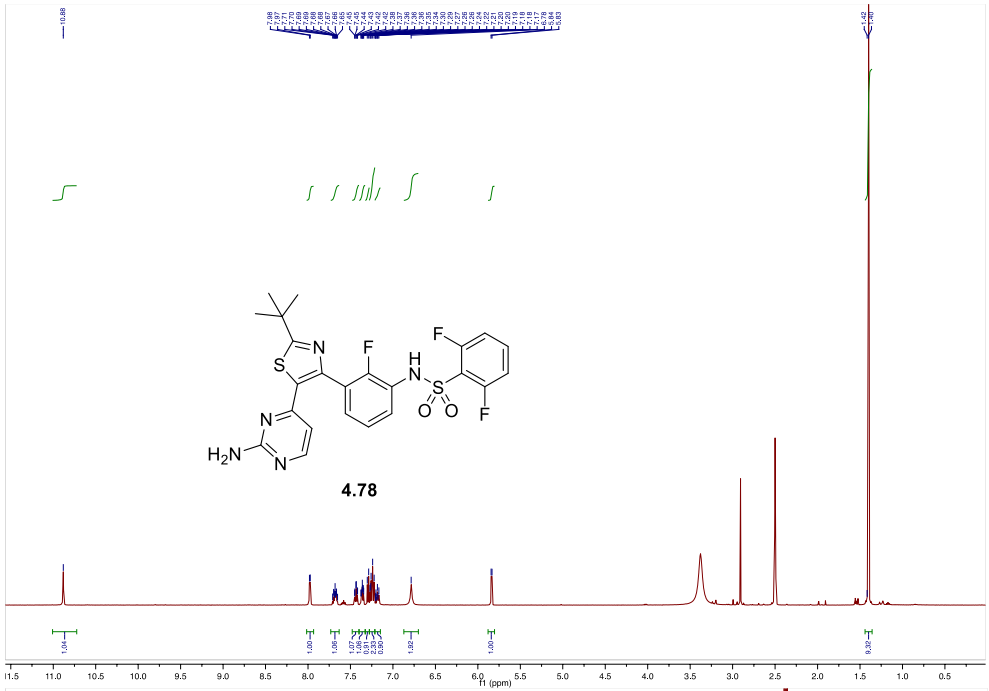
F
N
S
F
H
N
S
O
O
F
N
N
H_2N
4.78
f1 (ppm)

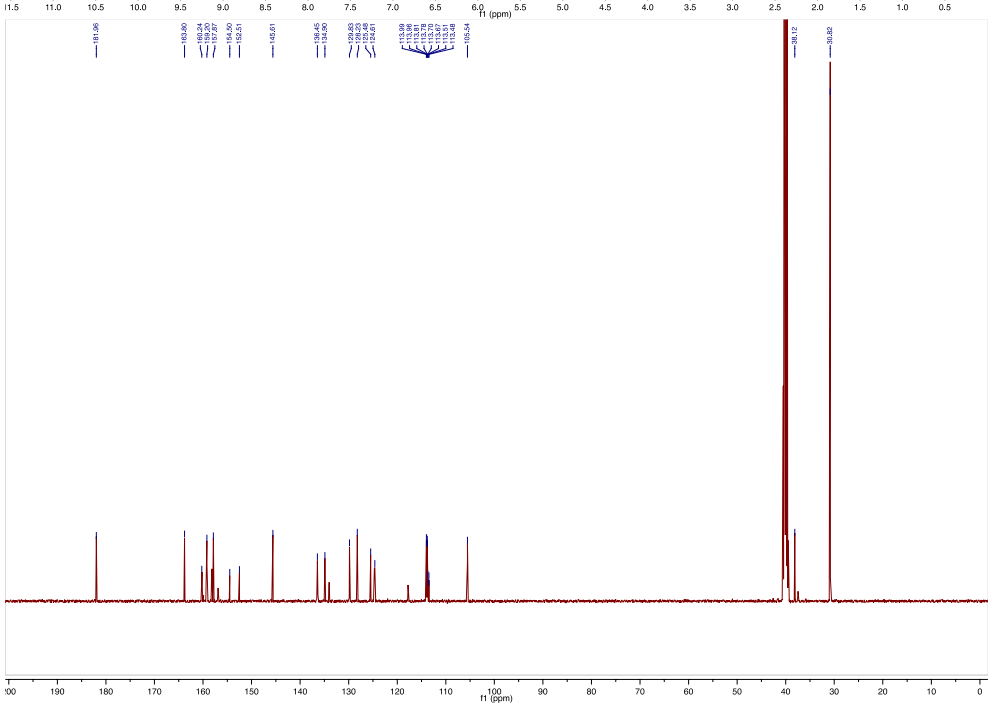
f1 (ppm)

Appendix B

Chapter 5. NMR Spectra

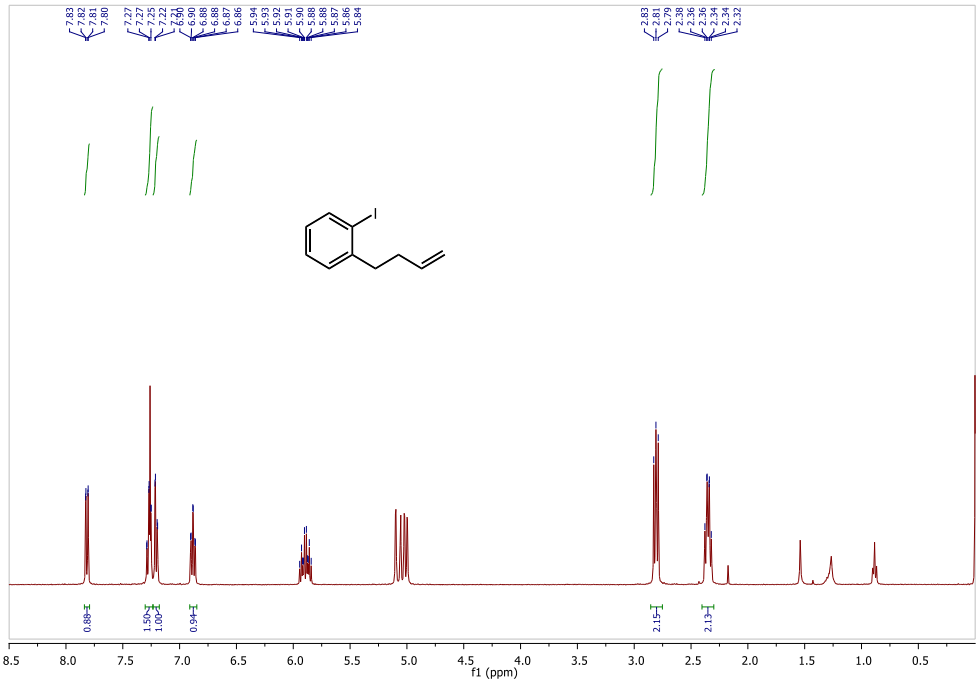
I
f1 (ppm)

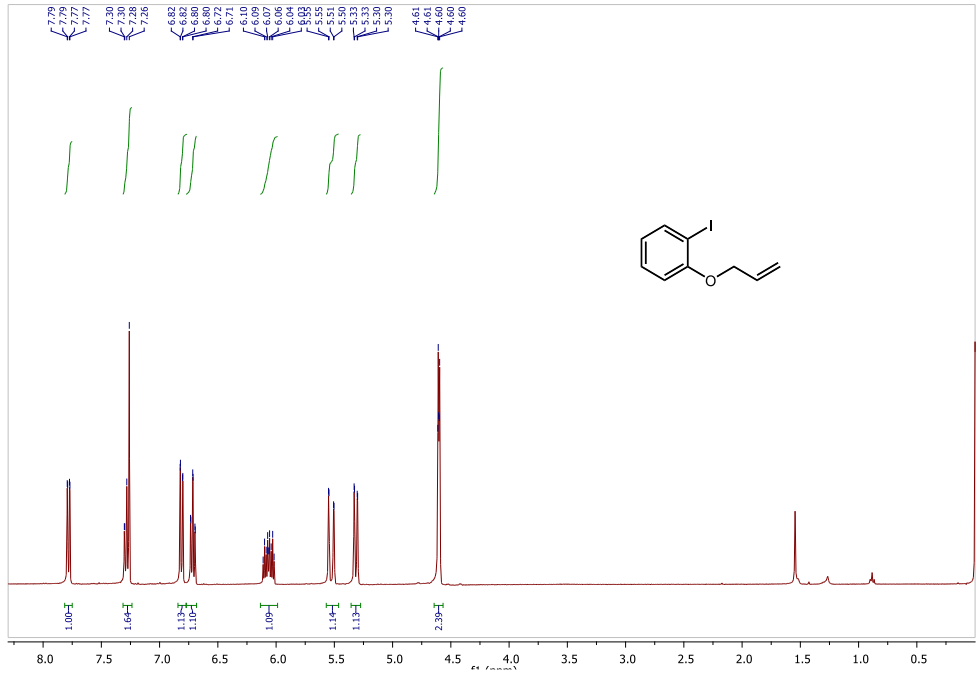
I
O

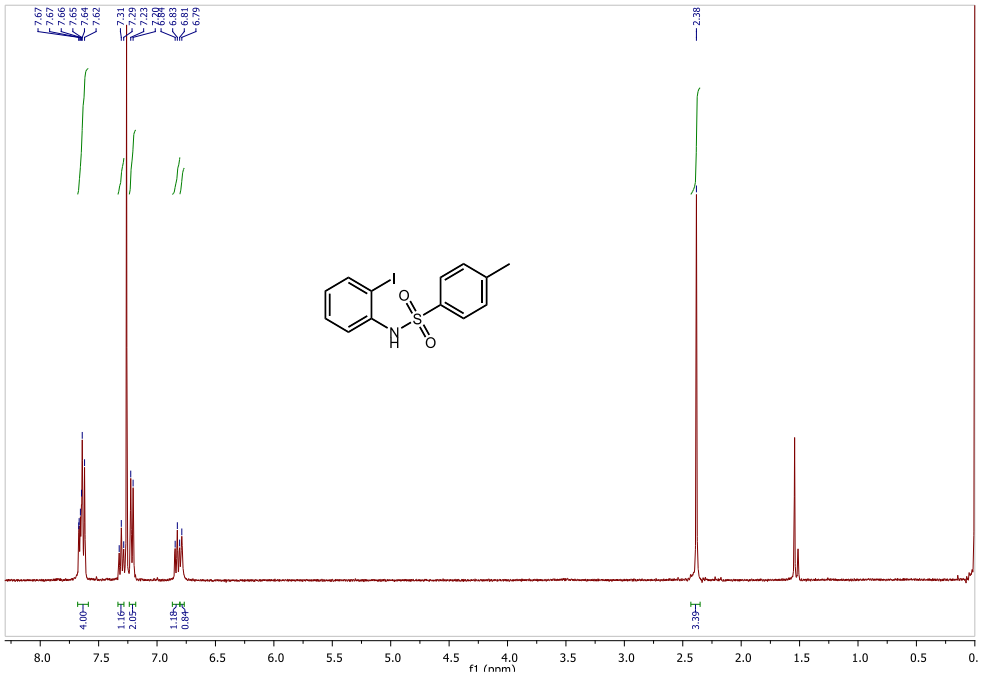

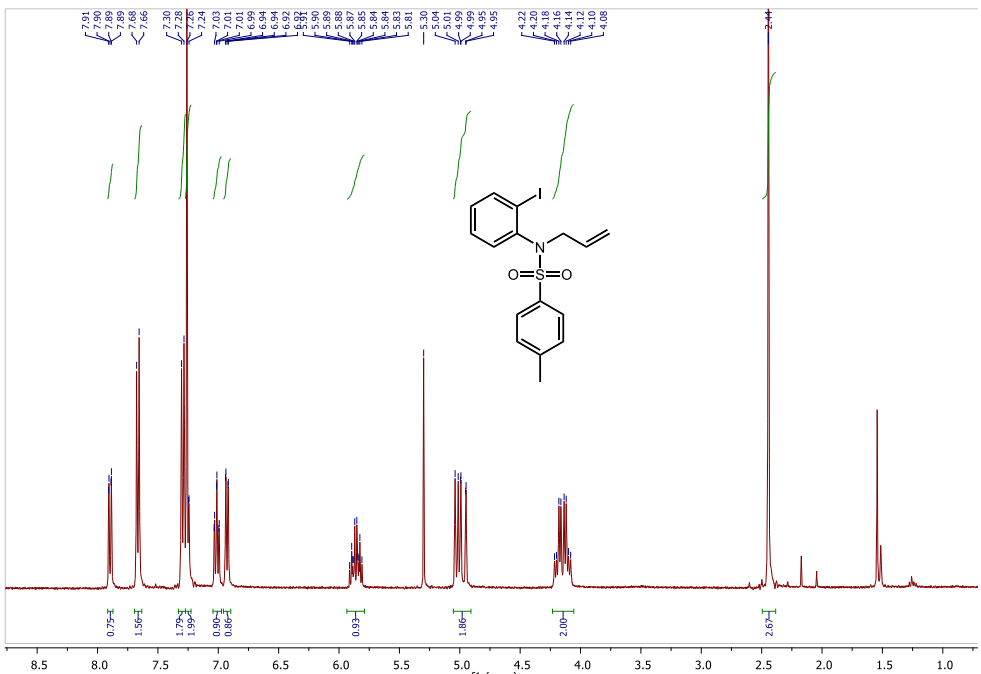

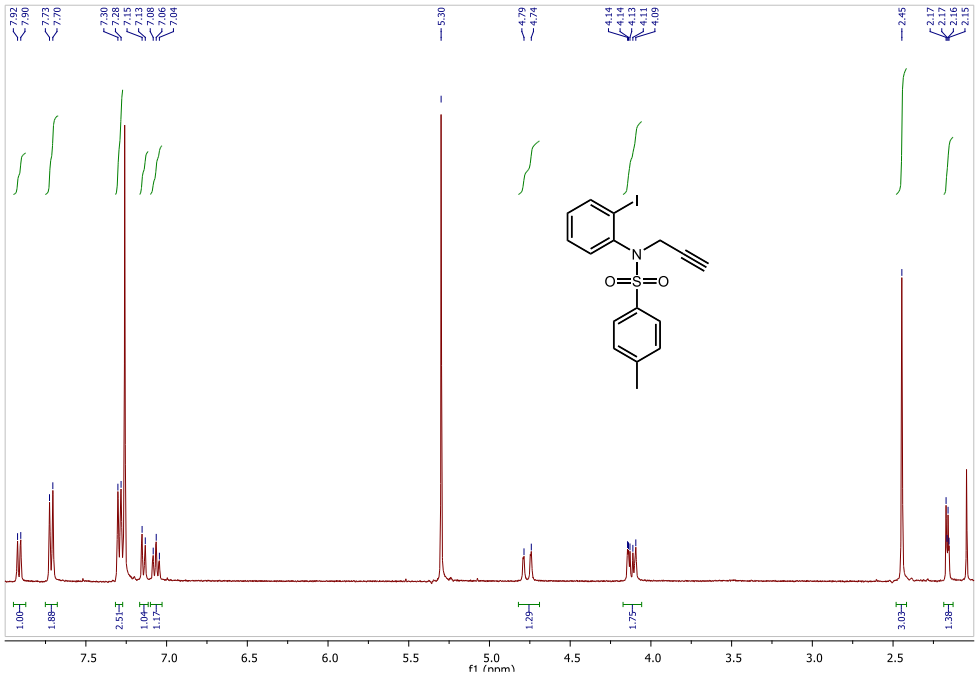
7.92
7.90
7.73
7.70
7.30
7.28
7.15
7.13
7.08
7.06
7.04
5.30
4.79
4.74
4.14
4.14
4.13
4.11
4.09
2.45
2.17
2.17
2.16
2.15
I
N
O=S=O
1.00
1.88
2.51
1.04
1.17
1.29
1.75
3.03
1.38
7.5
7.0
6.5
6.0
5.5
5.0
4.5
4.0
3.5
3.0
2.5

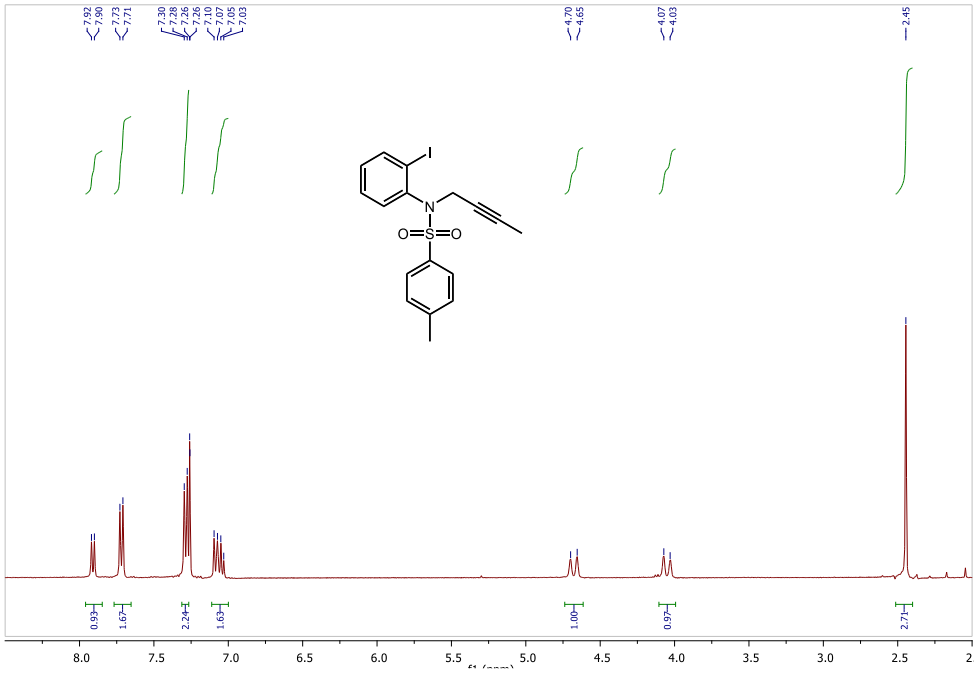
7.92
7.90
7.73
7.71
7.30
7.28
7.26
7.10
7.07
7.05
7.03
4.70
4.65
4.07
4.03
2.45
I
N
O=S=O
0.93
1.67
2.24
1.63
1.00
0.97
2.71
8.0
7.5
7.0
6.5
6.0
5.5
5.0
4.5
4.0
3.5
3.0
2.5

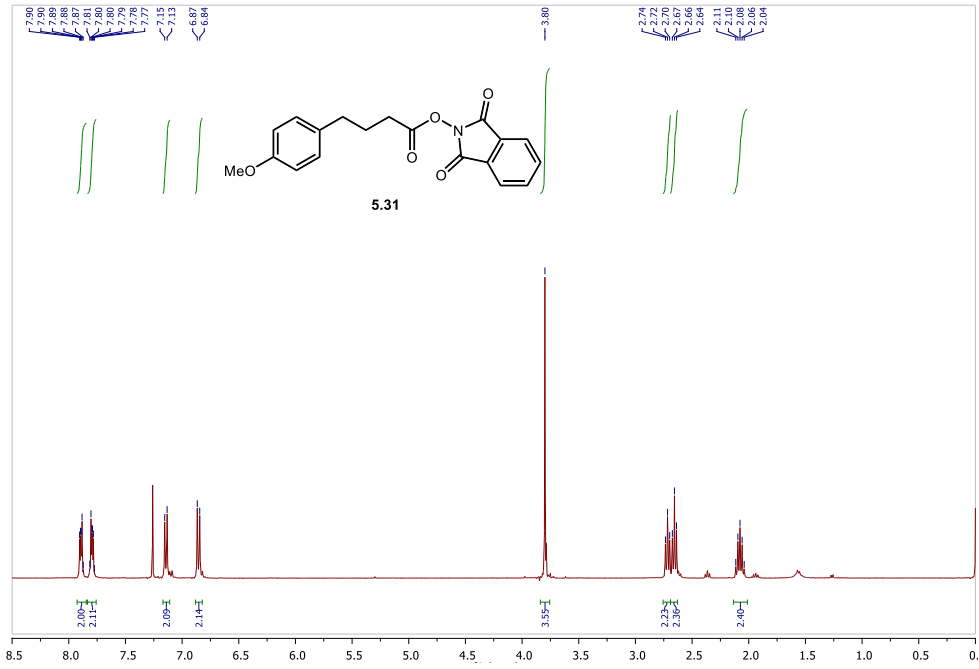
7.90
7.90
7.89
7.88
7.87
7.81
7.80
7.80
7.79
7.78
7.77
7.15
7.13
6.87
6.84
3.80
2.74
2.72
2.70
2.67
2.66
2.64
2.11
2.10
2.08
2.06
2.04
MeO
O
O
N
O
O
5.31
2.00
2.11
2.09
2.14
3.55
2.23
2.36
2.40
8.5
8.0
7.5
7.0
6.5
6.0
5.5
5.0
4.5
4.0
3.5
3.0
2.5
2.0
1.5
1.0
0.5
0.

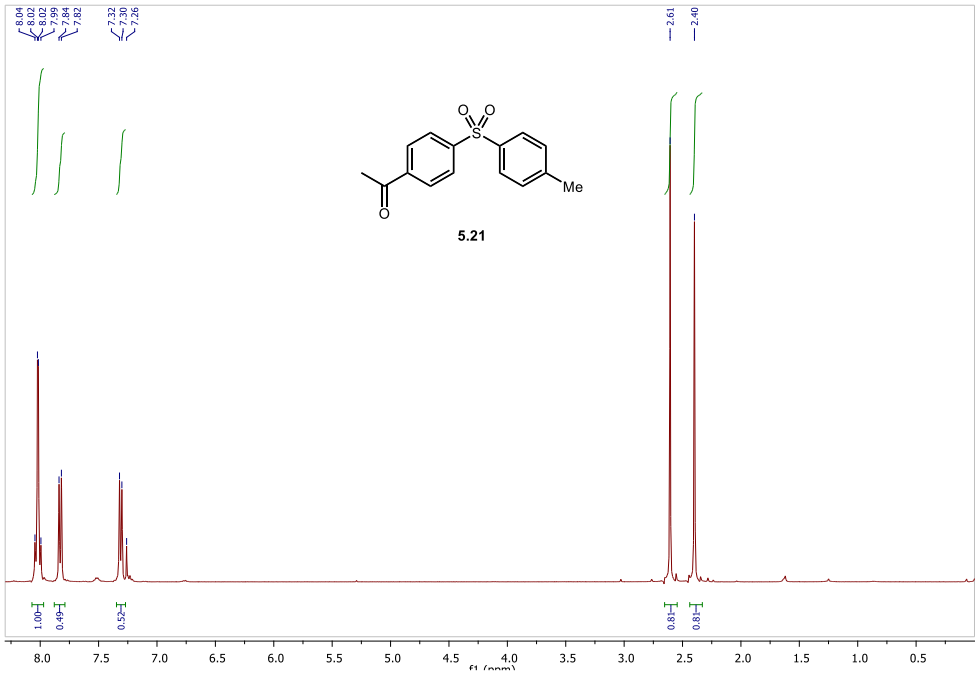
8.04
8.02
8.02
7.99
7.84
7.82
7.32
7.30
7.26
2.61
2.40
O
O
S
Me
O
5.21
1.00
0.49
0.52
0.81
0.81
8.0
7.5
7.0
6.5
6.0
5.5
5.0
4.5
4.0
3.5
3.0
2.5
2.0
1.5
1.0
0.5

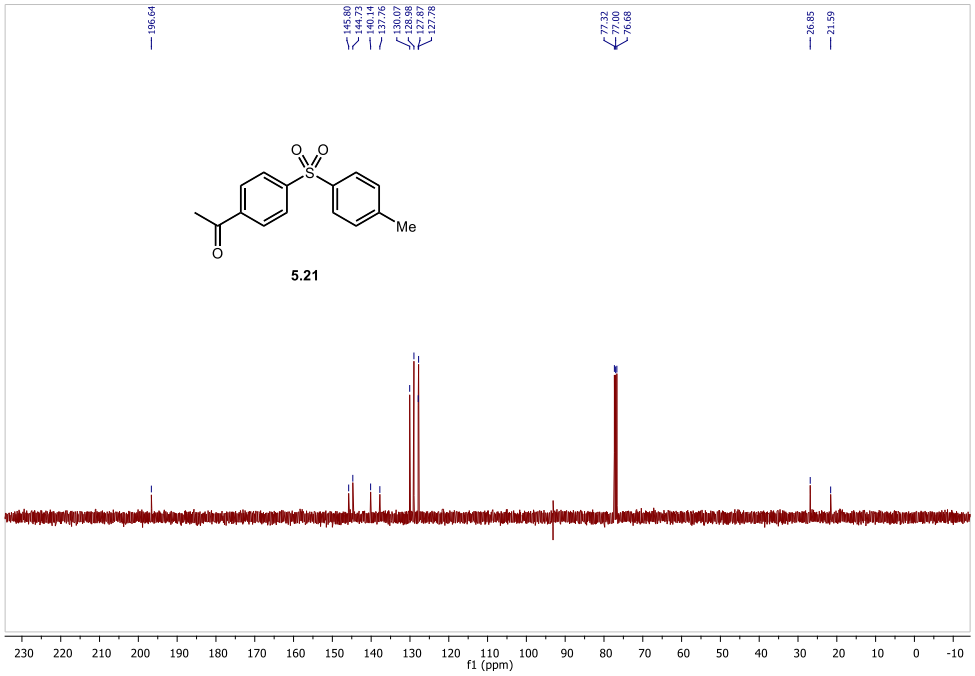
196.64
145.80
144.73
140.14
137.76
130.07
128.98
127.87
127.78
77.32
77.00
76.68
26.85
21.59
O
O
S
Me
O
5.21
230
220
210
200
190
180
170
160
150
140
130
120
110
100
90
80
70
60
50
40
30
20
10
0
-10
f1 (ppm)

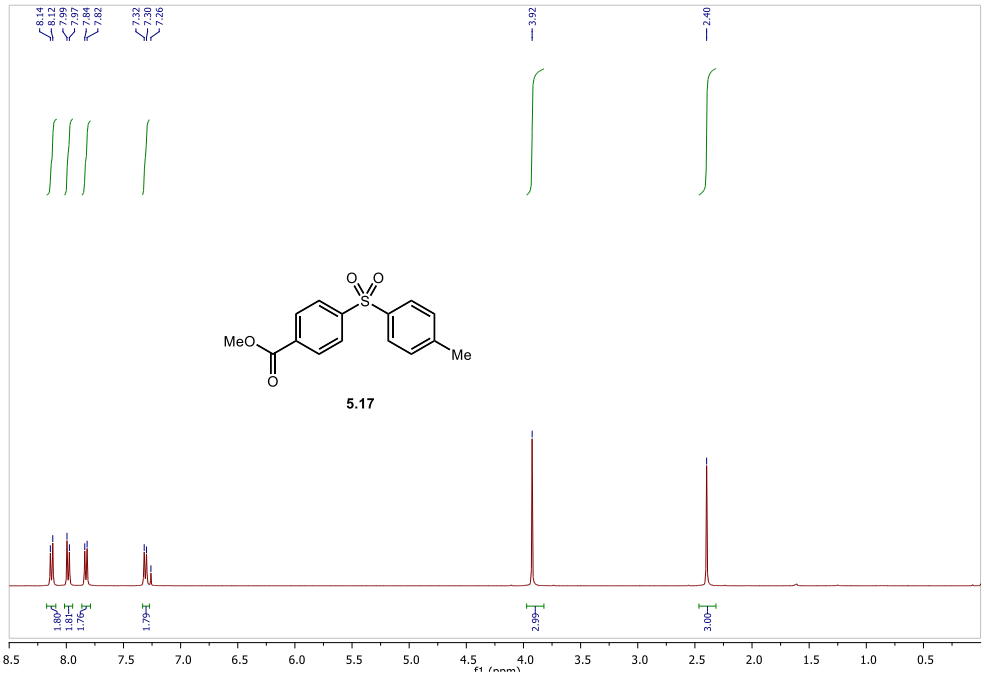
8.14
8.13
7.99
7.97
7.84
7.82
7.32
7.30
7.26
3.92
2.40
MeO
O
O
O
S
Me
5.17
1.80
1.81
1.76
1.79
2.99
3.00
8.5
8.0
7.5
7.0
6.5
6.0
5.5
5.0
4.5
4.0
3.5
3.0
2.5
2.0
1.5
1.0
0.5

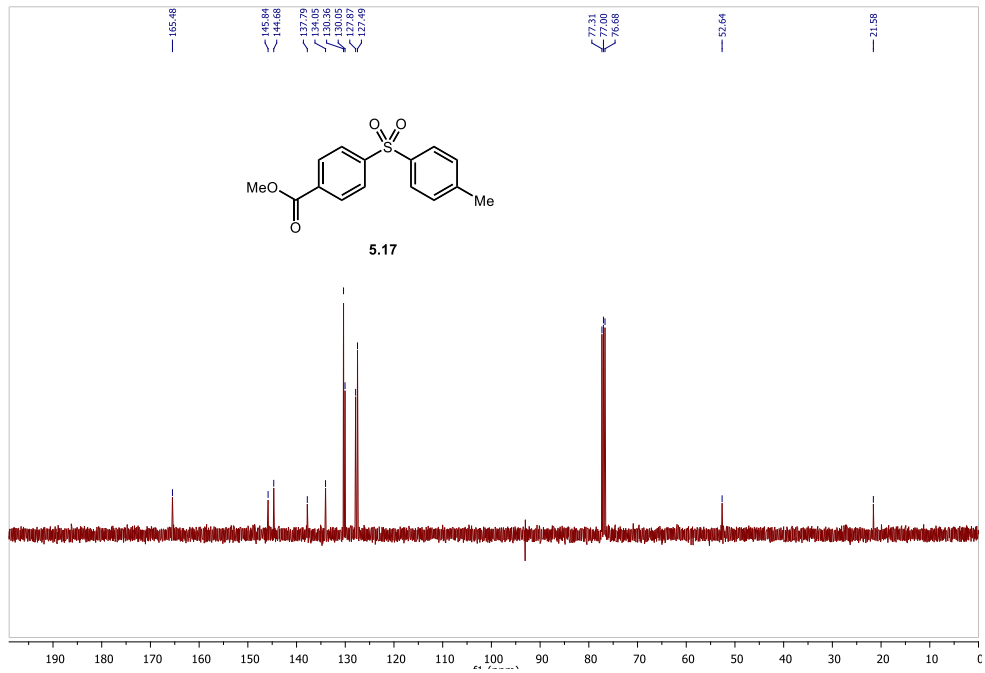
165.48
145.84
144.68
137.79
134.05
130.36
130.05
127.87
127.49
77.31
77.00
76.68
52.64
21.58
MeO
O
O
O
S
Me
5.17
190
180
170
160
150
140
130
120
110
100
90
80
70
60
50
40
30
20
10
0

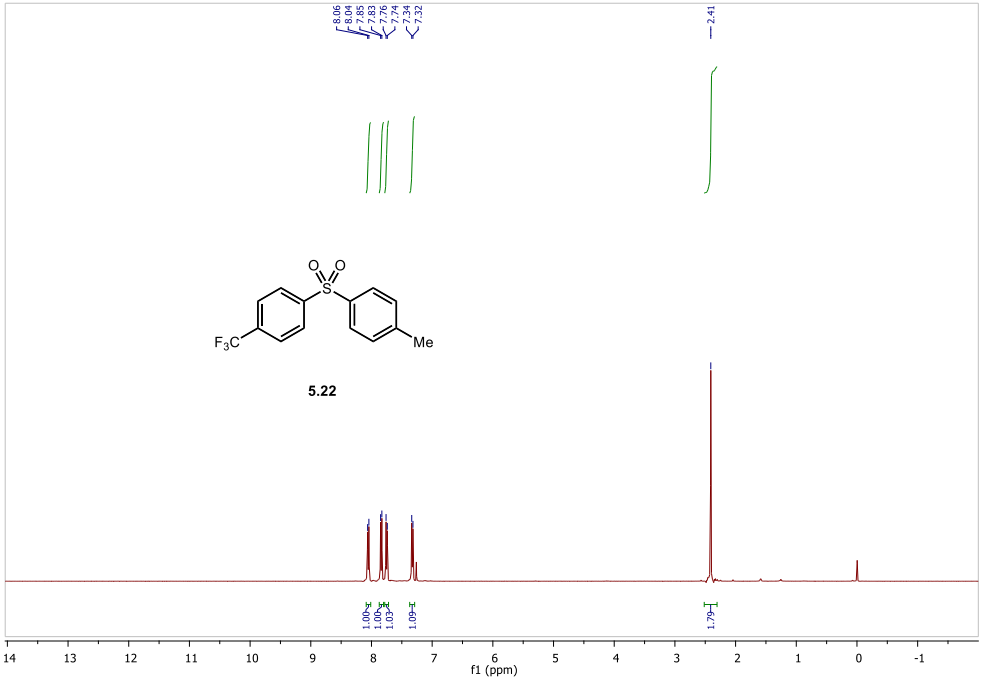
8.06
8.04
7.85
7.83
7.76
7.74
7.34
7.32
2.41
O
O
S
F3C
Me
1.00
1.00
1.03
1.09
1.79
14
13
12
11
10
9
8
7
6
5
4
3
2
1
0
-1
f1 (ppm)

5.22

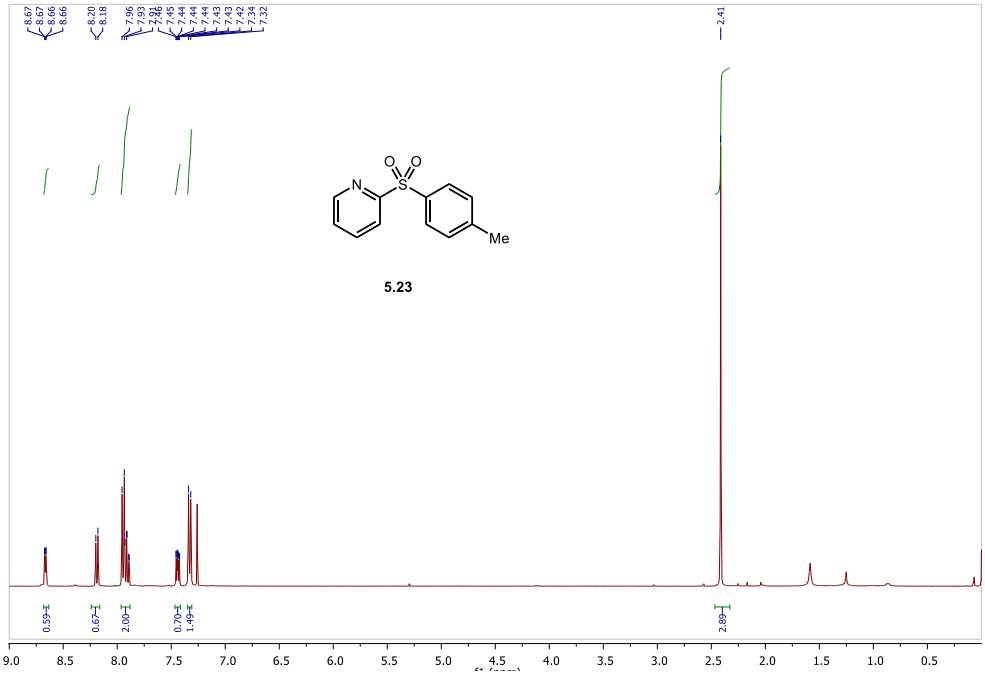
8.67
8.67
8.66
8.66
8.20
8.18
7.96
7.93
7.46
7.45
7.44
7.44
7.44
7.43
7.42
7.34
7.32
2.41
O
O
S
N
Me
0.59
0.67
2.00
0.70
1.49
2.89
9.0
8.5
8.0
7.5
7.0
6.5
6.0
5.5
5.0
4.5
4.0
3.5
3.0
2.5
2.0
1.5
1.0
0.5

5.23

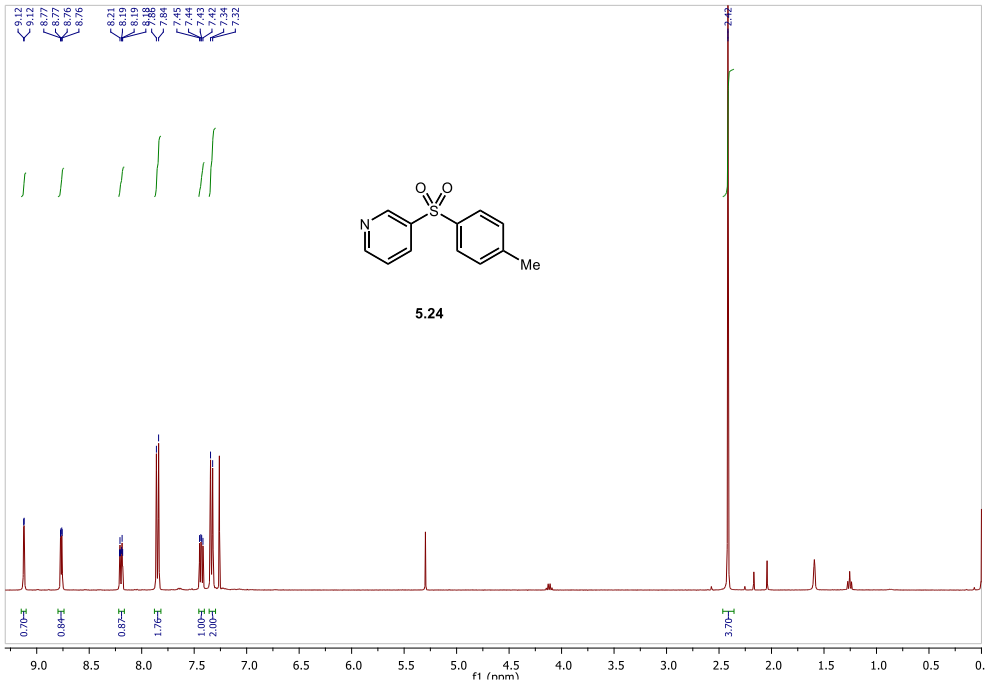
9.12
9.12
8.77
8.77
8.76
8.76
8.21
8.19
8.19
7.88
7.84
7.45
7.44
7.43
7.42
7.34
7.32
2.42
O
O
S
N
Me
5.24
0.70
0.84
0.87
1.76
1.00
2.00
3.70
9.0
8.5
8.0
7.5
7.0
6.5
6.0
5.5
5.0
4.5
4.0
3.5
3.0
2.5
2.0
1.5
1.0
0.5
0.0
f1 (ppm)